SCUOLA DI DOTTORATO
UNIVERSITÀ DEGLI STUDI DI MILANO-BICOCCA

Department of biotechnology and biosciences
PhD program in biology and biotechnology
XXX Cycle

Production of recombinant human MD-2 and development of protein-ligand binding assays for the characterization of novel TLR4 modulators

Surname: **Zaffaroni** Name: **Lenny**
Registration number: **072091**

Tutor: **Professor Francesco Peri**
Co-tutor: **Professor Paola Fusi**

Coordinator: **Professor Paola Branduardi**

ACADEMIC YEAR 2016/2017

Alla zia Giudy,
alla mia famiglia

"Considerate la vostra semenza:
fatti non foste a viver come bruti
ma per seguir virtute e canoscenza"

Dante

Table of Contents

Abstract

Abstract

Toll-like receptor 4 (TLR4) represents a central mediator of innate and adaptive immune responses in mammals. TLR4 activation in response to bacterial lipopolysaccharides (LPS) results in the rapid triggering of pro-inflammatory processes essential for optimal host immune responses. TLR4 activation mediated by LPS is a complex event which involves several proteins (lipid binding protein (LBP), cluster of differentiation 14 (CD14), and myeloid differentiation 2 (MD-2)) and it ends with the formation of the activated $(TLR4/MD\text{-}2/LPS)_2$ complex.

The TLR4 co-receptor MD-2 plays an important role in the interaction with LPS and subsequent TLR4 dimerization. MD-2 alone binds to LPS, whereas TLR4 alone does not. MD-2 is the ligand-binding component of the TLR4/MD-2 receptor complex. LPS binding to TLR4/MD-2 induces TLR4 dimerization; whereas TLR4 antagonists binding to TLR4/MD-2 does not induce TLR4 dimerization.

Deregulated TLR4 activation is related to an impressively broad spectrum of disorders still lacking specific pharmacological treatment. These include autoimmune disorders, chronic inflammations, allergies, asthma, infectious and central nervous system diseases, cancer, and sepsis. The TLR4 inhibition by small molecules of synthetic and natural origin provides access to new TLR-based therapeutics targeting this large array of diseases.

This thesis is part of an original structure-activity relationship (SAR) study on synthetic monosaccharide glycolipids in the context of TLR4 modulation. Thesis work focuses on the *in vitro* binding characterization of new synthetic monosaccharide glycolipids with the purified receptor MD-2.

Pure and functional human MD-2 (hMD-2) protein for binding studies has been obtained by expression in yeast cells. Two different expression systems for the production of recombinant hMD-2 were tested: mammalian (HEK293T) and yeast cells (*Pichia pastoris*). Recovery of hMD-2 from the medium of yeast cells was optimized, achieving a concentration of recombinant hMD-2 of 30 μM. An ELISA was developed in order to compare the biological activity of the hMD-2 expressed in different hosts. hMD-2 from mammalian cells obtained the highest biological activity, followed by the hMD-2 expressed by *P. pastoris*. hMD-2 expressed by *E. coli* presented the lowest biological activity of the three.

Due to the higher yield of recovery achieved, hMD-2 expressed in *P. pastoris* was used in four different types of binding experiments to assess its affinity for natural and synthetic molecules. The binding tests comprise two plate based ELISA with immobilized hMD-2, a fluorescence displacement assay and surface plasmon resonance (SPR) measurements.

Abstract

The two ELISA tests were based on: i) dose-dependent displacement of a monoclonal antibody from immobilized hMD-2. The antibody binds to hMD-2 in a region proximal to ligand binding site; ii) displacement of biotin-LPS from immobilized hMD-2. The fluorescence experiment was based on the displacement of the bis-ANS from hMD-2, whereas the SPR technique was used to study the direct interactions between small ligands and immobilized hMD-2.

The obtained binding affinities for hMD-2 of the tested molecules (which turned out to be in the low μM range) mirror their biological activity in modulating TLR4 signaling and cytokine production *in vitro* in cell models.

The results obtained from these *in vitro* cell-free studies indicate that the tested molecules bind to the hMD-2 pocket, with differences in the affinity values.

These data allow a systematic study on SAR for TLR4 modulators, opening the way for the development of a new generation of drug hits and leads targeting directly TLR4 signaling.

Riassunto

Riassunto

Il *toll-like receptor 4* (TLR4) rappresenta un mediatore centrale dell'immunità innata ed adattativa in mammiferi. L'attivazione di TLR4 in risposta al lipopolisaccaride (LPS) batterico induce un rapido innesco di processi pro-infiammatori essenziali per una risposta immunitaria ottimale. L'attivazione di TLR4 mediata da LPS è un meccanismo che coinvolge la partecipazione di diverse proteine (*lipid binding protein* (LBP), *cluster of differentiation 14* (CD14), e *myeloid differentiation 2* (MD-2)) e culmina con la formazione del complesso attivato $(TLR4/MD\text{-}2/LPS)_2$.

MD-2 è il co-rettore di TLR4, e svolge un importante ruolo nell'interazione con LPS e la susseguente dimerizzazione del TLR4. MD-2 da solo lega LPS, mentre TLR4 da solo no. MD-2 è la componente che interagisce con il ligando (LPS) nel complesso recettoriale TLR4/MD-2. Il legame di LPS al complesso TLR4/MD-2 induce la dimerizzazione del TLR4; mentre gli antagonisti del TLR4 sono in grado di legare il complesso TLR4/MD-2 ma non inducono la dimerizzazione del TLR4.

L'attivazione non regolata del TLR4 è correlata ad una serie di problematiche ancor prive di un trattamento farmacologico. Esse includono disordini autoimmuni, infiammazione cronica, allergie, asma, infezioni e malattie del sistema nervoso centrale, cancro, e setticemia. L'inibizione del TLR4 tramite l'uso di piccole molecole sintetiche o naturali può quindi rappresentare una via

per lo sviluppo di nuove terapie contro questa vasta gamma di problematiche.

Questa tesi è parte di un studio originale di relazione struttura-attività (SAR) svolto su glicolipidi monosaccaridici sintetici nel contesto della modulazione del TLR4. In particolare, essa si focalizza sulla caratterizzazione del legame *in vitro* di nuovi glicolipidi monosaccaridici sintetici con il recettore MD-2 purificato.

Per gli studi di interazione la proteina MD-2 umana (hMD-2) purificata e funzionale è stata espressa in cellule di lievito. Due diversi sistemi di espressione per la produzione di hMD-2 ricombinante sono stati testati: mammifero (HEK293T) e cellule di lievito (*Pichia pastoris*). La purificazione di hMD-2 da lievito è stata ottimizzata ottenendo una concentrazione finale di hMD-2 purificato di 30 μM. Per confrontare l'attività biologica di hMD-2 espresso nei diversi microorganismi è stato sviluppato un ELISA. hMD-2 da cellule di mammifero ha ottenuto l'attività biologica più elevata, seguito da hMD-2 espresso in *P. pastoris*. hMD-2 da *E. coli* ha ottenuto l'attività biologica più bassa dei tre.

Date le rese più elevate di purificazione in lievito, hMD-2 espresso in *P. Pastoris* è stato utilizzato nei quattro diversi tipi di esperimenti di legame per studiare l'affinità di molecole naturali e sintetiche. I test di legame comprendono due ELISA con hMD-2 immobilizzato, un saggio fluorescente di spiazzamento, e misure

di risonanza plasmonica di superficie (SPR). I due test ELISA sono basati su: i) spiazzamento dose-dipendente di un anticorpo da hMD-2 immobilizzato. L'anticorpo lega hMD-2 in una regione in prossimità del sito di legame del ligando; ii) spiazzamento di LPS biotinilato da hMD-2 immobilizzato. L'esperimento di florescenza è basato sullo spiazzamento di bis-ANS da hMD-2. Mentre la tecnica SPR è stata utilizzata per studiare la diretta interazione tra le molecole e hMD-2 immobilizzato.

L'affinità per hMD-2 delle molecole analizzate (che risulta essere nell'intervallo del basso μM) è in linea con i risultati di attività biologica e la produzione di citochine *in vitro* in modelli cellulari.

I risultati ottenuti da questi studi *in vitro* sul recettore hMD-2 purificato evidenziano l'interazione delle molecole con la tasca idrofobica di hMD-2, presentando differenze nei valori di affinità.

Questi dati generati permettono uno studio sistemico dei modulatori del TLR4, creando buone prospettive per lo sviluppo di una nuova generazione di farmaci *hits* e *leads* che agiscano direttamente sul recettore TLR4.

Introduction

1.1 The immune system

The immune system is a defense system that protects the host from viruses, microorganisms and cancer. It is the second most complex system that the human body has, after the nervous system. The immune system generates different group of cells and molecules which work together with the aim of recognizing, fighting, and eliminating a variety of pathogens. It includes innate and adaptive immunity, which are less and more specific components respectively (Figure 1) [1].

1.1.1 Innate immunity

Innate immunity is the first line of defense against pathogens, it aims at preventing infections and to maintain homeostasis, and it represents the less specific component of the immune system [1]. Innate immunity includes four types of barriers: anatomic, physiologic, phagocytic, and inflammatory. Skin and mucous membranes represent the anatomic barrier which blocks the entry of the pathogens into the body. Temperature, pH, and various body secretions represent the physiologic barrier which makes difficult to the invading pathogen to growth and survive. Endocytosis (defined as the uptake of material from its environment by cells) represents the phagocytic defense

mechanism, by which phagocytes (main classes are called macrophages and neutrophils) engulf microbes, viruses, and cellular debris. Finally, inflammation is a complex series of events that are triggered by an invading pathogen after tissue damage. The inflammatory process is activated by a variety of chemical mediators which are derived from invading microorganisms, released from damaged cells in response to tissue injury, generated by plasma enzyme systems, and produced by white blood cells. The innate immunity also plays a role in activate and regulate the adaptive immunity [2].

1.1.2 Adaptive immunity

The adaptive immunity is considered to be the specific component of the immune system, and it is activated within five to six days after an antigenic challenge to the organism occurred. Adaptive immunity possesses the characteristics of high specificity and memory. Thanks to this memory feature, the immune response to an already encountered antigen is typically faster, stronger, and more effective in fighting the pathogen compared to the first time. Lymphocytes, B cells, antibodies and other molecules are the key agents of adaptive immunity (Figure 1). Due to the slow response of adaptive immunity, innate immunity plays a crucial role, and it provides the first line of

defense against pathogens. In healthy people, invading pathogens are usually "cleared" by the defense mechanisms of innate immunity before the adaptive immunity can be activated [3].

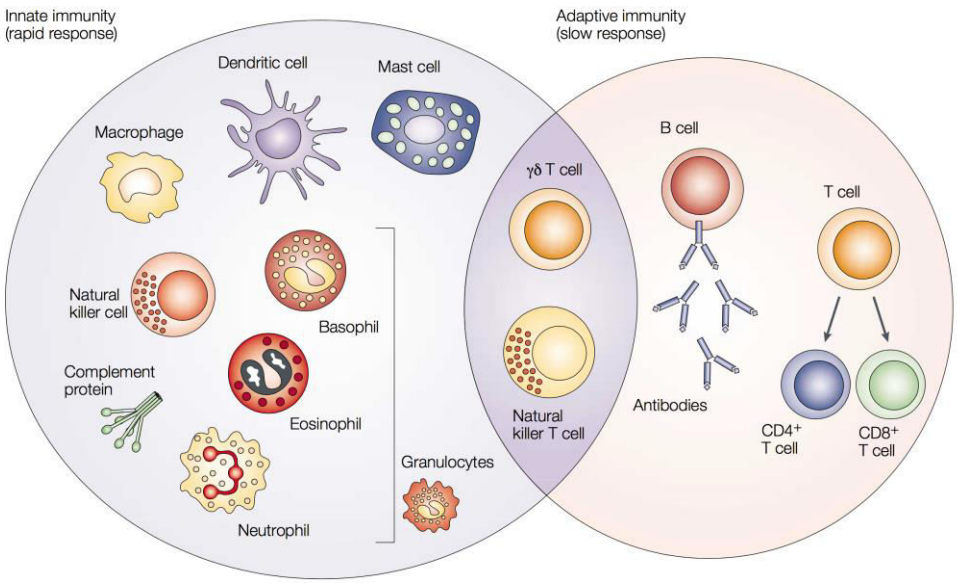

Figure 1. The innate immunity is the first line of defense against infection. It consists of soluble factors, such as complement proteins, and diverse cellular components including granulocytes (basophils, eosinophils and neutrophils), mast cells, macrophages, dendritic cells and natural killer cells. The adaptive immunity is slower to develop, but manifests as increased antigenic specificity and memory. It consists of antibodies, B cells, and CD4+ and CD8+ T lymphocytes. Natural killer T cells and γδ T cells are cytotoxic lymphocytes that straddle the interface of innate and adaptive immunity [4].

Innate immunity	Adaptive immunity
Response is antigen-independent	Response is antigen-dependent
There is immediate maximal response	There is a lag time between exposure and maximal response
Not antigen-specific	Antigen-specific
Exposure results in no immunologic memory	Exposure results in immunologic memory

Table 1. Summary of the main characteristics of innate and adaptive immunity.

1.2 Inflammation

The inflammatory response is a complex series of events activated after tissue damage or by an invading pathogen.

Inflammation fights infection in a finely-orchestrated way: it delivers specialized cells and molecules to the infection's site to support macrophages in fighting the invaders, it promotes injured tissue's repairing processes, and it provides a physical barrier preventing the spread of infection [5].

The Roman physician Celsus in 30 AD described the "four cardinal signs of inflammation" as *rubor* (redness), *tumor* (swelling), *calor* (heat), and *dolor* (pain) [6]. One century later, Galen, also a physician, added a fifth sign: *functio laesa* (loss of function) [7]. These cardinal signs are related with the 3 major events of the inflammatory response (Figure 2) [8], that are:

i) Vasodilatation (dilatation of blood vessel) and increased blood flow. Due to the dilatation of arterioles, more blood flows to the injured site. The vessels that carry blood away are constricted, resulting in an engorgement of the capillary network. This constriction (in combination with the increased blood flow) provokes to the injured area to become red and warm, which are the first two signs of inflammation;

ii) Increased vascular permeability. Following tissue injury the capillary permeability of blood vessels in the injured area

increases to facilitate fluid and cells to influx from the engorged capillaries into the tissue. During this stage, cytokines and chemokines (chemoattractant cytokines) are synthesized and secreted by macrophages;

iii) Leukocytic exudation and chemotaxis. The first cells attracted to the site of infection are generally neutrophils, followed by monocytes, and later on by other eosinophils and lymphocytes.

This complex process called inflammatory response which involves a series of mediators which interact with each other, is still only partially understood. The origin of these mediators can vary. They can be derived from microorganisms, be released from damaged cells, be generated by several plasma enzyme systems, or be a product of various white blood cells participating in the inflammatory response.

A well know example of these mediators is the bacterial lipopolysaccharide (LPS), a molecular component of Gram-negative bacteria, that can initiate an inflammatory response via interaction with cell surface receptors.

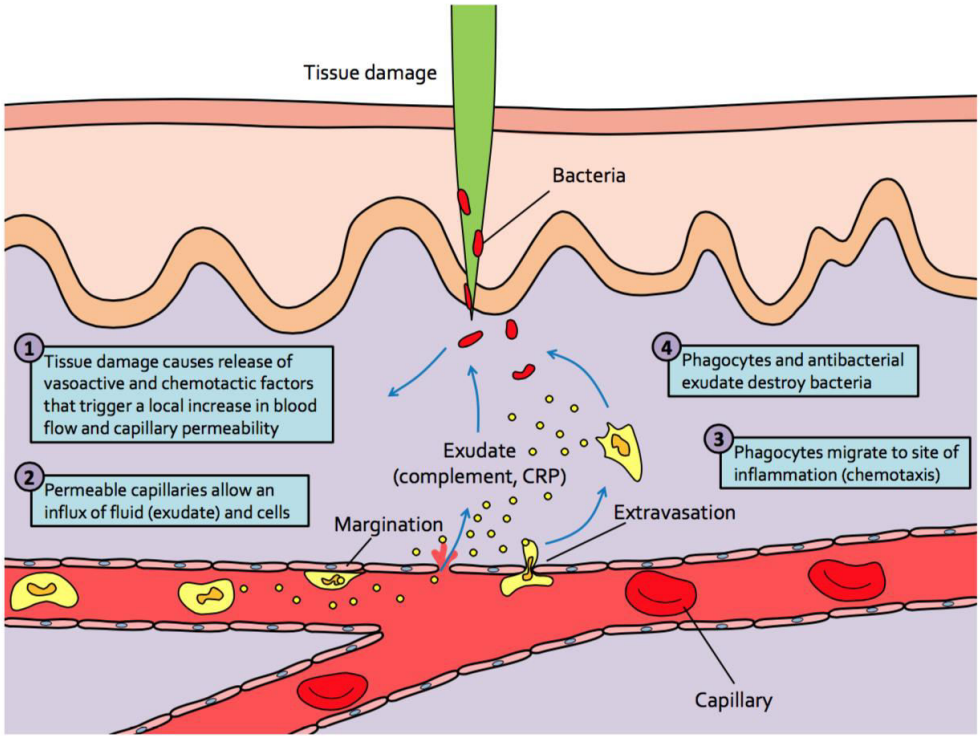

Figure 2. Major events in the inflammatory response. A bacterial infection causes tissue damage with release of various vaso-active and chemo-tactic factors. These factors induce increased blood flow to the area, increased capillary permeability, and an influx of white blood cells, including phagocytes and lymphocytes, from the blood into the tissues. The serum proteins contained in the exudate have antibacterial properties, and the phagocytes begin to engulf the bacteria [8].

1.2.1 Bacteria and Gram stain classification

Bacteria are the most common and widespread human pathogens. Of all the different classification systems, the Gram stain is the preferred method used [9]. Discovered by Hans Christian Joachim Gram in 1884, it allows bacteria to be classified as either Gram-positive or Gram-negative based on their morphology and differential staining properties. Gram-positive bacteria have a cell envelope that consists of a single membrane and a thick layer of peptidoglycan (or murein, a complex polysaccharide) known as cell wall (Figure 3). On the other hand, Gram-negative bacteria have a cell wall that is made up of two membranes, the inner and the outer membrane (OM), that enclose a region known as periplasm, in which lies a thin peptidoglycan layer linked with the overlaying OM (Figure 3).

The cell wall of Gram-positive bacteria tends to be two to eight times as thick as the Gram-negative wall. The iodine and crystal violet used in the Gram staining method, precipitate in the thickened cell wall and are not eluted by alcohol, whereas in the Gram-negative bacteria which present a thin peptidoglycan layer, the crystal violet is readily eluted. Bacteria can then be distinguished based on their morphology and staining properties, and in particular, Gram-negative bacteria stain red and Gram-positive bacteria stain blue-purple (Figure 4).

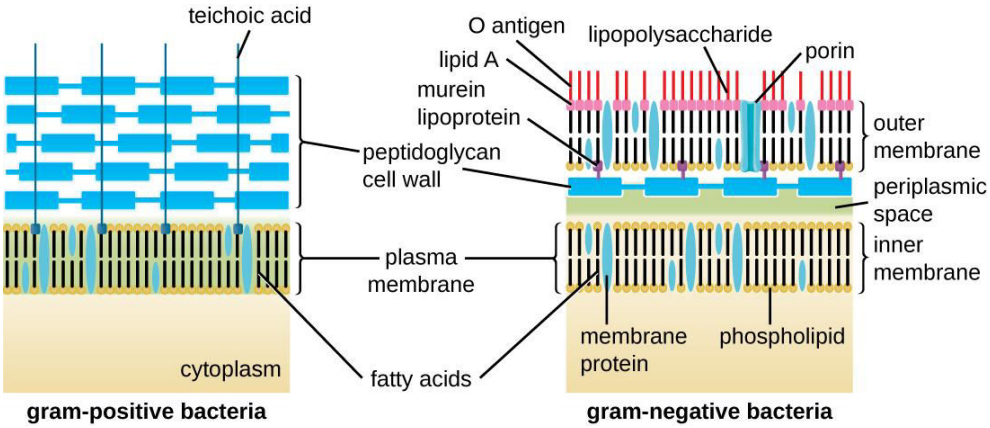

Figure 3. Scheme of the bacterial envelope composition of Gram-positive bacteria (left) and Gram-negative bacteria (right) [10].

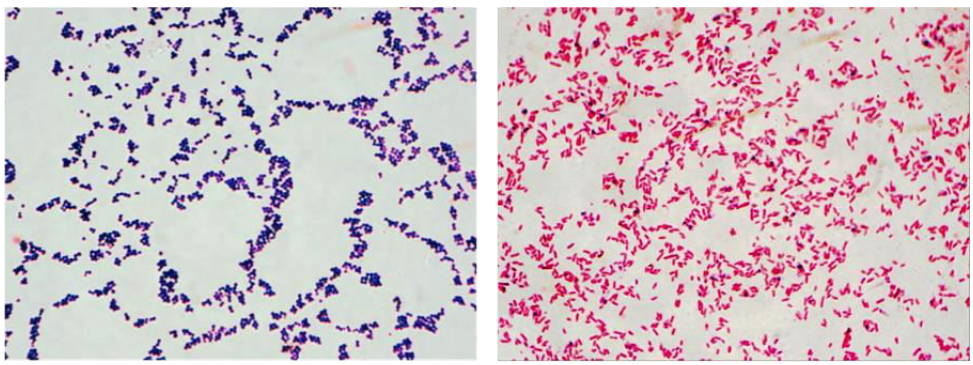

Figure 4. Gram staining of *Staphylococcus sp.* (Gram-positive, blue-purple, on the left) and *Escherichia coli* (Gram-negative, red, on the right) [8].

Bacterial membranes are composed by 40% of phospholipids and 60% of proteins. In the membrane of Gram-positive bacteria and in the inner membrane of Gram-negative bacteria, phospholipids are arranged evenly on either leaflet, whereas in the OM of Gram-negative bacteria phospholipids are asymmetrically distributed, with the majority of them located at the inner leaflet of the membrane. The outer leaflet of the OM of Gram-negative bacteria is mainly constituted by a glycolipid termed lipopolysaccharide (LPS), beside some phospholipids and proteins (Figure 3) like protein channels (*i.e.* porins) that allow the passage of small molecules across the OM, and other proteins that function as specific transporters in an energy-dependent manner. The periplasm has important functions, acting as a buffer between the external environment and the interior, and it is essential for the survival and operation of the bacterium [8,11,12].

1.2.2 The lipopolysaccharide (LPS)

LPS can cover up to 75% of the bacterium's cell surface and is present in almost all Gram-negative bacteria. LPS can act as a strong stimulator of immunity in diverse eukaryotic species ranging from insects to humans. LPS is typically organized into three structural domains (Figure 5): the O-polysaccharide chain, the core oligosaccharide, and the lipid A which is responsible for

the endotoxic activity of the entire molecule. LPS can present chemical arrangements that influence the ability to elude the host immune defenses [13,14].

1.2.3 LPS-mediated activation of the immune system

LPS is a potent elicitor of the immune system. It is a marker for the detection of bacterial pathogen invasion, responsible to initiate host immunological response leading to inflammation and in extreme cases septic shock [13]. Extracellular LPS is recognized by toll-like receptor 4 (TLR4) and this way represents the “canonical inflammasome” [15]. On the other hand, cysteine-aspartic protease (caspase)-11 in mouse and the human orthologues caspase-4/caspase-5 were recently identified as components of the “non-canonical inflammasome” that senses intracellular LPS during macrophage-mediated inflammatory responses [16].

The work of this thesis will be focused on the “canonical inflammasome” mediated by TLR4 signaling.

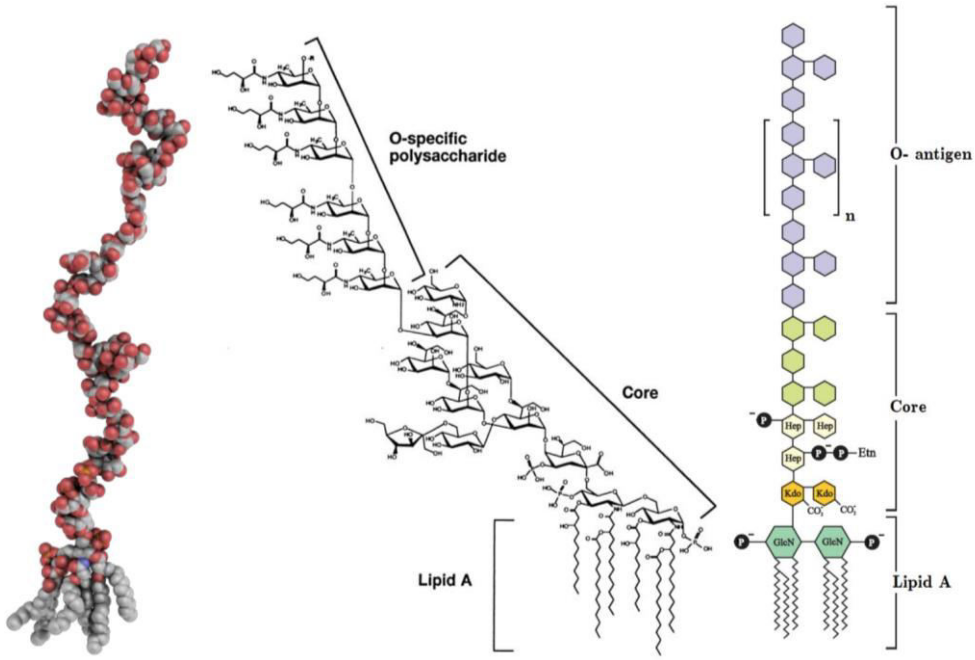

Figure 5. General Structure of bacterial LPS. The O-specific antigen is variable among species. Lipid A is a conserved structure, although some modifications of its structure have been reported. A pictorial sphere model of LPS is also shown [8].

1.3 Toll Like Receptors (TLRs)

TLRs belong to the class of pattern recognition receptors and they play a key role in the innate immune system.

TLRs are transmembrane, non-catalytic receptors, composed of an ectodomain (presenting a horseshoe-like structure) with leucine-rich repeats that mediates ligand recognition, a transmembrane domain, and a cytoplasmic Toll/IL-1 receptor (TIR) domain which is responsible for the intracellular downstream signaling.

TLRs are localized either on the cell surface or into intracellular compartments (endoplasmic reticulum, endosome, lysosome) and normally are expressed in B cells, macrophages, dendritic cells and specific types of T cells. TLRs recognise structurally conserved microbial molecules (lipid, lipoprotein, protein, and nucleic acid), which are denominated pathogen-associated molecular patterns (PAMPs), and that are broadly shared by pathogens and distinguishable from host molecules.

TLRs can recognise their respective PAMPs in two different way: homodimeric or heterodimeric, and they can present co-receptors or accessory molecules [17]. Once a pathogen has breached physical barriers such as the skin or intestinal tract mucosa, their conserved microbial molecules (PAMPs) are recognized by TLRs which activate immune cell responses [18].

TLRs name comes from their similarity to the protein coded by the *toll* gene identified in *Drosophila* in 1985 by Christiane Nüsslein-Volhard. Christiane was surprised and she shouted out in German, “Das ist ja toll!” which translates as “That's great!”.

1.3.1 TLRs diversity

To date, the TLRs family comprises 10 members in humans (TLR1 to TLR10) and 12 in mice (TLR1 to TLR9 and TLR11 to TLR13). TLRs can be divided based on their localization when sensing their respective ligands (Figure 6). Cell surface TLRs (1, 2, 4, 5, 6, 10) respond to microbial membrane materials, whereas intracellular TLRs (3, 7, 8, 9) recognize bacteria- and virus-derived nucleic acids [19]. In particular, TLR2 — sometimes in combination with other TLRs — senses lipoproteins and lipoteichoic acid; TLR5 recognizes flagellin of flagellated bacteria. TLR3, TLR7 and TLR8 are mostly responsible for detecting viral RNA, whereas TLR9 recognizes low-methylated DNA that contains CpG motifs, which are characteristic of bacterial DNA. TLR4 senses LPS [19], but can also bind endogenous molecules produced as a result of tissue injury, denominated danger-associated molecular patterns (DAMPs). Hence, TLR4 is a key receptor that plays a critical role in both infectious and noninfectious stimuli. TLR4-mediated

inflammation triggered by PAMPs and DAMPs is clearly involved in several acute and chronic diseases, making TLR4 a molecular target aiming to treat a broad spectrum of modern day disorders lacking pharmacological treatment [20-22].

In the next subchapter the last advancements on TLR4 modulation will be presented in a detailed manner.

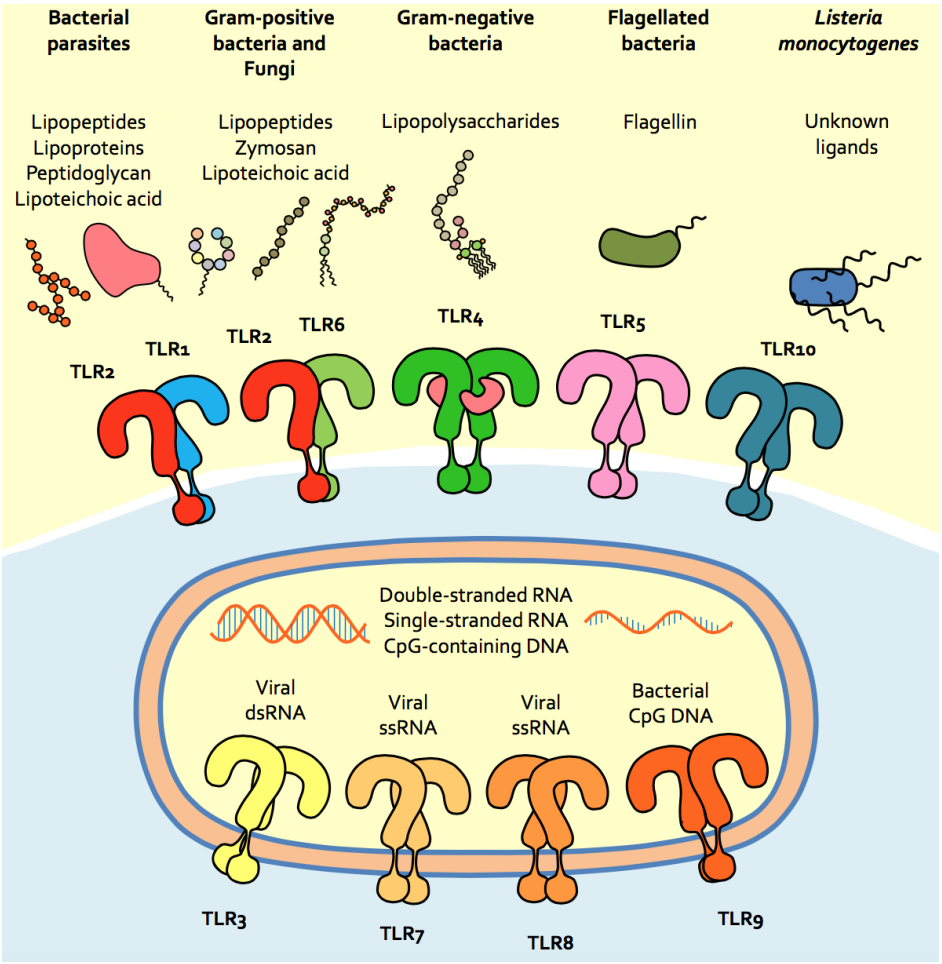

Figure 6. Toll like receptors (TLRs) in humans, their compartmentalization and their respective ligands [8].

1.3.2 Toll Like Receptor 4

This subchapter is based on a review paper published by *Future Medicinal Chemistry* on date 30 January 2018 (DOI: 10.4155/ fmc-2017-0172).

Recent advances on Toll-like receptor 4 modulation: new therapeutic perspectives

Lenny Zaffaroni[1] & Francesco Peri[1]

[1]Department of Biotechnology & Biosciences, University of Milano-Bicocca; Piazza della Scienza, 2; 20126 Milano, Italy

Abstract

Activation or inhibition of TLR4 by small molecules will provide in next few years a new generation of therapeutics. TLR4 stimulation (agonism) by high-affinity ligands mimicking lipid A gave vaccine adjuvants with improved specificity and efficacy that have been licensed and entered into the market. TLR4 inhibition (antagonism) prevents cytokine production at a very early stage, this is in principle a more efficient method to block inflammatory and autoimmune diseases compared to cytokine neutralization by antibodies. Advances in TLR4 modulation by drug-like small molecules achieved in the last years are reviewed.

Recently discovered TLR4 agonists and antagonists of natural and synthetic origin are presented, and their mechanism of action and structure-activity relationship are discussed.

Introduction

TLR4-associated pathologies and possible therapies

TLRs belong to the class of pattern recognition receptors (PRRs) and are the first line of defense from invading pathogens in humans and higher animals. TLRs recognize PAMPs, thus activating inflammation and innate immunity response [23]. Among TLRs, TLR4 is the specific sensor of LPS, one of the molecular components of Gram-negative outer membrane, and its truncated versions lipooligosaccharide (LOS) and lipid A, collectively termed as endotoxin [24,25]. TLR4 also recognizes endogenous molecules, called DAMPs, released by injured tissues and necrotic cells [26]. TLR4-mediated inflammation, triggered by PAMPs and DAMPs, is involved in several acute and chronic diseases. Hence, TLR4 is a key receptor on which both non-infectious and infectious stimuli converge to trigger a proinflammatory response. TLR4 can then have an inflammatory or repair role. Inflammation, in general, has a protective function, and TLR4 can play an important role in this context; in particular by activating the induction of specific resolution pathways that

restore tissue integrity and function [27]. However, when the TLR4 inflammatory response is not regulated, it can be harmful for the organism. In several diseases with microbial (Gram-negative infections) or non-microbial etiology (ischemia/ reperfusion injury, sterile and chronic inflammations, autoimmune diseases, neuroinflammations), TLR4 activation and signaling contribute to disease progression [28]. The most severe disease deriving from TLR4 excessive activation by PAMPs is sepsis. Sepsis is a dysregulated response of the host organism to outer pathogens, which leads to acute life-threatening organ dysfunction [29]. The global incidence of this syndrome accounts for 437 per 100,000 person-years between the years 1995 and 2015, according to the retrospective analysis of an international database [30]. In western countries, mortality in patients with severe sepsis is 20-50%, and if there is no organ dysfunction it can be diminished (less than 20%). Septic shock with increased LPS levels in blood, overexpression of pro-inflammatory cytokines, activation of blood coagulation system and accumulation of fibrinogen degradation products leads to a violation of local and general hemodynamics and endothelial dysfunction via TLR4 signaling pathway. Sepsis is one of the possible complications of severe influenza. The most typical bacterial species complicating diseases are *Streptococcus pneumoniae*, *Pseudomonas aeruginosa*, *Acinetobacter* species,

Staphylococcus aureus as well as *Enterobacteriaceae* species, *Aspergillus* species and others [31-33]. Sepsis is the most important example of pathology caused by TLR4 excessive and dysregulated activation mediated by LPS, that could be efficiently blocked by using TLR4 antagonists such as Eritoran [34]. However, despite its efficacy in contrasting acute sepsis in animal models, Eritoran failed to pass clinical Phase III trials on septic patients [35]. Other pathologies are associated to DAMP/TLR4 signaling, for instance TLR4 plays a key role in the central nervous system (CNS) neurodegeneration [36]. In CNS, TLRs activation can be either detrimental (neuroinflammations and neurodegeneration) or benefical (tissue repair), or have a mixed, still not fully understood, effect [37]. In the context of DAMP-associated pathologies, the inhibition of TLR4 stimulation by endogenous factors could be used to contrast a wide range of inflammatory and autoimmune disorders. These pathologies are caused by the release of reactive nitrogen or oxygen species (RNS/ROS) and inflammatory cytokines following “sterile inflammations” induced by DAMPs. In this context, TLR4 is a molecular target related to a broad spectrum of modern day disorders including asthma [20], allergies [21], chronic inflammations, autoimmune disorders, CNS diseases linked to neuroinflammation, and cancer [22].

TLR4 has also been suggested as a promising therapeutic target for drug abuse [38], major depressive disorder [39], and amyotrophic lateral sclerosis (ALS) [40]. Possible application of synthetic TLR4 antagonists in the treatment of neuropathic pain has also been shown [41,42]. From a molecular point of view, TLR4 activation by LPS is based on the successive interaction of LPS with lipid-binding protein (LBP) [43] that transfer a single molecule of LPS from aggregates in solution to cluster of differentiation 14 (CD14) [44], that in turns shuttles LPS to the TLR4/myeloid differentiation factor 2 (MD-2) [45] complex. The whole molecular process ends with the formation of the $(LPS/MD\text{-}2/TLR4)_2$ complex on plasma membrane [15]. The complex transmits the signal in the cell by recruiting the myeloid differentiation primary response gene 88 (MyD88) and the adapter myelin and lymphocyte protein (MAL). The MyD88-dependent pathway involves the early phase of nuclear factor-κβ (NF-κβ) activation, which leads to the production of inflammatory cytokines such as IL-1α/β, IL-18, IL-6, and TNFα. On the other hand the TIR-domain-containing adapter-inducing interferon-β (TRIF) (MyD88-independent pathway) activates interferon (IFN)-regulatory factor (IRF3) and involves the late phase of NF-κβ activation, both of which lead to the production of IFN-β and the expression of IFN-inducible genes [1-3] (Figure 7). In contrast, truncated LPS lacking the O-chain (LOS) can

directly interact with the TLR4/MD-2 complex and activate TLR4 signaling without the participation of LBP and CD14 co-receptors [14,46]. Molecules active as TLR4 antagonists, as Eritoran or TAK-242, have failed to block acute sepsis [35,47]. However, a new perspective is holding promise in using TLR4 antagonists to block TLR4 activation by endogenous factors (DAMPs) in chronic inflammatory diseases and sterile inflammations. DAMPs are released from inflamed and damaged tissues [48]. Unequivocal evidence that DAMPs are specific TLR4 agonists remains to be provided in some cases, because in biochemical experiments aimed at identifying endogenous TLR4 agonists, the activation of TLR4 pathway could actually derive from endotoxin contamination in DAMPs. While the molecular mechanisms of endotoxin (LPS, LOS) TLR4 activation are well understood [22], the mechanisms of DAMP/TLR4 signaling are only partially known. The high chemical diversity of recently discovered endogenous TLR4 ligands seem to be incompatible with the molecular specificity of TLR4 receptor. A recent critical paper on this subject recommended that some requirements are respected when assessing TLR4 agonism [32]. The most important condition is that the putative agonist should engage both TLR4 and MD-2 receptors for signaling and directly interacts with MD-2 and/or CD14 receptors [49].

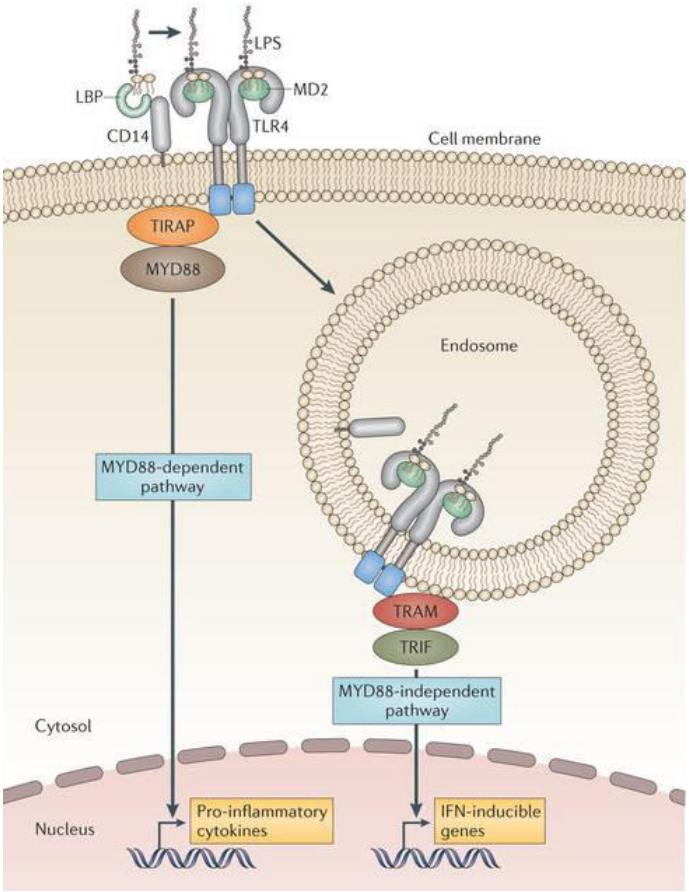

Figure 7. Scheme that illustrate a simplified TLR4/MD-2 signaling of the two responses — the myeloid differentiation primary response protein 88 (MYD88)-dependent and the TIR domain-containing adaptor inducing IFNβ (TRIF) (or MYD88-independent) pathways — that can be differentially stimulated on binding of endotoxin to the TLR4/MD-2 complex. The MYD88-dependent pathway leads to the production of pro-inflammatory cytokines, whereas the less inflammatory TRIF pathway occurs after endocytosis of the TLR4/MD-2 receptor and stimulates the expression of interferon (IFN)-inducible genes that are important for adjuvanticity but are less inflammatory than those cytokines induced by the MYD88-dependent pathway [50].

As a follow-up of our previous reviews on this topic [22], we present here last achievements on the discovery of natural and synthetic molecules that modulate TLR4 activity as agonists or antagonists. We focus on small molecules (MW less than 1 KDa) that have been validated as TLR4 ligands according to the rules above mentioned, and on their mechanism of action.

In the first part new synthetic TLR4 modulators are reported, in the second part are reported compounds of natural origin.

Synthetic TLR4 modulators

From lipid A mimetics to other compounds

The rational design of lipid A variants and analogues gave several TLR4 agonists and antagonists with glycolipid structures that have been reviewed by us [22] and others [51,52]. All these structures include the chemical determinant (pharmacophore) essential for MD-2 recognition and binding: a disaccharide core (GlcNAc-GlcNAc) with six lipid chains, and two negatively charged phosphates or phosphates bioisoster groups, at positions C1 and C4' of the disaccharide. These are Eritoran [53], monophosphoryl lipid A (MPL) [54], and aminoglycosides [55] lipid A mimetics. Other lipid A mimetics are based on a monosaccharide scaffold derived from lipid X, a biosynthetic precursor of lipid A, with activity as TLR4 antagonist [56]. All these compounds are sparingly soluble and have poor

pharmacokinetic *in vivo*. The new tendency is therefore to explore new chemical structures, often derived from natural compounds, to obtain new TLR4 ligands with improved solubility and pharmacokinetic. We report here on TLR4 ligands and modulators recently discovered. Generally, the chemical structures of these molecules are different from that of lipid A. Very often these compounds are structurally derived from natural compounds that have been found active on TLR4 or are the results of a random screening of libraries of compounds.

Glycolipid-based compounds

Fatty acid esters of monogalactosyl-diacylglycerol

Fatty acid esters of monogalactosyl-diacylglycerol (MGDG) are essential components of the thylakoid membrane in chloroplasts and di-linolenoyl MGDG has been reported to show anti-inflammatory effects in human peripheral blood neutrophils [57].

In order to understand the mechanism of action of these molecules, a derivative of di-linolenoyl MGDG, a bi-functional, MGDG-based probe (molecule **1**, Figure 8) has been synthesized.

1 contains two chemical functions, one reactive towards nucleophile groups target protein, another, the alkyne function, forms triazole adducts by reacting with azide groups (click reaction). **1** inhibited LPS-mediated TLR4 activation in a concentration-dependent manner in cells. Consistently with other

studies [58], **1** showed strong inhibition of p38 phosphorylation without influencing the total cell number being a more potent inhibitor than parent MGDG. Endogenous proteome labeling followed by pull-down/LC-MS/MS showed that compound **1** mainly interacts with the TLR4/MD-2 complex. By molecular modeling it has been calculated the lowest-energy binding pose of **1** with the TLR4/MD-2 complex. **1** binds to MD-2 similarly to Eritoran: both fatty acid (FA) chains of **1** insert into the hydrophobic pocket of MD-2, while the sugar part interacts with residues of the MD-2 cavity rim. The binding mode between **1** and TLR4/MD-2 shows that FA chains forms favorable hydrophobic interactions with human TLR4 (hTLR4) residues including F440, F463, L444, K388, Q436, which facilitate the subsequent formation of a covalent bond with hTLR4. Mutational studies showed that two residues of hTLR4, namely F440 and F463, are essential for binding to **1**. Previous functional studies have identified that both F440 and F463 are required for cell activation by LPS. These mutational data reinforce the vision of a mechanism of action of MGDG based on direct competition with LPS for MD-2 (TLR4) binding.

Trimannoside glycolipid conjugates (MGCs)

Tri-mannoside glycolipid conjugates (MGCs) (**2**, Figure 8) are formed by a branched core linked to three mannose units through tri-ethylenglycol linkers and to a saturated or unsaturated C24

lipophilic chain. MGCs selectively blocked TLR4-mediated activation of human monocytes and monocyte-derived dendritic cells (DCs) by LPS [59]. The mechanism of action of MGCs is unique: while these compounds inhibit both MyD-88 and TRIF-mediated intracellular pathways deriving from TLR4 activation and also block NF-κβ activation and nuclear translocation, they do not directly compete with LPS for TLR4 binding. The action of MGCs is therefore not based on a direct competition with LPS for CD14 and/or MD-2 binding as in the case of the majority of other TLR4 antagonists. **2** has a disruptive action on lipid raft-located GPI-anchored proteins, CD1a and CD14, and induce their rapid cell internalization. Thus, the plasma membrane may be a principal target through which the modulatory effects of MGCs are mediated. In the presence of LPS, **2** could prevent CD14 and TLR4 co-localization. These results suggest that the inhibitory action of **2** and other MGCs is mediated by their effect on the cell membrane: they alter lipid raft composition, interfere with the clustering of CD14 and TLR4 in rafts, leading to impaired receptor-complex formation and blocking of signal transduction. Moreover, selective deprivation of CD14 from the cellular membrane, and subsequent impairment of $(TLR4/MD\text{-}2)_2$ complex formation could be a new mechanism for TLR4 antagonism. A similar mechanism of action has been recently

described for monosaccharide **3**, a synthetic TLR4 antagonist [60].

Monosaccharide derivatives

The di-phosphorylated di-acylated monosaccharide FP7 (compound **3**, Figure 8), is a synthetic molecule with potent TLR4 antagonist action both in cells and in animals [60,61]. Monosaccharide **3** inhibits the LPS-stimulated, TLR4-dependent secretion of proinflammatory cytokines (IL-6, IL-8, and MIP-1β) by monocytes and DCs and prevents DCs maturation upon TLR4 activation by LPS [61]. The mechanism of action of **3** is based on the direct competition with LPS for MD-2 binding probably reinforced by direct binding to CD14 co-receptor. ^{1}H NMR experiments demonstrated that after addition of MD-2, the signals of the two FA chains (C14) of **3** is attenuated [60] thus suggesting that lipophilic chains are the main interacting units of **3** with MD-2 hydrophobic pocket. The capacity of **3** to induce CD14 and TLR4/MD-2 complex internalization in murine cells was analyzed [60]. Cell exposure to **3** caused endocytosis of CD14 but not of the TLR4/MD-2 complex. These results suggest that **3** interacts directly with CD14, causing its internalization, and deprivation of CD14 on plasma membrane could explain the antagonist action of **3**. *In vitro* binding data with purified, functional hMD-2 (unpublished data) show that **3** is able to displace LPS from hMD-2, and binds to hMD-2 with an affinity

(K_D) in the low μM range. The TLR4 antagonist Eritoran has been recently used to contrast influence lethality in animal models [62]. The infection of some influenza strains induces a TLR4-dependent cytokine storm similar to septic shock. Abnormal TLR4 stimulation is due to the release of endogenous TLR4 agonists (DAMPs) deriving form damage of lung tissue, such as oxidized phospholipids from infected tissue or circulating High Mobility Group Box 1 (HMGB1) protein. The DAMP/TLR4 signaling related to influenza inflection is inhibited by Eritoran [62]. Similarly to Eritoran, **3** selectively blocked DAMP/TLR4 signaling in animal models, protected mice from PR8 influenza virus-induced lethality and reduced proinflammatory cytokine gene expression in the lungs and acute lung injury (ALI) [61]. In a proof-of-concept experiment, compound **3** inhibited in a dose-dependent manner the DCs activation by endogenous HMGB1 [61]. This suggests that the mechanism of action of **3** in blocking influenza lethality could be based on inhibition of HMGB1/TLR4 signaling. The good bioavailability of **3**, together with its high water solubility, lack of toxicity, and selective TLR4 antagonist action, make it a new hit targeting TLR4-related microbial and sterile inflammatory diseases.

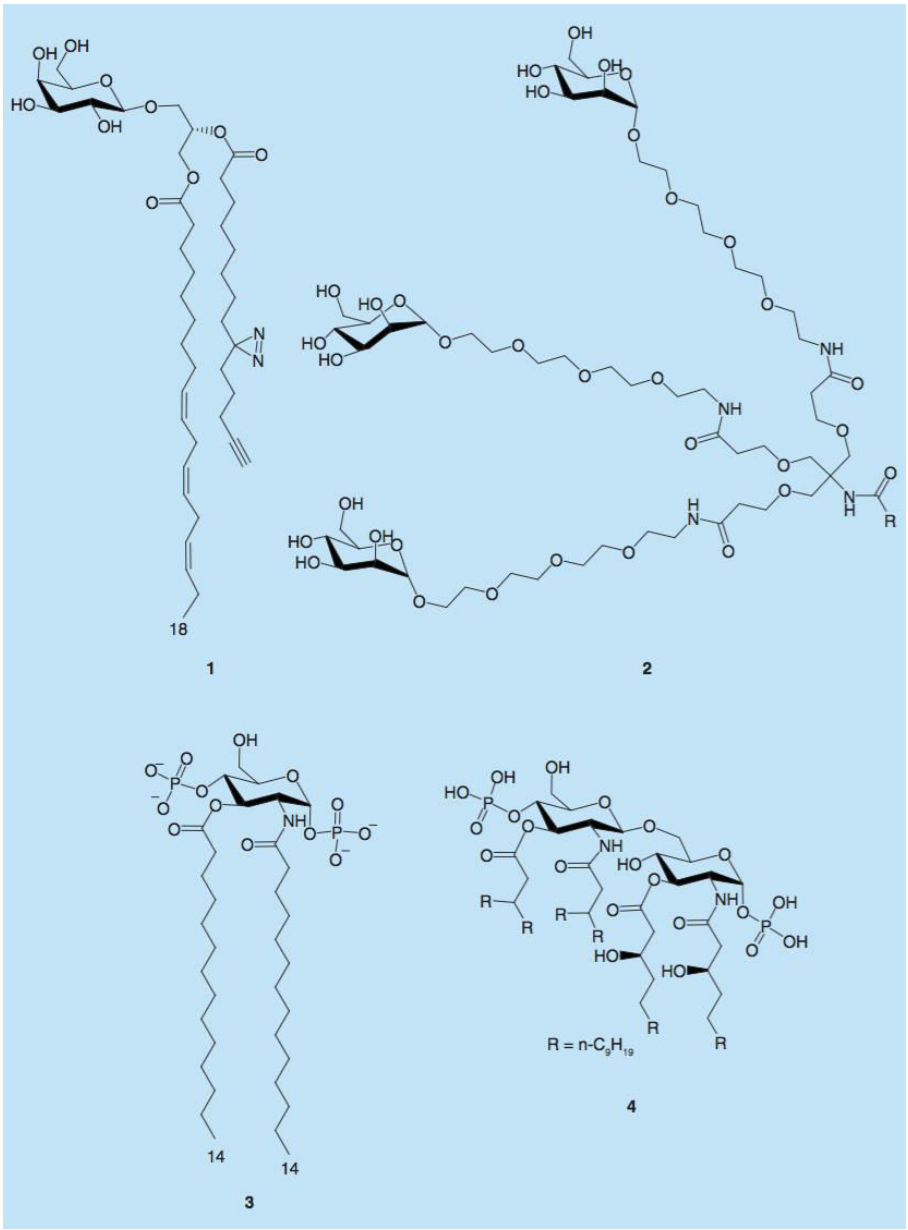

Figure 8. Recently discovered synthetic, glycolipid-based TLR4 modulators: bifunctional MGDG probe (**1**); tri-mannoside glycolipid conjugates (**2**) R= saturated or insaturated C24 lipophilic chain; monosaccharide FP7 (**3**); Vizantin-lipid A conjugate (**4**).

Lipid A mimetic with Vizantin-like branched chains

In a recent study was shown that the trehalose derivative named Vizantin (6,6′-bis-*O*-(3-nonyldodecanoyl)-*α*,*α*′-trehalose) displays adjuvant activity based on TLR4 agonism and binding to the TLR4/MD-2 complex. Based on the known biological activity of lipid A and Vizantin, the authors projected a novel bifunctional glycolipid, that combines the structural features of Vizantin (namely, the two branched FA chains 3-nonyldodecanoic acid, 3NDDA) with the glucosamine core of lipid A (compound **4,** Figure 8) [63]. Disaccharide **4** potently antagonizes the LPS/TLR4 signaling pathway in a concentration-dependent manner, in human THP-1 cells, with an IC_{50} of 3.8 nM. Molecular docking simulations with MD-2 and MD-2/TLR4 suggest that the two branched NDDA chains of compound **4** insert into MD-2 binding cavity thus stabilizing by hydrophobic interaction the complex with the receptor.

Non-glycolipid TLR4 modulators

Neoseptins

After a screening of 90,000 compounds tested for their ability to activate TNF-α in mouse peritoneal macrophages, a new TLR4 agonist, Neoseptin-1, has been identified. Structure-activity relationship (SAR) studies allowed to improve the design of these LPS-binding peptide mimetics, leading to Neoseptin-3 hit

compound (**5**, Figure 9) [64]. **5** is a peptidomimetic with no structural similarity to LPS that activates mouse TLR4 (mTLR4)/MD-2. *In vitro* dose–response experiments demonstrated that molecule **5** activates TLR4 in different mouse cells. Induction of TNF-α by **5** was completely abrogated in TLR4- or MD-2-deficient mouse macrophages, while CD14-deficient macrophages that do not respond to LPS, still produced TNF-α in response to **5**.

5 activates mTLR4/MD-2 independently of CD14 and triggers canonical MyD88 and TRIF-dependent signaling. On the other hand, **5** is unable to stimulate human TLR4, as turned out from experiments on human THP-1 monocytes. This supported the idea that the TLR4 agonist activity of **5** is species-specific, whit a preference towards mouse MD-2 (mMD-2). The direct interaction of **5** with mTLR4/MD-2 heterodimer with formation of a complex was observed by NMR binding experiments and, more directly, by X-ray analysis of the complex. The crystal structures of mTLR4/MD-2 complex in the "apo" form (*i.e.* without any ligand), in complex with lipid A, and with **5** were compared. In all the three different cases studied, the structure of the mTLR4/MD-2 complexes presented similar conformations. While having completely different chemical structures, lipid A and **5** are capable of inducing similar conformational changes of the MD-2 Phe126 loop region, the typical conformational switch induced by

agonists. Interestingly, two molecules of **5** were found asymmetrically bound to MD-2 cavity in the complex with mTLR4/MD-2. The two molecules occupy different sites at the rim of MD-2 binding cavity and interact with the second TLR4 molecule (TLR4*) thus promoting TLR4 dimerization and activation. The final activated complex (TLR4/MD-2/$\mathbf{5}_2$)$_2$ contains four molecules of **5**. This study provides new and interesting information on how a molecule different from lipid A can promote the formation of the activated TLR4/MD-2 heterodimer by binding MD-2 and TLR4*. The dissociation between CD14 function and MyD88/TRIF signaling pathways is reminiscent of the mechanism of action of other small-molecular TLR4 agonists, including Ugi compounds presented in the next paragraph. However, the lack of activity on human TLR4 receptor system limits the clinical development of Neoseptins as TLR4-directed therapeutics.

Ugi compounds

A panel of small molecules with TLR4 agonist activity was synthesized through a 4-component Ugi condensation reaction (the more potent molecule being AZ617, compound **6** in Figure 9) [65]. The majority of the synthetic Ugi compounds presented TLR4 agonist in HEK-293 cells transfected with hTLR4/hMD-2/hCD14 while were almost inactive in stimulating HEK cells transfected with mTLR4/mMD-2/mCD14. Species-specific TLR4

activation is due to higher affinity binding of Ugi compounds to hMD-2 than to mMD-2. By comparing the activity of Ugi compounds in HEK "hybrid" transfectants with a combination of human and mouse receptors, namely hTLR4/mMD-2 and mTLR4/hMD-2, authors observed that Ugi compounds turned out to be more active in the transfectants containing hMD-2. The capacity of Ugi compounds to stimulate human TLR4 receptor system was also confirmed on human peripheral blood mononuclear cells (PBMCs). The preference of human TLR4 receptor system over murine is however peculiar, because LPS and MPL, show an opposite preference for murine receptors giving a stronger activation in cells expressing mMD-2. Another important difference with LPS and lipid A-derived agonists, is that the TLR4 activation mediated by **6** is CD14-independent. *In silico* studies showed two possible sets of binding poses (with almost identical energy) of Ugi compounds into the hydrophobic pocket of MD-2. As Ugi compounds have a TLR4 agonist preference towards human species, and a better water solubility compared to other lipid A analogs, making them a good starting point for the development of adjuvants that can activate TLR4 in cells with physiological low levels of CD14, such as DCs.

Phospholipids

Lung alveolar epithelium secretes a mixture of proteins and lipids called pulmonary surfactants, which have important immunoregulatory properties, able to regulate the innate immune system by competitively antagonizing activation of TLR4 [66]. Phospholipids account for 90% of pulmonary surfactants (PS), and it has been reported that a small part of PS, palmitoyl-oleoyl-phosphatidylglycerol (POPG) and phosphatidylinositol (PI), are capable to inhibit LPS-induced inflammatory responses in U937 cells, primary rat alveolar macrophages, and primary human alveolar macrophages by blocking LPS-induced phosphorylation of MAPKs and Iκβα, and by preventing LPS-induced degradation of Iκβ and MKP-1 expression [66]. *In vitro* binding studies showed that POPG and PI bind to LBP, CD14 and MD-2 in a concentration-dependent manner. A recent study screened a library of POPG variants, with the aim to understand the phospholipids structural features that dictate the antagonistic activity against toll-like receptor 2 (TLR2) and TLR4 [67]. In summary, POPG analogs with polar head-group modifications, can antagonize TLR2 and TLR4 activation. POPG analogs strongly bind to CD14 and MD-2 proteins, thus causing TLR4 inhibition. The structural plasticity necessary for TLRs modulation open up possibilities for the design of new POPG-like molecules that can possess individual TLRs specificity.

Chalcone derivatives

Several chalcone derivatives that contain the moiety of (E)-4-phenylbut-3-en-2-one, considered the core structure of currently known MD-2 inhibitors of natural origin such as curcumin, caffeic acid phenethyl ester, and 1-dehydro-10-gingerdione, have been designed and synthesized in a recent study [68]. Amongst all the synthesized chalcone compounds, compound **7** (Figure 9) turned out to be the more potent in antagonizing the TLR4 pathway both *in vitro* and *in vivo*. Fluorescence spectroscopy experiments showed that **7** competitively inhibits the interactions between MD-2 and LPS and also between TLR4 and MD-2. The direct interaction between **7** and MD-2 was confirmed by surface plasmon resonance (SPR) experiments. Computational studies shown that in the lower energy binding pose, **7** would interact with MD-2 residues Arg90 and Tyr102, by forming two hydrogen bonds. This finding was experimentally confirmed by using MD-2 mutants [69]. **7** is also able to attenuate LPS-induced lung injuries, in particular by diminishing pulmonary inflammation and by preventing the interaction between MD-2 and TLR4 in lung tissue. Similarly to other TLR4 antagonists as Eritoran and **3**, chalcone derivative **7** can be considered a hit compound for the development of drugs for the treatment of ALI and other TLR4-dependent syndromes induced by pathogens infections.

Calcineurin inhibitors (CNIs)

CNIs cyclosporine A and tacrolimus are active in increasing the production of proinflammatory cytokines and endothelial activation markers through TLR4 activation in cultured murine endothelial and vascular smooth muscle cells, and in *ex vivo* cultures of murine aortas [70]. Data showed that CNIs were unable to induce inflammation in aortas from *Tlr4*$^{-/-}$ mice and after pharmacological inhibition of TLR4 in endothelial cells. However, further research is required to clarify the exact mechanisms of action by which CNIs are able to activate TLR4.

4,4′-Diisothiocyanostilbene-2,2′-disulfonic acid

The anti-inflammatory effects of 4,4′-Diisothiocyanostilbene-2,2′-disulfonic acid (compound **8**, Figure 9), a chloride channel blocker, were investigated in a recent study [71]. **8** significantly inhibits LPS-induced release of pro-inflammatory cytokines *in vitro* and *in vivo* studies, down-regulating the inflammatory cytokines via inhibition of the TLR4/NF-κβ pathway, with a clear indication that ClC-3 (a volume-activated chloride channel protein) is involved in the inhibitory effect of **8**. This study showed that abrogating ClC-3 inhibits the LPS-induced inflammatory response by inhibiting the TLR4/NF-κβ pathway *in vivo* and *in vitro*, and this mechanism could represent a novel way for TLR4/NF-κβ inhibition based on chloride channels.

Morphine derivatives

Compounds based on simplified morphine analogues (+)-naltrexone and (+)-noroxymorphone have been designed, synthesized and their TLR4 antagonist activities have been evaluated by their effects on inhibiting LPS induced TLR4 downstream nitric oxide production in microglia BV-2 cells [72]. Amongst all the compounds synthetized, the *N*-phenethyl-noroxymorphone (compound **9**, Figure 10) was the most potent TLR4 antagonist with an IC_{50} of 1.4 μM, and no cell cytotoxicity. This analog also showed *in vivo* efficacy in potentiating morphine analgesia, but further research is required to investigate its exact mechanism of TLR4 inhibition.

TLR4 modulators of natural origin

Plant secondary metabolism provides a vast source of chemically different bioactive and pharmacologically active compounds. Traditional Chinese and Indian medicine use a variety of herbs that are rich in molecules that very likely act as TLR4 modulators [73]. TLR4 activation or inhibition mediated by herbal extracts promoted a vast area of research which focuses on the molecular mechanism of action of these TLR4 modulators [74].

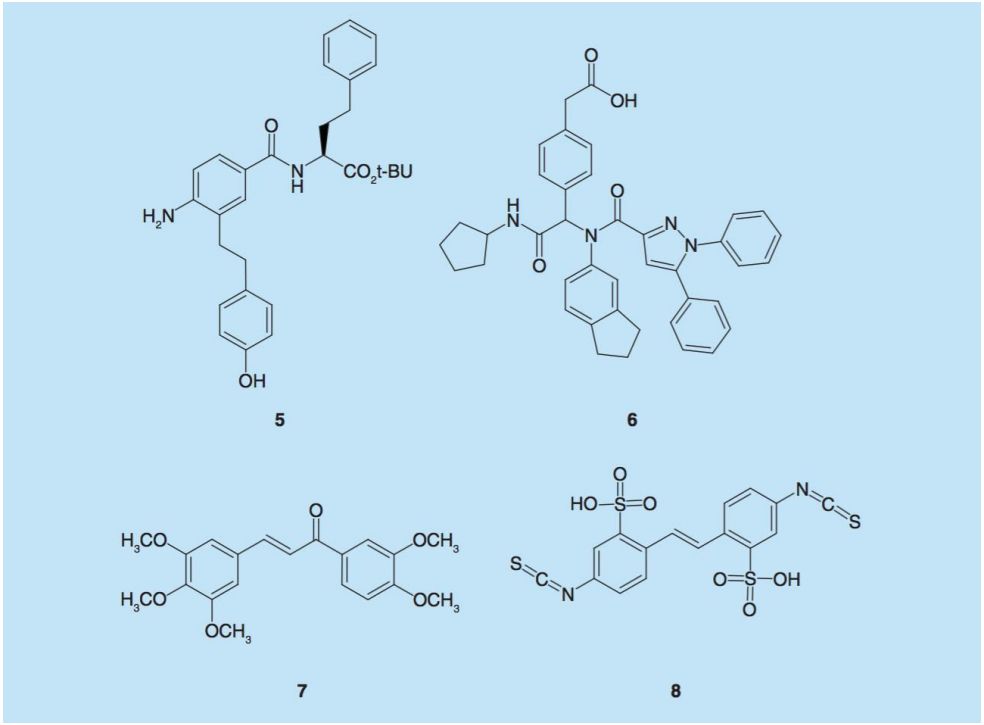

Figure 9. Non-glycolipid synthetic TLR4 modulators: Neoseptin-3 (**5**); compound AZ617 (**6**); chalcone compound 20 (**7**); 4,4′-Diisothiocyanostilbene-2,2′-disulfonic acid (**8**).

Saturated fatty acids (palmitic acid, PA)

The molecular mechanism explaining the inflammatory action of palmitic acid (PA, compound **10**, Figure 10) (the most abundant circulating saturated fatty acids, SFAs), has recently been proposed [75]. It has been observed that **10** induces myocardial inflammatory injury and dysfunction through MD-2 in mouse and cell culture experimental models. The paper presented studies of purified protein-ligand interactions indicating that **10** directly

binds to MD-2, supporting a mechanism of canonical, MD-2-dependent, TLR4 activation and signaling. However, the MD-2 binding affinity of **10** measured by SPR turned out to be very low (μM range). **10** is responsible for the production of pro-inflammatory cytokines in myocardial tissue, causing cardiac tissue remodeling and cardiac dysfunction in mice with hyper-lipidemia and/or obesity. In addition, murine cardiomyocytes and macrophages acquired an MD-2-dependent pro-inflammatory phenotype when challenged with **10**. The computational docking simulation results also supported the hypothesis of direct MD-2/**10** binding and predicted that three molecules of **10** can accommodate into the MD-2 binding cavity. The resulting MD-2/$\mathbf{10}_3$ complex appeared to be relatively stable, with appropriate positioning of the fatty acids. Interestingly, the findings from this study supported the idea that the ability of **10** (or other SFAs) to activate TLR4 signaling was likely attributed to its saturated nature. The change to unsaturated fatty acids on the lipid A moiety of LPS results in a complete loss of TLR4 agonist activity, and the unsaturated FA chain plays an important role in MD-2 binding of the antagonist Eritoran [76]. The authors found that, despite the binding to MD-2, unsaturated FAs did not induce TLR4/MD-2 complex formation nor activate downstream TLR4 signaling. Unsaturated FA were unable to induce cardiac inflammatory phenotype both *in vitro* and *in vivo* and did not

significantly contributed to myocardial remodeling and injury in obesity. The observation that unsaturated FAs bound MD-2 suggests an intriguing possibility that unsaturated FAs may competitively inhibit SFAs to modulate TLR4 signaling response and chronic inflammation. These results underscore MD-2 as a necessary protein in SFA-mediated myocardial inflammatory injury.

Morphine and opioids

The molecular mechanism of TLR4 stimulation by morphine and opioids has been investigated, and presents several common points with LPS activation [77]. In a recent paper the structural dynamics of the opioid-bound activation mechanism of TLR4/MD-2 complex has been studied using various computational tools [78]. The *in silico* results supported previous findings: the binding of morphine (**11**) and naloxone (**12**) (Figure 10) into the hydrophobic pocket of MD-2 is TLR4-dependent. Binding of **11** induce the typical conformational change of MD-2 into its active form (agonist switch). In particular this is mediated by interaction of **11** with the Phe126 loop of MD-2, that confers stability to the subsequently formed TLR4/MD-2/**11** complex. The interaction with TLR4 stabilizes also the MD-2/**12** complex. However, **12** switches the Phe126 loop of MD-2 to its inactive (antagonist) conformation form. These data confirmed that subtle changes on the morphine structure can induce agonism to

antagonism switch and that morphine scaffold could be used to generate potent TLR4 modulators.

Platycodin D

Platycodin D (**13**, Figure 10), the major triterpene saponin in the root of *Platycodon grandiflorum*, exhibits a broad spectrum of anti-inflammatory effects by inhibiting LPS-induced TNF-α and IL-1β production [79] and NF-κβ activation [80]. The mechanism of action of **13** in protecting LPS-induced ALI has been recently studied and clarified [81]. In *in vitro* and *in vivo* models, **13** acts as a TLR4 antagonist by mediating the depletion of cholesterol from plasma membrane and therefore by reducing the translocation of TLR4 to lipid rafts. This mechanism was confirmed by the fact that cholesterol replenishment prevented **13**-mediated TLR4 antagonism. Studies on raft-disrupting drugs supported this data, confirming that depletion of cholesterol can antagonize LPS-mediated TLR4 activation by the inhibition of TLR4 translocation into lipid rafts [82]. It has been reported that also ethanol acts by altering the LPS-induced redistribution of TLR4 complex within the lipid raft, thus interfering with receptor clustering, and subsequent signaling [83].

P4-ATPases

Phospholipids translocation from exoplasmic to cytoplasmic leaflet is mediated by integral membrane proteins, named P4-ATPases, which have a crucial function in the biogenesis of transport vesicles and in endocytic pathways [84,85]. The hypothesis that P4-ATPases (in particular CDC50A) can play a role in the TLR4 activation pathway has been investigated [86]. In this study, the LPS-mediated TLR4 activation has been analyzed by using CDC50A-depleted THP-1 and human monocyte-derived macrophages. LPS challenge of CDC50A-depleted THP-1 is responsible for a hyper-activation of the MyD88-dependent pathway, caused by the impaired endocytic TLR4 retrieval. There are two P4-ATPases (*i.e.* ATP8B1 and ATP11A) that are expressed in humans, and their deficiency is associated with severe chronic liver disease [87] and pulmonary disorders [88]. The exact contribution of P4-ATPases in TLR4-dependent inflammatory disease remains to be established.

Naringenin

Naringenin (**14**, Figure 10) is a flavonoid naturally present in grapefruit and other citrus species, that posses anti-inflammatory and antioxidant activities, particularly important for inflammatory-associated atherosclerosis, arthritis and metabolic syndrome [89]. In a recent study, the underlying mechanism of

the anti-inflammatory properties and life-protective efficacy of **14** in LPS-stimulated macrophages and in a murine endotoxaemia model was evaluated [90]. **14** was able to prevent TNF-α and IL-6 upregulation, to inhibit NF-κβ activation, and **14** was also responsible for the upregulatated expression of transcription factor 3 (ATF3) in LPS-stimulated murine macrophages. In lung tissues, the ATF3 expression is upregulated by the induction of 5' adenosine monophosphate-activated protein kinase (AMPK) that is provoke by **14**. In murine models of endotoxaemia **14** improved the pro-inflammatory reactions and the survival of mice. This AMPK-ATF3-dependent down regulation of the LPS/TLR4 signaling pathway mediated by **14** represents a novel mechanism of TLR4 modulation.

Nickel and Cobalt ions (Ni^{++}, Co^{++})

Allergic contact dermatitis (ACD) is a very common skin disease, and amongst all the over 3,000 allergens, nickel is one of the most common ones [91]. Recent findings revealed that hTLR4, but not TLR4 of other species including mouse, can be directly activated by nickel and cobalt ions [92]. This species-specific activation is due to the coordination of nickel or cobalt ions by a cluster of histidine residues on the ectodomain of hTLR4 that is absent in the majority of other species TLR4. This study identified TLR4 and MD-2 mutants not responsive to LPS, that can be activated

by nickel and cobalt ions. Starting form these observations, authors proposed a model for the activation of the TLR4/MD-2 complex mediated by transition metal bivalent cations. To enable TLR4 activation several interactions are required and interactions mediated by the histidine residues of the TLR4 ectodomains can be a driving force for TLR4 dimerization. This is confirmed by a study where a single TLR4 mutation (residue N433, important for the interactions of the two TLR4 ectodomains), prevented the dimerization of TLR4 in the presence of cobalt or nickel ions [93]. Interestingly, nickel and cobalt ions turned out to be able to induce the dimerization of TLR4 ectodomain in the absence of MD-2 *in vitro* in cell-free experiments. However, this effect was not observed *in vitro* in cells.

Lead (Pb^{++})

Lead (Pb) exposure is a worlwide problematic, and it has been shown that Pb exposure can impact the immune system integrity [94]. Pb neurotoxicity has been researched extensively, however, the pro-inflammatory role that this metal plays in the brain has not been fully understood. The inflammatory role of Pb has been recently presented [95], and experiments showed that exposure to Pb induces micro and astrogliosis by activating TLR4/MyD88/NF-κβ signaling pathway. Increased levels of pro-inflammatory cytokines was also observed.

Ferulic acid

Ferulic acid (**15**, Figure 10) is a phenolic compound abundant in vegetables and fruits, and it presents several anti-oxidative and anti-inflammatory activities [96]. **15** pharmacological effects and the underlying mechanisms in mice with acetaminophen-induced hepatotoxicity has been investigated in a recent study [97]. **15** attenuated acetaminophen-induced serum TNF-α and IL-1β production, suppressed TLR4 expression and dampened MAPK and NF-κβ activation. These data suggested that **15** is able to partially suppress TLR4-mediated inflammatory response. However, the molecular mechanism of action of **15** in relation with TLR4 still needs elucidation.

Corilagin

Corilagin (**16**, Figure 10) is a polyphenol isolated from the extract of *Arctostaphylos uvaursi*, it is identified in several plants and it presents anti-inflammatory and antibacterial activity [98]. A recent study found that **16** is able to inhibit both TLR4-dependent MyD88 and TRIF signaling pathways [99]. Cellular and animal models treated with LPS and **16** presented mRNA levels and expression of TLR4, MyD88, TRIF and TRAF6, as well as IL-5 and IL-1β cytokines levels significantly decreased compared to the group treated with LPS alone. The molecular mechanism of action of **16** still needs elucidation.

Alpinetin

Alpinetin (**17**, Figure 10) is a natural flavonoid with known antibacterial, anti-tumor and other therapeutic activities [100]. A recent study investigate the anti-inflammatory effect of **17** in dextran sulfate sodium (DSS)-induced colitis in mice [101]. **17** pre-treatment inhibited significantly the phosphorylation of IKKα/β, Iκβα and p65 NF-κβ activation, and TLR4 expression was down-regualted in LPS-induced PMA-differentiated THP-1 cells. According to this study, **17** has a protective effects on DSS-induced colitis and might be a promising therapeutic treatment. However, further research is required to understand the exact molecular mechanism of action of **17**.

Epigallocatechin-3-gallate

Green tea contains caffeine and polyphenolic compounds known as catechins. The most abundant catechol found in green tea is (−)-epigallocatechin-3-gallate (**18**, Figure 10**)** [102] which has been suggested to be responsible for many of the potential health effects of tea [100]. A recent study showed that **18** negatively regulates TLR4 pathway through the inhibition of downstream signaling [103]. **18** induced ubiquitination of TLR4, decreased TLR4 expression through E3 ubiquitin-protein ligase RNF216, and increased cGMP levels in macrophages. **18**-induced TLR4 downregulation is completely canceled by the soluble guanylate

cyclase (cGMP synthesis enzyme) inhibitor, and cGMP induction is sufficient to suppress TLR4 expression. This is a novel mechanism for the downregulation of TLR4 expression. Study the role of cGMP in the down-regulation of expression of TLR4 could be particularly valuable.

Celastrol

Celastrol (**19**, Figure 10) is a pharmacologically-active cyclic-penta-triterpene, extracted from the roots of the plant *Tripterygium wilfordii*. **19** can act as a potent immunosuppressive and anti-inflammatory agent [104]. A recent study investigated the protective effects of celastrol on TLR4-dependent liver injury in diabetic rats [105]. Diabetic rats presented steatohepatitis and proinflammatory cytokine significantly upregulated. Diabetic rats **19**-treated presented reduced hepatic inflammation and macrophages infiltration. TLR4, MyD88, and NF-κβ expression, as well as downstream inflammatory factors IL-1β and TNF-α in the hepatic tissue of **19**-treated rats were downregulated in a dose-dependent manner. Treatment with **19** delayed the progression of diabetic liver disease via the inhibition of TLR4/MyD88/NF-κβ signaling pathways and its downstream inflammatory effectors. Further studies are required to clarify the molecular mechanisms of action of **19**, and for the development of new treatments for diabetic liver injury.

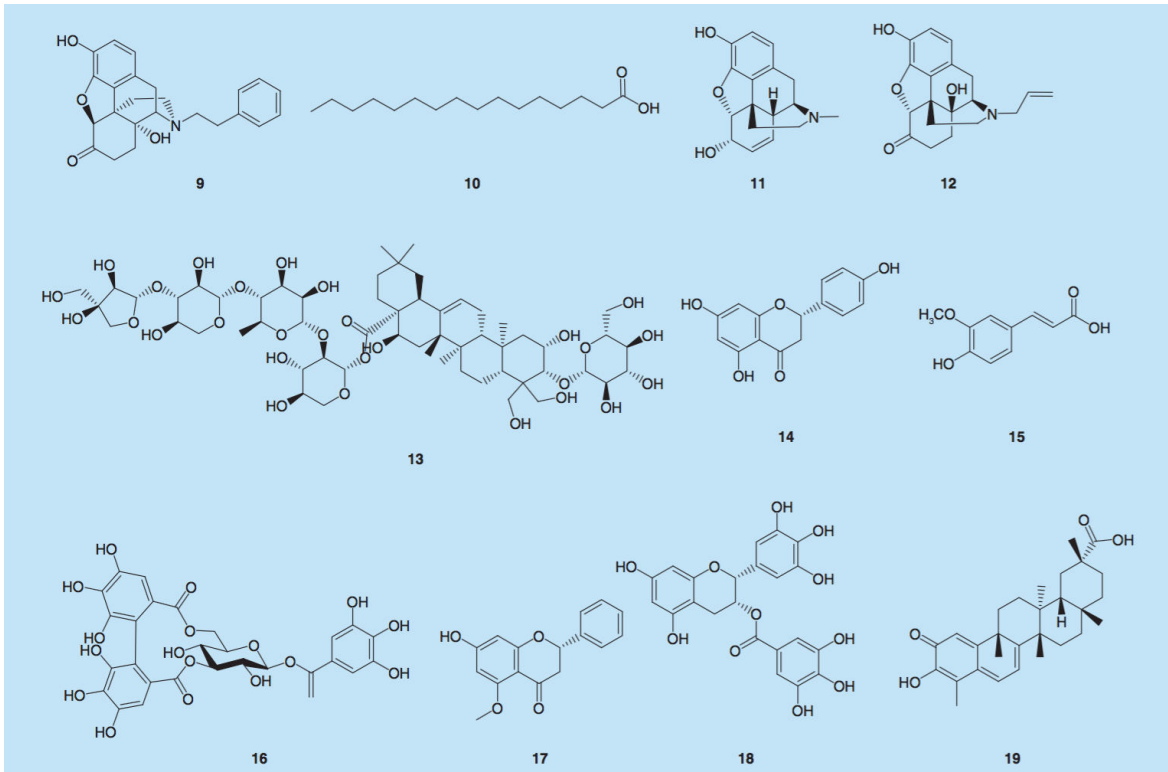

Figure 10. Natural TLR4 modulators: *N*-phenethyl-noroxymorphone (**9**); palmitic acid (**10**); morphine (**11**); naloxone (**12**); platycodin (**13**); naringenin (**14**); ferulic acid (**15**); corilagin (**16**); alpinetin (**17**); epigallocatechin-3-gallate (**18**); celastrol (**19**).

Conclusions

After the failure of TLR4 antagonists Eritoran and TAK-242 to pass clinical trials as drugs against acute sepsis and septic shock, the most recent change of direction in TLR4-directed therapeutics is to use TLR4 antagonist, included Eritoran, to block or reduce acute and chronic inflammatory diseases due to TLR4 activation by endogenous factors (DAMPs) [106]. Another important paradigm change in the rational design of small-molecular TLR4 modulators is to move away from the structure of lipid A, the natural agonist, and explore new hit compounds derived from combinatorial libraries and natural sources (mainly plant secondary metabolites). Besides the necessity for companies and academic groups to have proprietary structures, the main reason to leave the ligand-based design so far adopted, is the low solubility in aqueous media of lipid A and lipid A-like molecules and their poor pharmacokinetic (adsorption and distribution) properties. Concerning synthetic molecules, new promising directions have been suggested in the use of non-lipid A-like synthetic glycolipids, as in the case of monogalactosyl-diacylglycerol (MGDG) **1** and tri-mannoside Glycolipid Conjugates (MGC) **2** (Figure 8) reported in this review [58,59]. This last type of antagonists show a new mechanism of action based on targeting the membrane lipid rafts that would be essential to TLR4 organization in activated oligomeric species,

and in the selective deprivation of CD14 co-receptor from plasma membrane [59]. Interestingly, a very similar mechanism of action based on membrane rafts targeting seems to be at the base of natural molecules such as the steroid **13** [81]. Membrane rafts disruption and impairment of CD14 function are new strategies for TLR4 antagonism that could be used by other molecules and deserve to be investigated more in detail in the perspective to develop new generations of TLR4 modulators. Phosphorylated lipo-monosaccharides as compound **3** [60,61], deriving from molecular simplification of lipid A, present several advantages in the perspective of industrial development, due to the much simpler synthesis compared to Eritoran, and retention of selectivity and antagonist potency. Innovative peptidomimetics (neoseptins) have been proposed in 2016 as interesting hit compounds to develop non-lipid A-like TLR4 agonists [64], while the low potency and the lack of activity on human TLR4 limit the applicability of these compounds. Other non-lipid A-like TLR4 modulators have been reviewed here among synthetic and natural molecules. In general, the main limitation of the studies on new TLR4 modulators reported in this review and depicted in Figure 8, Figure 9, and Figure 10 is the lack or very limited investigation of selectivity and toxicity. The TLR4 activity has been rarely compared to the activity on other TLRs or other biological targets, and toxicity studies are lacking as well.

Future perspective

Despite the majority of the natural and synthetic molecules reviewed here are in the early stage of pre-clinical development, ongoing clinical studies and a few licensed compounds demonstrate the potential of TLR4 modulators (Table 2). TLR4 agonists with a structure related to lipid A (MPL and AS04) have been licenced as vaccine adjuvants. Other lipid A mimetics (AS04, GLA-SE, GSK1795091, OM-174) are in clinical phase I or II as anticancer therapeutics. Small molecular TLR4 antagonist AV-411 (Ibudilast) is in phase II clinical trials for the treatment of asthma and post-stroke disorders. NI-0101 is the first anti-TLR4 monoclonal antibody to pass phase I clinical trials for rheumatoid arthritis, showing safety and tolerability (Table 2). Because very reduced number of chemicals are in clinical phase of development as TLR4-based therapeutics, major efforts should be focused in the next future to progress in the preclinical characterization of newly discovered hit compounds. To do this, complete data on toxicity and specificity should be collected for every new hit compound presented here. In parallel, it is still important to extend the chemical variety of TLR4 modulators by discovering new active molecules from natural sources and from *de novo* designed synthetic molecules.

Compound	Action	Clinical phase	Indications	References/ clinical trial identifier
MPL plus pollen (Pollinex Quattro)	Agonist	Licensed	Allergy	[107]
AS04 (Stimuvax)	Agonist	Licensed	Protection from HPV	[108]
AS04 (Stimuvax)	Agonist	Phase II	Rectal, prostate and colorectal cancer	NCT01507103, NCT01496131, NCT01462513
AV-411 (Ibudilast)	Antagonist	Phase II	Asthma and post-stroke disorders	[109]
NI-0101[+]	Antagonist	Phase II	Rheumatoid arthritis	[110]
GLA-SE (Glucopyranosyl lipid A-stable emulsion)	Agonist	Phase I	Metastatic sarcoma	NCT02180698
GSK1795091	Agonist	Phase I	Cancer	NCT02798978
OM-174 (Lipid A analog)	Agonist	Phase I	Solid tumor and melanoma	NCT01800812, NCT01530698
E5564 (Eritoran)	Antagonist	Withdrawn	Severe sepsis	[35]
TAK-242 (Resatorvid)	Antagonist	Withdrawn	Severe sepsis	[47]

[+] First in human study of an anti-TLR4 monoclonal antibody

Table 2. Selection of clinical trials testing drugs targeting TLR4.

1.3.2.1 Monosaccharide glycolipids as TLR4 modulators

This thesis focuses on TLR4 modulators obtained by lipid A structure simplification, *i.e.* synthetic monosaccharide glycolipids (Figure 11), which present some advantages in the perspective of industrial development. They present a polar (charged) head linked to a variable number of lipophilic chains. Due to their amphiphilic nature, these molecules tend to form micelles in aqueous solutions, and their critical micellar concentration is normally in the nM range. Consequently, aggregated forms of these amphiphilic molecules (synthetic or natural) should predominate in the concentration range relevant for biological responses and for biochemical characterization *in vitro* [22]. Moreover, differences in the molecule aggregation and 3D state might influence kinetics and potency of TLR4 modulation [111]. The correlation of aggregates conformation in solution and bioactivity was investigated for natural TLR4 ligands, whereas only little is know for the synthetic ones. A SAR study approach can greatly support the characterization of these new synthetic TLR4 modulators.

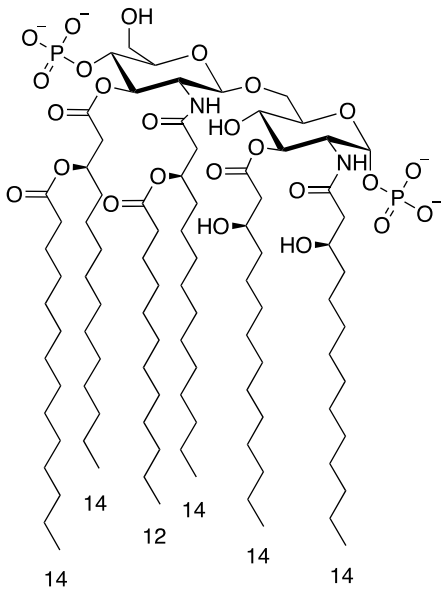

***E. coli* Lipid A**

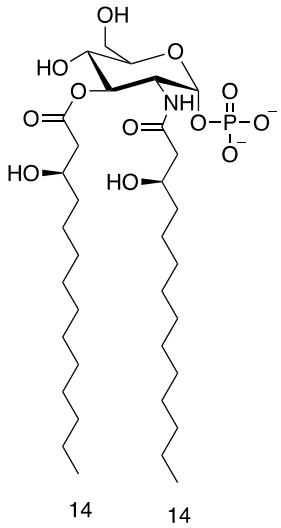

***E. coli* Lipid X**

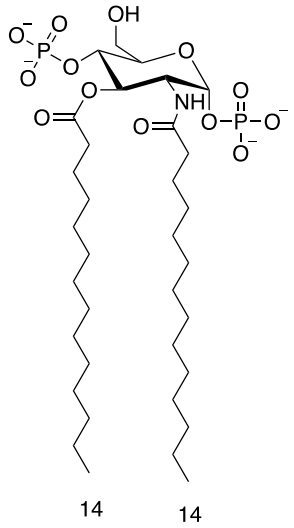

Monosaccharide FP7

Figure 11. Structure representations of *E. coli* lipid A, the lipid A precursor lipid X, and the monosaccharide FP7.

1.4 Structure activity relationship (SAR)

SAR studies play a fundamental role in drug discovery from the initial screening up to the lead optimization. The whole SAR study process involves the identification of a collection of molecules, the elucidation of their associated activities, and the characterization of their structural modifications. A SAR study is a complex process which aims at optimizing the molecular physicochemical and biological properties. In particular it aims at improving potency and selectivity, to decrease toxicity, to ensure bioavailability, to modulate metabolism, and to enable patentability of the drug candidate (Figure 12). A chemical set of molecules for a SAR study can essentially be infinite. Hence, there is the need to rapidly identify the most promising ones. *In silico* methods can help with this, allowing a fast and efficient characterization of SAR, and predicting activities for the new molecules. Computational methods are indeed an useful tool for the medicinal chemistry domain, suggesting potential structural modifications of the hit or lead [112]. However, *in silico* SAR studies have to be confirmed and complemented with *in vitro* and possibly *in vivo* experiments.

1.4.1 SAR of glycolipids as TLR4 modulators

TLR4 is clearly linked to an increasing number of pathologies, therefore there is a need for new drugs targeting TLR4. Though some principles for TLR4 modulation by lipid A and other ligands have been described, a thorough understanding of the monosaccharide glycolipids SAR is missing. In this thesis a SAR study is presented, first of its kind, on synthetic monosaccharide glycolipids as TLR4 modulators. My contibution to this SAR study concerned the *in vitro* binding characterization of molecules with hMD-2. Hence, next chapters focus on recombinant protein production, MD-2, and protein-ligand binding assays.

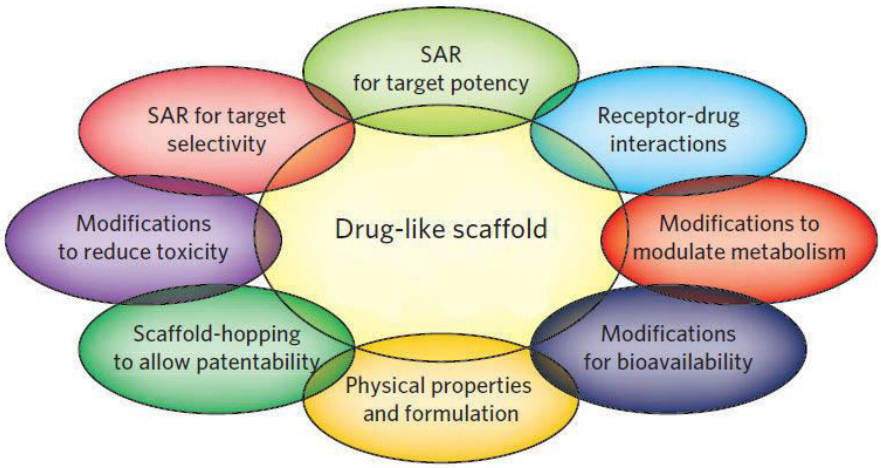

Figure 12. Discovery paradigm for a small-molecule drug. A drug-like scaffold is modified by structure activity relationship (SAR) studies aiming to ameliorate drug target features: potency, selectivity, toxicity, bioavailability, metabolism, and patentability [113].

1.5 Recombinant protein production (RPP)

RPP is one of the most rapidly growing sectors of biotechnology (Figure 13), and it steadily increased during the last 30 years. RPP is required for scientific research and in the therapeutic field: to date, more than 400 approved biopharmaceuticals are recombinant proteins and 1300 are under development [114]. Demand for high yields of therapeutic recombinant protein is very high. However, obtaining a high quality recombinant protein that is correctly folded can be an overriding requirement: for example, for the determination of the protein structure using NMR and X-ray crystallography, or for protein-ligand interaction studies, which togheter represent the basis for drug design and development of biopharmaceuticals. RPP has been underway for almost 40 years, however associated problems are still being investigated today. These include accumulation of the recombinant protein in inclusion bodies, proteolysis, plasmid loss, and stress of the utilised host. Strategies to improve the yields of correctly folded recombinant protein have therefore long been the focus of many international meetings in the RPP scientific community, which have failed to define generic protocols for successful outcomes [115,116].

1.5.1 RPP in *Escherichia coli*

Escherichia coli is widely used for RPP in both research and industrial settings. The popularity of *E. coli* is due to its attributes which include high growth rates in inexpensive media, high recombinant protein yields, simple scale-up process, and safety. The target protein can account for up to 50% of the total protein content of the bacteria [117]. However, other hosts may be more suitable than *E. coli* depending on the nature of the protein to be produced.

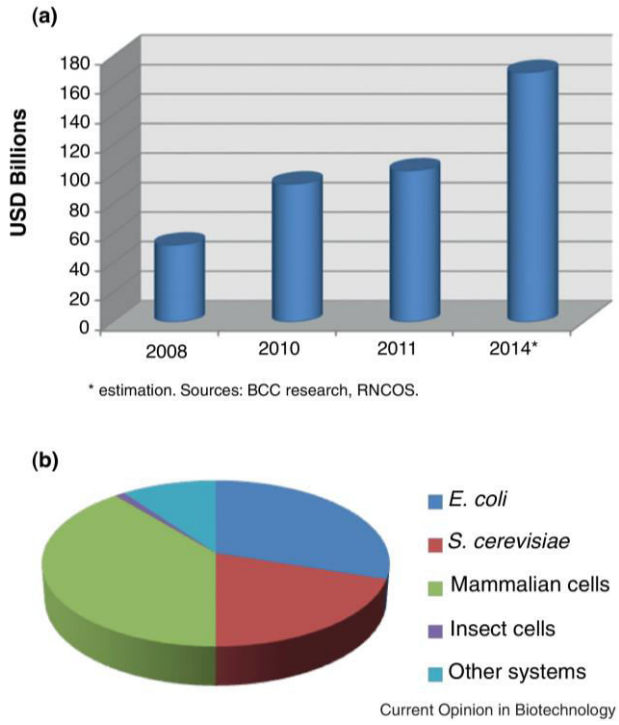

Figure 13. a) Global market for recombinant protein drugs; b) percentage of recombinant protein pharmaceuticals, produced by different hosts [118].

1.5.2 RPP in Gram-positive bacteria

The Gram-positive bacteria such as *Bacillus subtilis* and *Lactococcus lactis* are characterized by their natural tendency to secrete high-quality recombinant proteins in the extracellular medium by the Sec pathway. The advantage of secretion of recombinant protein is that both the proteolytic degradation within the cell is avoided and the downstream processing is minimized. Not surprisingly, therefore, *B. subtilis* is currently the microbial host responsible for the production of over 60% of commercially available enzymes. However, protein secretion in both these strains remains the bottleneck in RPP, in which the many steps involved in secretion and translocation are rate limiting [119]. This results in the accumulation of the protein in the cytoplasm and the increased aggregation of newly synthesised proteins in inclusion bodies [120].

Similar to *E. coli*, the rapid overproduction of recombinant protein in *B. subtilis* results in severe physiological stress [120]. Studies have reported the negative consequences of RPP on bacterial growth, particularly as the relative synthesis rate of the general stress proteins constituted up to 40% of the total protein synthesis of stressed cells [121,122].

The need to produce proteins requiring post-translational modifications (PTMs) such as glycosylation, proteolytic processing and disulphide bond formation also requires an expression host other than bacteria.

1.5.3 RPP in eukaryotes

Lower eukaryotes like yeast cells such as *Pichia pastoris*, and like filamentous fungi such as *Aspergillus niger* are a possible host of choice for RPP. During the last decades, yeast became increasingly popular for the production of antibodies and antibody fragments, whereas filamentous fungi have been widely used for large-scale production of industrial enzymes [123,124]. In these lower eukaryotic production hosts, the process of protein folding, post-translational modification and translocation for further secretion are accomplished in the endoplasmic reticulum (ER). Excessive accumulation of misfolded proteins in the ER, however, leads to activation of a set of genes associated with protein folding and transport as well as ER-associated protein degradation (ERAD), in which misfolded polypeptides are translocated back into the cytosol for degradation. This activation is known as the unfolded protein response (UPR) and constitutes an ER stress response in these hosts. ER stress is characterized by down-regulation of energy consuming biosynthetic pathways

such as for vitamin, amino acid, carbohydrate and lipid metabolism, which ultimately inhibits the growth of these production hosts [125].

Higher eukaryotes like human embryonic kidney 293 cells (HEK293) are a possible host of choice for RPP requiring PTMs. HEK293 have been widely used to produce research-grade proteins for many years and, more recently, five therapeutic agents produced in HEK293 have been approved by the Food and Drug Administration (FDA) or the European Medicines Agency (EMA) for therapeutic use. The major advantage of using human cell lines for RPP of human proteins, is the greater likelihood that the recombinant protein produced will possess the correct PTMs. Other mammalian cell lines can produce human PTMs, however they can also produce non-human PTMs, which can be potentially immunogenic. Human cell lines are currently widely used for biopharmaceutical research, vaccine production and production of licensed protein biotherapeutics [126].

Although various hosts, plasmids and protocols are available, the accumulation of each new recombinant protein presents challenges that require optimization.

1.6 Myeloid differentiation factor 2 (MD-2)

LPS is one of the best characterized TLR4 PAMPs, and TLR4 activation mediated by LPS involves several extracellular regulators, which can affect ligand specificity and activity [127].

Amongst TLR4 ancillary proteins LBP, CD14, and MD-2 (which is also known as lymphocyte antigen 96 (Ly96)), only MD-2 is absolutely required for TLR4 mediated LPS sensing [128,129].

Shimazu *et al.* reported the cDNA sequence of hMD-2 for the first time in 1999 [45]. The authors were searching for human proteins similar to myeloid differentiation factor 1 (MD-1, a protein involved in the regulation of LPS responses) and they found one protein presenting a high homology to MD-1 which was named MD-2 [130]. Thanks to a thorough characterization which involved Northern blots and FACS analysis, co-precipitation and *in vitro* cell experiments, strong evidence suggested, for the first time, that a role of MD-2 in TLR4 signaling was implied.

Only a year later (in 2000) the identification of mMD-2 was reported [131]. To date, MD-2 is the high-affinity co-receptor exclusive of TLR4. Hence, it is assumed that MD-2 is tethered to the cell surface primarily via TLR4 [132].

1.6.1 Structural features of MD-2

MD-2 is a small globular glycoprotein and its cDNA encodes for 160 amino acids. MD-2 signal sequence (the first 16 hydrophobic amino acids) directs MD-2 to the secretory pathway. On SDS-PAGE in reducing conditions, MD-2 migrates in two major bands with apparent molecular weights of 25-30 kDa [45]. Upon MD-2 treatment with endoglycosidase F (enzyme that strips N-linked sugars), on SDS-PAGE only one single band is visible, which corresponds to the predicted molecular weight of 18 kDa [133]. The three N-glycosylation sites mostly conserved among different species are Asn26, Asn114 and Asn150.

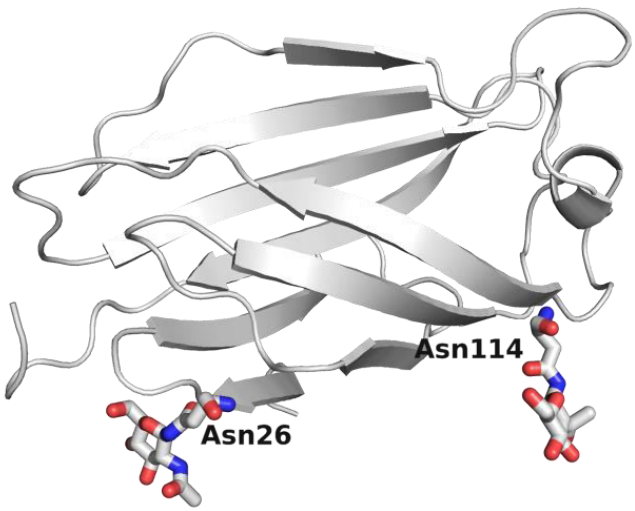

Figure 14. Human MD-2 and its residues carrying glycosylations (courtesy of Jean-Marc Billod).

Human and chimp MD-2 differ from other mammals as they lack the N-glycosylation site at position Ans150 [132] (Figure 14).

It was demostrated that mutated MD-2 presenting only one glycosylation site (Asn26 or Asn114) binds to TLR4, binds to LPS, and confers LPS responsiveness. On the other hand, mutated MD-2 without glycosylation sites binds to TLR4, but the LPS-induced activation via TLR4 is impaired unless CD14 is co-expressed [134,135]. In contrast, it was found that fully deglycosylated MD-2 expressed in baculovirus is able to confer normal LPS responsivness via TLR4 activation [136]. Other unpublished observations stated that fully deglycosylated MD-2 is active in LPS response via TLR4 [132]. These contrasting observations leave the role of MD-2 glycosylations related to LPS recognition and signaling in a position still to be fully clarified.

Known MD-2 orthologs, except chicken MD-2, posses seven cysteine residues in identical positions (Figure 15). It was hypothesized that due to the odd number of residues, the unpaired cysteine might be involved in interchain disulfide bond in the extracellular oxidizing environment. Mullen *et al.* found that with exception of Cys95 and Cys105, all the cysteine when changed into serines were able to trigger TLR4 activation mediated by LPS, although to a lower extent, suggesting that cysteines are involved in functionally structural features of MD-2 [137].

All the mutagenesis studies conducted on MD-2 suggest that several amino acids of MD-2 are important for its activity [138-140]. However, a thoroughly mutational characterization of MD-2 residues still need to be performed.

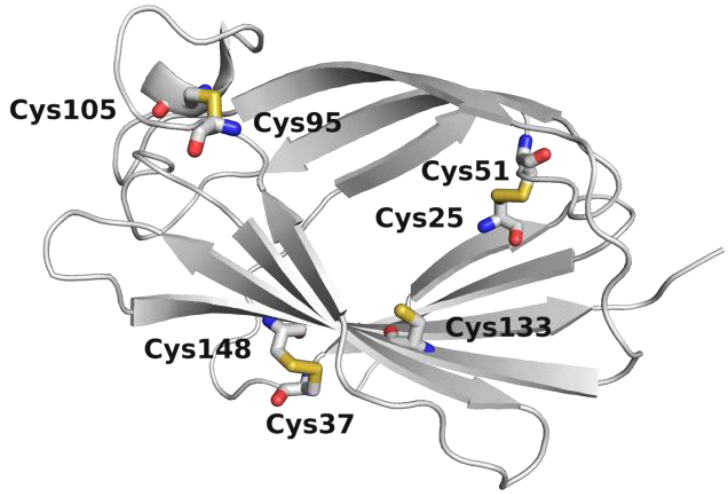

Figure 15. Human MD-2 with disulphide bonds and the free Cys133 (courtesy of Jean-Marc Billod).

1.6.2 Recombinant MD-2

The production of active, monomeric MD-2 is extremely difficult to achieve [132]. For this reason, and due to MD-2 tendency to multimerise, MD-2 characterization has been delayed. The role behind MD-2 multimerization is still unclear at present.

Jerala [141] and Tsuneyoshi [142] were the first two that independently obtained functional MD-2 expressed in

Escherichia coli. However, in the first case MD-2 was purified with a complex procedure due to the co-presence of MD-2 natural ligand (LPS). In the second case, MD-2 was purified in complexes containing LPS. It is clear that using an eukaryote host to express recombinant MD-2 would prevent the presence of LPS and would allow PTMs to take place.

Nowadays, functional MD-2 is commercially available, it is obtained by RPP in insect cells, and interestingly it is mostly monomeric or dimeric. However the high price of this recombinant MD-2 makes it accessible only to a very restricted portion of the scientific community.

Hence, in this thesis the possibility to produce functional recombinant hMD-2 by using eukaryotic expression systems was evaluated, in particular by using *Pichia pastoris* cells and human HEK293T cells.

1.7 Molecular recognition

Molecular recognition is a process in which biological macromolecules interact with each other or with other molecules through non-covalent interactions to form a specific complex [143]. This process possesses two essential features: specificity and affinity [144]. Molecular recognition is an element of complex mechanisms essential in life processes, such as self-replication, metabolism, and cell communication and signaling. For example, cell communication and signaling is a series of events which involve recognition, binding, and dissociation of certain molecular messengers that are recognised by receptors, and that culminate with the functional cascade response of the cell involved in the phenomena [145-147].

1.7.1 Ligand binding studies

In molecular recognition, the quantification of ligand binding to specific receptors is a key concept of both theoretical studies and drug development research. Ligand binding studies are essential to better characterize and quantify the mechanisms and energies which govern and drive the formation of receptor complexes and signaling. On the other hand, ligand binding studies are important for the characterization of the binding affinities of molecules as part of SAR studies. This helps to understand the molecular

interactions and hence to facilitate the discovery, design, and development of new hit or lead compounds.

Table 3 reports the main classes of ligand binding assays which include labeled, structure-based, thermodynamic, whole cell, and label-free ligand binding assays [148].

Although many different methods are available, the molecular characterization of novel protein-ligand interactions presents challenges that require an initial screening of possible ligand binding assays followed by their optimization.

Type	Assays	Mechanism	Advantages	Disadvantages
Labeled ligand-binding assays	Fluorescent-ligand binding	Detect the binding to a target	Broad spectrum of wavelengths	Fluorescence interferences; ligand-labeling can alterate the binding characteristics; difficult to find good fluorescent ligands for many receptors;
	Radio-ligand binding	Detect the binding to a target	Popular in membrane-bound targets; robust and good determination of receptor density and distribution; ligand binding sites and affinity;	Costly; hazards of handling high levels of radioactivity;
	Bio-luminescent binding (nano-luciferase)	Study the interactions of protein hormones with their receptors	High sensitivity; high stability; reproducibility;	Might influence the receptor binding;
Structurebased ligand-binding assays	Nuclear magnetic resonance (NMR)	Analyze the magnetic characteristics of atomic nuclei	Assist structure-based drug design; suitable for any class of compounds and almost all soluble proteins, natively unstructured proteins or membrane proteins;	Costly; time consuming; resolving power is lower than X-ray crystallography;
	X-ray crystallo-graphy	Produce a 3D image of molecules' structures	The solvent effect can be examined by X-ray cristallography. The whole 3D structure can be obtained by the systematic analysis of a crystallized material;	Time consuming; molecules in solution can not be examined; secondary structures including domain movements can not be determined;

Table 3. Ligand binding assays: mechanisms, advantages and disadvantages of the methods (continues on the next page).

Type	Assays	Mechanism	Advantages	Disadvantages
Thermo-dynamic binding assays	Thermal denaturation assays (TDA)	Detect the thermal denaturation of proteins by differential scanning fluorimetry	Applications in chemical profiling of different protein families; identification of novel ligands; investigation of stability of proteins in buffers in solution;	May not be suitable for analysis of very small proteins that do not aggregate upon denaturation;
	Isothermal titration calorimetry (ITC)	Measures of binding enthalpy variation	Detection of highly potent and entropy-driven ligands, compared to others;	Low throughput; low sensitivity; large sample volumes needed;
Whole cell ligand-binding assays	Surface acoustic wave (SAW) biosensor	Binding characteristics are indicated by a change in amplitude	Sequential binding of distinct ligands; targeting different cell surface molecules; detection in real time;	Lack of development of SAW biosensors for analysis of molecules on living cells;
	RWG biosensor	Make cell phenotypic signatures named dynamic mass redistribution	Measure the binding, and the stimulus-response interpretation of the initial interaction of drug and receptor; analyze the functional consequences of ligand binding and dissociation;	RWG biosensor may not be used to detect ligand binding directly;

Table 3. Ligand binding assays: mechanisms, advantages and disadvantages of the methods (continues on the next page).

Type	Assays	Mechanism	Advantages	Disadvantages
Labeled free ligand-binding assays	Surface plasmon resonance (SPR)	Surface plasmon polaritons tracks the binding of ligands to the receptors bound to a gold surface	Most popular label-free ligand binding assay; determination of binding kinetics;	Low sensitivity to binding-induced conformational change;
	Plasmon-waveguide resonance (PWR)	Polarized continuous wave laser excites electromagnetic waves in a resonator. Ligand binding changes amplitude, position and width of reflected lights	Examination of anisotropic optical contents of receptor-ligand complexes, thus differentiating mass density changes from conformational changes;	Lower sensitivity compared to SPR with regard to refractive index, thickness and mass parameters;
	Nanofluidic Fluorescent Microscopy (NFM)	Combination of nanofluidic-based biosensors and fluorescence microscopy to analyze the protein binding kinetics	Time of analysis shorter compared to other microfluidic assays; statistical errors are reduced and there are no limitations on the size of the analyzed molecules;	Limitations of fluorescence microscopy;
	Biolayer Interferometry Biosensor (BIB)	Detection of interference patterns formed by an optical layer and a biolayer containing proteins	Effective assay to study binding kinetics;	Not yet validated for small molecule detection;

Table 3. Ligand binding assays: mechanisms, advantages and disadvantages of the methods (continues from previous pages). Self work.

1.7.2 MD-2-ligand binding studies

Quantitative analysis of binding of purified hMD-2 receptor with small molecular ligands has been very difficult mainly due to the challenges in the expression and purification of functional recombinant MD-2.

The only available X-ray structures of MD-2/ligand complexes have been obtained with lipid IVa and to Eritoran, whereas it has been easier to use the MD-2/TLR4 complex for co-crystallization studies (Figure 16).

Molecular dynamics simulation is the most common way to study MD-2 interaction dynamics, since only few MD-2-ligand binding assays have been developed since MD-2 discovery in 1999.

In this thesis, four different techniques have been developed to study the interactions of small molecular ligands with functional hMD-2. In particular two plate-based ELISA with immobilized hMD-2, a fluorescence displacement assay, and surface plasmon resonance (SPR) measurements were performed. These techniques are presented in the following subchapters.

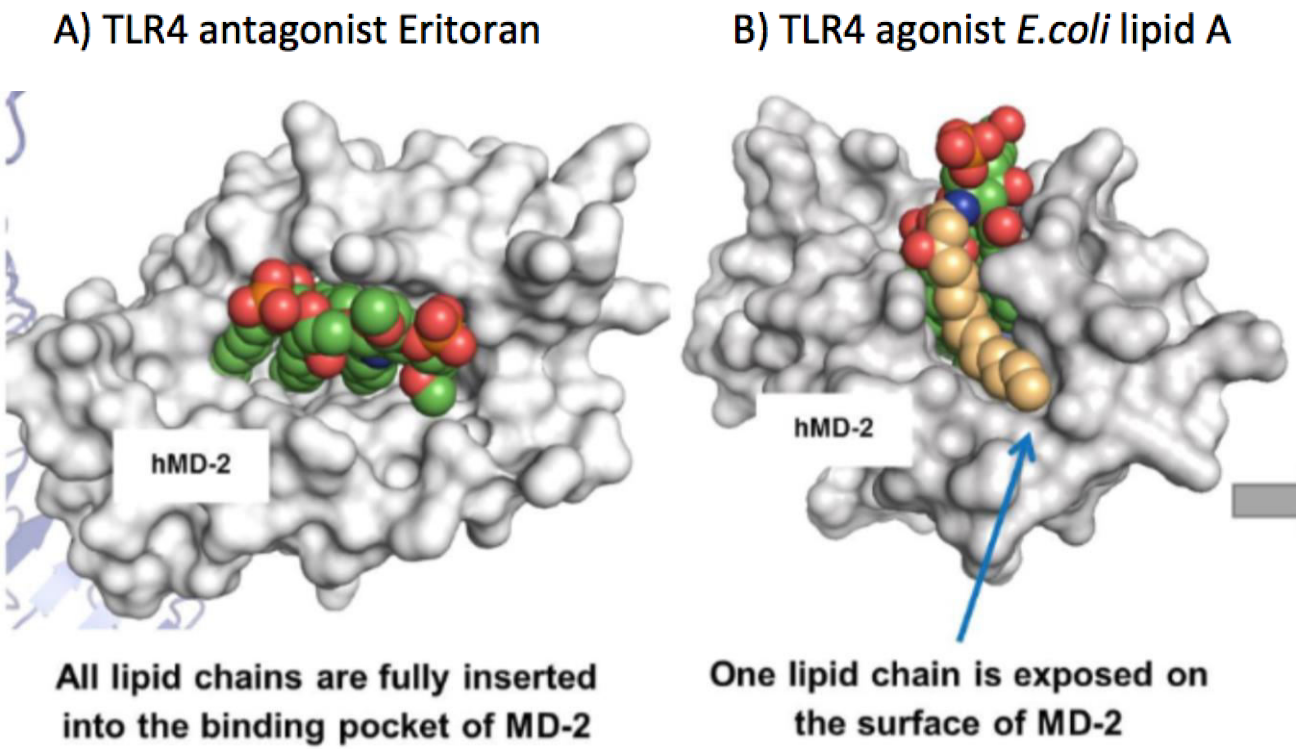

Figure 16. Co-crystal structures of A) TLR4/hMD-2 with the bound antagonist Eritoran (PDB: 2Z65, TLR4 is not shown); B) TLR4/hMD-2 with the bound agonist lipid A (PDB code: 3FXI, TLR4 is not shown). Modified from [149].

1.7.2.1 ELISA: competition with bound hMD-2

This ELISA was first developed by R. Jerala and coworkers in 2008 [150]. hMD-2 is immobilized on multiwell plates by means of the interaction of an anti-MD-2 antibody. The direct binding of the tested molecules is determined by using an anti-hMD-2 antibody (9B4) that binds to an epitope close to the rim of the LPS-binding pocket of hMD-2, that is available for the binding of 9B4 only when hMD-2 pocket is empty [151]. In the presence of LPS or of another hMD-2 ligands, the antibody binding to hMD-2 is therefore inhibited. Anti IgG-horseradish peroxidase (-HRP) was used to quantify the percentage of competition (Figure 17).

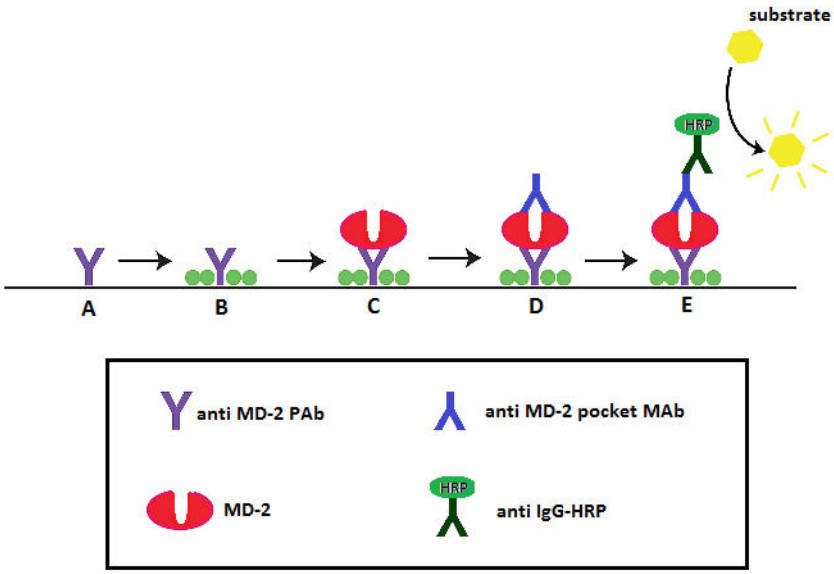

Figure 17. Schematic representation of the hMD-2-ligand binding assay "competition ELISA". Self work.

1.7.2.2 Displacement ELISA

Based on the previous "competition ELISA" a novel "displacement ELISA" was developed by using immobilized hMD-2 and biotin-labelled LPS (biotin-LPS) in combination with streptavidin conjugated to HRP (streptavidin-HRP). In particular, the tested molecules were added to immobilized hMD-2 that was previously incubated with biotin-LPS. Streptavidin-HRP was used to quantify the percentage of displacement of biotin-LPS from the pocket of hMD-2 mediated by the tested molecules (Figure 18).

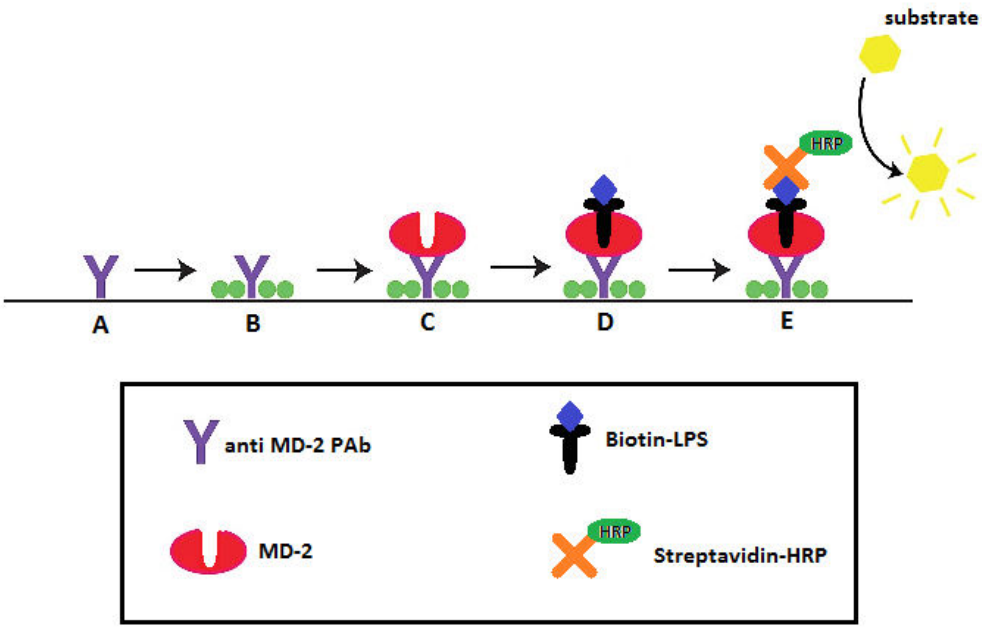

Figure 18. Schematic representation of the MD-2-ligand binding assay "displacement ELISA". Self work.

1.7.2.3 bis-ANS displacement assay

This assay was developed by R. Jerala and coworkers in 2006 [152]. It particular, it was shown that the fluorescent probe 1,1'-Bis(anilino)-4,4'-bis (naphthalene)−8,8' disulfonate (*bis*-ANS) binds to hMD-2 and it is displaced by LPS (Figure 19). bis-ANS probe presumably binds the same hMD-2 binding pocket that accommodate lipid A chains, so that LPS or another hMD-2 ligand competes with bis-ANS and is able to displace it from hMD-2 pocket. The displacement of bis-ANS probe is measured by calculating the decrease of the fluorescence at 495 nm [152].

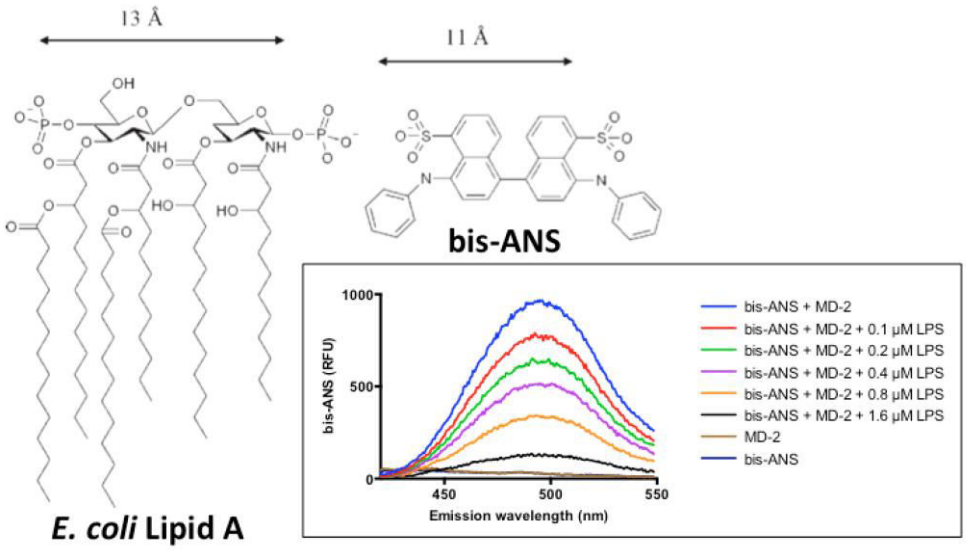

Figure 19. Structure similarities between *E. coli* lipid A and bis-ANS probe; fluorescence measurements showing a dose-dependent diplacement of bis-ANS probe from hMD-2 mediated by LPS. Self work.

1.7.2.4 Surface plasmon resonance (SPR)

SPR measures change in refractive index close to a sensor surface, allowing the study of interactions between immobilized hMD-2 and molecules in solution, in real time and label-free. hMD-2 (in SPR terms, the ligand) was adsorbed to the sensor surface by using its 6x-His tag. Binding response of the molecule (in SPR terms, the analyte) was measured in resonance units (RU), which are directly proportional to the concentration of molecules on the surface. The data were analysed with Biacore Evaluation software that provided the K_D of the molecules.

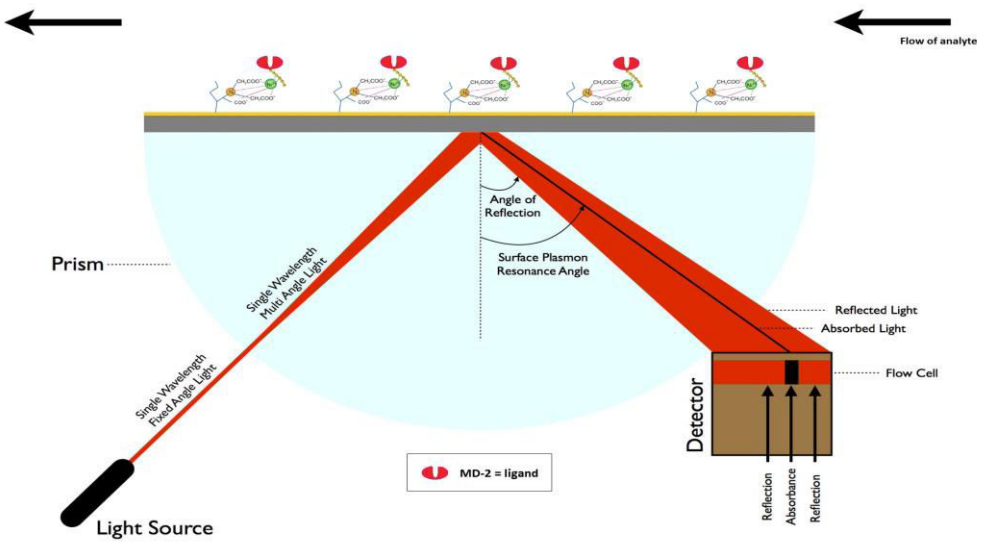

Figure 20. Schematic representation of SPR with MD-2 as ligand (modified from [153]).

1.8 The TOLLerant project

This PhD thesis is part of the MSCA-ITN-2014 ETN project "Toll-like receptor 4 activation and function in diseases: an integrated chemical-biology approach" (*www.tollerant.eu*, acronym TOLLerant) and is based on international group interactions and synergies. TOLLerant is a combination of chemistry, biology, biophysics, biochemistry and pharmacology expertise, and it is aiming to gain information on molecular aspects of TLR4 activation and signaling.

The short-term scientific objective is to develop novel, non-toxic, synthetic and natural TLR4 modulators and to assess their therapeutic potential. The long-term scientific objective is to develop a generation of innovative, TLR4-based therapeutics, to be used as vaccine adjuvants, anti-sepsis and anti-inflammatory agents to treat chronic inflammations (allergy, asthma).

Figure 21. The TOLLerant project logo

1.8.1 The training within TOLLerant

The training programme within the TOLLerant network provided me a broad range of competences, experiences and skills in the cutting-edge, inter-disciplinary research field of chemical biology related to the molecular mechanisms of innate immunity and inflammation.

During the training program I have been supported by senior scientists to cultivate my scientific, entrepreneurial and inter-cultural mindset.

The non-academic sector provided me with entrepreneurship and company management skills, in order to enhance my future employability by the private sector.

1.9 Purpose of the work

The systematic SAR study presented in this manuscript is the first of its kind on synthetic monosaccharide glycolipids in the context of TLR4 modulation. In its totality, this SAR study considers:

a) *in silico* interaction of molecules with hMD-2;

b) *in vitro* interaction of molecules with purified hMD-2;

c) *in vitro* biological activity of molecules in cell models;

d) aggregation properties of the molecules in solution;

My contibution to this SAR study concerned, in particular, the *in vitro* binding characterization of the new synthetic monosaccharide glycolipids with the purified receptor hMD-2.

Quantitative evaluation studies of MD-2-ligand interactions has been very difficult to achieve; mainly due to difficulties encountered in expressing functional hMD-2.

The purpose of this thesis' work has been:

1) produce functional recombinant hMD-2;

2) develop hMD-2-ligand binding assays to characterize TLR4 modulators as part of SAR studies;

Information obtained from this SAR study can contribute to the development process of new hits or leads targeting TLR4.

Results and discussion

2.1 SAR study part I

This chapter is based on a paper published by the *Journal of Medicinal Chemistry* on date 01 March 2018 (DOI: 10.1021/acs.jmedchem.7b01803).

Structure-activity relationship (SAR) in monosaccharide-based Toll-like receptor 4 (TLR4) antagonists

Fabio A. Facchini,[a] **Lenny Zaffaroni**,[a] Alberto Minotti,[a] Silvia Rapisarda,[a] Valentina Calabrese,[a] Matilde Forcella,[a] Paola Fusi,[a] Cristina Airoldi,[a] Carlotta Ciaramelli,[a] Jean-Marc Billod,[b] Andra B. Schromm,[c] Harald Braun,[d] Charys Palmer,[e] Rudi Beyaert,[d] Roman Jerala,[f] Grisha Pirianov,[e] Sonsoles Martin-Santamaria,[b] Francesco Peri[a]*

[a]University of Milano-Bicocca, Piazza della Scienza, 2; 20126 Milano (Italy); [b]CIB-CSIC. C/ Ramiro de Maeztu, 9. 28040-Madrid (Spain); [c]Research Center Borstel, Parkallee 1-40, 23845 Borstel (Germany); [d]VIB-UGent; Technologiepark 927 / 9052 Ghent (Belgium); [e]Anglia Ruskin Cambridge University, UK; [f]DepaNational Institute of Chemistry; Hajdrihova 19 SI-1000 Ljubljana (Slovenia);

Abstract

The structure-activity relationship was investigated in a series of synthetic TLR4 antagonists formed by a glucosamine core linked to two phosphate esters and two linear carbon chains. Molecular modeling showed that the compounds with C10, C12 and C14 chains are associated to higher stabilization of the MD-2/TLR4 antagonist conformation than in the case of the C16 variant.

Binding experiments with human MD-2 showed that the C12 and C14 variants have higher affinity than C10, while the C16 variant did not interact with the protein.

The molecules, with the exception of the C16 variant, inhibited the LPS-stimulated TLR4 signal in human and murine cells and the antagonist potency mirrored MD-2 affinity calculated from *in vitro* binding experiments.

FT-IR, NMR, and SAXS measurements suggested that the aggregation state in aqueous solution depends on fatty acid chains lengths and that this property can influence TLR4 activity in this series of compounds.

Introduction

TLRs are pattern recognition receptors (PRR) that recognize pathogen-associated molecular patterns (PAMPs). TLR4 is mainly expressed on haematopoietic cells including monocytes, dendritic cells and macrophages [23]. Lipopolysaccharide (LPS), lipooligosaccharide (LOS) and lipid A from Gram-negative bacteria are generally called endotoxin and are powerful TLR4 agonists [25]. TLR4 responds rapidly to minute amounts of circulating LPS through a multistep molecular recognition process, initiated by transfer of LPS monomers from aggregates in solution to LPS-binding protein (LBP), and subsequently to cluster of differentiation 14 (CD14), and to myeloid differentiation factor 2 (MD-2). MD-2 is associated with TLR4 in MD-2/TLR4 complexes on cell membrane. In the absence of agonist, the complex TLR4/MD-2 is in equilibrium between monomeric and dimeric species. Recent quantitative single-molecule localization microscopy (SMLM) studies [154] have shown that LPS binding to MD-2 [46] displaces the equilibrium towards homodimeric complexes $(TLR4/MD\text{-}2/LPS)_2$ [15,46,154]. The homodimer transmits the signal downstream through two distinct pathways. One pathway starts by recruitment of myeloid differentiation primary response gene 88 (MyD88) and adapter myelin and lymphocyte protein (MAL) (MyD88-dependent pathways and production of a number of pro-

inflammatory proteins), the other by the activation of TIR-domain-containing adapter-inducing interferon-β (TRIF) (MyD88-independent pathways and production of interferons) [60]. In addition to bacterial PAMPs, TLR4 can be also activated by damage-associated molecular patterns (DAMPs), endogenous agonists responsible for sterile inflammation, such as fibronectins [155], saturated palmitic acid [75], oxidized phospholipids [156] or high-mobility group box 1 (HMGB1) protein [157] have also been shown to activate TLR4. While different LPS chemotypes share a conserved lipid A moiety with chemical determinants that ensure optimal interaction with CD14 and MD-2 (5 or 6 lipophilic fatty acid chains attached to a disaccharide backbone, and one or two phosphate groups), DAMPs are chemically diverse molecules and the molecular mechanism of TLR4 activation and the role of CD14 and MD-2 in sensing these molecules are not entirely understood. DAMPs are implicated in many pathologies caused by TLR4 activation including atherosclerosis [158], rheumatoid arthritis [159], neuroinflammation [160], trauma [161] and hemorrhage [162]. These findings strongly support the idea that regulation of TLR4 activity appears as a potential target for therapeutic control of a variety of inflammatory-based diseases. Manipulation of TLR4-mediated immune responses as a potential approach for pharmacological intervention of diseases has been reported in the literature [163]. For the last few years several

TLR4 antagonists have been evaluated in preclinical studies but only two drugs, E5564 (Eritoran, Eisai Inc.) [35] and TAK-242 (Takeda Biological) [47] progressed to clinical trials for treatment of sepsis, which have been discontinued in different phases [164,165]. Efficient and selective TLR4 antagonists with a chemical structure simpler than lipid A are the basis for development of novel TLR4 modulators. Lipid A consists of a 1,4-β-diphosphorylated di-glucosamine backbone to which variable lengths and numbers of fatty acid (FA) acyl chains are covalently linked [25]. Lipid X [166], a biosynthetic precursor of lipid A with TLR4 antagonist activity, has been considered a simplified monosaccharide scaffold for the development of novel TLR4 modulators (Figure 22). Our group developed the lipid X mimetic FP7 [60], a glucosamine derivative with two phosphate groups and two myristic (C14) fatty acid (FA) chains, whose design was inspired by other glucosamine-based TLR4 modulators [167-169]. FP7 is active in inhibiting in a dose-dependent way human [60] and murine [61] TLR4 activation by LPS. Some preliminary observations from NMR experiments suggest that FP7 interact with MD-2, probably inserting FA chains into hydrophobic binding cavity [60]. This direct competition with LPS for MD-2 binding is probably reinforced by the capacity of FP7 to induce endocytosis of CD14 thus causing the absence of this receptor on the plasma membrane

[60]. FP7 is active in blocking PR8 virus lethality that is mainly due to TLR4 over-stimulation by endogenous DAMPs (mainly oxidized phospholipids and HMGB-1 protein) derived from viral damage to lung tissue [61]. In a proof-of-concept experiments in support of this *in vivo* mechanism, FP7 inhibited HMGB-1 activation of dendritic cells [61]. Other monosaccharide-based TLR4 modulators were developed and SAR studies showed that the length of FA chain is a critical factor determining the potency of TLR4 antagonism or agonism [167,170]. The biological activity and the agonist/antagonist behavior on TLR4 of lipid A variants and other amphiphilic glycolipids including FP7 is not only determined by the interaction with MD-2 but also by the aggregation state in solution. As LPS and lipid A, FP7 is an anionic amphiphile with a low value of CMC (9 μM) [60]. Even though the CMC value of FP7 is higher than its IC_{50} (about 2 μM in HEK cells assays), equilibrium between aggregates and single molecules in solution is present in the concentration range in which FP7 is active. It has been proposed for lipid A derivatives that size and 3D shape of aggregates influences the TLR4 activity, lamellar aggregates being associated to antagonism and aggregates with non-lamellar cubic symmetry to agonism [171,172]. While the last step of ligand presentation to TLR4 and formation of the activated heterodimer $(TLR4/MD\text{-}2/ligand)_2$ are dominated by single molecule interactions between the ligand and

CD14 and MD-2 receptors [173], the early phases of endotoxin (ligand) recognition by LBP are very likely influenced by the aggregation state of the ligand. We present here a SAR study on synthetic FP7 variants differing only for FA chains lengths (10, 12, 14 and 16 carbon atoms, Figure 22). In this study we will take into account both the interaction with MD-2 and the aggregation properties of the molecules. Additionally, we show the relationship between the chemical structure of FP7 variants with different fatty acid chains lengths and their effect on functional activity of TLR4 in different *in vitro* cell models.

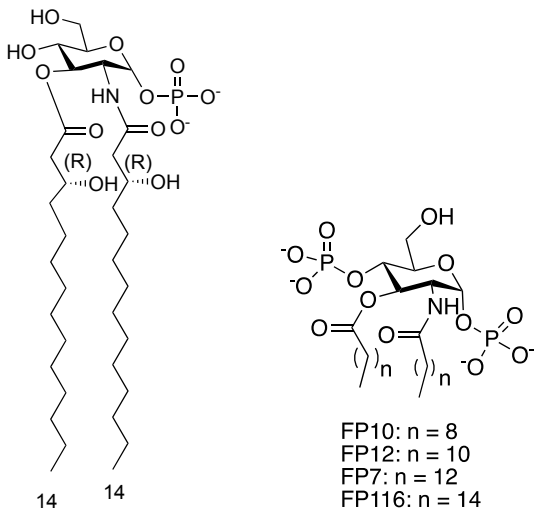

Figure 22. Chemical structures of lipid X (left) and FP7 variants (right).

Results

Computational design of FP7 variants as ligands of human MD-2 and CD14

Given our previous studies on the lipid X mimetic FP7 as ligand of TLR4/MD-2 and CD14 proteins, with TLR4/MD-2 antagonist activity [60], we were prompted to investigate the influence of the acyl chain length on the antagonist activity. To address this point, we designed three new FP7 (C14) derivatives with different FA lengths: FP10 (C10), FP12 (C12), and FP116 (C16). The ability of these ligands to bind to TLR4/MD-2 complex and to CD14, compared with FP7, was initially assessed through various computational techniques. We firstly docked the ligands in the binding site of CD14 using AutoDock Vina. For all the four ligands, docked poses inside the hydrophobic pocket were found. The obtained binding poses were very similar for all the ligands (SI Figure 33A) with also very close favorable predicted binding energies for the top poses (range from -6.5 kcal mol^{-1} to -5.9 kcal mol^{-1}). Therefore, the docking calculation showed that all four ligands are theoretically able to interact with CD14 inside its hydrophobic pocket and to engage in favorable interactions. In the most populated and most favorable docked poses, one phosphate group is interacting with the NH groups of Arg72 and Val73, and with the OH group of Tyr82 (SI Figure 33B), while the other phosphate group is exposed to the solvent. The FA

chains are accommodated inside the hydrophobic pocket of CD14 interacting with aliphatic residues, mainly Ala, Val, Leu, and Ile residues, and aromatic Phe49 (details are depicted in SI Figure 33C). The results were in agreement with previous docking studies of FP7 reported by us [174]. Figure 23 shows the docking calculations of ligands FP7, FP10, FP12 and FP116 inside the TLR4/MD-2 complex in the antagonist conformation. For all the compounds, favorable docked poses were found, with predicted binding energies, for the best ones, ranging from -7.8 to -6.5 kcal mol^{-1}. Figure 23B shows that the polar head groups are placed at the rim of MD-2 and the FA chains go deep inside the hydrophobic pocket interacting with many hydrophobic residues, namely Val24, Ala30, Ile32, Ile44, Ile46, Val48, Ile52, Leu54, Leu61, Ile63, Tyr65, Phe76, Leu78, Ile80, Phe104, Val113, Ile117, Phe119, Phe121, Ile124, Tyr131, Val135, Phe147, Leu149, Phe151, and Ile153. Additionally, it was possible to observe more diversity in the predicted binding poses in TLR4/MD-2 than in the case of CD14. Results for FP7 were in agreement with those previously reported in MD-2 [60]. Figure 23C shows that in many poses, one of the phosphate groups was close to the hydroxyl group of MD-2 Tyr102 where it establishes hydrogen bonds, and the other one was often close to MD-2 Arg90 establishing hydrogen bonds and electrostatic interactions. In some docked poses, the phosphate groups were observed to

interact with the backbone of residues Phe119, Ser120, and Phe121. Both phosphate groups were often placed at the rim of MD-2 where they are exposed to the solvent, in agreement with the reported X-ray crystallographic complexes of TLR4/MD-2 with glycolipids (*i.e.* complex with eritoran, PDB-ID 2Z65, or with lipid IVa, PDB-ID 2E59). Two different orientations were also found: type A (antagonist-like binding mode), similar to that found for lipid IVa; and type B (agonist-like binding mode), similar to that found for *E. coli* lipid A in PDB-ID 3FXI (SI Figure 34). It is well known that these two ligands, lipid IVa and *E. coli* lipid A, bind to TLR4/MD-2 in a different manner, one being rotated 180° compared to the other one, leading to opposed biological activities. Selected binding poses were used as starting structures for re-docking with AutoDock4 resulting in predicted binding energies ranging from -4.6 kcal mol^{-1} to +4.3 kcal mol^{-1}. Among the docked solutions, the best poses (from -4.6 kcal mol^{-1} to -2.5 kcal mol^{-1}) corresponded to binding poses very similar to those obtained with AutoDock Vina (data not shown). The narrow binding energy range did not permit to rank the ligands by predicted affinity, showing that the four ligands are putative binders of the TLR4/MD-2 system. Given that the main interactions (the polar ones) are common to the four ligands, and that the MD-2 pocket is big enough to host two longer FA chains, from the docking calculations it was not possible to clearly

correlate the subtle differences in FA chain length with preferred ligand binding.

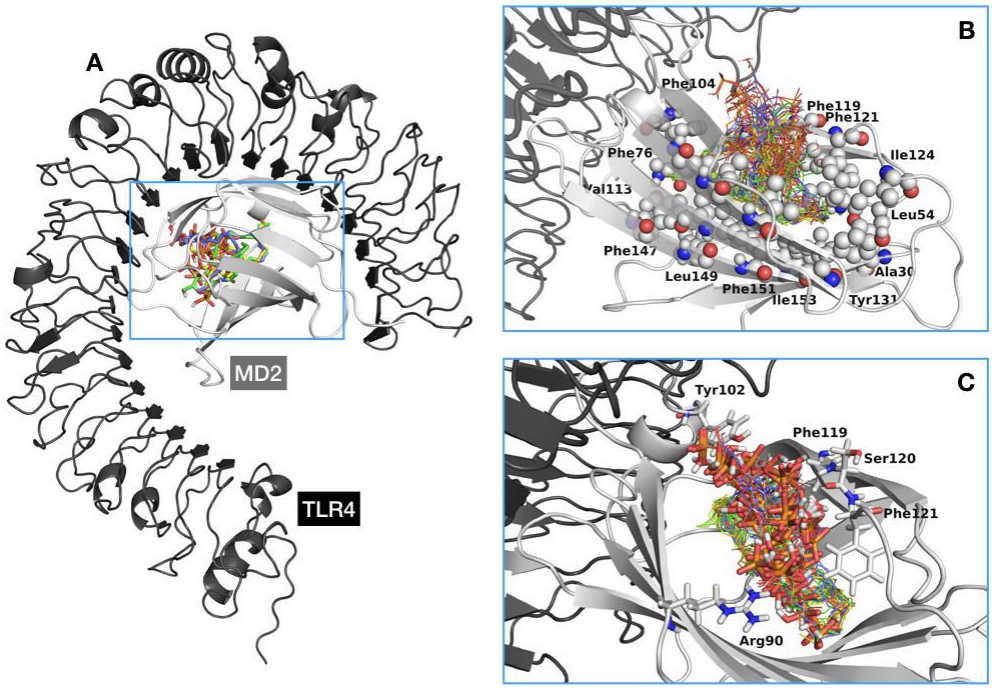

Figure 23. A) General view of FP10 (in orange), FP12 (in yellow), FP7 (in green), and FP116 (in violet) ligands are shown docked inside TLR4/MD-2 (TLR4 is shown in black and MD-2 in grey); B) Detail of the MD-2 hydrophobic pocket occupied by all the best docked poses for each ligand (represented as lines). Hydrophobic residues mentioned in the text as interacting with the FA chains of the ligands are represented in spheres; C) Detail of the polar interactions of the ligands inside the TLR4/MD-2 system. Phosphate groups of the best docked poses of each ligand and the MD-2 residues with which they interact are represented in sticks.

Stability of the predicted TLR4/MD-2/ligand complexes was further studied by molecular dynamics (MD) simulations. We selected two of the best binding poses for each ligand (SI Figure 35): one type A (antagonist-like binding pose), and one type B (agonist-like binding pose), plus two additional poses for compounds FP10 and FP7. Therefore, a total of eight 50 ns MD simulation were run. SI Figure 36 shows the motion of MD-2 over time and the RMSD and RMS fluctuation per residues, as well as the motion of Phe126 side chain over time. All the complexes showed stable ligand-receptor interactions along the MD simulation time as predicted by the docking calculations. In particular, in the MD simulation of the TLR4/MD-2/FP7 complex in the type A (antagonist-like) binding pose, the Phe126 side chain moves around its initial position staying largely exposed to the solvent in a conformation in agreement with the X-ray crystallographic antagonist conformation of MD-2 (Figure 24A). To evaluate the relative orientation between the ligands and MD-2, we arbitrarily defined two vectors, one from the amide α-carbon atom to the ester α-carbon atom of the ligand, and another one from the α-carbon of residues Pro78 to Thr105 of MD-2 (SI Figure 37A). SI Figure 38 shows the angle between these two vectors, both over time and as a percentage of frames per 0.1 degree angle range. It was observed that none of the ligands undergoes orientation flip during the 50ns simulations, all

remaining in the orientation from the docking process. Interestingly, Figure 24B shows that only in the case of the TLR4/MD-2/FP116 complex with FP116 in the type A (antagonist-like) binding pose, the orientation of Phe126 side chain flips over. We monitored this flipping behavior along the MD simulations, for all the ligands (data shown in SI Figure 37B and SI Figure 39), by arbitrary choosing two vectors, within MD-2, both starting from the α-carbon of residue Phe126 to, respectively, the phenyl C-4 atom of the same residue and the α-carbon of residue Ser21. This observation could suggest that FP116 is not able to efficiently retain an antagonist conformation of MD-2, thus pointing to a poor antagonist capacity. LogP values of compounds FP10, FP12, FP7 and FP116 were computationally calculated, ranging from approximately 4 to 10 with a linear distribution (SI Figure 40). The highest logP value was obtained for FP116 indicating a high lipophilicity that might result in low water solubility. This was in agreement with the lower acyl chain mobility as analysed by FT-IR spectroscopy (see below), and did not interfere with the performance of the cell assays. Summarizing, computational studies assessed the ability of ligands FP7, FP10, FP12, and FP116 to bind both CD14 and TLR4/MD-2, pointing to the long FP116 acyl chain (C16) as the maximum length bordering good (predicted) binding properties.

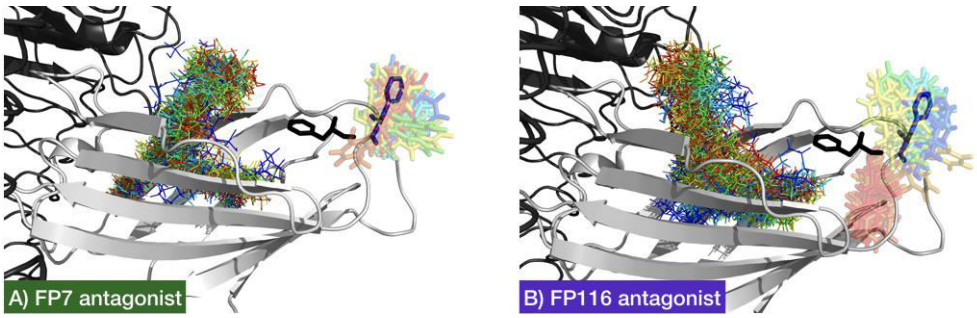

Figure 24. Superimposition of different snapshots (one for each simulated nanosecond), from the MD simulations of the TLR4/MD-2/ligand complexes, colored from blue (t=0 ns) to red (t=50 ns). Only ligands (as lines) and Phe126 (in sticks) are made visible. Side chains of Phe126 from the X-ray crystallographic structures have been superimposed to the snapshots to illustrate the antagonist (dark blue, PDB-ID 2E59) and agonist (black, PDB-ID 3FXI) conformations of MD-2. A) TLR4/MD-2/FP7 complex starting from the type A binding pose (antagonist-like); B) TLR4/MD-2/FP116 complex starting from the type A binding pose (antagonist-like).

Compounds were therefore synthesized and tested.

Synthesis of FP variants

Compounds FP7, FP10, FP12, and FP116 were synthesized according to a divergent synthetic strategy starting from the common precursor **4** (Scheme 1).

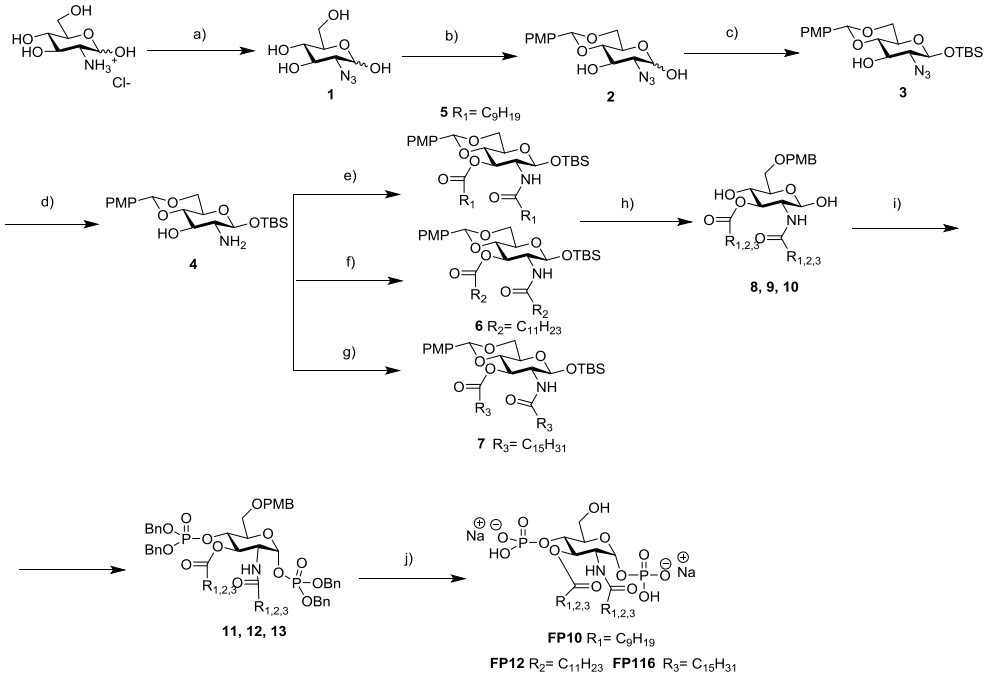

Scheme 1. Reagents and conditions: (a) $CuSO_4$, TEA, Py:H_2O, 0 °C, 30 min then TfN_3, Py, 0 °C-->rt, O.N., quant.; (b) p-MeOPhCH$(OMe)_2$, CSA, DMF dry, 40 °C, 8h, 68%; (c) TBSCl, imidazole, CH2Cl2 dry, rt, 1.5 h, 62%; (d) PPh_3, THF/H_2O, 60 °C, 2 h, quant.; (e) decanoic acid, EDC, DMAP, CH_2Cl_2 dry, rt, 6 h, 79%; (f) lauroyl chloride, DMAP, Py dry, 0 °C-> rt, O.N., 79%; (g) palmitoyl chloride, DMAP, Py dry, rt, O.N., 75%; (h) $NaCNBH_3$, 4 Å MS, THF dry, rt, O.N., then HCl 1 M in dioxane until pH 2, 12-70%; (i) $(BnO)_2PNiPr_2$, imidazolium triflate, CH_2Cl_2 dry, rt, 30 minutes, then m-CPBA, 0 °C--> rt, O.N., 51-56%; (j) I) H_2, Pd/C, MeOH dry/CH_2Cl_2 dry, rt, O.N., II) Et_3N, III) IRA 120 H^+ resin, IV) IR 120 Na^+, 84%-quant.

Commercially available D-glucosamine hydrochloride was converted into the intermediate **4** by subsequent protection of C4 and C6 positions as *p*-methoybenzylidene and the anomeric (C1) position as *tert*-butyldimethylsislyl (TBDMS) ether [60]. Intermediate **4** was then acylated in positions C2 and C3 according to three different procedures, obtaining monosaccharides **8**, **9**, and **10** with, respectively, C10, C12 and C16 carbon FA chains. Compound FP7, with C14 chains, was obtained similarly following a published procedure [60]. Regioselective *p*-methoxybenzylidene ring opening as *p*-methoxybenzyl (PMB) ether in C-6, followed by phosphorylation of free hydroxyls in positions C1 and C4, and final deprotection of PMB ethers gave final compounds as triethylammonium ions. Exchange of triethylamonium with sodium (IR120 Na^+ ion exchange resin) followed by reverse-phase purification gave final compounds FP10, FP12 and FP116 with a purity ≥ 85%.

Aggregation properties of FP compounds

FT-IR studies

The mobility of the acyl chains is an important biophysical parameter of aggregated lipids. Biological lipids typically show a temperature-dependent phase transition from a highly ordered gel (Lβ) phase of the hydrocarbon chains at low temperatures (indicated by an absorption peak around 2850 cm^{-1}) to a fluid

liquid-cystalline (Lα) phase at higher temperatures (indicated by a absorption peak around 2852 cm^{-1}). The phase transition temperature (Tc) is characteristic of the chemical structure of the lipids. The FP compounds were analysed by FT-IR spectroscopy to determine the lipid phase in dependence of temperature. FP compounds with shorter acyl chains (FP10, C10 and FP12, C12) were found to be in a fluid Lα phase with high mobility of their acyl chains at all temperatures. FP compounds with a longer acyl chains (FP7, C14 and FP116, C16) showed a biphasic behavior with a clear Lβ to Lα phase transition with Tc around 28.5 °C for FP7 and around 40.2 °C for FP116 (Figure 25). Notably, the main phase transition of FP116 at 40.2 °C occurs along a broad temperature range and a second phase transition is observed around 65 °C. Thus, at a biological relevant temperature of 37 °C, FP10, FP12, and FP7 exhibit a fluid membrane phase, whereas FP116 is still in a rigid membrane phase and requires much higher temperatures for acyl chain melting to occur.

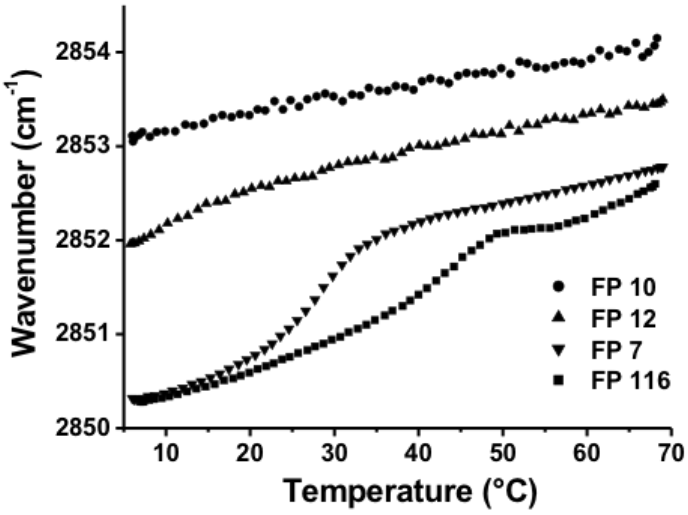

Figure 25. Acyl chain mobility of the aggregated FP compounds in dependence on temperature. The infrared absorption around wavenumbers 2850 - 2852 cm−1 corresponds to the symmetric stretching vibrations νs of the CH2 groups of the acyl chains. The wavenumbers indicated were derived from the peak absorption of νs(CH2) determined upon constant heating of the samples. Data are representative of two independent measurements.

NMR studies

The comparison of the ^{1}H NMR spectra recorded after compound dissolution in buffer, pH 7.4, 25 °C (SI Figure 41) suggested a different aggregation state of the bioactive compounds in solution in the μM concentration range. The ^{1}H NMR spectrum acquired on a 100 μM FP7 sample (SI Figure 41A) showed the presence of two set of signals (spectral region between 5.5 and 5.2 ppm).

In addition to a doublet of doublet and a triplet, corresponding to H1 and H3 protons (*), also two broad resonances (§) are present that can be assigned to aggregated species.

This hypothesis was supported by the comparison of spectrum SI Figure 41 with FP7 spectra recorded at higher concentrations, in particular 125 μM (Figure S9B) and 250 μM (SI Figure 41C), where the gradual decrease in sharp signal (*) intensity is associated with the increase of the broad resonance (§) ones, as expected as a consequence of FP7 aggregation. A further confirmation was achieved through the acquisition of relaxation-edited (SI Figure 41D) and diffusion-edited (SI Figure 41E) spectra, employed to partially filter out resonances from high molecular weight and low molecular weight species respectively.[31, 32] Indeed, the spectrum acquired with the CPMG sequence (SI Figure 41D), edited on the basis of relaxation times and thus highlighting the signals from low molecular weight species, showed a decrease of broad signal (§) intensities compared to spectrum SI Figure 41C; on the contrary, in the diffusion-edited spectrum (SI Figure 41E), whose parameters were set up to erase resonances from low molecular weight compounds, sharp resonances (*) disappeared. We can conclude that, under our experimental condition, FP7 was present in solution as a mixture of monomer/small aggregates and higher aggregated species (micelles), whose equilibrium changes

coherently to the variation of the nominal concentration of the molecule. Instead, only one set of sharp signals was observed in the ^{1}H NMR spectra recorded on FP10 and FP12 solutions containing the compounds in the concentration range 100 μM - 1 mM. Representative spectra acquired on 500 μM samples are depicted in SI Figure 41F-H for FP10 and SI Figure 41I-M for FP12. Furthermore, FP10 and FP12 resonances appear considerably narrower compared to FP7 signals (SI Figure 41A). Collectively, these findings suggest an appreciably higher solubility of FP10 and FP12 in aqueous buffer solution and thus a lower propensity to form micelles. A different behaviour can be described for FP116. All the ^{1}H-NMR spectra acquired on this compound present broad resonances and no sharp signals, expected for the free monomer. Thus, in the range of tested concentrations (125 - 500 μM), FP116 is always present in an aggregated form. Representative spectra acquired on a 250 μM FP116 sample are reported in SI Figure 41 N-P.

SAXS studies

SAXS profiles were measured in dependence of temperature to obtain information on the supramolecular organization of the molecules. The data are given in the range of the scattering vectors relevant for structure assignment. All FP compounds showed isotropic scattering, indicating no preference for a predominant orientation of the aggregates. On Figure 26 FP10

and FP12 showed diffuse symmetric scattering curves dominated by the form factor, characteristic of unilamellar aggregates with large interbilayer distance and probably owing to the negative surface charge of the two phosphate groups that leads to a net electrostatic repulsion of the bilayers. The scattering of FP10 shows two maxima at 5.58 and 3.38 nm, the latter could indicate the formation of interdigitated bilayers (3.38 nm). For FP12, a single peak is observed at 20 °C (up to 35 °C, data not shown) indicating the formation of correlated multilayers with a d-spacing of 4.14 nm, which is also consistent with the formation of an interdigitated bilayer structure. In contrast, FP7 does show a different scattering pattern, which indicates the occurrence of a non-lamellar structure. The spacing relationship exhibits clear similarity with cubic structures with a space group relationship of aQ 12.7 nm (not visible), aQ/√3 (7.29 nm), aQ/√5 (5.68 nm), aQ/√8 (4.53 nm), and aQ/√11 (3.86 nm), agreeing most likely with space group Q_{212}. The tendency to a non-lamellar structure of FP7 however could explain the slightly lower antagonistic activity of FP7 compared to FP12. In contrast to the above FP compounds, FP116 showed very weak scattering intensities hardly displaying a form factor which can be explained by a much lower solubility observed for the FP116 preparation and supports the results obtained by NMR.

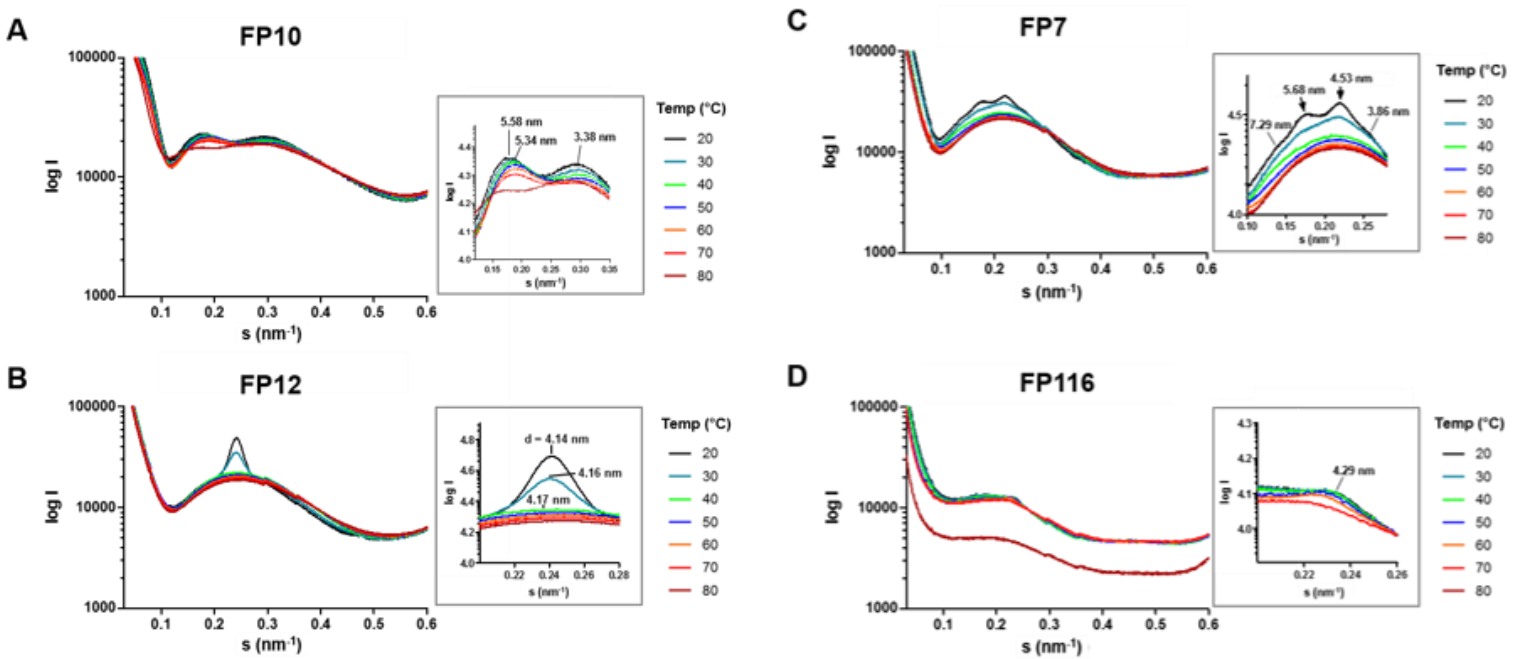

Figure 26. Small angle X-ray diffraction of aggregates in solution for FP10 (A), FP12 (B), FP7 (C), and FP116 (D). Scattering vectors are indicated for temperatures between 20 °C and 80 °C. Grey squares show enlargements of the relevant scattering vectors. The spacing of the diffraction maxima is indicted as d = 1/s (nm).

In vitro binding experiments with purified hMD-2

Expression, purification and activity of hMD-2

Recombinant human MD-2 (hMD-2) was used in *in vitro* binding experiments.

The functionality of this protein is a crucial prerequisite to obtain reliable results representative of specific, high-affinity molecular recognition of ligands [49]. Recombinant hMD-2 was expressed in *E. coli*, *Pichia pastoris* and mammalian HEK293 cells.

hMD-2 from different hosts was tested for its activity by incubating HEK/hTLR4 cells and then treating the cells with a mixture of hMD-2 and LPS (100 ng/mL). The TLR4-dependent IL-8 secretion by HEK/hTLR4 cells is indicative of functional MD-2. Figure 27 reports the lowest concentration of MD-2 required for maximum activation of TLR4 (quantified by IL-8 production), for each of the different expressed and purified hMD-2 proteins. hMD-2 produced and purified from HEK293T displayed the highest activity in stimulating the LPS/TLR4 inducible reporter at a concentration of 12 nM, followed by the hMD-2 expressed and purified from *P. pastoris* with its highest biological activity obtained at a concentration of 15 nM. Finally, hMD-2 purified from *E. coli* gave the lowest IL-8 production at the concentration of 245 nM.

The difference in activity of hMD-2 expressed in different hosts most likely reflects minor differences in protein folding and/or glycosylation [134,135]. The higher expression yield and the good activity prompted us to use hMD-2 from *P. pastoris* in *in vitro* binding experiments with synthetic compounds.

Binding studies were carried out by means of fours different techniques: two ELISA-type plate-based assays with immobilized protein, a fluorescence displacement assay and Surface Plasmon Resonance (SPR).

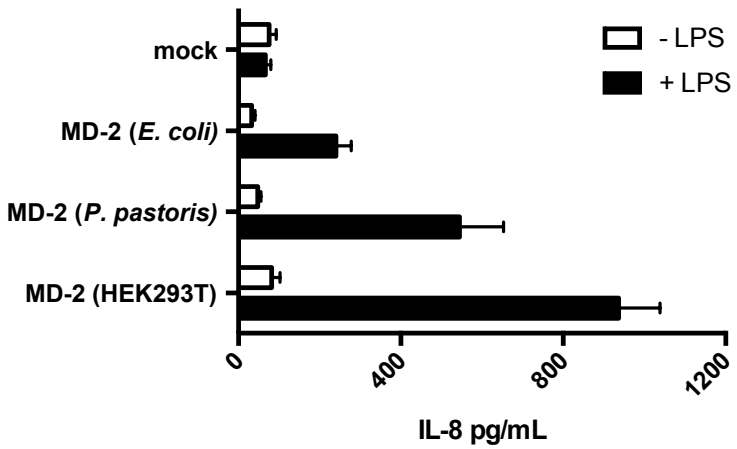

Figure 27. Activity of hMD-2 expressed in different hosts: maximum activation of TLR4 (quantified by IL-8 production) at the lowest concentration of hMD-2 under the different expressed conditions (bacteria 245 nM, yeast 15 nM, and mammalian 12 nM). Results are mean ± SEM from three parallels representative of at least three independent experiments.

ELISA competition experiments with anti-hMD-2 antibody

Direct binding of LPS, FP7, FP10 and FP12 to MD-2 was determined using a monoclonal antibody that binds to free hMD-2 but not to hMD-2 bound to LPS [151]. Monoclonal mouse anti-hMD-2 (9B4) antibody specifically binds to an epitope close to the rim of the LPS-binding pocket of hMD-2, available for recognition by the antibody only when the hMD-2 pocket is empty. This assay detected a decrease in binding to MD-2 in the presence of LPS (Figure 28A), similar to what previously reported [150]. A dose-dependent inhibition of antibody/MD-2 interaction was observed when adding FP7 and FP12, with a 90-95% decrease in binding obtained at concentrations of FP7 and FP12 of 20 μM (Figure 28A). 70% decrease in binding to hMD-2 was obtained with 20 μM of FP10 (Figure 28A), and 20% decrease was obtained with 20 μM of FP116 (Figure 28A).

These data showed that while FP7 and FP12 bind hMD-2 with high affinity, FP10 and FP116 are less potent ligands.

ELISA displacement experiment with biotinylated LPS

The ability of FP compounds to displace LPS from the pocket of hMD-2 was assessed by an ELISA plate-based assay.

The synthetic molecules were added at increasing concentration to hMD-2 that was already incubated with biotinylated LPS. FP7 and FP12 were able to displace biotin-LPS from hMD-2 in a

dose-dependent manner, with the highest displacement of 60-65% obtained at a concentration of 160 μM (Figure 28B). FP10 and FP116, at a concentration of 160 μM, gave a displacement of biotin-LPS of 20-30% (Figure 28B). LPS at a concentration of 40 μM gave the highest displacement of biotin-LPS of 70% (Figure 28B).

Fluorescence displacement assay

It has been previously shown that the fluorescent probe 1,1'-Bis(anilino)-4,4'-bis (naphthalene)−8,8' disulfonate (*bis*-ANS) binds to MD-2 and is displaced by LPS. bis-ANS presumably binds the same MD-2 binding site as lipid A and of other lipid A-like ligands [152].

TLR4 ligands interacting with MD-2 in a lipid A-like manner, are supposed to compete with bis-ANS and displace it from MD-2.

LPS, FP7, FP10, and FP12 caused a concentration-dependent decrease of bis-ANS fluorescence, indicating competitive binding to hMD-2 (Figure 28C). FP116 induces only a modest decrease of bis-ANS fluorescence at the tested concentrations (Figure 28C), thus confirming that the lack of activity on cells could be related to low affinity binding of this molecule to hMD-2.

Surface Plasmon Resonance (SPR) analysis

SPR data with immobilized hMD-2, showed direct interaction of the receptor with LPS (control) and with the tested synthetic compounds. K_D values derived from sensorgrams analysis were 3 μM, 13.7 μM, 22 μM, and 66.8 μM for FP12, FP7, FP10, and FP116, respectively (Figure 28E-H). SPR experimental curves optimal fitting was obtained by assuming 1:1 ligand/MD-2 stoichiometry.

Together, the results obtained from these *in vitro* cell-free studies clearly indicate that FP7, FP10, FP12, and FP116 directly interacted with MD-2, with the same order of potency found in human and murine cell experiments FP12(C12)>FP7(C14)>FP10(C10)>>FP116(C16).

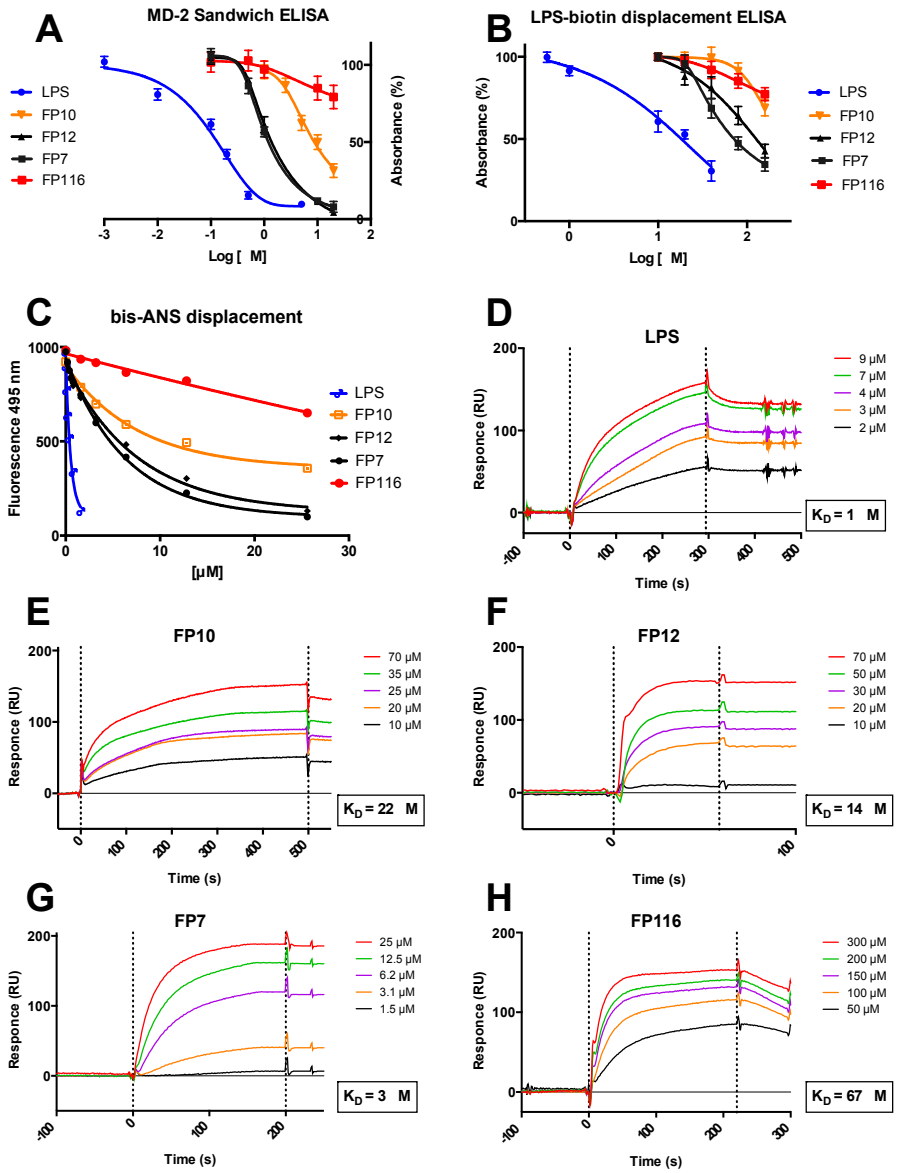

Figure 28. Binding studies on purified hMD-2**.** A) Molecules prevent anti-hMD-2 MAb binding in a dose-dependent manner; B) Molecules competion with biotin-LPS for hMD-2 binding; C) Molecules dose-dependently inhibit bis-ANS binding to hMD-2; D-H) SPR analysis show direct interaction between LPS, FP10, FP12, FP7, and FP116 and MD-2. Results are mean ± SEM from 3 parallels representative of at least 3 independent experiments.

Cell experiments

Modulation of LPS-stimulated TLR4 signaling in HEK cells

In order to evaluate the influence the fatty acids length on the TLR4 antagonist activity, molecules FP10, FP12, FP7, and FP116, constituting the homologous series with fatty acid chain lengths C10, C12, C14, and C16, were first tested on HEK-Blue hTLR4 cells. These cells are engineered to stably express the human receptors of the LPS recognition complex (hTLR4, hMD-2 and hCD14) and a reporter gene (SEAP) placed under the control of two TLR4-dependent transcription factors (NF-κβ and AP-1). Results from MTT assay revealed that all compounds did not have a negative effect on cell viability at the concentration of 10 μM used in experiments (SI Figure 42). FP7, FP10 and FP12, but not FP116, inhibited in concentration-dependent manner the TLR4 signaling in HEK-Blue cells (Figure 29). FP7 displayed the expected antagonistic activity [60]. FP10 and FP12 showed IC_{50} respectively higher (5.45 μM) and lower (0.63 μM) than FP7 (2.0 μM) (Figure 8B).

These results demonstrated the efficacy of fatty acid chains lengths (C10, C12 and C14) of FP7 variants to negatively modulate TLR4 signaling in HEK-Blue cells, the order of activity being: FP12(C12)>FP7(C14)>FP10(C10)>>FP116(C16).

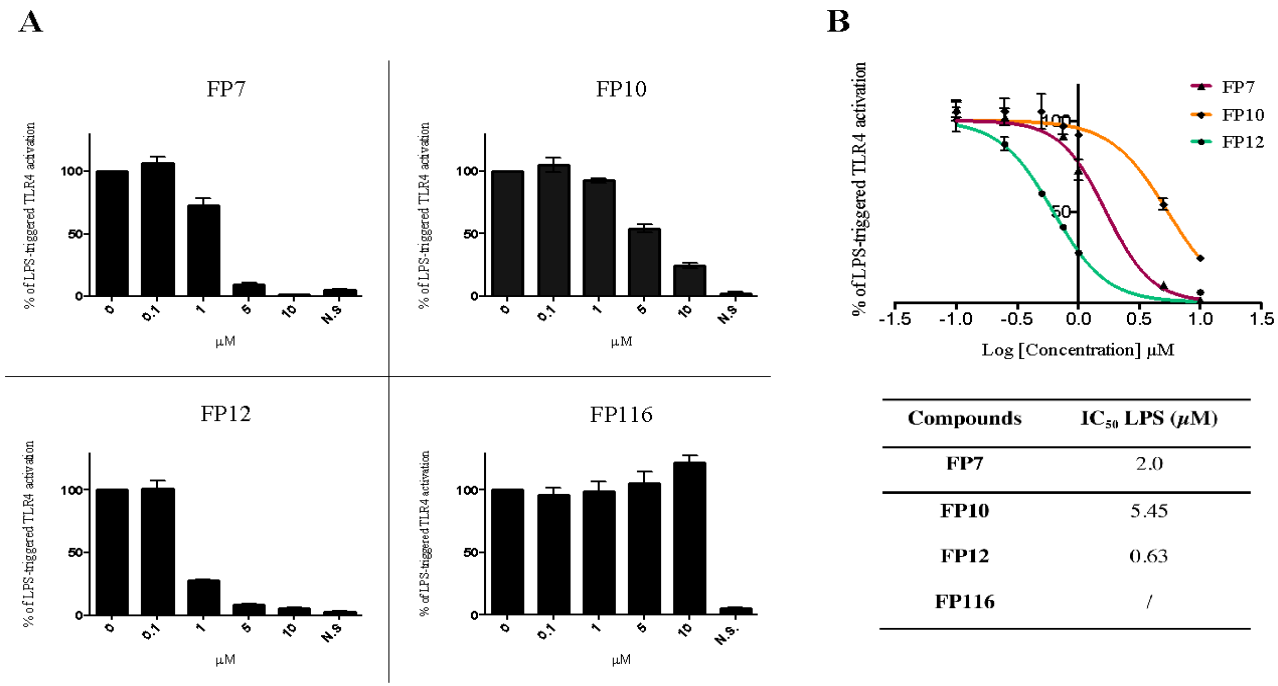

Compounds	IC_{50} LPS (μM)
FP7	2.0
FP10	5.45
FP12	0.63
FP116	/

Figure 29. LPS-triggered TLR4-dependent NF-κβ activation in HEK cells. A) Cells were pre-incubated with the indicated compounds and stimulated with LPS (100 ng/mL); B) TLR4-dependent NF-κβ dose-dependent inhibition curves of compounds. IC_{50} values in the table on the bottom. Data were normalized to stimulation with LPS alone. Results are mean ± SEM from three parallels representative of at least three independent experiments.

Modulation of LPS-stimulated TLR4 signaling in murine macrophages

Several TLR4 modulators mimicking lipid A have different effect on human and murine TLR4. For certain compounds when passing from murine to human TLR4/MD-2/CD14 system the agonistic effect switched to antagonistic effect [175]. The species-specificity is due to differences between hMD-2 and mMD-2 binding regions that induce different positioning of the same ligand thus causing different activity. In this experiment we aimed to investigating the effect of glucosamine derivatives in murine RAW-Blue macrophages. These cells are derived from RAW 264.7 and possess the same reporter gene present in HEK-Blue hTLR4 cells (SEAP). We first verified the capacity of FP compounds to stimulate the TLR4 response in RAW-Blue cells and we found all molecules inactive (SI Figure 43). When administrated before LPS, FP7, FP10, and FP12 were active in inhibiting TLR4-dependent NF-κβ activation in RAW-Blue macrophages (Figure 30A-B). Similarly to what happened in the case of human HEK cells, FP116 turned out to be inactive as antagonist. Notably, FP12 was the most active antagonist compound (IC_{50} = 1.7 μM). The activity order of the tested compounds was found to be the same than in human HEK cells: FP12(C12)>FP7(C14) >FP10(C10)>>FP116(C16).

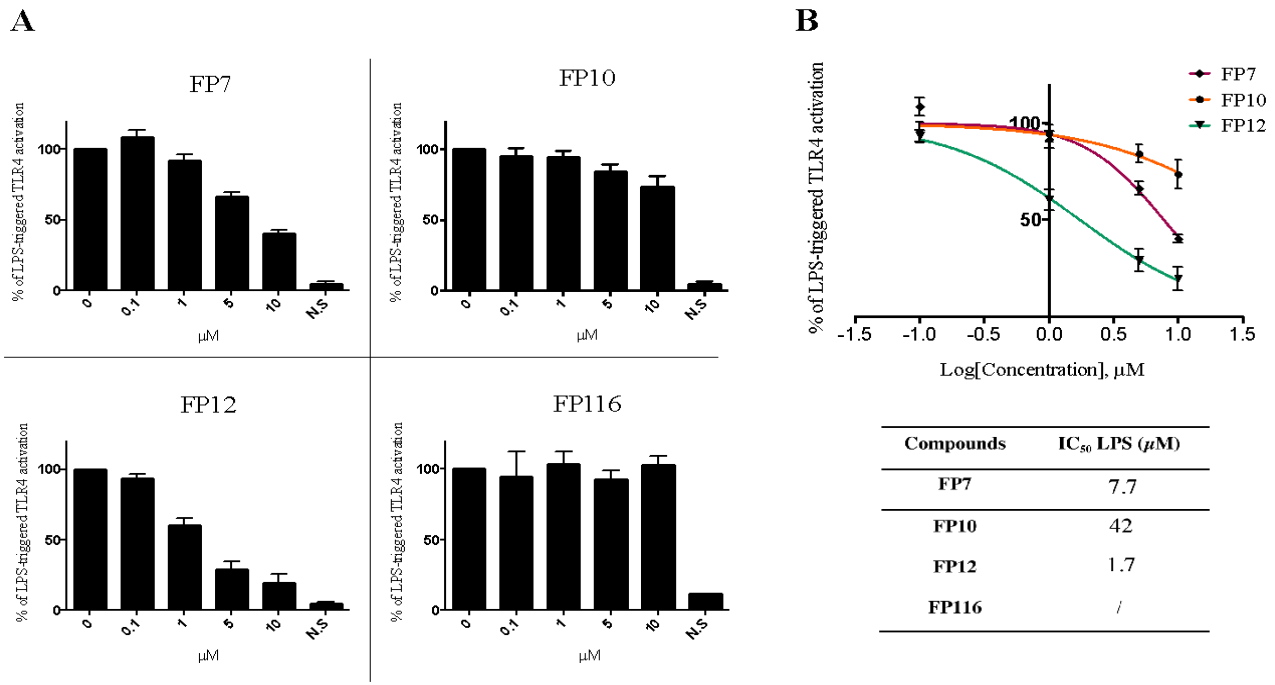

Compounds	IC_{50} LPS (μM)
FP7	7.7
FP10	42
FP12	1.7
FP116	/

Figure 30. LPS-triggered TLR4-dependent NF-κβ activation in RAW cells**.** A) Cells were pre-incubated with the indicated compounds and stimulated with LPS (10 ng/mL); B) TLR4-dependent NF-κβ dose-dependent inhibition curves of compounds. IC_{50} values in the table on the bottom. Data were normalized to stimulation with LPS alone. Results are mean ± SEM from three parallels representative of at least three independent experiments.

Effect of FP variants on LPS-induced TLR4 signaling in THP-1 cells

Haematopoietic TLR4 has been shown to play a critical role in any stage of inflammatory process. Furthermore, immune competent cells use TLR4 signaling to sense danger molecules and produce proinflammatory proteins that initiate and amplify the inflammatory process. To test the potential of FP variants to modulate TLR4 signaling pathways we utilised THP-1 cells as an *in vitro* model. Initially, we evaluated the effect of FP variants on THP-1 cell viability. THP-1 cells were exposed to different concentrations of FP variants (0-10 μM) in the presence or absence of LPS (100 ng/mL) for up to 24 h. Results from MTT assay demonstrated that FP variants/LPS did not affect cell viability (SI Figure 44). To determine the effect of FP variants on TLR4 signaling, next we analysed IL-8 expression, a well known TLR4-dependent proinflammatory cytokine produced in THP-1 cells in response to LPS. ELISA results clearly demonstrated the potential of FP7 and FP12 at 10 μM to inhibit LPS driven IL-8 production (Figure 31). In contrast, FP10 and FP116 had a modest or non-significant impact on IL-8 expression respectively (Figure 31). We have demonstrated that FP7 exerted a negative effect on TLR4 signaling in different cell types (unpublished data).

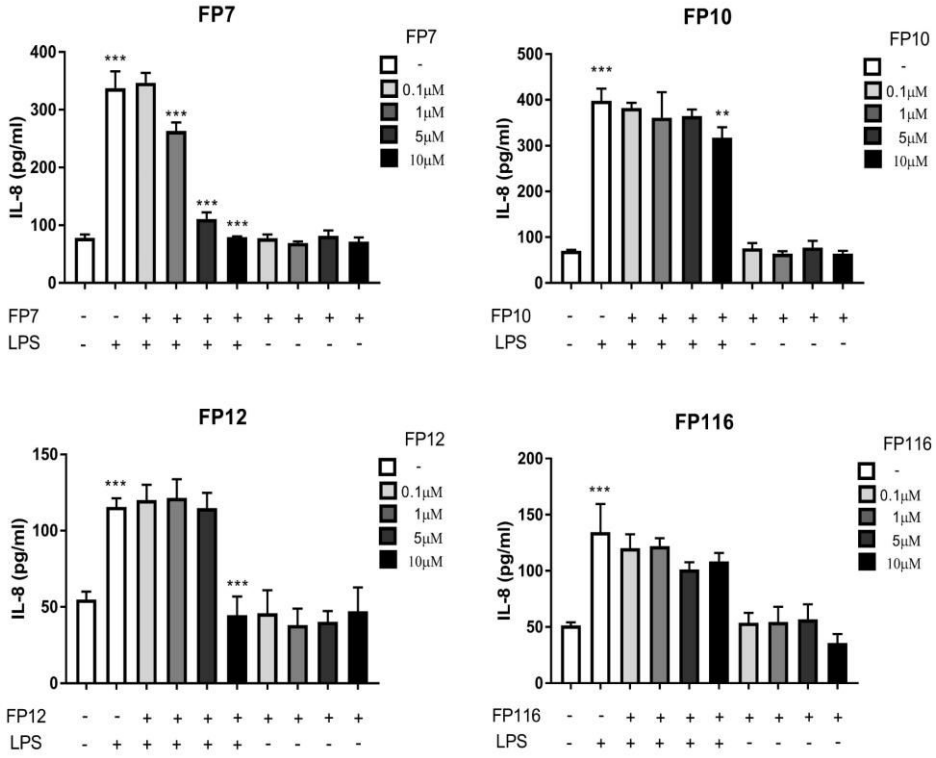

Figure 31. The Effect of FP variants on LPS/TLR4 induced production of IL-8 in THP-1 cells. THP-1 cells were pre-treated with FP variants (0 - 10 μM) for 1 h prior to LPS exposure. Cells were then left to incubate 16 h further in the presence or absence of LPS (100 ng/mL). IL-8 production was measured by ELISA. Results are displayed as mean concentration ± SD of three independent experiments. Significant results are indicated as *P>0.05 **P>0.01 ***P>0.001 for LPS vs Control and LPS vs FPs treated samples (Anova).

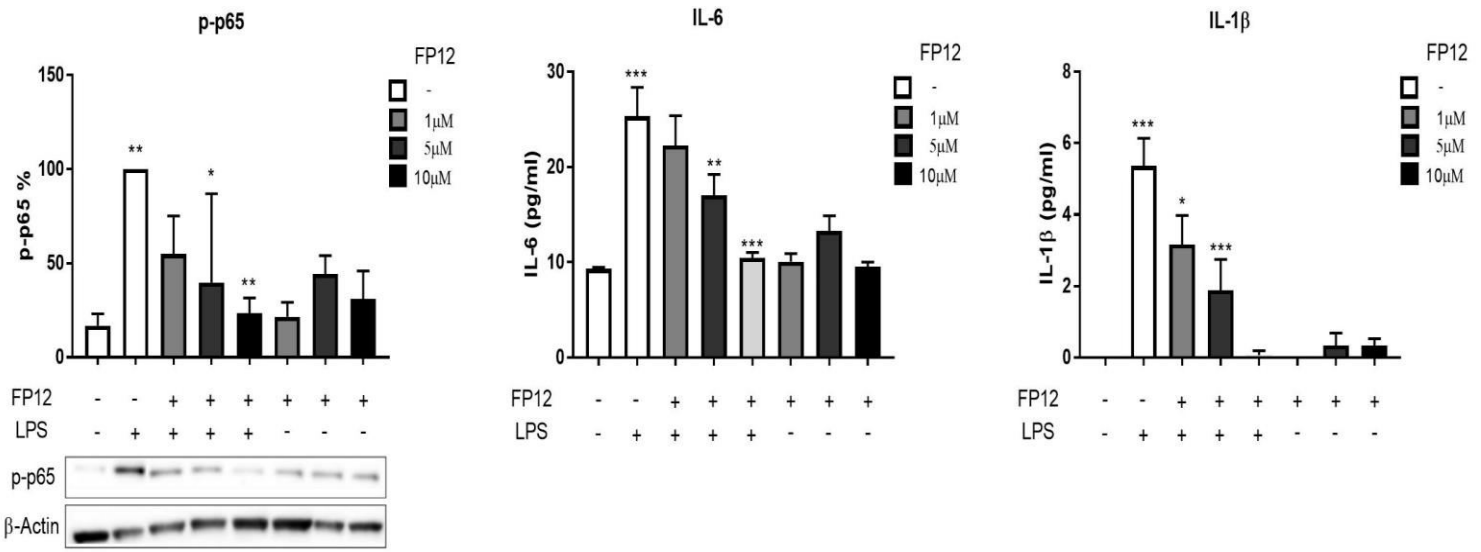

Figure 32. FP12 negatively regulates p65 NF-κβ phosphorylation and production of IL-6 and IL-1β in THP-1 cells. THP-1 cells were pre-treated with compound FP12 (0 - 10 μM) for 1 h prior to LPS exposure. Cells were then left to incubate 1 and 16 h further in presence or absence of LPS (100 ng/mL). p65 NF-κβ phosphorylation was determined in cell lysates using Western Blot analysis and cytokine production was measured by ELISA after 16 h of LPS exposure respectively. Results are displayed as mean concentration ± SD of three independent experiments. Significant results are indicated as *P>0.05 **P>0.01 ***P>0.001 for LPS vs Control and LPS vs FP12 treated samples (Anova).

Following on from comparative analysis based on TLR4-dependent IL-8 expression and tendency on the binding affinity with MD-2 of FP7 variants we found that the structural modification of FP12, but not FP10 and FP116 is related to antagonistic activity of the compound. In support to this notion, we further investigated the ability of FP12 to modulate second messengers in TLR4 signaling. Immunoblotting data revealed that FP12 significantly downregulated p65 NF-κβ phosphorylation that was associated with a strong inhibition of the expression of additional TLR4-dependent cytokines (IL-6 and IL-1β) in a dose-dependent manner (Figure 32). These data demonstrate that FP12 is a negative regulator of TLR4 signaling in THP-1 cells.

Discussion

The homologous series of FP glycolipids with fatty acid chain lengths varying from 10 to 16 carbon atoms were rationally designed as MD-2 ligands and synthesized.

In a first set of *in vitro* experiments we aimed at studying the SAR of these molecules in binding experiments with functional hMD-2. For this purpose hMD-2 expressed in yeast (*P. pastoris*), was used because it showed higher activity in responding to LPS stimulus than bacterial (*E. coli*) hMD-2 and was produced with higher yields than hMD-2 from mammalian (HEK) cells. Four different binding experiments between synthetic compounds and

hMD-2 were carried out. These were competition (displacement) experiments in which the synthetic glycolipids compete with biotin-LPS, with the fluorescent MD-2 ligand bis-ANS and with anti-MD-2 antibody for MD-2 binding. SPR measurements allowed to analyze directly the binding between synthetic glycolipids and hMD-2. All binding experiments consistently provided the same order of affinity among hMD-2 and synthetic molecules: FP12(C12)>FP7(C14) >FP10(C10)>>FP116(C16).

The biological activity was then assessed on cells: when provided alone, the synthetic FP compounds did not display any TLR4 agonist activity in human and murine cells. On the contrary, when administrated with LPS, the molecules with C10, C12, and C14 chains (respectively, FP10, FP12 and FP7) were active in blocking LPS/TLR4 signal (antagonism) in human and murine cells, while the molecule with C16 chains (FP116) showed very weak, or no activity. The order of activity of FP variants as TLR4 antagonists was confirmed in human (HEK-TLR4 and THP-1) and murine (RAW macrophages) cells. The molecules with C10, C12, and C14 chains seem to be non-species specific TLR4 antagonists, because these compounds are active in both human and murine cells, with higher potency in human ones. The compound with higher biological activity was FP12, with 12 carbons, followed by FP7 and FP10 with 14 and 10 carbons, while FP116 with 16 carbons showed very weak or no activity in

cell models. The variation of compounds' functional activity was related to the number of carbon atoms of the aliphatic chains which could be described by a bell-shaped curve with a maximum at C12. This is a common structure-activity trend that is found in a number of series of homologous compounds in medicinal chemistry and can be explained in terms of docking within the binding pocket of the pharmacological target (as it exists an optimal number of carbon atoms that can be accommodated into the pocket) and also in terms of variation of solubility and bioavailability (when the chain length is too long the solubility and the biological activity decreases). The difference of TLR4 functional activity of FP monosaccharides related to FA chains length can be explained in terms of their interaction with MD-2(/TLR4) and/or by their aggregation properties in a solution.

The docking and MD simulation studies have shown that FP10, FP7 and FP12 would accomplish optimal binding properties while FP116 could be bordering the limits of the maximum length compatible with a proper MD-2 binding. Although MD-2 pocket is able to host until five FA chains, the highly long and flexible C16 acyl chains present in FP116 seem to point to less efficient ability to interact with TLR4/MD-2 in an antagonistic binding mode, given that the required exposed conformation of Phe126 side chain could be jeopardized.

Additionally, calculated logP values for the FP variants point to a very high lipophilicity for FP116, maybe affecting the aggregation properties in solution.

Taken together, these data strongly suggest that the mechanism of TLR4 antagonism of that class of compounds is mainly based on the competition with LPS (or other ligands, as bis-ANS) in the binding to the MD-2/TLR4 complex.

Interestingly, an identical order of activity on TLR4 has been found in a series of monosaccharide TLR4 agonists, the Gifu Lipid A (GLA), and the following order of potency in inducing the production of TNF-α in murine cells was detected: C12>C14>C10>>C16 [167]. Also in the case of GLA compounds, with three FA chains and one phosphate in C-4 position, the C12 and C14 variants were the most active ones, C10 less active and C16 were inactive. Similarly to FP compounds, GLA are more active on murine than on human cells [167]. However, the authors did not provide any evidences or explanation about the link between TLR4 activity of monosaccharide and FA chain length.

Regarding the aggregation properties some important differences among FP compounds were detected by FT-IR analysis in solution. These measurements showed marked variations in acyl chain fluidity of aggregated FP compounds depending on the

chemical structure. The phase transition temperature Tc exhibits a clear inverse correlation with the length of the acyl chains with Tc C16 >> Tc C14 > Tc C12 > Tc C10. Of note, this behavior results in marked differences at the biological relevant temperature of 37 °C, where FP10, FP12, and FP7 are in a fluid membrane phase, whereas FP116 is still in a rigid membrane phase and requires much higher temperatures for acyl chain melting to occur. The occurrence of a very broad phase transition at temperatures above 37 °C and occurrence of a second phase transition at higher temperature as observed for FP116 was also found for inactive glucosamine monosaccharide GLA compounds [176]. Differences in phase behavior have also been shown for the TLR4 ligands lipid A and LPS. The antagonistic tetraacylated synthetic compound 406 is highly fluid at 37 °C, whereas the biologically active hexaacylated compound 506 and LPS Re have phase transition temperatures above 37 °C [177]. The fluidity state of the acyl chains in aggregated glycolipids is thus not an exclusive determinant of inflammatory or antagonistic activity of chemically different compounds. It is rather a modifying parameter of biological activity by affecting aggregate properties such as hydrophobic thickness, packing density, and aggregate stability. NMR and SAXS analysis revealed striking differences in aggregate formation of FP compounds which are likely to explain differences in their biological activity. Concentration-

dependent NMR analysis of the two most antagonistic compounds FP12 and FP7 revealed aggregation of FP7 (C14) at much lower concentrations than FP12 (C12), reflecting further differences in the biophysical state and bioavailability of these compounds. Aggregate structures resolved by SAXS analysis provided evidence for lamellar bilayer structures for FP10 and FP12, which are associated with antagonistic activity, for FP7 a tendency to for non-lamellar structures was determined. Considering the crucial role of lipid supramolecular aggregate structure for the presentation to LPS receptor molecules, the different aggregate structures observed by SAXS might explain the slightly lower antagonistic activity of FP7 compared to FP12 in some biological systems.

The present study provides structural and functional biological data demonstrating the ability of novel FP variants to negatively regulate TLR4 signaling in different cell model systems. Having shown the strong potential of FP12 to modulate second messengers activation and various end points of TLR4 signaling pathways including its lack of toxicity, this study supports the idea of further drug development of FP12 as a lead compound in preclinical and clinical studies for pharmacological intervention of inflammatory-based diseases.

Supplementary information (SI Figures):

Molecular Modeling

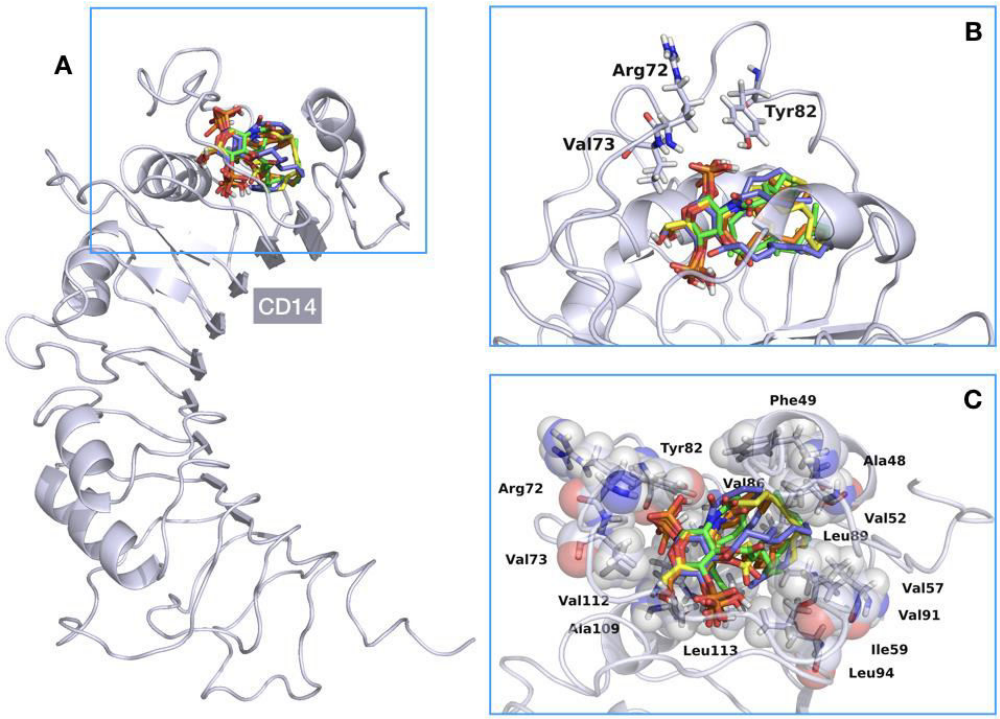

Figure 33. A) Full view of CD14 (in light blue). Superimposed best-score docked poses of FP10 (in orange), FP12 (in yellow), FP7 (in green), and FP116 (in violet) ligands are shown; B) Close-up of the binding pocket of CD14, showing the major interactions of the head groups of the ligands docked within the protein; C) Top view of the binding pocket of CD14. CD14 residues that form the hydrophobic pocket and whose side chains are close to the FA chains of the docked ligands are displayed in sticks and partially transparent spheres.

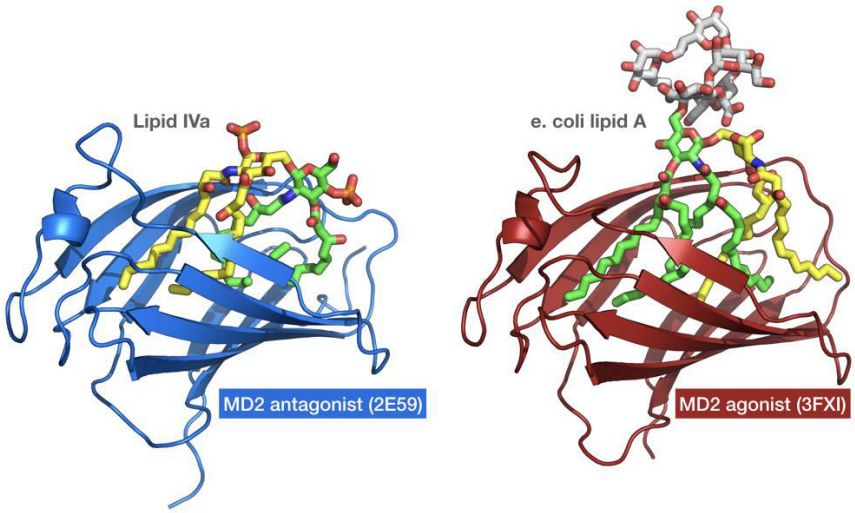

Figure 34. Left: representation of type A (antagonist-like) binding mode as known from lipid IVa in PDB-ID 2E59; right: representation of type B (agonist-like) binding mode as for *E. coli* lipid A in PDB-ID 3FXI.

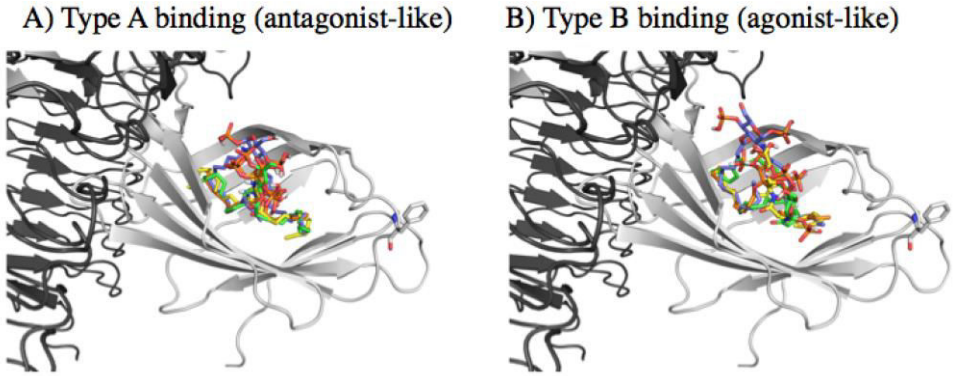

Figure 35. Selected docked poses of each ligand for MD simulations. A) Type A antagonist-like binding pose; B) Type B agonist-like binding pose. Ligands are depicted following the CPK coloring scheme, excepting the carbon atoms that are shown in orange for FP10, in yellow for FP12, in green for FP7, and in violet for FP116. TLR4 is colored dark, MD-2 is shown in light grey and Phe126 side chain is represented in sticks.

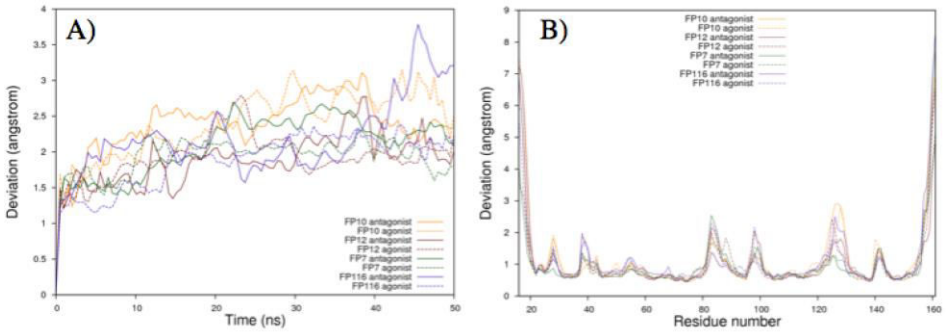

Figure 36. Molecular dynamics simulations of the TLR4/MD-2 system in complex with ligands FP10, FP12, FP7, and FP116. A) RMSD of the MD-2 backbone over time; B) RMS fluctuations per residues of MD-2.

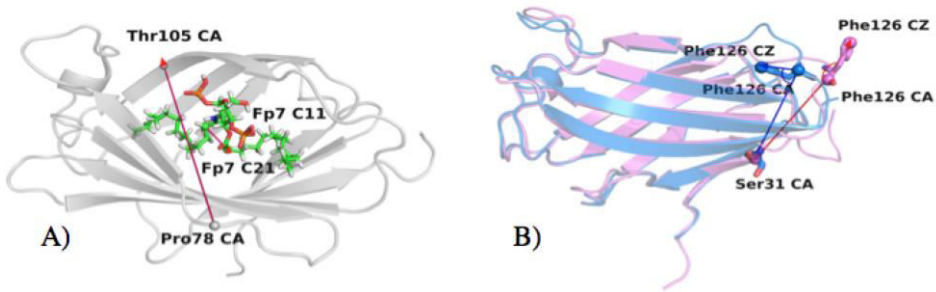

Figure 37. A) Representation of the vector from the α-carbon (CA) of Pro78 to the α-carbon of Thr105, and the vector from amide α-carbon atom (C11) and the ester α-carbon atom (C21) of FP7, used to follow the orientation of the ligands along the MD simulations (cf. S4). FP7 is used as an example; the same applies for the other ligands. MD-2 is represented in grey an FP7 is depicted in CPK coloring at the exception of the carbon atoms that are in green; B) Representation of two vectors, within MD-2, starting both from the alpha-carbon (CA) of residue Phe126 to, respectively, the phenyl C-4 atom (CZ) of the same residue and the α-carbon (CA) of residue Ser21. Agonist MD-2 from PDB-ID 2E59 and antagonist MD-2 from PDB-ID 3FXI are in semi-transparent blue and pink cartoons respectively.

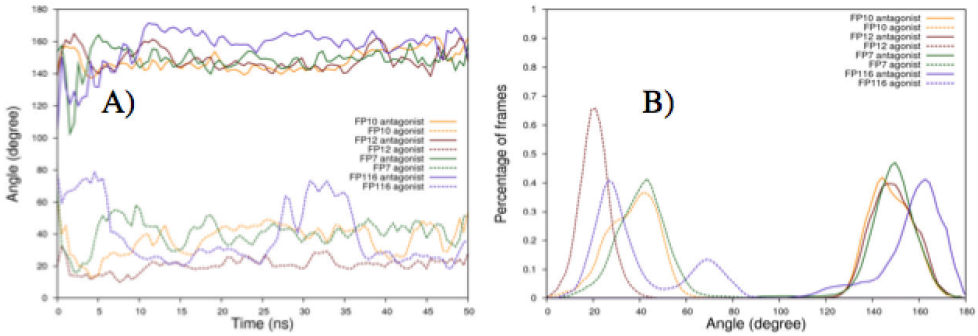

Figure 38. A) Angle between two vectors along the MD simulation. First was defined between the amide α-Carbon atom and the ester α-carbon atom of the ligand, and the second between the α-Carbon atoms of residues Pro78 and Thr105 of MD-2 (cf. S5A). Angle between 0 and 90 degrees is characteristic of the type B binding (agonist-like) as observed in the PDB-ID 3FXI (TLR4/MD-2/lipid-A complex); angle between 90 and 180 degrees is characteristic of the type A binding mode (antagonist-like) as observed in the PDB-ID 2E59 (TLR4/MD-2/lipid-IVa complex); B) Percentage of time frames along the MD simulation projected over angle.

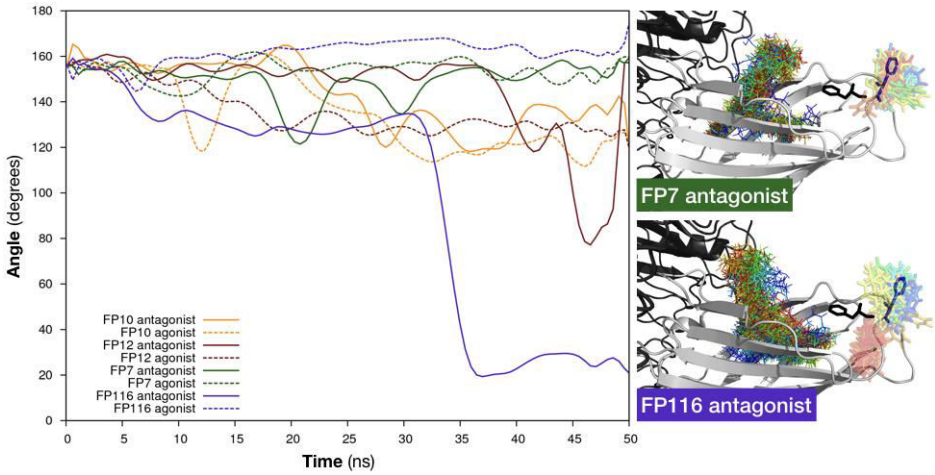

Figure 39. On the left: angle between two vectors defined in Figure S5B. The angle between these two arbitrarily selected vectors plotted over time illustrates the flip that residue Phe126 undergoes during the MD simulation when MD-2 is engaged by FP116 in the type A binding mode. On the right: superimposition of different snapshots (one for each simulated nanosecond), from the MD simulations, colored from blue (t=0ns) to red (t=50ns). From these snapshots only ligands (as lines) and residue Phe126 (as sticks) are made visible.

Figure 40. Computed logP values for compounds FP10, FP12, FP7 and FP116, as calculated in Maestro (www.schroedinger.com).

NMR spectroscopy

Freeze-dried compounds were reconstituted in 10 mM deuterated phosphate buffer at different concentration, ranging from 100 µM to 1 mM. pH values were measured with a Microelectrode (Mettler-Toledo, Greifensee, Switzerland) for 5 mm NMR tubes and adjusted to 7.4 with small amounts (few µL) of NaOD or DCl. The pH* reading in D_2O was corrected for the deuterium isotope effect at the glass electrode. The acquisition temperature was 25 °C. All spectra were acquired on a Bruker AVANCE III 600 MHz NMR spectrometer equipped with a QCI (^{1}H, ^{13}C, $^{15}N/^{31}P$, and 2H lock) cryogenic probe. 1D ^{1}H NMR spectra were recorded with water suppression (*noesygppr1d* pulse sequences in Bruker library), T_2-editing (*cpmgpr1d* pulse sequences in Bruker library) or diffusion-editing (*ledbpgppr2s1d* pulse sequences in Bruker library), 256 scans, a spectral width of 20 ppm, and a relaxation delay of 5 s. They were processed with a line broadening of 0.3 Hz and automatically phased and baseline corrected. Chemical shift values were internally calibrated to the D_2O peak at 4.79 ppm of a spectrum recorded without water saturation.

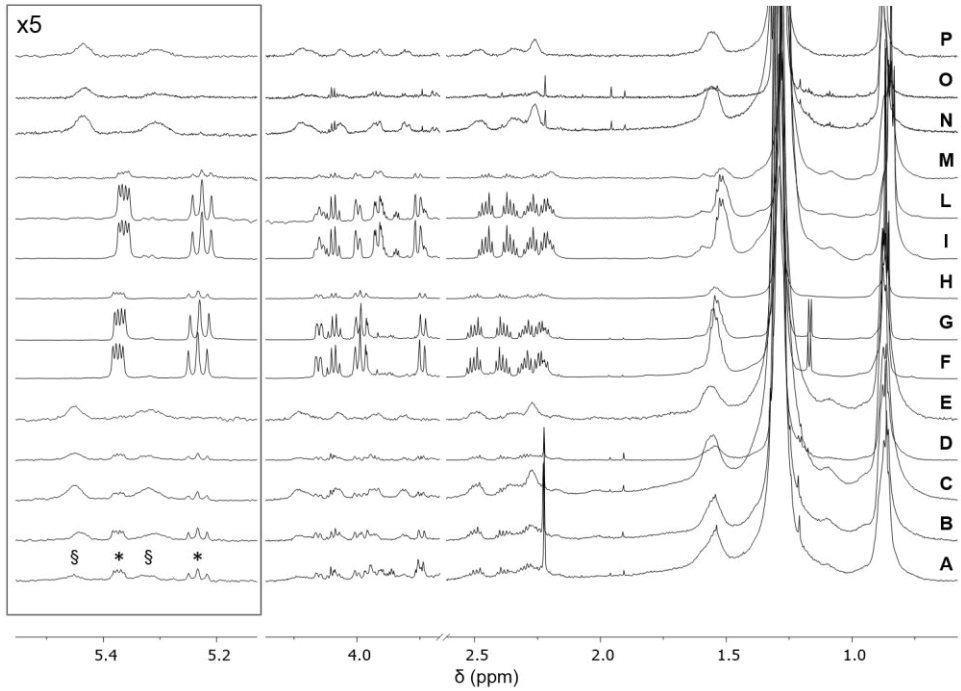

Figure 41. Comparison between FP7 (spectra A, B, C, D and E), FP10 (spectra F, G and H), FP12 (spectra I, L and M) and FP116 (spectra N, O and P) ^{1}H NMR spectra after compound dissolution in deuterated phosphate buffer 10 mM, pH 7.4, 25 °C. A) FP7 100 μM, ^{1}H NMR spectrum; B) FP7 125 μM, ^{1}H NMR spectrum; C) FP7 250 μM, ^{1}H NMR spectrum; D) FP7 250 μM, T_2-edited ^{1}H NMR spectrum; E) FP7 250 μM, diffusion-edited ^{1}H NMR spectrum; F) FP10 500 μM, ^{1}H NMR spectrum; G) FP10 500 μM, T_2-edited ^{1}H NMR spectrum; H) FP10 500 μM, diffusion-edited ^{1}H NMR spectrum, I) FP12 500 μM, ^{1}H NMR spectrum; L) FP12 500 μM, T_2-edited ^{1}H NMR spectrum; M) FP12 500 μM, diffusion-edited ^{1}H NMR spectrum; N) FP116 250 μM, ^{1}H NMR spectrum; O) FP116 250 μM, T_2-edited ^{1}H NMR spectrum; P) FP116 250 μM, diffusion-edited ^{1}H NMR spectrum.

Fourier transform infrared (FT-IR) spectroscopy

For FT-IR measurements, lyophilized FP compounds were dissolved in chloroform:methanol 1:1 (v/v) and dried under a stream of nitrogen. The dried lipid film was solubilized in 20 mM HEPES, 150 mM NaCl, pH 7.4 to a final concentration of 10 mM and incubated in a ultrasound bath for 30 min at 60 °C for aggregate formation. Aggregate preparations were temperature cycled three times between 4 °C and 60 °C (30 min each) and stored over night at 4 °C before measurements. FT-IR measurements were performed on a IFS-55 spectrometer (Bruker, Billerica, MA, USA). Aggregate preparations were placed between CaF_2 crystals and cooled to 4 °C. Temperature scans were performed automatically between 5 °C and 75 °C with a heating rate of 0.6 °C/min. For each measurement, 65 interferograms were accumulated, apodized, Fourier-transformed and converted to absorbance spectra. The main vibrational band used for the evaluation of the acyl chain mobility was the symmetrical stretching vibration ν_s (CH_2) located around 2852 cm^{-1} as described in detail by Brandenburg *et al.* [174]. The temperature of phase transition (Tc) between the ordered β-phase and the fluid α-phase was determined as the temperature of the inflection point of the peak absorption wavenumber.

Small angle X-Ray scattering (SAXS)

SAXS scattering experiments of aggregates in solution were performed at the BioSAXS beamline P12 of the European Molecular Biology Laboratory at the highly brilliant synchrotron light source PETRA III at DESY (Hamburg, Germany). An automatically xy- adjustable capillary sample holder with temperature control was used to analyze the phase dependent structure of aggregates in solution. For SAXS measurements, lyophilized compounds were dissolved in chloroform:methanol 1:1 (v/v) and dried under a stream of nitrogen. The lipid film was solubilized in 20 mM HEPES, 150 mM NaCl, pH 7.4 to a final concentration of 80 mg/ml. Aggregate formation was induced by ultrasound bath for 30 min at 60 °C. Preparations were then cycled three times for 30 min at 4 °C and 60 °C and stored over night at 4 °C. Samples were placed in 80 mm long 1 mm thick glas capillaries (Hilgenberger GmbH, Malsfeld, Germany). Diffraction experiments were performed with 0.04 s exposure time. 20 frames per sample were averaged. Scattering patterns were investigated in the range of the scattering vector $0.1 < s < 1.0\ nm^{-1}$ ($s = 2 \sin \theta/\lambda$, 2θ scattering angle and $\lambda = 0.124$ nm) and were recorded in dependence of temperature between 20 °C and 80 °C. Diffraction was detected on a 2D photon counting Pilatus 2M detector calibrated with silver behenate.

Characterization of chemical reactions

The reactions were carried out under a nitrogen atmosphere. TLC were performed using prepared plates of silica gel (Merck 60 F254 on aluminium) and revealed using UV light or staining reagents (H_2SO_4 (5% in EtOH), ninhydrin (5% in EtOH), basic solution of $KMnO_4$ (0.75% in H_2O), molibdate solution (molybdatophosphorus acid and Ce(IV) sulphate in 4% sulphuric acid). ^{1}H NMR (400 MHz) and ^{13}C NMR spectra (100 MHz) were recorded on a Varian spectrometer using partially deuterated solvents as internal standards. Purity of final compounds was ≥ 95% as assessed by quantitative NMR analysis.

MTT viability assay on HEK cells

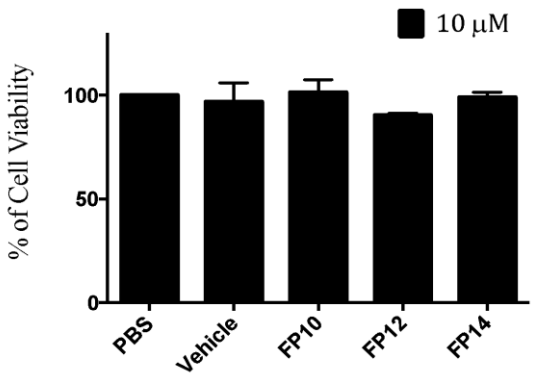

Figure 42. MTT viability assay on HEK cells. Cells were treated with compounds and incubated overnight. The DMSO:H_2O 1:1 solution is used as vehicle control to check for solvent toxicity. FP116 was not included in the assay as it is not active. Data is normalized to PBS treatment and represent the mean percentage ± SEM of at least 3 independent experiments.

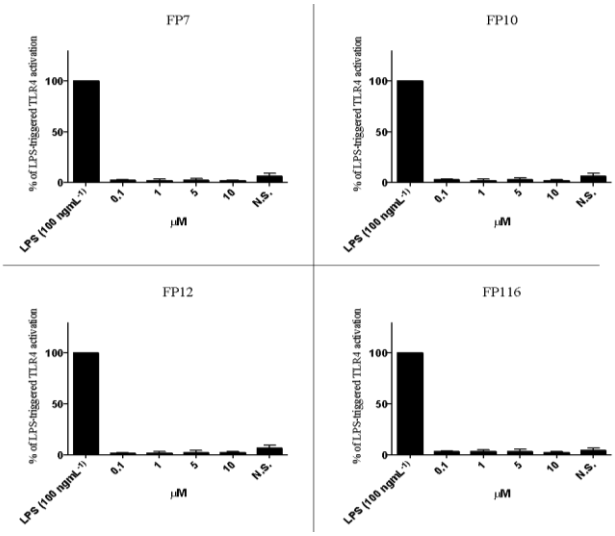

Figure 43. Dose-dependent activation of TLR4 signal in RAW-Blue™. The results were normalized to stimulation with the LPS alone.

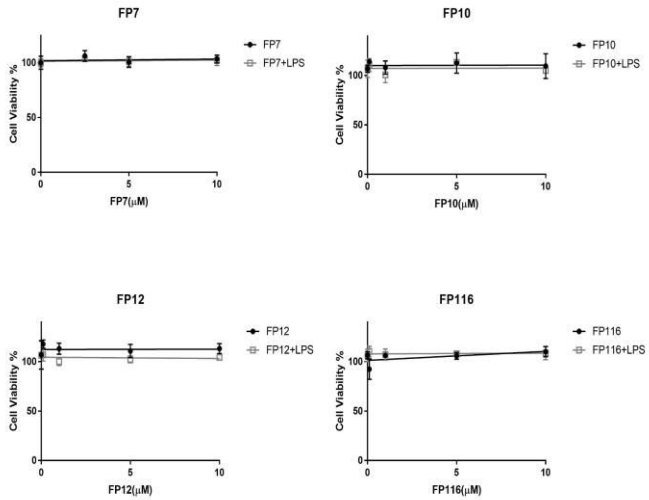

Figure 44. Effect of FP derivatives on cell viability in THP-1 cells. Cells were pre-treated with FP variants (0-10 μM) in the presence (grey) and absence (black) of LPS. Plates were incubated overnight and cell viability was measured using an MTT assay. Results are expressed as percentage of untreated cells accepted as (100% cell viability)

2.2 SAR study part II

This chapter is based on a manuscript in preparation.

New carboxylate-based TLR4 antagonists that bind to MD-2

Florent Cochet[1], Fabio A. Facchini[1], **Lenny Zaffaroni[1]**, Jean-Marc Billod[2], Helena Coelho[3], Aurora Holgado[4], Sonsoles Martin Santamaria[2], Jesus Jimenez Barbero[3], Rudi Beyaert[4], Francesco Peri[1*]

[1]Department of Biotechnology and Biosciences, University of Milano-Bicocca, Piazza della Scienza, 2; 20126 Milano (Italy); [2]Department of Chemical and Physical Biology, Centro de Investigaciones Biologicas, CIB-CSIC, C/Ramiro de Maeztu, 9, 28040 Madrid, Spain; [3]CIC bioGUNE, Bizkaia Technology Park, Building 801A, 48170 Derio (Spain); [4]Unit for Molecular Signal Transduction in Inflammation VIB-UGent Center for Inflammation Research, VIB Technologiepark 927, 9052 Zwijnaarde, Ghent (Belgium);

Introduction

The toll-like receptor 4 (TLR4) is the sensor of bacterial endotoxin (LPS), and it is present on immune cells of humans and animals (mainly macrophages and dendritic cells) [178]. TLR4 can senses minute amounts of LPS released by the Gram-negative bacteria. Upon bacterial infection, LPS triggers innate immune response by the TLR4 recognition pathway which activates the signaling cascade and lead to the production of pro-inflammatory molecules such as cytokines and chemokines [23]. Deragulated TLR4 activation can lead to a series of problematics, of which the more serious and often deadly is the acute sepsis syndrome [2]. On the other hand, TLR4 can also be activated by endogenous factors (DAMPs), which are the result of damaged tissues as a consequence of inflammatory and auto-immune diseases [179]. There is therefore a growing pharmacological interest in developing hit or lead compounds that are able to modulate TLR4 signaling [56]. These compounds (of synthetic or natural origin) should ideally compete with the natural ligands (PAMPs or DAMPs) for the binding site of the TLR4 co-receptor MD-2.

One of the most potent TLR4 antagonist is the synthetic compound E5564 (Eritoran) [35], a lipid A mimetic consisting of a glucosamine disaccharide with two phosphate groups in C1 and C4' positions, and four lipophilic chains. Other TLR4 antagonists deriving from structural simplification of Eritoran or of lipid A,

are based on a monosaccharide scaffold on which are present different acylated lipophilic chains, mimicking the reducing and non-reducing part of the lipid A molecule (Figure 45) [22].

Several research groups have worked intensively on lipid A mimetics. In some cases the anionic phosphate group has been replaced by the bioisosteric carboxylate group which mantains the negative charges (Figure 46) [180-185]. Some of these lipid A analogues were synthesized with different acylation pattern and substitution of the phosphate in the C1 position by carboxymethyl group [180-182], or carboxyl group [183]. In other lipid A analogues, the reducing sugar and phosphate have been replaced by an acylated diethanolamine bound to a phosphate or a carboxylic acid [184,185]. These last compounds, called glucosaminide-4-phosphates (AGP, Figure 46) were the first of their kind, and were designed and synthesized by Johnson *et al.* in 1999 [186].

AGP were subsequently developed as vaccine adjuvants as they retained the immune-stimulant activity TLR4 dependent. This TLR4 agonistic activity of AGP is a good indication that the bioisosteric substitution of the phosphate group in C1, with a carboxylic acid (thus maintaining the negative charge), does not alter the TLR4 agonistic effect of the starting compounds.

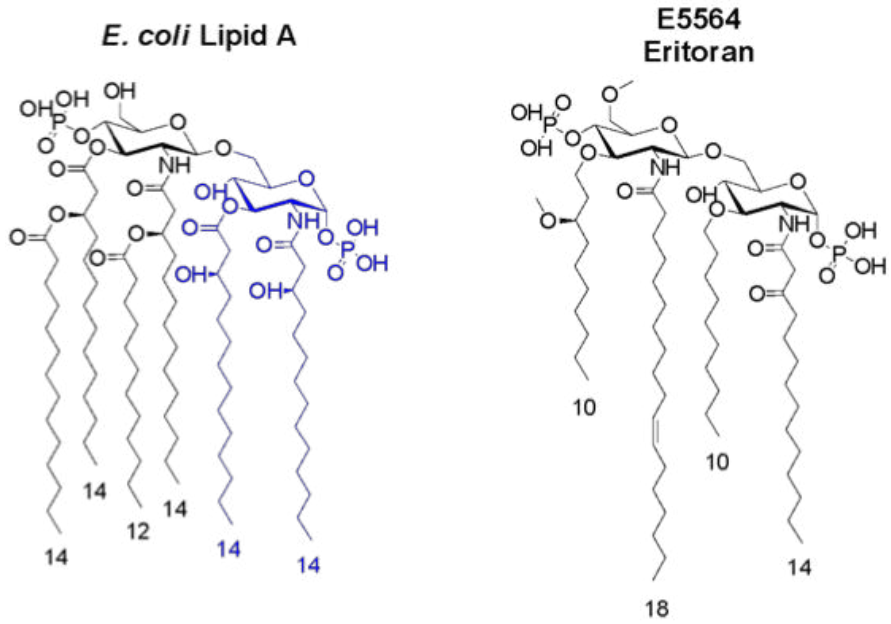

Figure 45. Chemical structure of *E. coli* lipid A (reducing part in black, non-reducing part in blue) and of synthetic TLR4 antagonist E5564 (Eritoran).

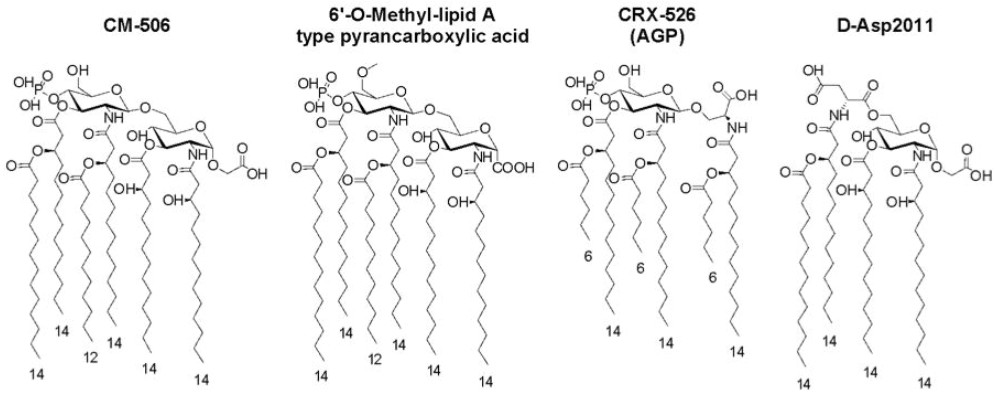

Figure 46. Collection of chemical structure of synthetic lipid A mimetics containing carboxylic acids, that are active as TLR4 modulators.

Herein we present a SAR study based on ligand-based drug design. It consists of combining partial structures which are derived from different active molecules, in order to obtain new TLR4 modulators.

In particular the compounds FP13, FP14, FP15, FP16, and FP17 (FP13-17, Figure 47) have been designed and synthetised. The idea behind these molecules is based on two considerations:

i) the well known TLR4 antagonist FP7 is a simple structure for the design of new molecules [61];

ii) substitution of phosphates with carboxylat allows in many cases reported in literature to maintain TLR4 activity [180-185];

The FP13-17 series consist of a monosaccharide derived from β-glucopyranoside conforming glucosamine, to which two units of succinate have been bound at C1 and C4 positions. The two carboxylic groups in C1 and C4 are in the form of β-carboxylated anions at neutral pH and therefore mimic the two negative phosphates of the FP7 molecule. In this context the carboxy groups are phospate bioisostere.

The FP13-17 series have in common the basic structure of the glucosamine skeleton bound to succinate groups at the C1 and C4 positions and differ with one another for the lipophilic chains attached to the monosaccharide in positions C2 and C3.

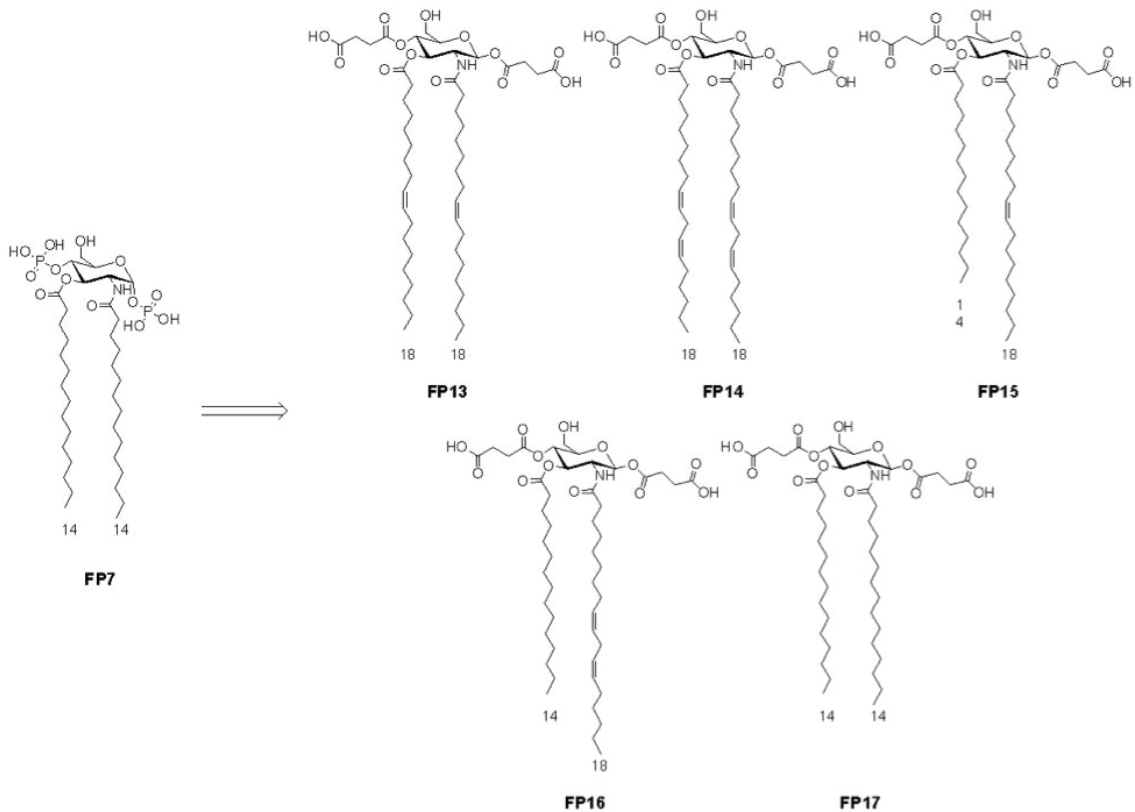

Figure 47. Chemical structures of the lead compound FP7 and the newly synthesized carboxylate monosaccharides derivatives FP13, FP14, FP15, FP16, and FP17 developed by our group,

As TLR4 antagonist Eritoran presents unsaturated chains (C18, cis-11), we thought to investigate the effect of saturated and unsaturated chains to the C2 and C3 positions of the glucosamine moiety. FP13 contains two oleic chains (C18, cis-9), FP14 two linoleic chains (C18, cis, cis-9,12), FP15 myristic at C3 (C14) and oleic at C2, FP16 myristic at C3 and linoleic at C2 and FP17 two myristic chains.

Experimental Section

Synthesis of FP variants

For the synthesis of FP13-17 compounds, a divergent strategy was initiated from D-glucosamine which was first treated with sodium azide and triflic anhydride to obtain the azido derivative at position C2. Subsequently, positions C4 and C6 were protected as 4,6-di-O-benzylidene and, finally, position C1 was protected in as *tert*-butyldimethylsilyl ether (TBDMS) to obtain compound **1** as a common intermediate of all molecules (Scheme 2).

For the synthesis of FP13, FP14 and FP17, compounds having C2 and C3 two identical chains, intermediate **1** was treated with triphenylphosphine (PPh_3) in tetrahydrofuran (THF) / water to reduce the azide to an amine and produce the intermediate **2** (Scheme 3A). The C2 and C3 positions were then esterified with myristic, oleic or linoleic acid in the presence of the 1-ethyl-3-(3-dimethyl-aminopropyl) carbodiimide (EDC) as a condensing

agent and a catalytic amount of dimethyl aminopyridine (DMAP) in dichloromethane giving, respectively, compounds **3**, **4** and **5**.

For the synthesis of compounds with two different chains in C2 and C3, another synthetic route was followed (Scheme 3B) where azido-glucose intermediate **1** was esterified at position C3 using myristic acid, in the presence of DMAP and EDC in dichloromethane, to give intermediate **6**. After reduction of the azide to an amine with triphenylphosphine in THF / water (**7**) and subsequent esterification with linoleic or oleic acid was obtained, respectively, compounds **8** (R_1=myristic; R_2=linoleic) and **9** (R_1=myristic; R_2=oleic). Intermediates **3**, **4**, **5**, **8** and **9** were transformed into final products through the same sequence of reactions (Scheme 4).

The regioselective opening of benzylidene with sodium cyanoborohydride and hydrochloric acid followed by succinic anhydride treatment and, finally, deprotection of the para-methoxybenzyl group in position C6 by acid treatment (trifluoro acetic acid, TFA) gave final products FP 13-17 (Scheme 4). Compounds were soluble in DMSO up to a concentration of 100 mg/mL.

Scheme 2. Synthesis of intermediate **1**

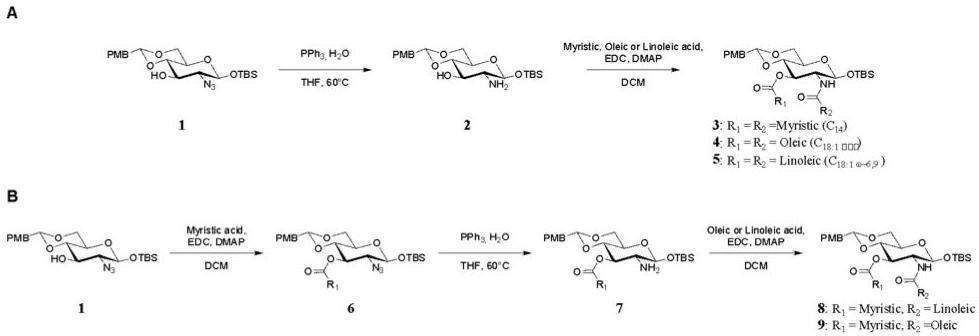

Scheme 3. Two pathways: A) compounds **3**, **4** and **5** with two identical lipophilic chains; B) compounds **8** and **9** possessing two different chains.

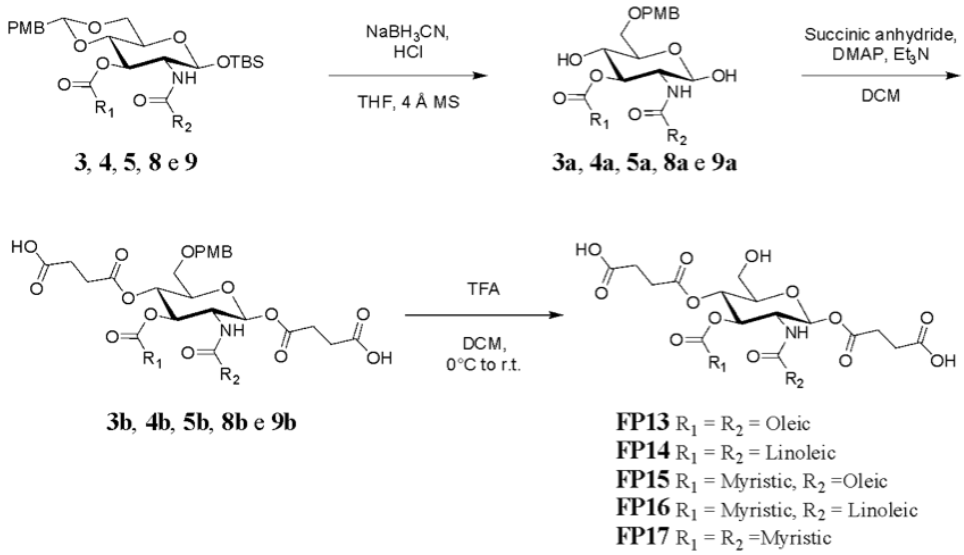

Scheme 4. Common pathway to obtain the final compounds FP13-17.

Results and discussion

In vitro binding experiments

The interaction of the synthetic compounds FP13-17 with purified hMD-2 has been studied by fours different techniques: two ELISA-type plate assays with immobilized protein, a fluorescence displacement assay and SPR measurements.

ELISA competition experiments with anti-hMD-2 antibody

Direct binding of FP13-17 to hMD-2 was determined by using a monoclonal antibody that binds to free hMD-2 but not to hMD-2 bound to LPS [151]. Monoclonal mouse anti-hMD-2 (9B4) antibody specifically binds to an epitope close to the rim of the hMD-2 pocket, available for the binding only when hMD-2 pocket is empty. This assay detected a decrease in binding to hMD-2 in the presence of LPS (Figure 48A), similar to what previously reported [150]. A similar dose-dependent inhibition of antibody/MD-2 interaction was found when adding FP13-17 molecules, with a 85-90% decrease in binding obtained at the highest concentrations tested (10-20 μM) (Figure 48A).

ELISA displacement experiment with biotinylated LPS

The ability of FP13-17 to displace LPS from the hMD-2 pocket was assessed by ELISA. FP13-17 molecules were added at increasing concentration to hMD-2 that was previously incubated with biotinylated LPS. FP13-17 were able to displace biotin-LPS

from the hMD-2 pocket in a similar dose-dependent manner. A displacement of 40-60% was obtained at a higest concentration tested (160 μM) (Figure 48B). LPS obtained a displacement of 70% at a concentration of 40 μM (Figure 48B).

Fluorescence displacement assay

It has been previously shown that the fluorescent probe 1,1'-Bis(anilino)-4,4'-bis (naphthalene)−8,8' disulfonate (*bis*-ANS) binds to hMD-2 and it is displaced by LPS [152]. bis-ANS presumably binds the same hMD-2 binding pocket that accommodates the fatty acid chains of lipid A and of other lipid A-like ligands, so that TLR4 modulators interacting with MD-2 in a lipid A-like manner, compete with bis-ANS and displace it from MD-2. FP13-17 compounds caused a similar concentration-dependent decrease of bis-ANS fluorescence, thus indicating competitive binding to hMD-2 (Figure 48C).

Surface Plasmon Resonance (SPR) analysis

SPR data with immobilized hMD-2, showed direct interaction of the receptor with LPS (data not shown) and with synthetic compound FP13-17. All the K_D values derived from sensorgrams analysis fall in the low μM range (Figure 48D-H).

The results of these *in vitro* cell-free studies clearly indicate that all the FP13-17 compounds directly interacted with hMD-2.

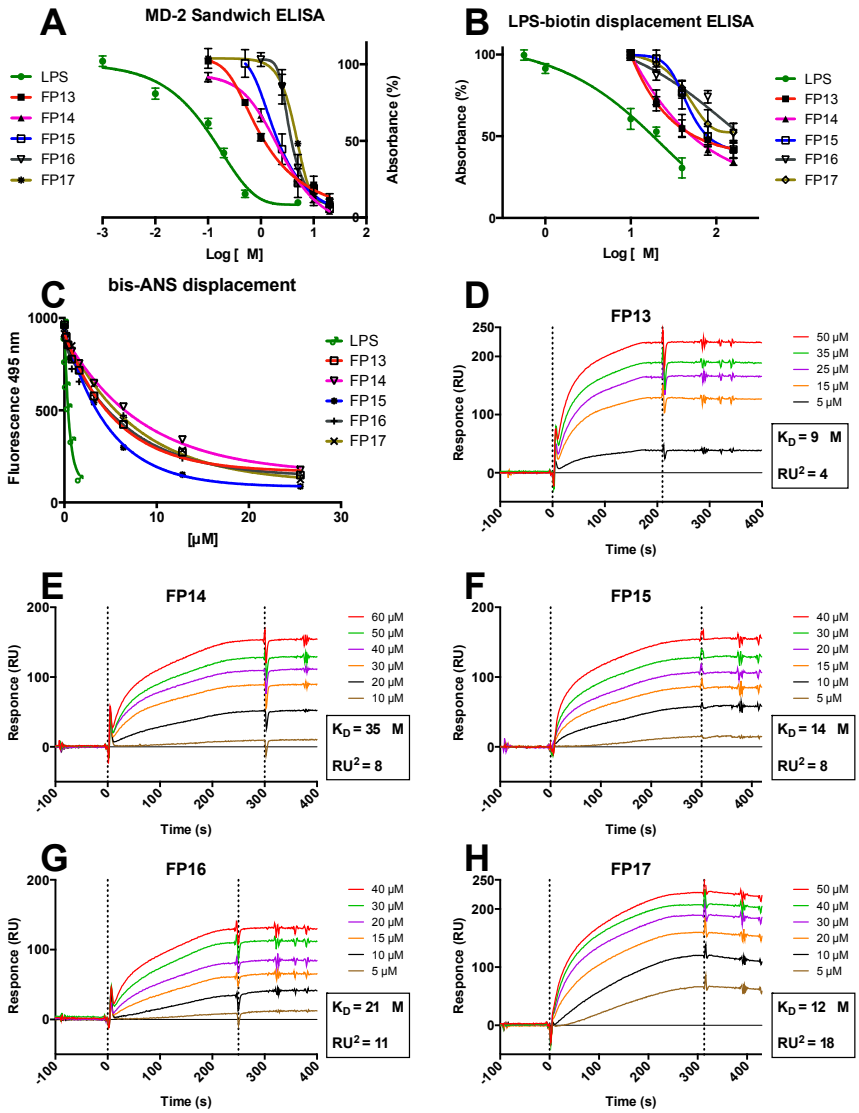

Figure 48. Cell-free binding studies on purified hMD-2 receptor. A) FP13-17 prevent anti-human hMD-2 monoclonal antibody binding in a dose-dependent manner; B) FP13-17 compete with biotin-LPS for hMD-2 binding; C) FP13-17 dose-dependent inhibit the binding of bis-ANS to hMD-2; D-H) SPR analysis show direct interaction between FP13-17 and hMD-2; K_D values are reported. Results are mean ± SEM from 3 parallels representative of at least 3 independent experiments.

Experiments on HEK-Blue hTLR4 cells

Monosaccharides FP13-17 were tested for their capacity to activate or inhibit LPS-stimulated TLR4 activation and signaling in HEK-Blue^{TM} hTLR4 cells. These cells are engineered to stably express the human receptors of the LPS recognition complex (hTLR4, hMD-2 and hCD14) and a reporter gene (SEAP) placed under the control of two TLR4-dependent transcription factors (NF-κβ and AP-1). Results from MTT assay revealed that all compounds did not have a negative effect on cell viability at the concentration of 10 μM used in experiments (data not shown).

Compounds FP13-17 alone were inactive to stimulate TLR4 signal up to a concentration of 50 μM (data not shown). Instead, compounds FP13-17 inhibited in a concentration-dependent manner the TLR4 signaling in HEK-Blue cells (Figure 49). FP13-17 series showed a similar IC_{50} that is in the range 2.7 to 6.6 μM, only slightly higher compared to the IC_{50} of FP7 (2.0 μM) (Figure 49).

These results demonstrated the efficacy of the new FP13-17 series to negatively modulate TLR4 signaling in HEK-Blue cells.

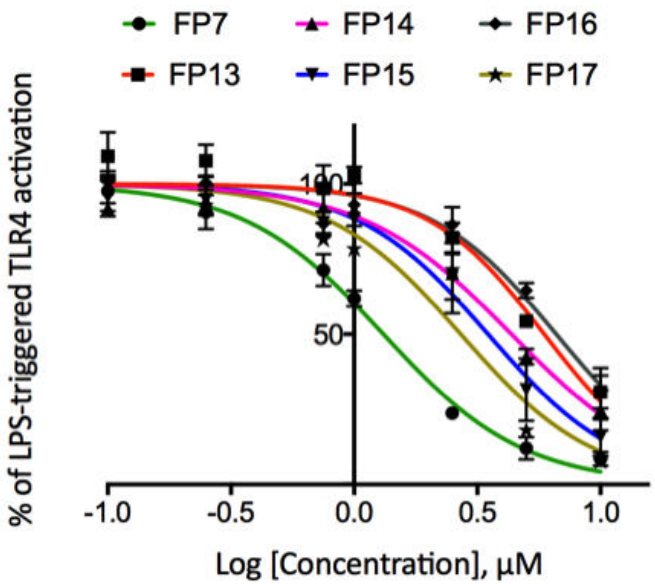

Compound	IC_{50} LPS (µM)
FP7	1.32
FP13	5.91
FP14	4.35
FP15	3.50
FP16	6.61
FP17	2.70

Figure 49. Dose-dependent inhibition of LPS-triggered TLR4-dependent NF-κβ activation in HEK-Blue™ hTLR4 cells by compounds FP13-17. HEK-Blue™ hTLR4 cells were pre-incubated with increasing concentrations (0.1-10 µM) of compounds FP13-17 and stimulated with LPS (100 ng/mL) after 30 minutes. Comparison between dose-effect curves for compounds FP13-17 in inhibiting the LPS-triggered, TLR4-dependent NF-κβ activation (left panel). Data were normalized to stimulation with LPS alone and fitted to a sigmoidal 4 parameter logistic equation to determine IC_{50} values (right panel). Data points represent the mean of percentage ± SEM of at least 3 independent experiments.

Cryogenic Transmission Electron Microscopy (Cryo-TEM)

In a recent paper, we described the aggregation properties of FP7, which represents the starting point for the design of the molecules presented in this paper (FP13-17). NMR and TEM data (cryogenic and negative staining) showed that FP7 is able to form micellar structures [187], and that the FP7 critical micelle concentrations (CMC) is 9 μM [60]. For the FP13-17 series we selected compound FP15 as a candidate, to further investigate the glycolipids' behavior in solution. In particular we used cryogenic transmission electron microscopy (Cryo-TEM) (Figure 50).

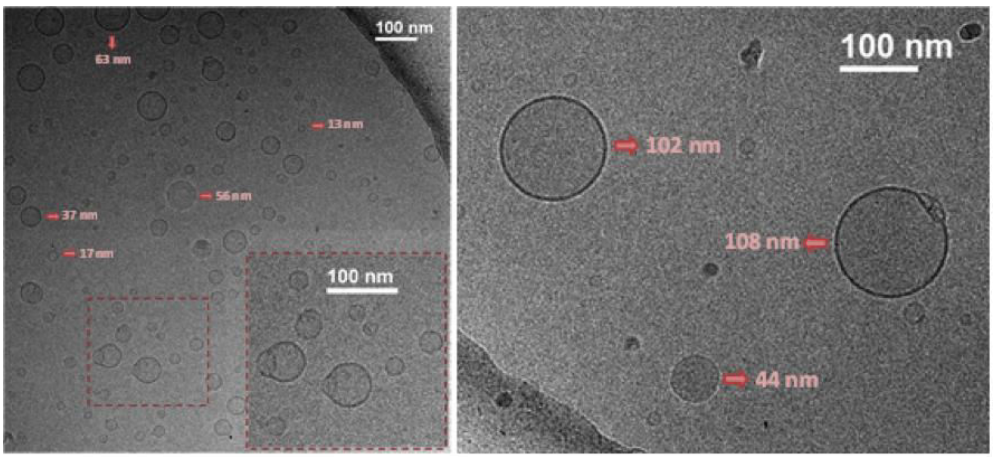

Figure 50. Cryogenic transmission electron microscopy (Cryo-TEM) of FP15 (7 mg/mL) nominal magnification of 40,000 X (0.26 nm/pixel).

Analysis of the cryo-TEM data of FP15 show that the glycolipid displays a different aggregation behavior in solution compared to the previously reported for FP7 molecule. FP15 mainly generates circular and homogeneous small unilamellar vesicles (SUV), with rather different size distributions, from 10 to 110 nm of diameter. Moreover, it was possible to detect the presence of fusion events (as highlighted in the zoomed picture in Figure 50, in the dark red squares) as well as the existence of open bilayers. Indeed, the use of vitrified samples allowed the trapping of the potentially unstable structures associated with the formed intermediates in the solubilization process of the vesicles.

These data show that FP15 when in solution is able to form vesicles/liposomes displaying a double layer.

Conclusions

This study presented a new series of monosaccharide glycolipids compounds that present TLR4 antagonist activity.

The FP13-17 series of monosaccharide glycolipids presenting two carboxylic groups in C1 and C4 (in the form of β-carboxylated anions) with a different combination of saturated and/or unsaturated fatty acid chains attached to the C2 and C3 positions of the glucosamine moiety (Figure 47) were rationally designed as MD-2 ligands and synthesized.

Firstly we study the SAR of these molecules in *in vitro* binding experiments with functional hMD-2. For this purpose hMD-2 expressed in yeast (*P. pastoris*) was used. Four different binding experiments between synthetic compounds FP13-17 and hMD-2 were carried out. These were competition (displacement) experiments in which the synthetic glycolipids compete with biotin-LPS, with the fluorescent hMD-2 ligand bis-ANS and with anti-hMD-2 antibody for hMD-2 binding. SPR measurements allowed to analyze directly the binding between synthetic glycolipids FP13-17 and hMD-2. All binding experiments consistently provided an almost identical affinity among hMD-2 and molecules, in particular FP13>FP14=FP15>FP16>FP17.

Secondly the biological activity was assessed *in vitro* on cell models: when provided alone, the synthetic FP13-17 compounds did not display any TLR4 agonist activity in human cell models. On the contrary, when administrated with LPS, all the FP13-17 molecules were active in blocking LPS/TLR4 signal (antagonism) in human cell models in a similar way to the well characterized monosaccharide FP7. The activity of FP13-17 present very similar IC_{50} that is in the 3.5 to 6.6 μM range, which is a slightly higher value compared to the IC_{50} of FP7 (2.0 μM).

The analysis of the cryo-TEM data of the chosen representative candidate, FP15, indicates that this molecule mainly generates

circular and homogeneous small unilamellar vesicles (SUV), with rather different size distributions, from 10 to 110 nm of diameter, with the presence of fusion events as well as open bilayers. These data indicate that this series of similar amphiphilic molecules when in solution possess a tendency to form vesicles/liposomes displaying a double layer. This is a crucial point to consider for the presentation of the molecules to the LPS receptor proteins, LBP, CD14, and MD-2.

Taken together, these data strongly suggest that the mechanism of TLR4 antagonism of these new FP13-17 compounds is mainly based on the competition with LPS (or other ligands, as bis-ANS) in the binding to the MD-2/TLR4 complex.

We confirm that the carboxylic acid represents an interesting bioisosteric replacement of phosphoric acid, as in our case it was used without loss of biological activity. This kind of substitiution could be of important interest as it allows to improve the synthesis and chemical stability of the final product. It also allows a further conjugation at positions C1 and C4 and an easier purification on the final product. The contribution of the unsaturated chains has a minor importance since the level of activity *in vitro* in cell models as well as the affinity *in vitro* for the purified hMD-2 receptor is almost identical for all the FP13-17 series.

The present SAR study demonstrates the ability of a new series of monosaccharide glycolipids, FP13-17 series, to negatively regulate TLR4 signaling.

The potential of the patented FP13-17 molecules to antagonise TLR4 signaling, in combination with the lack of toxicity, supports the idea to further invest resources for the development of FP13-17 series as potential TLR4-based therapeutics.

2.3 SAR study part III

This chapter is based on a manuscript in preparation.

A novel monosaccharide-based TLR4 agonist

Alberto Minotti[1], **Lenny Zaffaroni[1]**, Fabio A. Facchini[1], Jean-Marc Billod[2], Sonsoles Martin Santamaria[2], Francesco Peri[1*]

[1]Department of Biotechnology and Biosciences, University of Milano-Bicocca, Piazza della Scienza, 2; 20126 Milano (Italy); [2]Department of Chemical and Physical Biology, Centro de Investigaciones Biologicas, CIB-CSIC, C/Ramiro de Maeztu, 9, 28040 Madrid, Spain;

Introduction

Toll-like receptor 4 (TLR4) is an innate immunity receptor which selectively recognizes LPS of the Gram-negative bacteria that eluded the physical and anatomical barriers [129,188,189]. TLR4 responds to bacterial LPS and to different endogenous ligands (DAMPs) in association with the adaptor protein MD-2 and triggers the innate immune response [45,128,190,191]. The TLR4 co-receptors LBP and CD14 are also involved in the LPS recognition process, in particular by mediating the transfer of LPS monomers from aggregates in solution to the TLR4/MD-2 complex [44,192-194]. TLR4 has been vastly related to many important pathologies still lacking specific pharmacological treatment: from diseases caused by bacterial infection such as sepsis and septic shock, to more complex such as cancer and acute or chronic inflammatory diseases, atherosclerosis, allergies, asthma, cardiovascular disorder, and diabetes [195,196].

Compounds that block TLR4 activation (antagonists) can represent drug candidates against these vast range of pathologies [35], whereas compounds that activate TLR4 (agonists) can represent potential antitumoral agents or vaccine adjuvants [197].

Lipid A (Figure 51), which anchors LPS to the outer membranes of Gram-negative bacteria, is the moiety responsible for its TLR4 immunostimulatory activity [13]. Lipid A generally consist of a

1,4-β-diphosphorylated diglucosamine backbone to which acyl chains of various structure and length are covalently linked. The numbers and position of these acyl chains, as well as the number of phosphate groups, can greatly influence the TLR4 activity of different types of lipid A. The lipid A structures of LPS derived from numerous Gram-negative bacterial species have been fully elucidated and characterized especially in terms of biological activities [193]. Several *E. Coli* lipid A derivatives have been developed with variations of the number, length and type of FA chains, or with variations in the number of phosphate groups. This provided important information regarding SAR of lipid A as TLR4 modulators. However since the disaccharide lipid A derivatives can be only obtained through complex synthesis, the current disaccharides adjuvants used in clinics are still extracted from the natural sources [197]. The insufficient scalability, the difficult and costly synthesis of these disaccharides lipid A derivatives are the main reasons why, after their discoveries, chemists shifted the focus towards a structural simplification of the lipid A moiety, such as monosaccharide (Figure 51). In particular, compound SDZ MRL 953, a monosaccharide acylated with the 3-hydroxymyristoyl chains and with one phosphate group in C1, demonstrated a powerful immunostimulatory activity both in murine and in human [198,199]. A phase I

clinical trial of SDZ MRL 953 (Figure 51) was conducted to evaluate the biologic response and safety, showing an improved tolerability of SDZ MRL 953 compared to endotoxin [199]. A limited understanding of structure-activity requirements of monosaccharides represent one of the limitation for the development of monosaccharides as immunostimulators. Funatogawa and Matsuura shown that several lipid A derivatives monosaccharide molecules possess immunostimulatory properties both in human and in murine. These compounds present some common structural features: one phopshate group and three fatty acyl chains of C12 or C14 length [167,170].

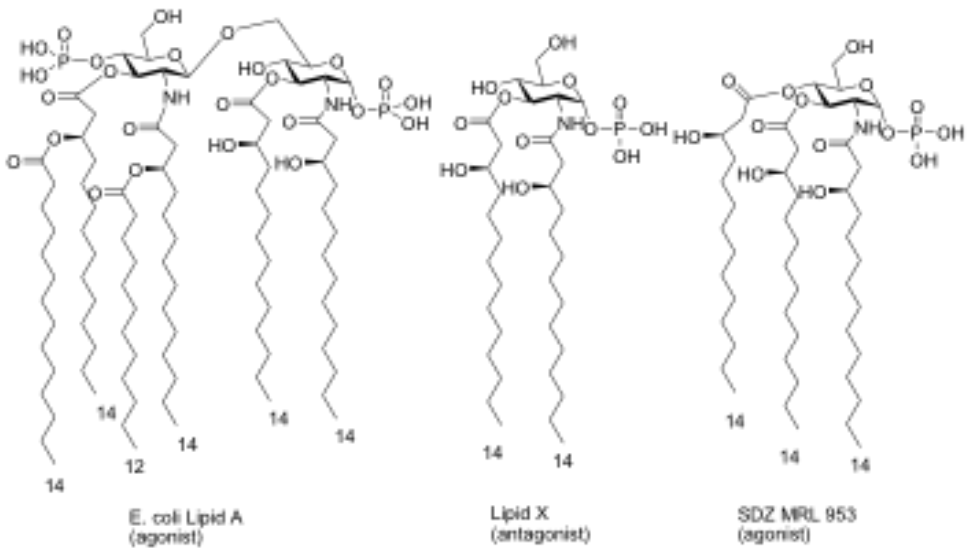

Figure 51. *E. coli* lipid A and monosaccharide molecular simplifications lipid X, a TLR4 antagonist, and SDZ MRL 953 an immunostimulator.

While for lipid A analogs, the TLR4 biological activity have been correlated to the binding to TLR4 co-receptor MD-2, and to the shapes in solution of aggregates (they must be non-lamellar to be TLR4 agonist), the characterization of monosaccharides glycolipids as TLR4 modulators is lacking [15,171,172,200,201]. In particular, even if a specific correlation between the shape of the aggregates and the activity of these compounds still seems to exist, and a clear dependence of the activity of some monosaccharide compounds on TLR4 receptor has been confirmed [169], no proof of direct role of MD-2 has been demonstrated yet.

With the aims to obtain new monosaccharide-based TLR4 modulators, to explore their SAR, and to study their binding affinities to MD-2, we have developed two SDZ MRL 953 derivatives: FP11 and FP111 (Figure 52). Compound FP11 (as SDZ MRL 953) possess all the features depicted by Funatogawa and Matsuura important for a monosaccharide to present immunostimulatory agonistic activity, while FP111 presents an additional phosphate compared to FP11. The ratio 1:1:3 (phospate:sugar moiety:fatty acid chains) seems important for monosaccharide TLR4 agonists, so the insertion of the second phosphate, which changes the ratio to 2:1:3, might impaired this TLR4 agonistic property.

This extra phosphate in C6 position of FP111 is a modification rarely explored in literature.

The syntheses of FP11 and FP111 compounds is herein described, followed by their biological *in vitro* characterization on cell-free and cell-based experiments.

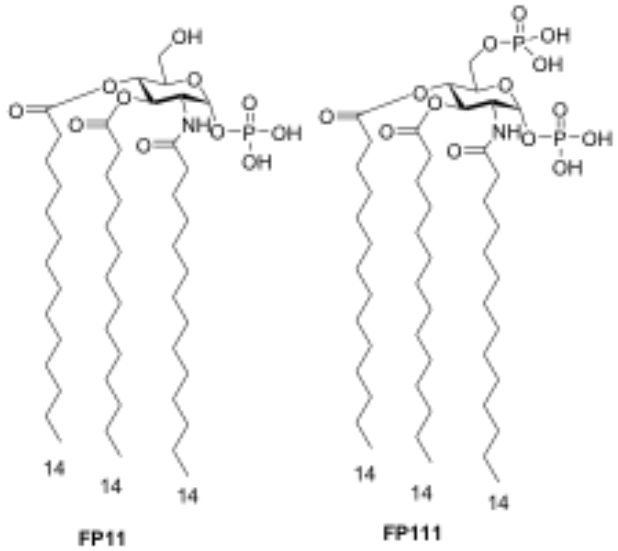

Figure 52. Representation of synthesized compounds FP11 and FP111.

Experimental section

Synthesis of FP11 and FP111

Compounds FP11 and FP111 were synthesized by using a divergent strategy starting from the common intermediate 8, obtained from commercial D-glucosamine hydrochloride (Scheme 5).

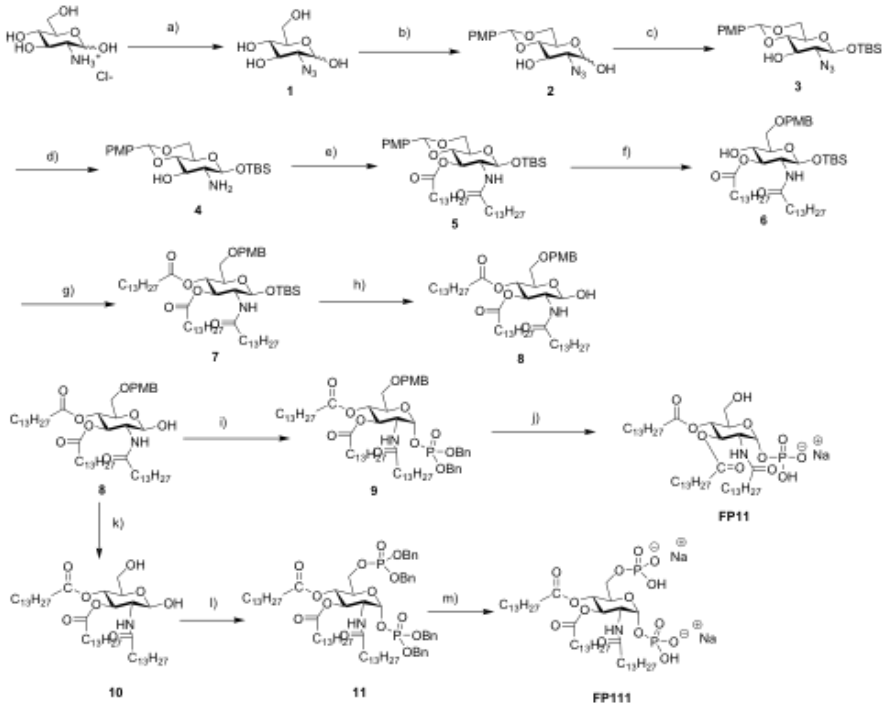

Scheme 5. Reagents and conditions: a) $CuSO_4$, TEA, Py:H_2O, 0°C, 30 min then TfN_3, Py, 0°C-->rt, O.N., quant.; b) p-MeOPhCH$(OMe)_2$, CSA, DMF dry, 40 °C, 8h, 68%; c) TBSCl, imidazole, CH_2Cl_2 dry, rt, 1.5 h, 62%; d) PPh_3, THF/H_2O, 60°C, 2h, quant.; e) myristic acid, EDC, DMAP, CH_2Cl_2 dry, rt, O.N., 73%; f) $NaCNBH_3$, 4 Å MS, THF dry, rt, 1h., then HCl 1M in dioxane, 0°C-->rt, 45 min, 85%; g) myristic acid, DCC, DMAP, CH_2Cl_2 dry, rt, 1h, 98%; h) TBAF (1M in THF), AcOH, THF dry, -15°C-->rt, 30 min, 87%; i) $(BnO)_2PNiPr_2$, imidazolium triflate, CH_2Cl_2 dry, rt, 30 min, then m-CPBA, 0°C-->rt, O.N., 55%; j) I) H_2, Pd/C, MeOH dry/CH_2Cl_2 dry, rt, O.N., II) Et_3N, III) resin IRA 120 H^+ , IV) resin IR 120 Na^+, 82%; k) H_2, Pd/C, MeOH dry/CH_2Cl_2 dry, rt, O.N., 96%; l) $(BnO)_2PNiPr_2$, imidazolium triflate, CH_2Cl_2 dry, rt, 1 h 30 min, then m-CPBA, 0°C-->rt, O.N., 44%; m) I) H_2, Pd/C, MeOH dry/CH_2Cl_2 dry, rt, O.N., II) Et_3N, III) resin IRA 120 H^+ , IV) resin IR 120 Na^+, 68%.

The complete synthetic pathway consists in a series of selective protection and deprotection steps. After Staudinger reduction of the azide in position 2 of intermediate 3 (obtained according to previously reported procedures), compound 4 is acylated in 2 and 3 with myristic acid. Following deprotection of C4 with $NaCNBH_3$ and HCl, acylation with the third myristic acid chain is conducted to give intermediate 7. Deprotection of C1 with TBAF gave intermediate 8. From this point on, the synthesis of FP11 and FP111 diverge: phosphorilation followed by hydrogenation gave compound FP11, while a hydrogenation prior to the phosphorylation step resulted in compound FP111.

Following this synthetic route compound FP11 and FP111 have been obtained as confirmed by NMR and mass analysis (data not shown).

Results and discussion

In vitro binding experiments

The interaction of the synthetic compounds FP11 and FP111 with purified hMD-2 has been studied by fours different techniques: two ELISA-type plate assays with immobilized protein, a fluorescence displacement assay and SPR measurements.

ELISA competition experiments with anti-hMD-2 antibody

Direct binding of FP11 and FP111 to hMD-2 was determined by using a monoclonal antibody that binds to free hMD-2 but not to hMD-2 bound to LPS [151]. Monoclonal mouse anti-hMD-2 (9B4) antibody specifically binds to an epitope close to the rim of the hMD-2 pocket, available for the binding only when hMD-2 pocket is empty. This assay detected a decrease in binding to hMD-2 in the presence of LPS, similar to what previously reported [150]. A similar dose-dependent inhibition of antibody/MD-2 interaction was found when adding FP11, with a 80-85% decrease in binding obtained at the highest concentrations tested of 20 μM (Figure 53A). In contrast, FP111 was unable to dose-dependent inhibit the antibody/MD-2 interaction at the tested concentrations (Figure 53A).

ELISA displacement experiment with biotinylated LPS

The ability of FP11 and FP111 to displace LPS from the hMD-2 pocket was assessed by ELISA. FP11 and FP111 molecules were added at increasing concentration to hMD-2 that was previously incubated with biotinylated LPS. FP11 was able to displace biotin-LPS from the hMD-2 pocket in a dose-dependent manner. A displacement of 50% was obtained at the higest concentration tested (160 μM) (Figure 53B). On contrary, FP111 was unable to displace LPS at the tested concentrations (Figure 53B).

Fluorescence displacement assay

It has been previously shown that the fluorescent probe 1,1'-Bis(anilino)-4,4'-bis (naphthalene)−8,8' disulfonate (*bis*-ANS) binds to hMD-2 and it is displaced by LPS [152]. bis-ANS presumably binds the same hMD-2 binding pocket that accommodates the fatty acid chains of lipid A and of other lipid A-like ligands, so that TLR4 modulators interacting with MD-2 in a lipid A-like manner, compete with bis-ANS and displace it from MD-2. Compound FP11 caused a similar concentration-dependent decrease of bis-ANS fluorescence, thus indicating competitive binding to hMD-2 (Figure 53C). FP111 was unable to do displace the bis-ANS probe at the tested concentrations (Figure 53C).

Surface Plasmon Resonance (SPR) analysis

SPR data with immobilized hMD-2, showed direct interaction of the receptor with LPS and with synthetic compound FP11 (Figure 53D and E). The K_D derived from sensorgrams analysis for FP11 is 6 μM, and for LPS is 1 μM, which is a similar value to a previously reported paper [202].

The results of these *in vitro* cell-free studies clearly indicate that FP11 (but not FP111) directly interacted with hMD-2.

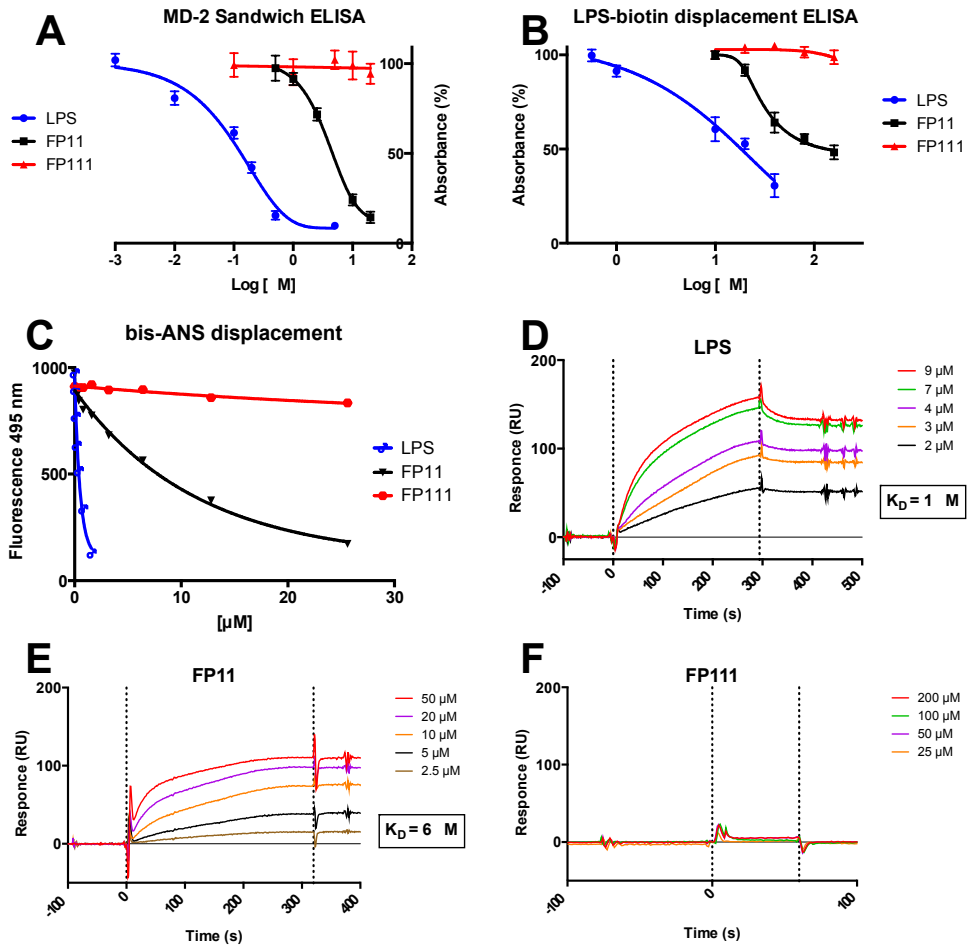

Figure 53. Cell-free binding studies on purified hMD-2 receptor. A) LPS and FP11 prevent anti-human hMD-2 monoclonal antibody binding in a dose-dependent manner; B) LPS and FP11 compete with biotin-LPS for hMD-2 binding; C) LPS and FP11 dose-dependent inhibit the binding of bis-ANS to hMD-2; D-F) SPR analysis show direct interaction of LPS and FP11 with hMD-2; K_D values are reported. Results are mean ± SEM from three parallels representative of at least three independent experiments.

Experiments on HEK-Blue hTLR4 cells

Monosaccharides FP11 and FP111 were tested for their capacity to activate or inhibit LPS-stimulated TLR4 activation and signaling in HEK-Blue^{TM} hTLR4 cells. These cells are engineered to stably express the human receptors of the LPS recognition complex (hTLR4, hMD-2 and hCD14) and a reporter gene (SEAP) placed under the control of two TLR4-dependent transcription factors (NF-κβ and AP-1). All compounds did not have a negative effect on cell viability at the concentration of 10 μM used in MTT assay (data not shown). Compounds FP11 and FP111 were inactive in antagonise TLR4 signaling up to a concentration of 50 μM (data not shown). Instead, only compound FP11 was active in agonise TLR4 signaling in a concentration-dependent manner in HEK-Blue cells to a less extent compared to LPS (Figure 54).

FP11 presents a calculated EC_{50} of 12 μM (Figure 54).

In order to verify whether the immunostimulatory activity of FP11 was TLR4 dependent, HEK-Blue^{TM} Null2 cells were used. These cells are derived from HEK-Blue^{TM} hTLR4 cells but do not express TLR4, CD14 and MD-2 proteins. In HEK-Blue^{TM} Null2 cells FP11 (and FP111) were unable to activate the production of transcription factors NF-kb e AP-1 (data not shown), indicating that the immunostimulatory effect of FP11 is TLR4 dependent.

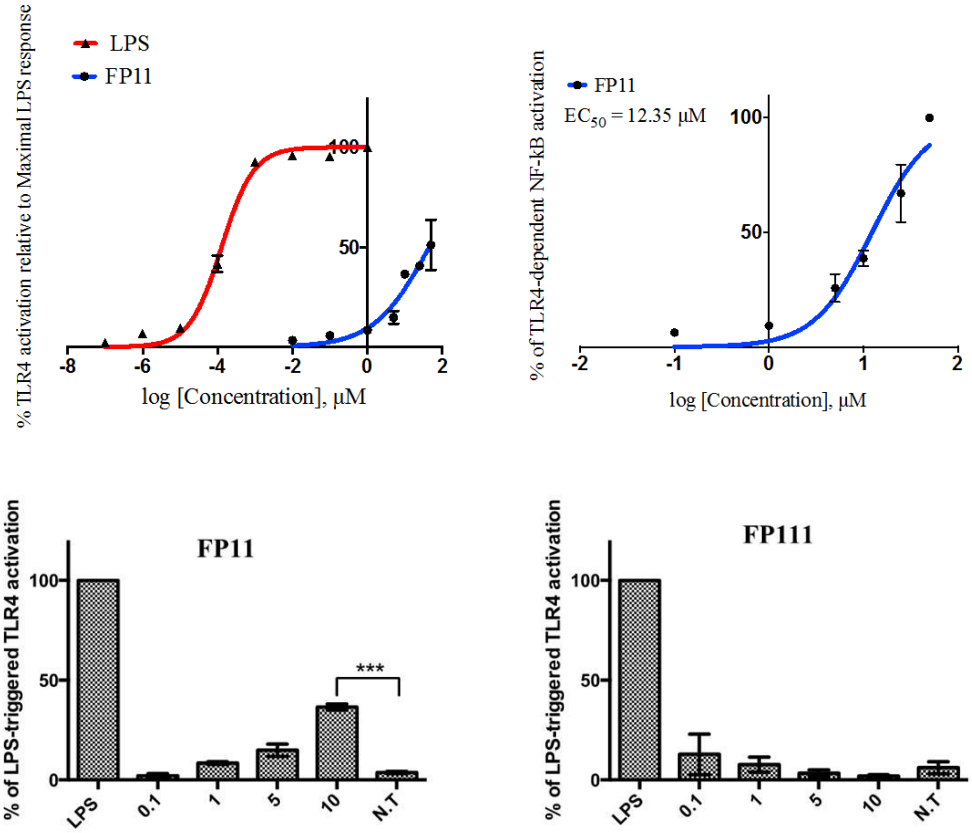

Figure 54. Dose-dependent activation of TLR4-dependent NF-κβ activation in HEK-Blue™ hTLR4. HEK-Blue™ hTLR4 cells were incubated with increasing concentrations (0.1-10 µM) of compounds FP11 and FP111 and incubated for 16-18 hours. The results are normalized to maximal activation by LPS alone and expressed as the mean of percentage ± SD of 3 independent experiments. Data have then been interpolated to a 4-parameter sigmoid logic equation to determine the EC_{50} values. Results are mean ± SEM from three parallels representative of at least three independent experiments.

Conclusions

This study presented a new monosaccharide glycolipid compound (FP11) which presents TLR4 agonist activity.

We confirm the SAR rule for TLR4 agonism of monosaccharides depicted by Funatogawa and Matsuura (one phosphate and three acyl chains of C14/C12 length). In fact FP11 possess the ratio 1:1:3 (phosphate groups : sugar moiety : fatty acid chains), while FP111 which possess an additional phosphate in C6 position which changes the ratio to 2:1:3, is not active as TLR4 agonist.

We study the SAR of FP11 and FP111 compounds in *in vitro* binding experiments with functional hMD-2. For this purpose hMD-2 expressed in yeast (*P. pastoris*) was used. Four different binding experiments between synthetic FP11 and FP111 compounds and hMD-2 were carried out. These were competition (displacement) experiments in which the synthetic glycolipids compete with biotin-LPS, with the fluorescent hMD-2 ligand bis-ANS and with anti-hMD-2 antibody for hMD-2 binding. SPR measurements allowed to analyze directly the binding between synthetic glycolipids FP11 and FP111 and hMD-2. All binding experiments consistently provided a strong affinity among hMD-2 and FP11, while FP111 did not bind to hMD-2.

The biological activity was assessed *in vitro* on a cell model: when administrated with LPS, FP11 and FP111 compounds were

inactive in blocking LPS/TLR4 signal (antagonism) in a human cell model. On the contrary, when provided alone, only the synthetic FP11 compound presented a TLR4 agonistic activity in a human cell model. TLR4 agonistic activity of FP11 presents an EC_{50} of 12 μM which is higher compared to the EC_{50} of LPS.

By using HEK-Blue™ Null2 cells we confirm that the immunostimulatory effect of FP11 is TLR4 dependent. Similar results were obtained for Gifu lipid A (GLA) monosaccharide, a TLR4 agonist discovered in 2003 [169].

The patented FP11 compound represents an important discovery, as it presents mild TLR4 agonistic activity and non-toxicity, making FP11 a potential candidate for the development as an antitumoral agent or a vaccine adjuvant.

Conclusions

Conclusions

Purpose of the work

This thesis presented a systematic structure− activity relationship (SAR) study; the first of its kind on synthetic monosaccharide glycolipids in the context of TLR4 modulation.

In particular this SAR considered the following aspects:

a) *in silico* interaction of molecules with hMD-2;

b) *in vitro* interaction of molecules with purified hMD-2;

c) *in vitro* biological activity of molecules on cell models;

d) aggregation properties of molecules;

My personal contribution focuses mainly on the point “b”.

Expression, purification and activity of hMD-2

In order to complete point “b”, we firstly screen various expression systems for the production of recombinant hMD-2. As outcome, we established two different ways to produce functional recombinant hMD-2 by using eukaryotic expression systems, in particular HEK293T cells and *Pichia pastoris* cells.

As the functionality of hMD-2 is a prerequisite to obtain reliable results representative of specific, high-affinity molecular recognition of ligands [49], an ELISA was developed. In particular, HEK/hTLR4 cells stably transfected with the human TLR4a gene but lacking the *MD-2* gene were used. After the co-administration of LPS and recombinant hMD-2, TLR4-dependent IL-8 production was quantified as an indicator of functionality of the recombinant hMD-2.

hMD-2 expressed and purified from HEK293T cells displayed a slightly higher activity in stimulating the LPS/TLR4 inducible reporter compared to the hMD-2 expressed and purified from *P. pastoris*. hMD-2 expressed and purified from *E. coli* displayed the lowest activity out of the three. This difference in activity of hMD-2 expressed in different hosts most likely reflects minor differences in protein folding and/or glycosylation [134,135].

Subsequently, the recovery of hMD-2 from the medium of yeast cells was optimized, and a final concentration of purified recombinant hMD-2 of 30 μM was achieved. The recovery yield in combination with the good activity, prompted us to use hMD-2 expressed in *P. pastoris* for the development of *in vitro* hMD-2-ligand binding experiments.

In vitro binding experiments with purified hMD-2

Four different techniques to study the interactions of TLR4 modulators with functional hMD-2 have been established. Two of them were optimized from procedures already present in literature [151,152], and the other two were designed and developed in an original way. They are two plate-based ELISA with immobilized hMD-2, a fluorescence displacement assay, and SPR:

i) ELISA competition experiments with anti-hMD-2 antibody: the direct binding of molecules to hMD-2 was determined using a monoclonal antibody that binds to free hMD-2 but not to hMD-2 bound to LPS [151]. Monoclonal mouse anti-hMD-2 (9B4) antibody specifically binds to an epitope close to the rim of the LPS-binding pocket of hMD-2, available for recognition by the antibody only when the hMD-2 pocket is empty. Whit this assay it is possible to determine in a quantitative manner whether a molecule binds into the hMD-2 pocket.

ii) ELISA displacement experiment with biotinylated LPS: the ability of molecules to displace biotinylated LPS from the pocket of hMD-2 was assessed by ELISA. Whit this assay it is possible to determine in a quantitative manner whether a molecule is able to displace biotinylated LPS from the hMD-2 pocket.

iii) Fluorescence displacement assay: the ability of molecules to compete with bis-ANS and displace it from hMD-2 is based on

previously reported experiments that showed that the fluorescent probe bis-ANS binds to hMD-2 and it is displaced by LPS. bis-ANS presumably binds the same hMD-2 binding site as lipid A and of other lipid A-like ligands [152]. With this assay it is possible to determine in a quantitative manner whether a molecule is able to displace the bis-ANS molecule from hMD-2.

iiii) SPR analysis: this technique is used to show direct interaction between immobilized hMD-2 and tested molecules. Sensorgrams analysis provided K_D values based on the assumption of a 1:1 ligand/MD-2 stoichiometry. With SPR it is possible to determine in a quantitative manner whether a molecule binds to hMD-2.

Since quantitative evaluation studies of hMD-2-ligand interactions has been very difficult to achieve, this established array of binding assays represents an important step towards a more complete characterization of TLR4 modulators.

This array of binding assays contributed to the SAR study of synthetic monosaccharide glycolipids as TLR4 modulators and it is presented in the three chapters of this thesis.

SAR study part I (chapter 2.1)

An homologous series of monosaccharide glycolipids with fatty acid chain lengths varying from 10 to 16 carbon atoms was presented.

In silico data show that the FP molecules with short FA chains (C10-C14) would accomplish optimal binding properties while the C16 version is on the limits of the maximum length compatible with a proper hMD-2 binding.

The four *in vitro* binding experiments described previously (2 ELISA, bisANS and SPR) on functional hMD-2 consistently provided the same order of affinity among hMD-2 and synthetic molecules: FP12(C12)>FP7(C14)>FP10(C10)> >FP116(C16).

The biological activity assessed on various cell models (human (HEK-TLR4 and THP-1) and murine (RAW macrophages)) provided similar results for the FP variants as TLR4 antagonists. The molecules with C10, C12, and C14 chains are active in both human and murine cell models, with higher potency in human ones. The molecule with C16 showed very weak or no activity in cell models. The number of carbon atoms of FA chains is clearly related to the activity that can be described as a bell-shaped curve with the maximum at C12. This can be explained in terms of docking of the molecules to the binding pocket of hMD-2, and in terms of variation of solubility and bioavailability of the

molecules. Thus, the differences in binding to hMD-2 and activity on cell models of FP monosaccharides related to FA chains length can be explained in terms of their interaction with hMD-2 and/or by their aggregation properties in solution.

Taken together, these data suggest that the TLR4 antagonistic property of FP7, FP10 and FP12 is based on the competition with LPS for the binding to the MD-2/TLR4 complex.

FT-IR, NMR, and SAXS analysis suggested that the aggregation state of this series of compounds in aqueous solution depends on fatty acid chain lengths and that this property can influence TLR4 activity.

SAR study part II (chapter 2.2)

A new series of monosaccharide glycolipids compounds (FP13, FP14, FP15, FP16, and FP17) presenting two carboxylic groups in C1 and C4 with a different combination of saturated and/or unsaturated fatty acid chains attached to the C2 and C3 positions of the glucosamine moiety was presented.

The four *in vitro* binding experiments described previously (2 ELISA, bisANS and SPR) on functional hMD-2 consistently provided the same order of affinity among hMD-2 and synthetic molecules: FP13>FP14=FP15>FP16>FP17. The biological activity assessed on human HEK-TLR4 cells provided results for

the FP13-17 series as TLR4 antagonists whit IC_{50} values in the low μM range, very similar to the IC_{50} of TLR4 antagonist FP7.

These data suggest that the TLR4 antagonistic property of this FP13-17 series is based on the competition with LPS for the binding to the MD-2/TLR4 complex.

Cryo-TEM data from a representative of this series of amphiphilic molecules, showed that when in solution there is a tendency to form vesicles/liposomes displaying a double layer. This can influence the TLR4 activity in this series of compounds.

We found that the carboxylic acid represents a suitable substitute of phosphoric acid in the case of monosaccharide glycolipids as TLR4 modulators without loosing any biological activity. The contribution of unsaturated chains seems to play a minor role.

SAR study part III (chapter 2.3)

A new monosaccharide glycolipid compound (FP11) with mild TLR4 agonistic activity was presented. Based on the rule for TLR4 agonism depicted by Funatogawa and Matsuura (one phosphate, one sugar moiety and three FA chains of C14/C12 length) [176] FP11 was design and synthesized as it possess the ratio 1:1:3 (phosphate groups : sugar moiety : fatty acid chains).

FP111 (ratio 2:1:3) was synthesized as negative control and it possesses an additional phosphate in C6 position.

The four *in vitro* binding experiments described previously (2 ELISA, bisANS and SPR) on functional hMD-2 consistently provided similar binding affinity among hMD-2 and FP11 compound, whereas FP111 did not bind to hMD-2.

The biological activity assessed on human HEK-TLR4 cells showed that FP11 and FP111 compounds were inactive in blocking LPS/TLR4 signal (antagonism). On the contrary, only FP11 compound presented a mild TLR4 agonistic activity in human cells, presenting an EC_{50} of 12 μM. By using HEK-Blue™ Null2 cells we confirm that the immunostimulatory effect of FP11 is TLR4 dependent.

Taken together, these data suggest that the TLR4 agonistic activity of FP11 compound is based on the binding to hMD-2. The mild TLR4 agonistic activity and non-toxicity of the patented FP11 compound, makes FP11 a good candidate to be developed as antitumoral agent or a vaccine adjuvant.

Future prospectives

A complete understanding of the aggregation properties in solution of the synthetic monosaccharide glycolipids (*i.e.* FP compounds) presented in this thesis is crucial. In fact, FT-IR, NMR, SAXS, and cryo-TEM analysis of these compounds is ongoing, and will soon help to clarify this important point.

However, the systematic SAR study presented in this manuscript already provides important structural and functional biological data, demonstrating the ability of these novel monosaccharide glycolipids (*i.e.* FP variants) to regulate (negatively or positively) TLR4 signaling in different cell model systems, in particular by direct interaction with TLR4 co-receptor MD-2.

These novel FP compounds which modulate (antagonise or agonise) TLR4 signaling pathway in combination with their lack of toxicity, can be potential lead compounds for further drug development in preclinical and clinical studies for the development of future TLR4-based therapeutics.

Materials and methods

Materials:

Suppliers

Chemicals/reagents were from Sigma, BDH, otherwise stated.

Growth media

Liquid and solid media were prepared by dissolving specified quantities in distilled water and autoclaving at 121°C and 6894 Pa for 20 minutes. Solutions and media used for growth were made in cleaned glassware. Other solutions such as antibiotics were sterilised by filtration through a sterile 0.2 μm filter (Millipore).

Solid media

11.2 g of nutrient agar was dissolved by autoclaving in 400 mL of distilled water. The sterile molten agar was left to cool to 60°C prior to addition of antibiotics. 20 mL of molten agar was poured into each Petri dish and allowed to solidify. Plates were dried for 20 minutes at 60°C and stored at 4°C for up to four weeks.

Liquid medium for bacteria

Lennox broth (LB) was prepared by dissolving 10 g Bacto-tryptone, 5 g yeast extract and 5 g NaCl in 1 L of distilled water.

Liquid media for yeast

Yeast extract peptone dextrose (YPD) was prepared by dissolving 10 g of Yeast extract, 20 g of each of BactoPeptone and Dextrose in 1 L of water.

Buffered Glycerol complex Medium (BMGY) was prepared by dissolving 10 g yeast extract, 20 g peptone, 13.4 g yeast nitrogen base without amino acids, 100 mM potassium phospate buffer (pH 6.0) and 10 g of glycerol in 1 L of distilled water.

Buffered Methanol complex Medium (BMMY) 0.05% Tween 20 was prepared by dissolving 10 g yeast extract, 20 g peptone, 13.4 g yeast nitrogen base without amino acids, 100 mM potassium phospate buffer (pH 6.0), 10 mL of methanol and 0.5 mL of Tween 20 in 1 L of distilled water.

Liquid medium for mammalian cells

Dulbecco's Modified Eagle Medium (DMEM).

Antibiotics

Carbenicillin/Zeocin were added from freshly made stock solutions of 100 mg/mL. Carbenicillin/Zeocin were supplement to liquid/solid media at a final concentration of 100 μg/mL.

Antibodies

Chicken anti-hMD-2 polyclonal Ab (GenTel).

Mouse anti-hMD-2 9B4 monoclonal Ab (eBioscience).

Goat anti-mouse MAb conjugated with HRP (Santa Cruz Biotec).

Mouse anti-His(c-term)-MAb conjugated with HRP (Invitrogen).

Mouse anti-His-MAb conjugated with HRP (Invitrogen).

Plasmid for bacterial expression

The coding sequence of mature human MD-2 amplified by PCR (primers F-ACGTCCATGGCGCA- R-GAAGCAGTATTGGGT CTG) was introduced through NcoI and XhoI sites into the pET14b cloning vector.

Plasmid for yeast expression

The coding sequence of mature human MD-2 was amplified by PCR (primers F- CAGAAGCAGTATTGGGTCTGC and R-TTT ACTAGTATTTGAATTAGGTTG GTGTAGG) from a plasmid template and ligated into the SnaBI/SpeI opened pPpT4AlphaS-His expression vector (under the control of AOX1 promoter), in frame with the N-terminal *S.cerevisiae* α-MF pre-pro leader sequence and at the C-terminal 6xHis tag. Positive recombinant plasmid were confirmed by DNA sequencing, linearized and transformed into *Pichia pastoris* GS115.

Plasmid for mammalian expression

The coding sequence of mature human MD-2 was amplified by PCR (primers F- ATACTCGAGAAAAGACAGAAGCAGTATT GGGTCTGC and R-TTTACTAGT ATTTGAATTAGGTTGGT GTAGG) from a plasmid template and ligated into the XhoI/SpeI opened pEF vector mammalian expression vector for secreted proteins carrying a N-terminal FLAG-tag and the C-terminal 6xHis tag. The resulting recombinant plasmid was transformed into *E. coli* DH5α competent cells. Positive recombinant plasmid were confirmed by DNA sequencing, linearized and transiently transfected into HEK cells.

Buffers and solutions:

PBS

Potassium phosphate buffered saline (PBS) (pH 7.4) was prepared by dissolving 1 tablet (Oxoid) in 100 mL of distilled water and sterilised by autoclaving.

For SDS-PAGE

Ultrapure Protogel 30% (w/v) acrylamide and 0.8% (w/v) NN'-methylenebisacrylamide was used in the stacking and resolving gel. The resolving gel buffer was 0.75 M Tris HCl (pH 8.3) and

the stacking gel buffer was 1.2 M Tris-HCl (pH 6.8). This was used to make 15% resolving and 5% stacking gels, respectively. Sample buffer contained 2 g SDS (sodium dodecyl sulphate), 20 mL glycerol and 5 mg of bromophenol blue in 0.1× stacking gel buffer in a final volume of 92 mL. This was dispensed into 1 mL aliquots and 87 μL of β-mercaptoethanol was added before use.

Stock electrode buffer (10x) contained 30 g Tris, 150 g of glycine per litre of distilled water. A working electrode buffer solution of a 1× concentration that contained 0.1% SDS was used.

For staining gels

Haem staining solution contained 0.113 g of 3,3',5,5'-tetramethylbenzidine dissolved in 75 mL methanol. Immediately before use, the stain solution was mixed with 175 mL of 0.25 M sodium acetate pH 5.0. Stop solution contained 175 mL 0.25 M sodium acetate pH 5.0 and 75 mL propan-2-ol.

Coomassie stain solution contained 0.2% (w/v) coomassie blue in 50% (v/v) methanol and 10% (v/v) acetic acid in distilled water.

This was filtered before use to remove any undissolved solid.

Fast destain solution contained 40% (v/v) methanol, 10% (v/v) acetic acid in distilled water.

Shrink solution contained 48% (v/v) methanol, 2% (v/v) glycerol in distilled water.

Methods:

Measuring optical density

The optical density of cultures was measured using a CamSpec spectrophotometer (M501 single beam scanning). When required, cultures were diluted with PBS in 1.5 mL cuvettes such that the OD was between 0.1 and 0.7 units. The cuvettes were inverted to ensure proper mixing of the diluted culture.

Making calcium chloride competent bacteria

This method was used routinely to prepare E. coli for transformation with plasmids and ligation reaction products. A 20 mL culture of E. coli DH5α was grown aerobically at 37 °C until the OD_{650} was between 0.45 and 0.6. Bacteria were incubated on ice for 20 minutes to stop further growth, then harvested in 10 mL test tubes at 5,000 rpm for 5 minutes. The pellet was resuspended in 5 mL of ice-cold 0.1 M $CaCl_2$ and incubated on ice for 20 minutes. The centrifugation step was repeated and the pellet was resuspended in 1 mL of ice-cold 0.1 M calcium chloride and left on ice for at least 1 hour. For long-term storage, 40% (v/v) glycerol was added and bacteria were stored at -80 °C.

Heat shock transformations of bacteria

Competent bacteria (20 µL) mixed with 2-5 ng/µL of plasmid DNA was incubated on ice for 30 minutes. Bacteria were heat-shocked in a water bath at 42 °C for 2 minutes, supplemented with 0.5 mL LB and incubated aerobically at 30 °C for 1 hour. Recovered bacteria were then plated onto nutrient agar containing the appropriate antibiotics and incubated at 30 °C overnight.

Small-scale isolation of plasmid DNA (minipreps)

A single colony, freshly transformed with the plasmid to be isolated and purified, was used to inoculate 2 mL of LB supplemented with the appropriate antibiotic. The culture was grown aerobically by shaking at 30 °C, and the plasmid was extracted using a QIAprep Miniprep kit (Qiagen).

Transformation of yeast

150-300 ng of linearized recombinant plasmid DNA was mixed with 80 µL of GS115 competent cells. The mixture was transferred into an ice cold 2 mm electroporation cuvette and incubated on ice for 5 minutes. The cells were then pulsed at 1.5 kV, 25 µF and 200 ohm. After pulsing, the cells were then washed immediately with 1 mL of 1 M ice cold sorbitol and the contents were transferred to a 1.5 mL sterile eppendorf. The tube was then incubated for 1.5 hours at 30°C. 100 µL were spread on

YPD plates containing 100 μg/mL Zeocin and incubated at 30°C for 2-3 days. Few colonies that grew were screened for a small scale MD-2 production. Positive clones were stock in 30% (v/v) glycerol and stored at -80°C and used for the production of recombinant MD-2.

Transfection of mammalian cells

HEK cells were harvested by trypsinization and plate at required density. Medium was changed 1 hour before trasfection. A solution of calcium phosphate-DNA (plasmid) coprecipitate was preperred: 100 μL of 2.5 M $CaCl_2$ and 25 μg of DNA diluted with TE buffer (1mM Tris-HCl, 0.1mM EDTA, pH7.6) to a final volume of 1 mL. One volume of this 2x Ca/DNA solution was addedd quickly to an equal volume of 2x HEPES solution (140 mM NaCl, 1.5 mM Na_2HPO_4, 50 mM HEPES, pH 7.05 at 23°C. The two solutions were mixed quickly for 1 min and 0.1 mL was added to the suspension of every 1 mL of medium. Cells were incubated at 37°C for 2-6 hours. DMEM growth medium was addedd and cells were incubated for 2 days.

Isolation of recombinant hMD-2 from *Escherichia coli*

hMD-2 was produced in *E. coli* as described previously [141], analysed by SDS–PAGE and its biological activity tested on 293/hTLR4a cells.

Isolation of recombinant hMD-2 from *Pichia pastoris*

hMD-2 was produced in *Pichia pastoris*, analysed by SDS–PAGE and its biological activity tested on 293/hTLR4a cells. The coding sequence of mature hMD-2 was amplified by PCR (primers F-hMD2-Q19 CAGAAGCAGTATTGGGTCTGC and R-Spe-hMD2 TTTACTAGTATTTGAATTAGGTTGGTGTAGG) from a plasmid template and ligated into the SnaBI/SpeI opened pPpT4AlphaS-His expression vector (under the control of AOX1 promoter), in frame with the N-terminal *S.cerevisiae* α-MF pre-pro leader sequence and the C-terminal 6xHis tag. The resulting recombinant plasmid pPpT4AlphaS-His was transformed into *E. coli* DH5α competent cells, and the positive recombinant plasmid which was confirmed by DNA sequencing, was linearized and transformed into *Pichia pastoris* GS115 by electroporation. MD-2 expressing transformant was selected and cultured in a 250 mL shake flask containing 10 mL of YPD liquid media at 28 °C for 24 h. 2 L flasks containing 250 mL of BMGY (1% glycerol) medium at 28 °C were inoculated with 1 mL of overnight inoculum. After being cultured for 24 h, cells were aseptically collected by centrifugation at room temperature 10 minutes at 5,000 rpm. BMGY medium was replaced with 250 mL of methanol-complex medium BMMY (1% methanol) to induce protein expression at 28 °C (250 rpm), adding 1% of methanol

every 12 h. After 2 days of fermentation in BMMY, cells were removed by centrifugation 10 minutes at 5,000 rpm. Supernatant was supplemented with 2 mM $MgCl_2$, 100 mg/L of reduced glutathione, and pH was adjusted to 7.5 with NaOH. Precipitate was removed by centrifugation for 20 minutes at 1,900 g, followed by filtration using Stericup-GP 0.22 μm (Sigma). A 0.5 M solution of TRIS HCl pH 7.5, 1.5 M NaCl was added to the medium to a final concentration of 50 mM TRIS HCl, 150 mM NaCl. High Density Nickel resin (ABT) was added to the medium (30 mL every liter of medium) and incubated in batch at room temperature for 4 h. High Density Nickel resin was washed several times with 50 mM TRIS HCl pH 7.5, 150 mM NaCl solution. hMD-2 was eluted with 0.5 M imidazole in 2 mL fractions, which were analysed for protein concentration and by SDS-PAGE. Pooled fractions containing hMD-2 were extensively dialysed against 50 mM TRIS, 150 mM NaCl, 0.5% Tween 20, pH 7.5 at 4 °C and purified hMD-2 biological activity was tested on 293/hTLR4a cells.

Isolation of recombinant hMD-2 from HEK293T cells

hMD-2 was produced in HEK293T cells, analysed by SDS–PAGE and its biological activity tested on 293/hTLR4a cells. HEK293T cells were grown in high-glucose DMEM medium supplemented with 10% fetal calf serum, 106 units per L penicillin G and 1 g L-L streptomycin in a 5% CO_2 atmosphere at

37 °C. Mammalian expression constructs for secreted proteins carrying a N-terminal FLAG-tag were generated in the pEF vector (Thermo Fisher Scientific). pEF-Flag-DEVD-hMD2-myc/His plasmid was transiently transfected to HEK293T cells, and the cells were harvested 48 h after transfection and resuspended in lysis buffer containing 50 mM TRIS, 150 mM NaCl, 1 mM EDTA, 1% TRITON X-100. The cell suspension was homogenized by Dounce homogenizer and clarified by centrifugation at 10,000 g for 20 minutes. ANTI-FLAG M2 affinity gel beads (SIGMA) was added to the lysate and then it was left shaking at 4 °C overnight. Solution was spin down at 1,000 rpm for 2 minutes and eluted with TBS Flag peptide (100 μL/mL). Recombinant protein hMD-2 was confirmed by western blot analysis using an HRP-coupled antibody directed against the FLAG-tag.

SDS-PAGE and Western blot

Purified recombinant hMD-2 was analysed on 15% SDS-PAGE under reducing conditions followed by Coomassie Brilliant Blue staining. For Western blot analysis, proteins were separated by SDS-PAGE under reducing conditions and then electrophoretically transferred onto polyvinylidene difluoride membranes (Amersham Biosciences). After protein transfer, the membranes were treated with blocking buffer followed by

incubation with anti-His-HRP antibodies. Then, the bands were visualized by 3,3'-diaminobenzidine as a peroxidase substrate.

Protein concentration determination

The total protein concentration was determined using ultraviolet absorption at 280 nm. The theoretical extinction coefficient (19.285) was obtained using the protein sequence of hMD-2.

hMD-2 activity test using 293/hTLR4a cells

For measuring the activity of recombinant expressed hMD-2, HEK 293 cells stably transfected with the human TLR4a gene (293/hTLR4a (Invivogen)) were used. Various dilutions of hMD-2 (stock concentration was 10 μM) were incubated with 100 ng/mL of LPS prior to stimulation of 293/hTLR4a cells. Supernatants were analysed for IL-8 secretion by ELISA assay.

Determination of IL-8 secretion by sandwich ELISA

IL-8 concentrations were assayed using the IL-8 Cytosets™ (Invitrogen) antibody pair kit containing matched, pre-titrated and fully optimized capture and detection antibodies, recombinant IL-8 standard and streptavidin-horseradish peroxidase. The assay was conducted according to the manufacturer's specifications.

Antibody-sandwich ELISA for the detection of binding of compounds to hMD-2

The method of antibody-sandwich ELISA for the detection of the binding of compounds to MD-2 was modified from a previous study [151]. A microtiter plate was coated overnight at 4 °C with 100 µL/well of 5 µg/mL of chicken polyclonal anti-hMD-2 antibodies, diluted in 50 mM Na_2CO_3 buffer, pH 9.6 and blocked with 1% BSA in PBS. After washing, 1 µM hMD-2 with tested compounds was added and incubated for 2 h. 0.1 µg/mL mouse anti-hMD-2 MAb (9B4) and 0.1 µg/mL goat anti-mouse IgG conjugated with HRP in PBS were added, followed by detection at 420 nm after the addition of 100 µL of ABTS (Sigma).

According to authors finding, MAb anti-hMD-2 (clone 9B4) can be used in Western blotting, in immunostaining and in an ELISA to detect hMD-2 [151].

Fluorescence spectroscopy assay

Fluorescence was measured on Perkin Elmer fluorimeter LS 55 (Perkin Elmer, UK) as previously described [152]. All measurements were done at 20 °C in a 5 x 5 mm quartz glass cuvette (Hellma Suprasil, Müllheim, Germany). hMD-2 protein (200 nM) and 1,1'-Bis(anilino)-4,4'-bis (naphthalene)−8,8' disulfonate (bis-ANS, 200 nM) were mixed and incubated until reaching stable relative fluorescence units (RFUs) emitted at 420–

550 nm under excitation at 385 nm. Compounds, at different concentrations, were then added, followed by relative fluorescence unit (RFU) measurement at 420–550 nm.

LPS displacement ELISA

The ability of the compounds to displace LPS from hMD-2 hydrophobic pocket was determined by ELISA. A microtiter plate was coated overnight at 4 °C with 100 µL/well of 5 µg/mL of chicken polyclonal anti-hMD-2 antibodies, diluted in 50 mM Na_2CO_3 buffer, pH 9.6 and blocked with 1% BSA in PBS. After washing, 1 µM of hMD-2 with biotin-labeled LPS was added and incubated for 2 h. After washing, the compounds were added at different concentration and incubated for 1.5 h. After washing, 0.5 µg/mL HRP-conjugated streptavidin in PBS was added, followed by detection at 420 nm after addition of 100 µL ABTS.

Surface plasmon resonance (SPR) analysis

The binding affinity of the compounds to recombinant hMD-2 was determined using a Biacore X100 with an NTA sensor chip (Biacore, GE Healthcare, Uppsala, Sweden). Briefly, 0.5 µM hMD-2 (in 50 mM TRIS, 150 mM NaCl, 0.5% Tween 20, pH 7.5) was immobilized onto the sensor chip previously activated with 1-minute pulse of 10 mM $NiSO_4$. First flow cell was used as a reference surface to control non-specific binding. Both flow cells were injected with the analyte (in PBS, 5% DMSO, 5%

EtOH, pH 7.5) at a flow rate of 10 μL/min at 25 °C in increasing concentrations. The data were analysed with Biacore Evaluation software. K_D values were calculated by global fitting of the equilibrium binding responses from various concentrations of analytes using a 1:1 Langmuir binding model.

HEK-Blue hTLR4 cells assay

HEK-Blue hTLR4 cells (InvivoGen) were cultured according to manufacturer's instructions. Briefly, cells were cultured in DMEM high glucose medium supplemented with 10% fetal bovine serum, 2 mM glutamine, antibiotics and 1× HEK-Blue Selection. Cells were detached, counted and seeded in a 96-well multiwell plate at a density of 4×10^4 cells per well. After overnight incubation (37 °C, 5% CO_2, 95% humidity), supernatants were replaced with medium supplemented by the compound to be tested dissolved in water or DMSO - H_2O (1:1). After 30 minutes, cells were stimulated with 100 ng/mL LPS from *E. coli* O55:B5 and incubated o.n. The SEAP-containing supernatants were collected and incubated with paranitrophenylphosphate (pNPP) for 2−4 h in the dark at room temperature. The wells optical density was determined using a microplate reader set to 405 nm.

RAW-Blue cells

Raw-Blue cells (InvivoGen) were cultured according to manufacturer's instructions. Briefly, cells were cultured in DMEM high glucose medium supplemented with 10% fetal bovine serum, 2 mM glutamine, 100 µg/mL Normocin, 200 µg/mL Zeocin. Cells were detached and concentration was estimated by using Trypan Blue. The cells were diluted in DMEM high glucose medium supplemented as described before and seeded in 96-well multiwell plate at a density of 6×10^4 cells per well in 200 µL. After overnight incubation (37 °C, 5% CO_2, 95% humidity), supernatant was removed, cell monolayers were washed with warm PBS and treated with increasing concentrations of compounds dissolved in DMSO - H_2O (1:1) and diluted in DMEM. After 30 minutes, cells were stimulated with 10 ng/mL of LPS from *E. coli* O55:B5 (Sigma-Aldrich) for 16 h. The supernatants were collected and incubated with paranitrophenylphosphate (pNPP) for 2−4 h in the dark at room temperature. The optical density of wells were determined using a microplate reader set to 405 nm.

THP-1 cells

THP-1 cells were cultured in RPMI (+10% heat inactivated fetal bovine serum (HiFPS), +1% Glutamine, +1% Penacillin/Streptamycin). Cells were split 3 times weekly and

maintained at a density of 0.3 × 10^6 cells/mL. For experimental procedure THP-1 were used at a density 0.5 x 10^6 cells/mL, 100 μL/well (96 wells) and 3 mL/well (6 wells) plates respectively. All cells were pre-treated with FP7 variants (0-10 μM) for 1 h, then exposed to LPS (100 ng/mL) for 1 or 16 h.

MTT Cell Viability Assay

HEK-Blue hTLR4 cells were grown in DMEM supplemented with 10% FBS, 2 mM glutamine and antibiotics. Cells were seeded in 100 μL of DMEM without Phenol Red at a density of 4×10^4 cells per well and incubated overnight (37 °C, 5% CO_2, 95% humidity). Cells were treated with the higher dose of compound used in the previous experiments and incubated overnight. MTT solution (5 mg/mL in PBS) was added to each well and after 3 h incubation, HCl 0.1 N in 2-propanol solution was used to dissolve formazan crystals. Formazan concentration was determined by measuring the absorbance at 570 nm.

Structure construction and refinement

The 3D structures of ligands FP10, FP12, FP7, and FP116 were built with PyMOL [203] using 6YA monosaccharide found in the GLYCAM database (http://glycam.org) as a template. The 3D coordinates of human TLR4/MD-2 model in the antagonist conformation is reported elsewhere [204].

Parameters derivation

The parameters needed for MD simulations were obtained using the standard Antechamber procedure in Amber14 [205]. Briefly, ligand structures, already refined at the AM1 level of theory, were optimized and their atomic partial charges were calculated with Gaussian g09/e1 [206] at the Hartree−Fock level (HF/6-31G* Pop=MK iop(6/33=2) iop(6/42=6)), then the partial charges were derived and formatted for AmberTools15 and Amber14 with Antechamber, assigning the general AMBER force field (GAFF) atom types. Later, the atom types of the atom constituting the saccharide ring were changed to the GLYCAM force field atom types [207]. The GAFF parameters for the phosphate group were modified as shown in SI.

Docking calculations of ligands FP10, FP12, FP7, and FP116.

The Gasteiger charges were computed within the AutoDockTools 1.5.6 program [208], and the nonpolar hydrogens were merged for all the ligands, the human TLR4/MD-2 antagonist model and human CD14 (PDB-ID 4GLP). AutoDock VINA 1.1.2 was used for the docking of the ligands and AutoDock 4.2 was used to redock the best-predicted binding poses. In AutoDock 4.2, the Lamarckian evolutionary algorithm was chosen and all parameters were kept default except for the number of genetic algorithm runs that was set to 200 to enhance the sampling.

AutoDockTools 1.5.6 was used to assign the Gasteiger−Marsili empirical atomic partial charges to the atoms of both the ligands and the receptors. The structure of the receptors was always kept rigid, whereas the structure of the ligand was set partially flexible by providing freedom to some appropriately selected dihedral angles. Regarding the docking boxes, spacing was set to the default value of 1Å for VINA, and 0.375 Å for AutoDock. For human CD14 structure, the size of the box was set to 33.00 Å in the x-axis, 33.75Å in the y-axis and 33.75 Å in the z-axis, and the center of the box was located equidistant to the center of mass of residues Phe69, Tyr82 and Leu89. For the human TLR4/MD-2 system, the size of the box was set to 33.00 Å in the x-axis, 40.50Å in the y-axis and 35.25 Å in the z-axis, and the center of the box was located equidistant to the center of mass of residues Arg90 (MD-2), Lys122 (MD-2) and Arg264 (TLR4).

Molecular dynamics (MD) simulations

Selected docked complexes were submitted to MD simulations for 50 ns in Amber14 suite. All the complexes followed the same procedure. First, the system is submitted to 1000 steps of steepest descent algorithm followed by 7000 steps of conjugate gradient algorithm. A 100 $kcal.mol^{-1}.A^{-2}$ harmonic potential constraint is applied on both the proteins and the ligand. In the subsequent steps, the harmonic potential is progressively lowered

(respectively to 10, 5 and 2.5 kcal.mol^{-1}.A^{-2}) for 600 steps of conjugate gradient algorithm each time, and then the whole system is minimized uniformly. Next, the system is heated from 0 K to 100 K using the Langevin thermostat in the canonical ensemble (NVT) while applying a 20 kcal.mol^{-1}.A^{-2} harmonic potential restraint on the proteins and the ligand. Finally, the system is heated up from 100 K to 300 K in the Isothermal–isobaric ensemble (NPT) under the same restraint condition than the previous step, followed by a simulation for 100 ps with no harmonic restraint. Production runs were performed for 50 ns.

LogP calculations

LogP value of FP10, FP12, FP7, and FP116 were calculated within the Maestro package [209].

Cryo-TEM

All samples were prepared in 10 mM buffer phosphate (pH 7.4) with 16% of DMSO. Cryo-TEM data were collected on a JEM-2200FS/CR transmission electron microscope (JEOL, Japan), equipped with an UltraScan 4000 SP (4008×4008 pixels) cooled slow-scan CCD camera (GATAN, UK).

Three microliters of the compound were vitrified on Quantifoil 2/2 grids, using Vitrobot (FEI) and were analyzed at nitrogen liquid temperature with a TEM operated at 200 kV in low dose conditions.

Secondments

- March - June 2017 and November 2017:
  National institute of chemistry (KI); Ljubljana, Slovenia

- November 2016 and January 2018:
  Lofarma; Milan, Italy

- November 2015 - March 2016:
  Flemish institute for biotechnology (VIB); Gent, Belgium

Communications

- **5th TOLLerant meeting**; Ghent, Belgium (12/2017)

Oral: "Update on research activities"

- **BtBs PhD meeting**; Milan, Italy (10/2017)

Oral: "Scientific results of the last year of the PhD"

- **EFMC International Symposium**; Vienna, Austria (08/2017)

Poster: "*In vitro* characterization of synthetic TLR4 modulators"

- **4th TOLLerant meeting**; Naples, Italy (06/2017)

Oral: "Update on research activities"

- **BtBs Day 2016**; Milan, Italy (12/2016)

Poster: "hMD-2 and the characterization of TLR4 modulators"

- **3rd TOLLerant meeting**; Ljubljana, Slovenia (12/2016)

Oral: "Update on research activities"

- **BtBs PhD meeting**; Verbania, Italy (10/2016)

Oral: "Interaction studies on MD-2 receptor with TLR4 ligands"

- **3rd Summer School ESSIB**; Barcelona, Spain (09/2016)

Oral: "My PhD topic"

- **2nd TOLLerant meeting**; Madrid, Spain (05/2016)

Oral: "Update on research activities"

- **BtBs PhD meeting**; Verbania, Italy (10/2015)

Poster and oral: "Production of recombinant human MD-2"

- **Congress TOLL2015**; Marbella, Spain (10/2015)

Poster: "New TLR-directed small-molecule therapeutics"

Publications

- **Zaffaroni L** & Peri F. **Recent advances on toll-like receptor 4 modulation: new therapeutic perspectives**
  Published on *Future medicinal chemistry* (30/01/2018)
  DOI: 10.4155/fmc-2017-0172

- Facchini A. F, **Zaffaroni L**, Minotti A. *et al.* **Structure-activity relationship (SAR) in monosaccharide-based toll-like receptor 4 (TLR4) antagonists**
  Published on *Journal of Medicinal Chemistry* (01/03/2018)
  DOI: 10.1021/acs.jmedchem.7b01803

- Cochet F, Facchini A. F, **Zaffaroni L** *et al*. **New carboxylate-based TLR4 antagonists that bind to MD-2**
  Manuscript in preparation

- Minotti A, **Zaffaroni L** *et al*. **A novel monosaccharide-based TLR4 agonist**
  Manuscript in preparation

- Facchini A. F, Di Fusco D, Barresi S, **Zaffaroni L** *et al*. **TLR4 synthetic antagonist FP7 inhibits LPS-induce production of pro-inflammatory cytokines in mononuclear cells of IBD patients and show anti-inflammatory effects in dextran-sulfate-sodium (DSS)-induced colitis model**

  Manuscript in preparation

- Wang T, Cochet F, **Zaffaroni L** *et al*. **A novel LOS conjugate (Alexa568-LPS-like) for imaging studies**

  Manuscript in preparation

- Cochet F, Facchini A. F, **Zaffaroni L** *et al*. **Synthesis and biological characterization of iron oxide nanoparticles functionalized with TLR4 and TLR7 agonists**

  Manuscript in preparation

References

1. Medzhitov R, Janeway C, Jr. Innate immunity. *N Engl J Med*, 343(5), 338-344 (2000).

2. Beutler B. Innate immunity: an overview. *Mol Immunol*, 40(12), 845-859 (2004).

3. Bonilla FA, Oettgen HC. Adaptive immunity. *J Allergy Clin Immunol*, 125(2 Suppl 2), S33-40 (2010).

4. Dranoff G. Cytokines in cancer pathogenesis and cancer therapy. *Nat Rev Cancer*, 4(1), 11-22 (2004).

5. Mayer G. IMMUNOLOGY - CHAPTER ONE: INNATE (NON-SPECIFIC) IMMUNITY. (Immunology Section of Microbiology and Immunology On-line. University of South Carolina, 2010)

6. Scott A, Khan KM, Cook JL, Duronio V. What is "inflammation"? Are we ready to move beyond Celsus? *Br J Sports Med*, 38(3), 248-249 (2004).

7. Heidland A, Klassen A, Rutkowski P, Bahner U. The contribution of Rudolf Virchow to the concept of inflammation: what is still of importance? *J Nephrol*, 19 Suppl 10, S102-109 (2006).

8. Cighetti R. Design, synthesis and biological characterization of new small-molecule TLR4 modulators. *PhD Thesis*, (2013).

9. Beveridge TJ. Use of the gram stain in microbiology. *Biotech Histochem*, 76(3), 111-118 (2001).

10. [ONLINE]. cnx.org/contents/W1kvc5fi@4/Unique-Characteristics-of-Prok. (Ed.^(Eds)

11. Silipo AM, A. Lipid A structure. In Bacterial lipopolysaccharides. Structure, chemical, synthesis, biogenesis and interaction with host cells. (Eds. Springer, 2011)

12. Actor JK. *Elsevier's Integrated Review Immunology and Microbiology* (Elsevier Health Sciences, 2011).

13. Alexander C, Rietschel ET. Bacterial lipopolysaccharides and innate immunity. *J Endotoxin Res*, 7(3), 167-202 (2001).

14. Huber M, Kalis C, Keck S *et al.* R-form LPS, the master key to the activation ofTLR4/MD-2-positive cells. *Eur J Immunol*, 36(3), 701-711 (2006).

15. Park BS, Song DH, Kim HM, Choi BS, Lee H, Lee JO. The structural basis of lipopolysaccharide recognition by the TLR4-MD-2 complex. *Nature*, 458(7242), 1191-1195 (2009).

16. Yi YS. Caspase-11 non-canonical inflammasome: a critical sensor of intracellular lipopolysaccharide in macrophage-mediated inflammatory responses. *Immunology*, 152(2), 207-217 (2017).

17. Botos I, Segal DM, Davies DR. The structural biology of Toll-like receptors. *Structure*, 19(4), 447-459 (2011).

18. Kawasaki T, Kawai T. Toll-like receptor signaling pathways. *Front Immunol*, 5, 461 (2014).

19. Kaufmann SH. The contribution of immunology to the rational design of novel antibacterial vaccines. *Nat Rev Microbiol*, 5(7), 491-504 (2007).

20. Racila DM, Kline JN. Perspectives in asthma: molecular use of microbial products in asthma prevention and treatment. *J Allergy Clin Immunol*, 116(6), 1202-1205 (2005).

21. Herrick CA, Bottomly K. To respond or not to respond: T cells in allergic asthma. *Nat Rev Immunol*, 3(5), 405-412 (2003).

22. Peri F, Calabrese V. Toll-like receptor 4 (TLR4) modulation by synthetic and natural compounds: an update. *J Med Chem*, 57(9), 3612-3622 (2014).

23. Akira S, Takeda K. Toll-like receptor signalling. *Nat Rev Immunol*, 4(7), 499-511 (2004).

24. Knirel YA, Valvano MA. *Bacterial lipopolysaccharides*.

25. Molinaro A, Holst O, Di Lorenzo F *et al.* Chemistry of lipid A: at the heart of innate immunity. *Chemistry*, 21(2), 500-519 (2015).

26. Yu L, Wang L, Chen S. Endogenous toll-like receptor ligands and their biological significance. *J Cell Mol Med*, 14(11), 2592-2603 (2010).

27. Molteni M, Gemma S, Rossetti C. The Role of Toll-Like Receptor 4 in Infectious and Noninfectious Inflammation. *Mediators Inflamm*, 2016 (2016).

28. Heneka MT, Carson MJ, El Khoury J *et al.* Neuroinflammation in Alzheimer's disease. *Lancet Neurol*, 14(4), 388-405 (2015).

29. Singer M, Deutschman CS, Seymour CW *et al.* The Third International Consensus Definitions for Sepsis and Septic Shock (Sepsis-3). *Jama*, 315(8), 801-810 (2016).

30. Fleischmann C, Scherag A, Adhikari NK *et al.* Assessment of Global Incidence and Mortality of Hospital-treated Sepsis. Current Estimates and Limitations. *Am J Respir Crit Care Med*, 193(3), 259-272 (2016).

31. Keynan Y, Fowke KR, Ball TB, Meyers AFA. Toll-Like Receptors Dysregulation after Influenza Virus Infection: Insights into Pathogenesis of Subsequent Bacterial Pneumonia. *ISRN Pulmonology*, 2011, 6 (2011).

32. Shah NS, Greenberg JA, McNulty MC *et al.* Bacterial and viral co-infections complicating severe influenza: Incidence and impact among 507 U.S. patients, 2013-14. *J Clin Virol*, 80, 12-19 (2016).

33. Crum-Cianflone NF. Invasive Aspergillosis Associated With Severe Influenza Infections. *Open Forum Infect Dis*, 3(3), ofw171 (2016).

34. Shirey KA, Lai W, Scott AJ *et al.* The TLR4 Antagonist, Eritoran, Protects Mice from Lethal Influenza Infection. *Nature*, 497(7450), 498-502 (2013).

35. Opal SM, Laterre PF, Francois B *et al.* Effect of eritoran, an antagonist of MD2-TLR4, on mortality in patients with severe sepsis: the ACCESS randomized trial. *Jama*, 309(11), 1154-1162 (2013).

36. van Noort JM, Bsibsi M. Toll-like receptors in the CNS: implications for neurodegeneration and repair. *Prog Brain Res*, 175, 139-148 (2009).

37. Hanamsagar R, Hanke ML, Kielian T. Toll-like receptor (TLR) and Inflammasome Actions in the Central Nervous System: New and Emerging Concepts. *Trends Immunol*, 33(7), 333-342 (2012).

38. Bachtell R, Hutchinson MR, Wang X, Rice KC, Maier SF, Watkins LR. Targeting the Toll of Drug Abuse: The Translational Potential of Toll-Like Receptor 4. *CNS Neurol Disord Drug Targets*, 14(6), 692-699 (2015).

39. Wu MK, Huang TL, Huang KW, Huang YL, Hung YY. Association between toll-like receptor 4 expression and symptoms of major depressive disorder. *Neuropsychiatr Dis Treat*, 11, 1853-1857 (2015).

40. De Paola M, Sestito SE, Mariani A *et al.* Synthetic and natural small molecule TLR4 antagonists inhibit motoneuron death in cultures from ALS mouse model. *Pharmacol Res*, 103, 180-187 (2016).

41. Thakur KK, Saini J, Mahajan K *et al.* Therapeutic implications of toll-like receptors in peripheral neuropathic pain. *Pharmacol Res*, 115, 224-232 (2017).

42. Bettoni I, Comelli F, Rossini C *et al.* Glial TLR4 receptor as new target to treat neuropathic pain: efficacy of a new receptor antagonist in a model of peripheral nerve injury in mice. *Glia*, 56(12), 1312-1319 (2008).

43. Gioannini TL, Zhang D, Teghanemt A, Weiss JP. An essential role for albumin in the interaction of endotoxin with lipopolysaccharide-binding protein and sCD14 and resultant cell activation. *J Biol Chem*, 277(49), 47818-47825 (2002).

44. Wright SD, Ramos RA, Tobias PS, Ulevitch RJ, Mathison JC. CD14, a receptor for complexes of lipopolysaccharide (LPS) and LPS binding protein. *Science*, 249(4975), 1431-1433 (1990).

45. Shimazu R, Akashi S, Ogata H *et al.* MD-2, a molecule that confers lipopolysaccharide responsiveness on Toll-like receptor 4. *J Exp Med*, 189(11), 1777-1782 (1999).

46. Gioannini TL, Teghanemt A, Zhang D, Levis EN, Weiss JP. Monomeric endotoxin:protein complexes are essential for TLR4-dependent cell activation. *J Endotoxin Res*, 11(2), 117-123 (2005).

47. Rice TW, Wheeler AP, Bernard GR *et al.* A randomized, double-blind, placebo-controlled trial of TAK-242 for the treatment of severe sepsis. *Crit Care Med*, 38(8), 1685-1694 (2010).

48. Miyake K. Innate immune sensing of pathogens and danger signals by cell surface Toll-like receptors. *Semin Immunol*, 19(1), 3-10 (2007).

49. Mancek-Keber M, Jerala R. Postulates for validating TLR4 agonists. *Eur J Immunol*, 45(2), 356-370 (2015).

50. Needham BD, Trent MS. Fortifying the barrier: the impact of lipid A remodelling on bacterial pathogenesis. *Nat Rev Microbiol*, 11(7), 467-481 (2013).

51. Li J, Csakai A, Jin J, Zhang F, Yin H. Therapeutic Developments Targeting Toll-like Receptor-4-Mediated Neuroinflammation. *ChemMedChem*, 11(2), 154-165 (2016).

52. Billod JM, Lacetera A, Guzman-Caldentey J, Martin-Santamaria S. Computational Approaches to Toll-Like Receptor 4 Modulation. *Molecules*, 21(8) (2016).

53. Rossignol DP, Lynn M. Antagonism of in vivo and ex vivo response to endotoxin by E5564, a synthetic lipid A analogue. *J Endotoxin Res*, 8(6), 483-488 (2002).

54. Mata-Haro V, Cekic C, Martin M, Chilton PM, Casella CR, Mitchell TC. The vaccine adjuvant monophosphoryl lipid A as a TRIF-biased agonist of TLR4. *Science*, 316(5831), 1628-1632 (2007).

55. Bowen WS, Minns LA, Johnson DA, Mitchell TC, Hutton MM, Evans JT. Selective TRIF-dependent signaling by a synthetic toll-like receptor 4 agonist. *Sci Signal*, 5(211), ra13 (2012).

56. Peri F, Piazza M. Therapeutic targeting of innate immunity with Toll-like receptor 4 (TLR4) antagonists. *Biotechnol Adv*, 30(1), 251-260 (2012).

57. Liu X, Dong T, Zhou Y, Huang N, Lei X. Exploring the Binding Proteins of Glycolipids with Bifunctional Chemical Probes. *Angew Chem Int Ed Engl*, 55(46), 14330-14334 (2016).

58. Ulivi V, Lenti M, Gentili C, Marcolongo G, Cancedda R, Descalzi Cancedda F. Anti-inflammatory activity of monogalactosyldiacylglycerol in human articular cartilage in vitro: activation of an anti-inflammatory cyclooxygenase-2 (COX-2) pathway. *Arthritis Res Ther*, 13(3), R92 (2011).

59. Flacher V, Neuberg P, Point F *et al.* Mannoside Glycolipid Conjugates Display Anti-inflammatory Activity by Inhibition of Toll-like Receptor-4 Mediated Cell Activation. *ACS Chem Biol*, 10(12), 2697-2705 (2015).

60. Cighetti R, Ciaramelli C, Sestito SE *et al.* Modulation of CD14 and TLR4.MD-2 activities by a synthetic lipid A mimetic. *Chembiochem*, 15(2), 250-258 (2014).

61. Perrin-Cocon L, Aublin-Gex A, Sestito SE *et al.* TLR4 antagonist FP7 inhibits LPS-induced cytokine production and glycolytic reprogramming in dendritic cells, and protects mice from lethal influenza infection. *Sci Rep*, 7, 40791 (2017).

62. Shirey KA, Lai W, Scott AJ *et al.* The TLR4 antagonist Eritoran protects mice from lethal influenza infection. *Nature*, 497(7450), 498-502 (2013).

63. Yamamoto H, Oda M, Kanno M *et al.* Chemical Hybridization of Vizantin and Lipid A to Generate a Novel LPS Antagonist. *Chem Pharm Bull (Tokyo)*, 64(3), 246-257 (2016).

64. Morin MD, Wang Y, Jones BT *et al.* Discovery and Structure-Activity Relationships of the Neoseptins: A New Class of Toll-like Receptor-4 (TLR4) Agonists. *J Med Chem*, 59(10), 4812-4830 (2016).

65. Marshall JD, Heeke DS, Rao E *et al.* A Novel Class of Small Molecule Agonists with Preference for Human over Mouse TLR4 Activation. *PLoS One*, 11(10) (2016).

66. Kuronuma K, Mitsuzawa H, Takeda K *et al.* Anionic pulmonary surfactant phospholipids inhibit inflammatory responses from alveolar macrophages and U937 cells by binding the lipopolysaccharide-interacting proteins CD14 and MD-2. *J Biol Chem*, 284(38), 25488-25500 (2009).

67. Kandasamy P, Numata M, Berry KZ *et al.* Structural analogs of pulmonary surfactant phosphatidylglycerol inhibit toll-like receptor 2 and 4 signaling. *J Lipid Res*, 57(6), 993-1005 (2016).

68. Zhang Y, Wu J, Ying S *et al.* Discovery of new MD2 inhibitor from chalcone derivatives with anti-inflammatory effects in LPS-induced acute lung injury. *Sci Rep*, 6, 25130 (2016).

69. Peluso MR, Miranda CL, Hobbs DJ, Proteau RR, Stevens JF. Xanthohumol and related prenylated flavonoids inhibit inflammatory cytokine production in LPS-activated THP-1 monocytes: structure-activity relationships and in silico binding to myeloid differentiation protein-2 (MD-2). *Planta Med*, 76(14), 1536-1543 (2010).

70. Rodrigues-Diez R, González-Guerrero C, Ocaña-Salceda C *et al.* Calcineurin inhibitors cyclosporine A and tacrolimus induce vascular inflammation and endothelial activation through TLR4 signaling. *Sci Rep*, 6 (2016).

71. Xiang N, Liu J, Liao Y *et al.* Abrogating ClC-3 Inhibits LPS-induced Inflammation via Blocking the TLR4/NF- κ B Pathway. *Sci Rep*, 6 (2016).

72. Selfridge BR, Wang X, Zhang Y *et al.* Structure-Activity Relationships of (+)-Naltrexone-Inspired Toll-like Receptor 4 (TLR4) Antagonists. *J Med Chem*, 58(12), 5038-5052 (2015).

73. Chen CY. TCM Database@Taiwan: the world's largest traditional Chinese medicine database for drug screening in silico. *PLoS One*, 6(1), e15939 (2011).

74. Jeong E, Lee JY. Intrinsic and extrinsic regulation of innate immune receptors. *Yonsei Med J*, 52(3), 379-392 (2011).

75. Wang Y, Qian Y, Fang Q *et al.* Saturated palmitic acid induces myocardial inflammatory injuries through direct binding to TLR4 accessory protein MD2. *Nat Commun*, 8 (2017).

76. Huang S, Rutkowsky JM, Snodgrass RG *et al.* Saturated fatty acids activate TLR-mediated proinflammatory signaling pathways. *J Lipid Res*, 53(9), 2002-2013 (2012).

77. Wang X, Loram LC, Ramos K *et al.* Morphine activates neuroinflammation in a manner parallel to endotoxin. *Proc Natl Acad Sci U S A*, 109(16), 6325-6330 (2012).

78. Shah M, Anwar MA, Yesudhas D, Krishnan J, Choi S. A structural insight into the negative effects of opioids in analgesia by modulating the TLR4 signaling: An in silico approach. *Sci Rep*, 6 (2016).

79. Wang C, Schuller Levis GB, Lee EB *et al.* Platycodin D and D3 isolated from the root of Platycodon grandiflorum modulate the production of nitric oxide and secretion of TNF-alpha in activated RAW 264.7 cells. *Int Immunopharmacol*, 4(8), 1039-1049 (2004).

80. Chung JW, Noh EJ, Zhao HL *et al.* Anti-inflammatory activity of prosapogenin methyl ester of platycodin D via nuclear factor-kappaB pathway inhibition. *Biol Pharm Bull*, 31(11), 2114-2120 (2008).

81. Hu X, Fu Y, Lu X *et al.* Protective Effects of Platycodin D on Lipopolysaccharide-Induced Acute Lung Injury by Activating LXR α -ABCA1 Signaling Pathway. *Front Immunol*, 7 (2016).

82. Olsson S, Sundler R. The role of lipid rafts in LPS-induced signaling in a macrophage cell line. *Mol Immunol*, 43(6), 607-612 (2006).

83. Szabo G, Dolganiuc A, Dai Q, Pruett SB. TLR4, ethanol, and lipid rafts: a new mechanism of ethanol action with implications for other receptor-mediated effects. *J Immunol*, 178(3), 1243-1249 (2007).

84. Lopez-Marques RL, Theorin L, Palmgren MG, Pomorski TG. P4-ATPases: lipid flippases in cell membranes. *Pflugers Arch*, 466(7), 1227-1240 (2014).

85. van der Mark VA, Elferink RP, Paulusma CC. P4 ATPases: flippases in health and disease. *Int J Mol Sci*, 14(4), 7897-7922 (2013).

86. van der Mark VA, Ghiboub M, Marsman C *et al.* Phospholipid flippases attenuate LPS-induced TLR4 signaling by mediating endocytic retrieval of Toll-like receptor 4. *Cell Mol Life Sci*, 74(4), 715-730 (2017).

87. Pawlikowska L, Strautnieks S, Jankowska I *et al.* Differences in presentation and progression between severe FIC1 and BSEP deficiencies. *J Hepatol*, 53(1), 170-178 (2010).

88. Fingerlin TE, Murphy E, Zhang W *et al.* Genome-wide association study identifies multiple susceptibility loci for pulmonary fibrosis. *Nat Genet*, 45(6), 613-620 (2013).

89. Mulvihill EE, Burke AC, Huff MW. Citrus Flavonoids as Regulators of Lipoprotein Metabolism and Atherosclerosis. *Annu Rev Nutr*, 36, 275-299 (2016).

90. Liu X, Wang N, Fan S *et al.* The citrus flavonoid naringenin confers protection in a murine endotoxaemia model through AMPK-ATF3-dependent negative regulation of the TLR4 signalling pathway. *Sci Rep*, 6 (2016).

91. Vocanson M, Hennino A, Rozieres A, Poyet G, Nicolas JF. Effector and regulatory mechanisms in allergic contact dermatitis. *Allergy*, 64(12), 1699-1714 (2009).

92. Oblak A, Pohar J, Jerala R. MD-2 determinants of nickel and cobalt-mediated activation of human TLR4. *PLoS One*, 10(3), e0120583 (2015).

93. Raghavan B, Martin SF, Esser PR, Goebeler M, Schmidt M. Metal allergens nickel and cobalt facilitate TLR4 homodimerization independently of MD2. *EMBO Rep*, 13(12), 1109-1115 (2012).

94. Bunn TL, Parsons PJ, Kao E, Dietert RR. Exposure to lead during critical windows of embryonic development: differential immunotoxic outcome based on stage of exposure and gender. *Toxicol Sci*, 64(1), 57-66 (2001).

95. Chibowska K, Baranowska-Bosiacka I, Falkowska A, Gutowska I, Goschorska M, Chlubek D. Effect of Lead (Pb) on Inflammatory Processes in the Brain. *Int J Mol Sci*, 17(12) (2016).

96. Das U, Manna K, Sinha M *et al.* Role of ferulic acid in the amelioration of ionizing radiation induced inflammation: a murine model. *PLoS One*, 9(5), e97599 (2014).

97. Yuan J, Ge K, Mu J *et al.* Ferulic acid attenuated acetaminophen-induced hepatotoxicity though down-regulating the cytochrome P 2E1 and inhibiting toll-like receptor 4 signaling-mediated inflammation in mice. *Am J Transl Res*, 8(10), 4205-4214 (2016).

98. Dang YP, Chen YF, Li YQ, Zhao L. Developments of Anticoagulants and New Agents with Anti-Coagulant Effects in Deep Vein Thrombosis. *Mini Rev Med Chem*, 17(4), 338-350 (2017).

99. Li HR, Liu J, Zhang SL *et al.* Corilagin ameliorates the extreme inflammatory status in sepsis through TLR4 signaling pathways. *BMC Complement Altern Med*, 17 (2017).

100. Wolfram S, Wang Y, Thielecke F. Anti-obesity effects of green tea: from bedside to bench. *Mol Nutr Food Res*, 50(2), 176-187 (2006).

101. He X, Wei Z, Wang J *et al.* Alpinetin attenuates inflammatory responses by suppressing TLR4 and NLRP3 signaling pathways in DSS-induced acute colitis. *Sci Rep*, 6 (2016).

102. Kovacs EM, Lejeune MP, Nijs I, Westerterp-Plantenga MS. Effects of green tea on weight maintenance after body-weight loss. *Br J Nutr*, 91(3), 431-437 (2004).

103. Kumazoe M, Nakamura Y, Yamashita M *et al.* Green Tea Polyphenol Epigallocatechin-3-gallate Suppresses Toll-like Receptor 4 Expression via Upregulation of E3 Ubiquitin-protein Ligase RNF216. *J Biol Chem*, (2017).

104. Shrivastava S, Jeengar MK, Reddy VS, Reddy GB, Naidu VG. Anticancer effect of celastrol on human triple negative breast cancer: possible involvement of oxidative stress, mitochondrial dysfunction, apoptosis and PI3K/Akt pathways. *Exp Mol Pathol*, 98(3), 313-327 (2015).

105. Han L, Li C, Sun B *et al.* Protective Effects of Celastrol on Diabetic Liver Injury via TLR4/MyD88/NF-κB Signaling Pathway in Type 2 Diabetic Rats. *J Diabetes Res*, 2016 (2016).

106. Dickinson SE, Wondrak GT. TLR4-directed Molecular Strategies Targeting Skin Photodamage and Carcinogenesis. *Curr Med Chem*, (2017).

107. DuBuske LM, Castells M, Holdich T. Significant Reduction In Combined Symptom And Medication Score Compared With Placebo Following MPL-Adjuvanted uSCIT In Patients With Seasonal Grass Pollen Allergy. *Journal of Allergy and Clinical Immunology*, 123(2, Supplement), S216 (2009).

108. Romanowski B, Schwarz TF, Ferguson L *et al.* Sustained immunogenicity of the HPV-16/18 AS04-adjuvanted vaccine administered as a two-dose schedule in adolescent girls: Five-year clinical data and modeling predictions from a randomized study. *Hum Vaccin Immunother*, 12(1), 20-29 (2016).

109. Jia ZJ, Wu FX, Huang QH, Liu JM. [Toll-like receptor 4: the potential therapeutic target for neuropathic pain]. *Zhongguo Yi Xue Ke Xue Yuan Xue Bao*, 34(2), 168-173 (2012).

110. Monnet E, Lapeyre G, Poelgeest EV *et al.* Evidence of NI-0101 pharmacological activity, an anti-TLR4 antibody, in a randomized phase I dose escalation study in healthy volunteers receiving LPS. *Clin Pharmacol Ther*, 101(2), 200-208 (2017).

111. Schromm AB, Howe J, Ulmer AJ *et al.* Physicochemical and biological analysis of synthetic bacterial lipopeptides: validity of the concept of endotoxic conformation. *J Biol Chem*, 282(15), 11030-11037 (2007).

112. Guha R. On exploring structure-activity relationships. *Methods Mol Biol*, 993, 81-94 (2013).

113. Evans JF, Hutchinson JH. Seeing the future of bioactive lipid drug targets. *Nat Chem Biol*, 6(7), 476-479 (2010).

114. Sanchez-Garcia L, Martín L, Mangues R, Ferrer-Miralles N, Vázquez E, Villaverde A. Recombinant pharmaceuticals from microbial cells: a 2015 update. *Microb Cell Fact*, 15 (2016).

115. Sevastsyanovich Y, Alfasi S, Cole J. Recombinant protein production: a comparative view on host physiology. *N Biotechnol*, 25(4), 175-180 (2009).

116. Zaffaroni L. Improved protein production in bacteria. (Ed.^(Eds) (University of Milano Bicocca, 2011)

117. Sevastsyanovich YR, Leyton DL, Wells TJ *et al.* A generalised module for the selective extracellular accumulation of recombinant proteins. *Microb Cell Fact*, 11, 69 (2012).

118. Martinez JL, Liu L, Petranovic D, Nielsen J. Pharmaceutical protein production by yeast: towards production of human blood proteins by microbial fermentation. *Curr Opin Biotechnol*, 23(6), 965-971 (2012).

119. Westers L, Westers H, Quax WJ. Bacillus subtilis as cell factory for pharmaceutical proteins: a biotechnological approach to optimize the host organism. *Biochim Biophys Acta*, 1694(1-3), 299-310 (2004).

120. Jurgen B, Hanschke R, Sarvas M, Hecker M, Schweder T. Proteome and transcriptome based analysis of Bacillus subtilis cells overproducing an insoluble heterologous protein. *Appl Microbiol Biotechnol*, 55(3), 326-332 (2001).

121. Bernhardt J, Volker U, Volker A *et al.* Specific and general stress proteins in Bacillus subtilis--a two-deimensional protein electrophoresis study. *Microbiology*, 143(Pt 3), 999-1017 (1997).

122. Eymann C, Homuth G, Scharf C, Hecker M. Bacillus subtilis functional genomics: global characterization of the stringent response by proteome and transcriptome analysis. *J Bacteriol*, 184(9), 2500-2520 (2002).

123. Mattanovich D, Gasser B, Hohenblum H, Sauer M. Stress in recombinant protein producing yeasts. *J Biotechnol*, 113(1-3), 121-135 (2004).

124. Gasser B, Saloheimo M, Rinas U *et al.* Protein folding and conformational stress in microbial cells producing recombinant proteins: a host comparative overview. *Microb Cell Fact*, 7, 11 (2008).

125. Graf A, Gasser B, Dragosits M *et al.* Novel insights into the unfolded protein response using Pichia pastoris specific DNA microarrays. *BMC Genomics*, 9, 390 (2008).

126. Dumont J, Euwart D, Mei B, Estes S, Kshirsagar R. Human cell lines for biopharmaceutical manufacturing: history, status, and future perspectives. *Crit Rev Biotechnol*, 36(6), 1110-1122 (2016).

127. Jiang Z, Georgel P, Du X *et al.* CD14 is required for MyD88-independent LPS signaling. *Nat Immunol*, 6(6), 565-570 (2005).

128. Nagai Y, Akashi S, Nagafuku M *et al.* Essential role of MD-2 in LPS responsiveness and TLR4 distribution. *Nat Immunol*, 3(7), 667-672 (2002).

129. Hoshino K, Takeuchi O, Kawai T *et al.* Cutting edge: Toll-like receptor 4 (TLR4)-deficient mice are hyporesponsive to lipopolysaccharide: evidence for TLR4 as the Lps gene product. *J Immunol*, 162(7), 3749-3752 (1999).

130. Nagai Y, Shimazu R, Ogata H *et al.* Requirement for MD-1 in cell surface expression of RP105/CD180 and B-cell responsiveness to lipopolysaccharide. *Blood*, 99(5), 1699-1705 (2002).

131. Kato K, Morrison AM, Nakano T, Tashiro K, Honjo T. ESOP-1, a secreted protein expressed in the hematopoietic, nervous, and reproductive systems of embryonic and adult mice. *Blood*, 96(1), 362-364 (2000).

132. Visintin A, Iliev DB, Monks BG, Halmen KA, Golenbock DT. MD-2. *Immunobiology*, 211(6-8), 437-447 (2006).

133. Visintin A, Mazzoni A, Spitzer JA, Segal DM. Secreted MD-2 is a large polymeric protein that efficiently confers lipopolysaccharide sensitivity to Toll-like receptor 4. *Proc Natl Acad Sci U S A*, 98(21), 12156-12161 (2001).

134. Ohnishi T, Muroi M, Tanamoto K-i. N-Linked Glycosylations at Asn26 and Asn114 of Human MD-2 Are Required for Toll-Like Receptor 4-Mediated Activation of NF-κB by Lipopolysaccharide. *The Journal of Immunology*, 167(6), 3354-3359 (2001).

135. da Silva Correia J, Ulevitch RJ. MD-2 and TLR4 N-linked glycosylations are important for a functional lipopolysaccharide receptor. *J Biol Chem*, 277(3), 1845-1854 (2002).

136. Zhang H, Tay PN, Cao W, Li W, Lu J. Integrin-nucleated Toll-like receptor (TLR) dimerization reveals subcellular targeting of TLRs and distinct mechanisms of TLR4 activation and signaling. *FEBS Lett*, 532(1-2), 171-176 (2002).

137. Mullen GE, Kennedy MN, Visintin A *et al.* The role of disulfide bonds in the assembly and function of MD-2. *Proc Natl Acad Sci U S A*, 100(7), 3919-3924 (2003).

138. Viriyakosol S, Tobias PS, Kirkland TN. Mutational analysis of membrane and soluble forms of human MD-2. *J Biol Chem*, 281(17), 11955-11964 (2006).

139. Kawasaki K, Nogawa H, Nishijima M. Identification of mouse MD-2 residues important for forming the cell surface TLR4-MD-2 complex recognized by anti-TLR4-MD-2 antibodies, and for conferring LPS and taxol responsiveness on mouse TLR4 by alanine-scanning mutagenesis. *J Immunol*, 170(1), 413-420 (2003).

140. Hamann L, Kumpf O, Muller M *et al.* A coding mutation within the first exon of the human MD-2 gene results in decreased lipopolysaccharide-induced signaling. *Genes Immun*, 5(4), 283-288 (2004).

141. Gruber A, Mancek M, Wagner H, Kirschning CJ, Jerala R. Structural model of MD-2 and functional role of its basic amino acid clusters involved in cellular lipopolysaccharide recognition. *J Biol Chem*, 279(27), 28475-28482 (2004).

142. Tsuneyoshi N, Fukudome K, Kohara J *et al.* The functional and structural properties of MD-2 required for lipopolysaccharide binding are absent in MD-1. *J Immunol*, 174(1), 340-344 (2005).

143. Janin J. Protein-protein recognition. *Progress in Biophysics and Molecular Biology*, 64(2), 145-166 (1995).

144. Demchenko AP. Recognition between flexible protein molecules: induced and assisted folding. *J Mol Recognit*, 14(1), 42-61 (2001).

145. Steinbrecher T, Labahn A. Towards accurate free energy calculations in ligand protein-binding studies. *Curr Med Chem*, 17(8), 767-785 (2010).

146. Acuner Ozbabacan SE, Gursoy A, Keskin O, Nussinov R. Conformational ensembles, signal transduction and residue hot spots: application to drug discovery. *Curr Opin Drug Discov Devel*, 13(5), 527-537 (2010).

147. Du X, Li Y, Xia YL *et al.* Insights into Protein-Ligand Interactions: Mechanisms, Models, and Methods. *Int J Mol Sci*, 17(2) (2016).

148. Yakimchuk K. Protein Receptor-Ligand Interaction/Binding Assays. Karolinska Institutet, S (Ed.^(Eds) (2011)

149. Zamyatina A. Aminosugar-based immunomodulator lipid A: synthetic approaches. *Beilstein J Org Chem*, 14, 25-53 (2018).

150. Resman N, Gradisar H, Vasl J, Keber MM, Pristovsek P, Jerala R. Taxanes inhibit human TLR4 signaling by binding to MD-2. *FEBS Lett*, 582(28), 3929-3934 (2008).

151. Viriyakosol S, McCray PB, Ashbaugh ME *et al.* Characterization of monoclonal antibodies to human soluble MD-2 protein. *Hybridoma (Larchmt)*, 25(6), 349-357 (2006).

152. Mancek-Keber M, Jerala R. Structural similarity between the hydrophobic fluorescent probe and lipid A as a ligand of MD-2. *Faseb j*, 20(11), 1836-1842 (2006).

153. [ONLINE]. en.wikipedia.org/wiki/Surface_plasmon_resonance. (Ed.^(Eds)

154. Kruger CL, Zeuner MT, Cottrell GS, Widera D, Heilemann M. Quantitative single-molecule imaging of TLR4 reveals ligand-specific receptor dimerization. *Sci Signal*, 10(503) (2017).

155. Okamura Y, Watari M, Jerud ES *et al.* The extra domain A of fibronectin activates Toll-like receptor 4. *J Biol Chem*, 276(13), 10229-10233 (2001).

156. Mancek-Keber M, Frank-Bertoncelj M, Hafner-Bratkovic I *et al.* Toll-like receptor 4 senses oxidative stress mediated by the oxidation of phospholipids in extracellular vesicles. *Sci Signal*, 8(381), ra60 (2015).

157. Goligorsky MS. TLR4 and HMGB1: partners in crime? *Kidney Int*, 80(5), 450-452 (2011).

158. Erridge C. The roles of Toll-like receptors in atherosclerosis. *J Innate Immun*, 1(4), 340-349 (2009).

159. Abdollahi-Roodsaz S, Joosten LA, Roelofs MF *et al.* Inhibition of Toll-like receptor 4 breaks the inflammatory loop in autoimmune destructive arthritis. *Arthritis Rheum*, 56(9), 2957-2967 (2007).

160. Cao L, Tanga FY, Deleo JA. The contributing role of CD14 in toll-like receptor 4 dependent neuropathic pain. *Neuroscience*, 158(2), 896-903 (2009).

161. Casula M, Iyer AM, Spliet WG *et al.* Toll-like receptor signaling in amyotrophic lateral sclerosis spinal cord tissue. *Neuroscience*, 179, 233-243 (2011).

162. Fan J, Li Y, Levy RM *et al.* Hemorrhagic shock induces NAD(P)H oxidase activation in neutrophils: role of HMGB1-TLR4 signaling. *J Immunol*, 178(10), 6573-6580 (2007).

163. Kuzmich NN, Sivak KV, Chubarev VN, Porozov YB, Savateeva-Lyubimova TN, Peri F. TLR4 Signaling Pathway Modulators as Potential Therapeutics in Inflammation and Sepsis. *Vaccines (Basel)*, 5(4) (2017).

164. Salluh JI, Povoa P. Biomarkers as end points in clinical trials of severe sepsis: a garden of forking paths. *Crit Care Med*, 38(8), 1749-1751 (2010).

165. Kalil AC, LaRosa SP, Gogate J, Lynn M, Opal SM. Influence of severity of illness on the effects of eritoran tetrasodium (E5564) and on other therapies for severe sepsis. *Shock*, 36(4), 327-331 (2011).

166. Danner RL, Van Dervort AL, Doerfler ME, Stuetz P, Parrillo JE. Antiendotoxin activity of lipid A analogues: requirements of the chemical structure. *Pharm Res*, 7(3), 260-263 (1990).

167. Matsuura M, Kiso M, Hasegawa A. Activity of monosaccharide lipid A analogues in human monocytic cells as agonists or antagonists of bacterial lipopolysaccharide. *Infect Immun*, 67(12), 6286-6292 (1999).

168. Yang D, Satoh M, Ueda H, Tsukagoshi S, Yamazaki M. Activation of tumor-infiltrating macrophages by a synthetic lipid A analog (ONO-4007) and its implication in antitumor effects. *Cancer Immunol Immunother*, 38(5), 287-293 (1994).

169. Tamai R, Asai Y, Hashimoto M *et al.* Cell activation by monosaccharide lipid A analogues utilizing Toll-like receptor 4. *Immunology*, 110(1), 66-72 (2003).

170. Funatogawa K, Matsuura M, Nakano M, Kiso M, Hasegawa A. Relationship of structure and biological activity of monosaccharide lipid A analogues to induction of nitric oxide production by murine macrophage RAW264.7 cells. *Infect Immun*, 66(12), 5792-5798 (1998).

171. Mueller M, Lindner B, Kusumoto S, Fukase K, Schromm AB, Seydel U. Aggregates are the biologically active units of endotoxin. *J Biol Chem*, 279(25), 26307-26313 (2004).

172. Gutsmann T, Schromm AB, Brandenburg K. The physicochemistry of endotoxins in relation to bioactivity. *Int J Med Microbiol*, 297(5), 341-352 (2007).

173. Gioannini TL, Teghanemt A, Zhang D *et al.* Isolation of an endotoxin-MD-2 complex that produces Toll-like receptor 4-dependent cell activation at picomolar concentrations. *Proc Natl Acad Sci U S A*, 101(12), 4186-4191 (2004).

174. Ciaramelli C, Calabrese V, Sestito SE *et al.* Glycolipid-based TLR4 Modulators and Fluorescent Probes: Rational Design, Synthesis, and Biological Properties. *Chem Biol Drug Des*, 88(2), 217-229 (2016).

175. Ohto U, Fukase K, Miyake K, Shimizu T. Structural basis of species-specific endotoxin sensing by innate immune receptor TLR4/MD-2. *Proc Natl Acad Sci U S A*, 109(19), 7421-7426 (2012).

176. Brandenburg K, Matsuura M, Heine H *et al.* Biophysical characterization of triacyl monosaccharide lipid a partial structures in relation to bioactivity. *Biophys J*, 83(1), 322-333 (2002).

177. Seydel U, Schromm AB, Brade L *et al.* Physicochemical characterization of carboxymethyl lipid A derivatives in relation to biological activity. *Febs j*, 272(2), 327-340 (2005).

178. Elson G, Dunn-Siegrist I, Daubeuf B, Pugin J. Contribution of Toll-like receptors to the innate immune response to Gram-negative and Gram-positive bacteria. *Blood*, 109(4), 1574-1583 (2007).

179. Liu Y, Yin H, Zhao M, Lu Q. TLR2 and TLR4 in autoimmune diseases: a comprehensive review. *Clin Rev Allergy Immunol*, 47(2), 136-147 (2014).

180. Kusama T, Soga T, Ono Y *et al.* Synthesis and biological activities of lipid A analogs: modification of a glycosidically bound group with chemically stable polar acidic groups and lipophilic groups on the disaccharide backbone with tetradecanoyl or N-dodecanoylglycyl groups. *Chem Pharm Bull (Tokyo)*, 39(12), 3244-3253 (1991).

181. Wen-Chi L, Masato O, Koichi F, Yasuo S, Shoichi K. A Divergent Synthesis of Lipid A and Its Chemically Stable Unnatural Analogues. *Bulletin of the Chemical Society of Japan*, 72(6), 1377-1385 (1999).

182. Fujimoto Y, Adachi Y, Akamatsu M *et al.* Synthesis of lipid A and its analogues for investigation of the structural basis for their bioactivity. *J Endotoxin Res*, 11(6), 341-347 (2005).

183. Mochizuki T, Iwano Y, Shiozaki M, Kurakata S, Kanai S, Nishijima M. Synthesis and biological activities of lipid A-type pyrancarboxylic acid derivatives. *Carbohydr Res*, 324(4), 225-230 (2000).

184. Lewicky JD, Ulanova M, Jiang ZH. Improving the immunostimulatory potency of diethanolamine-containing lipid A mimics. *Bioorg Med Chem*, 21(8), 2199-2209 (2013).

185. Fort MM, Mozaffarian A, Stover AG *et al.* A synthetic TLR4 antagonist has anti-inflammatory effects in two murine models of inflammatory bowel disease. *J Immunol*, 174(10), 6416-6423 (2005).

186. Johnson DA, Sowell CG, Johnson CL *et al.* Synthesis and biological evaluation of a new class of vaccine adjuvants: aminoalkyl glucosaminide 4-phosphates (AGPs). *Bioorg Med Chem Lett*, 9(15), 2273-2278 (1999).

187. Facchini FA, Coelho H, Sestito SE *et al.* Co-administration of Antimicrobial Peptides Enhances Toll-like Receptor 4 Antagonist Activity of a Synthetic Glycolipid. *ChemMedChem*, 13(3), 280-287 (2018).

188. Poltorak A, He X, Smirnova I *et al.* Defective LPS Signaling in C3H/HeJ and C57BL/10ScCr Mice: Mutations in Tlr4 Gene. *Science*, 282(5396), 2085-2088 (1998).

189. Medzhitov R, Preston-Hurlburt P, Janeway CA, Jr. A human homologue of the Drosophila Toll protein signals activation of adaptive immunity. *Nature*, 388(6640), 394-397 (1997).

190. Wright SD. Toll, a new piece in the puzzle of innate immunity. *J Exp Med*, 189(4), 605-609 (1999).

191. Schromm AB, Lien E, Henneke P *et al.* Molecular genetic analysis of an endotoxin nonresponder mutant cell line: a point mutation in a conserved region of MD-2 abolishes endotoxin-induced signaling. *J Exp Med*, 194(1), 79-88 (2001).

192. Wright SD, Tobias PS, Ulevitch RJ, Ramos RA. Lipopolysaccharide (LPS) binding protein opsonizes LPS-bearing particles for recognition by a novel receptor on macrophages. *J Exp Med*, 170(4), 1231-1241 (1989).

193. Schumann RR, Leong SR, Flaggs GW *et al.* Structure and function of lipopolysaccharide binding protein. *Science*, 249(4975), 1429-1431 (1990).

194. Tobias PS, Soldau K, Gegner JA, Mintz D, Ulevitch RJ. Lipopolysaccharide binding protein-mediated complexation of lipopolysaccharide with soluble CD14. *J Biol Chem*, 270(18), 10482-10488 (1995).

195. Lucas K, Maes M. Role of the Toll Like receptor (TLR) radical cycle in chronic inflammation: possible treatments targeting the TLR4 pathway. *Mol Neurobiol*, 48(1), 190-204 (2013).

196. Leon CG, Tory R, Jia J, Sivak O, Wasan KM. Discovery and development of toll-like receptor 4 (TLR4) antagonists: a new paradigm for treating sepsis and other diseases. *Pharm Res*, 25(8), 1751-1761 (2008).

197. Ireton GC, Reed SG. Adjuvants containing natural and synthetic Toll-like receptor 4 ligands. *Expert Rev Vaccines*, 12(7), 793-807 (2013).

198. Lam C, Schutze E, Hildebrandt J *et al.* SDZ MRL 953, a novel immunostimulatory monosaccharidic lipid A analog with an improved therapeutic window in experimental sepsis. *Antimicrob Agents Chemother*, 35(3), 500-505 (1991).

199. Knopf HP, Otto F, Engelhardt R *et al.* Discordant adaptation of human peritoneal macrophages to stimulation by lipopolysaccharide and the synthetic lipid A analogue SDZ MRL 953. Down-regulation of TNF-alpha and IL-6 is paralleled by an up-regulation of IL-1 beta and granulocyte colony-stimulating factor expression. *J Immunol*, 153(1), 287-299 (1994).

200. Kim HM, Park BS, Kim JI *et al.* Crystal structure of the TLR4-MD-2 complex with bound endotoxin antagonist Eritoran. *Cell*, 130(5), 906-917 (2007).

201. Ohto U, Fukase K, Miyake K, Satow Y. Crystal structures of human MD-2 and its complex with antiendotoxic lipid IVa. *Science*, 316(5831), 1632-1634 (2007).

202. Shin HJ, Lee H, Park JD *et al.* Kinetics of binding of LPS to recombinant CD14, TLR4, and MD-2 proteins. *Mol Cells*, 24(1), 119-124 (2007).

203. Schrodinger L. The PyMOL Molecular Graphics System, Version 1.8. (Ed.^(Eds) (2015)

204. Sestito SE, Facchini FA, Morbioli I *et al.* Amphiphilic Guanidinocalixarenes Inhibit Lipopolysaccharide (LPS)- and Lectin-Stimulated Toll-like Receptor 4 (TLR4) Signaling. *J Med Chem*, 60(12), 4882-4892 (2017).

205. Yang L, Skjevik Å A, Han Du WG, Noodleman L, Walker RC, Götz AW. Data for molecular dynamics simulations of B-type cytochrome c oxidase with the Amber force field. *Data Brief*, 8, 1209-1214 (2016).

206. Frisch MJT GW, Schlegel HB, Scuseria GE *et al.* Gaussian 09 Wallingford. (2009).

207. Kirschner KN, Yongye AB, Tschampel SM *et al.* GLYCAM06: a generalizable biomolecular force field. Carbohydrates. *J Comput Chem*, 29(4), 622-655 (2008).

208. Morris GM, Huey R, Lindstrom W *et al.* AutoDock4 and AutoDockTools4: Automated docking with selective receptor flexibility. *J Comput Chem*, 30(16), 2785-2791 (2009).

209. Schrödinger. *Release 2017-4: Maestro, Schrödinger, LLC, New York* (2017).

Review

For reprint orders, please contact: reprints@future-science.com

Future Medicinal Chemistry

Recent advances on Toll-like receptor 4 modulation: new therapeutic perspectives

Lenny Zaffaroni[1] & Francesco Peri*,[1]

[1]Department of Biotechnology & Biosciences, University of Milano-Bicocca; Piazza della Scienza, 2; 20126 Milano, Italy

* Author for correspondence: Tel.: +39 02 64483453; francesco.peri@unimib.it

Activation or inhibition of TLR4 by small molecules will provide in the next few years a new generation of therapeutics. TLR4 stimulation (agonism) by high-affinity ligands mimicking lipid A gave vaccine adjuvants with improved specificity and efficacy that have been licensed and entered into the market. TLR4 inhibition (antagonism) prevents cytokine production at a very early stage; this is in principle a more efficient method to block inflammatory diseases compared to cytokines neutralization by antibodies. Advances in TLR4 modulation by drug-like small molecules achieved in the last years are reviewed. Recently discovered TLR4 agonists and antagonists of natural and synthetic origin are presented, and their mechanism of action and structure–activity relationship are discussed.

First draft submitted: 4 August 2017; Accepted for publication: 9 November 2017; Published online: 30 January 2018

Keywords: CD14 • MD-2 • natural compounds • structure–activity relationship • synthetic compounds • TLR4

TLR4-associated pathologies & possible TLR4-based therapies

Toll-like receptors (TLRs) belong to the class of pattern recognition receptors and are the first line of defense from invading pathogens in humans and higher animals. TLRs recognize pathogen-associated molecular patterns (PAMPs), thus activating inflammation and innate immunity response [1]. Among TLRs, TLR4 is the specific sensor of lipopolysaccharide (LPS), one of the molecular components of Gram-negative outer membrane, and its truncated versions lipooligosaccharide (LOS) and lipid A, collectively termed as endotoxin [2,3]. TLR4 also recognizes endogenous molecules, called damage-associated molecular pattern (DAMPs) molecules, released by injured tissues and necrotic cells [4]. TLR4-mediated inflammation, triggered by PAMPs and DAMPs, is involved in several acute and chronic diseases. Hence, TLR4 is a key receptor on which both noninfectious and infectious stimuli converge to trigger a proinflammatory response. TLR4 can then have an inflammatory or repair role. Inflammation, in general, has a protective function, and TLR4 can play an important role in this context; in particular by activating the induction of specific resolution pathways that restore tissue integrity and function [5]. However, when the TLR4 inflammatory response is not regulated, it can be harmful for the organism. In several diseases with microbial (Gram-negative infections) or nonmicrobial etiology (ischemia/reperfusion injury, sterile and chronic inflammations, autoimmune diseases and neuroinflammation), TLR4 activation and signaling contribute to disease progression [6].

The most severe disease deriving from TLR4 excessive activation by PAMPs is sepsis. Sepsis is a dysregulated response of the host organism to outer pathogens, which leads to acute life-threatening organ dysfunction [7]. The global incidence of this syndrome accounts for 437 per 100,000 person-years between the years 1995 and 2015, according to retrospective analysis of an international database [8]. In western countries, mortality in patients with severe sepsis is 20–50%, and if there is no organ dysfunction it can be diminished (less than 20%). Septic shock with increased LPS levels in blood, overexpression of proinflammatory cytokines, activation of blood coagulation system and accumulation of fibrinogen degradation products leads to a violation of local and general hemodynamics and endothelial dysfunction via TLR4 signaling pathway.

Sepsis is one of the possible complications of severe influenza. The most typical bacterial species complicating disease are *Streptococcus pneumoniae*, *Pseudomonas aeruginosa*, *Acinetobacter* species, *Staphylococcus aureus* as well as *Enterobacteriaceae* species, *Aspergillus* species and others [9–11]. Sepsis is the most important example of pathology caused by TLR4 excessive and dysregulated activation by LPS that could be efficiently blocked by using TLR4

newlands press

antagonists such as Eritoran [12]. However, despite its efficacy in contrasting acute sepsis in animal models, Eritoran failed to pass clinical Phase III trials on septic patients [13].

Other pathologies are associated to DAMP/TLR4 signaling, for instance TLR4 plays a key role in the CNS neurodegeneration [14]. In CNS, TLRs activation can be either detrimental (neuroinflammation and neurodegeneration) or beneficial (tissue repair), or have a mixed, still not fully understood effect [15].

In the context of DAMP-associated pathologies, the inhibition of TLR4 stimulation by endogenous factors could be used to contrast a wide range of inflammatory disorders. These pathologies are caused by the release of reactive nitrogen or oxygen species and inflammatory cytokines following 'sterile inflammations' induced by DAMPs. In this context, TLR4 is a molecular target related to a broad spectrum of modern day diseases including asthma [16], allergies [17], chronic inflammations, autoimmune disorders, CNS diseases linked to neuroinflammation and cancer [18].

TLR4 has also been suggested as a promising therapeutic target for drug abuse [19] and major depressive disorder [20], as well as amyotrophic lateral sclerosis [21]. Possible application of synthetic TLR4 antagonists in the treatment of neuropathic pain has also been shown [22,23]. From a molecular point of view, TLR4 activation by LPS is based on the successive interaction of LPS with LBP [24] that transfers a single molecule of LPS from aggregates in solution to CD14 [25], that in turns shuttles LPS to the TLR4/MD-2 [26] complex. The whole molecular process ends with the formation of the $(LPS/MD\text{-}2/TLR4)_2$ complex on plasma membrane [27]. The complex transmits the signal in the cell by recruiting the MyD88 and the adapter MAL (MyD88-dependent pathways and production of a number of proinflammatory cytokines) or TRIF (MyD88-independent pathways and production of interferons) [1–3]. On the other hand, LOS can directly interact with the TLR4/MD-2 complex and activate TLR4 signaling without the participation of LBP and CD14 co-receptors [28,29].

Molecules active as TLR4 antagonists, Eritoran or TAK-242, have failed to block acute sepsis [13,30]. However, a new perspective is holding promise in using TLR4 antagonists to block TLR4 activation by DAMPs in chronic inflammatory diseases and sterile inflammations. DAMPs are released from inflamed and damaged tissues [31]. Unequivocal evidence that DAMPs are specific TLR4 agonists remains to be provided in some cases, because in biochemical experiments aimed at identifying endogenous TLR4 agonists, the activation of TLR4 pathway could actually derive from endotoxin contamination in DAMPs. While the molecular mechanisms of endotoxin (LPS and LOS) TLR4 activation are well understood [18], the mechanisms of DAMP/TLR4 signaling are only partially known. The high chemical diversity of recently discovered endogenous TLR4 ligands seems to be incompatible with the molecular specificity of TLR4 receptor. A recent critical paper on this subject recommended that some requirements are respected when assessing TLR4 agonism [32]. The most important condition is that the putative agonist should engage both TLR4 and MD-2 receptors for signaling and directly interacts with MD-2 and/or CD14 receptors [32].

As a follow-up of our previous reviews on this topic [18], we present here last achievements on the discovery of natural and synthetic molecules that modulate TLR4 activity as agonists or antagonists. We focus on small molecules (MW less than 1 KDa) that have been validated as TLR4 ligands according to the rules above mentioned, and on their mechanism of action.

In the first part, new synthetic TLR4 modulators are reported, in the second part are described compounds of natural origin.

Synthetic TLR4 modulators

From lipid A mimetics to other compounds

The rational design of lipid A variants and analogs afforded several TLR4 agonists and antagonists with glycolipid structures that have been reviewed by us [18] and others [33,34]. All these structures include the chemical determinant (pharmacophore) essential for MD-2 recognition and binding: a disaccharide core (GlcNAc–GlcNAc) with six lipid chains, and two negatively charged phosphates or phosphates bioisostere groups, at positions C1 and C4′ of the disaccharide. These are Eritoran [35], monophosphoryl lipid A (MPLA) [36] and aminoglycosides [37] lipid A mimetics. Other lipid A mimetics are based on a monosaccharide scaffold derived from lipid X, a biosynthetic precursor of lipid A, with activity as TLR4 antagonist [38]. All these compounds are sparingly soluble and have poor pharmacokinetic *in vivo*. The new tendency is therefore to explore new chemical structures, often derived from natural compounds, to obtain new TLR4 ligands with improved solubility and pharmacokinetics. We report here on TLR4 ligands and modulators recently discovered. Generally, the chemical structures of these molecules are

different from that of lipid A. Very often these compounds are structurally derived from natural compounds that have been found active on TLR4 or are the results of a random screening of libraries of compounds.

Glycolipid-based compounds

Fatty acid esters of monogalactosyldiacylglycerol

Fatty acid (FA) esters of monogalactosyldiacylglycerol (MGDG) are essential components of the thylakoid membrane in chloroplasts and dilinolenoyl MGDG has been reported to show anti-inflammatory effects in human peripheral blood neutrophils [39].

In order to understand the mechanism of action of these molecules, a derivative of dilinolenoyl MGDG, a bifunctional, MGDG-based probe (molecule **1**; Figure 1) has been synthesized.

1 contains two chemical functions, one reactive toward nucleophile groups in the target protein, another, the alkyne function, forms triazole adducts by reacting with azide groups (click reaction). **1** inhibited LPS-mediated TLR4 activation in a concentration-dependent manner in cells. Consistently with other studies [40], **1** showed strong inhibition of p38 phosphorylation without influencing the total cell number being a more potent inhibitor than parent MGDG.

Endogenous proteome labeling followed by pull down/LC–MS/MS showed that compound **1** mainly interacts with the TLR4/MD-2 complex. By molecular modeling it has been calculated the lowest-energy binding pose of **1** with the TLR4/MD-2 complex. **1** binds to MD-2 similarly to Eritoran, both FA chains of **1** insert into the hydrophobic pocket of MD-2, while the sugar part interacts with residues of the MD-2 cavity rim. The binding mode between **1** and TLR4/MD-2 shows that FA chains forms favorable hydrophobic interactions with human TLR4 (hTLR4) residues including F440, F463, L444, K388 and Q436, which facilitate the subsequent formation of a covalent bond with TLR4.

Mutational studies showed that two residues of hTLR4, namely F440 and F463, are essential for binding to **1**. Previous functional studies have identified that both F440 and F463 are required for cell activation by LPS. These mutational data reinforce the vision of a mechanism of action of MGDG based on direct competition with LPS for MD-2 binding.

Trimannoside glycolipid conjugates

Trimannoside glycolipid conjugates (MGCs; **2**; Figure 1) are formed by a branched core linked to three mannose units through triethylene glycol linkers and to a saturated or unsaturated C_{24} lipophilic chain. MGCs selectively blocked TLR4-mediated activation of human monocytes and monocyte-derived dendritic cells (DCs) by LPS [41].

The mechanism of action of MGCs is unique: while these compounds inhibit both MyD-88 and TRIF-mediated intracellular pathways deriving from TLR4 activation and also block NF-κB activation and nuclear translocation, they do not directly compete with LPS for MD-2/TLR4 binding. The action of MGCs is therefore not based on a direct competition with LPS for CD14 and/or MD-2 binding as in the case of the majority of other TLR4 antagonists.

2 has a disruptive action on lipid raft-located GPI-anchored proteins, CD1a and CD14, and induces their rapid cell internalization. Thus, the plasma membrane may be a principal target through which the modulatory effects of MGCs are mediated. In the presence of LPS, **2** could prevent CD14 and TLR4 co-localization. These results suggest that the inhibitory action of **2** and other MGCs is mediated by their effect on the cell membrane: they alter lipid raft composition, interfere with the clustering of CD14 and TLR4 in rafts, leading to impaired receptor complex formation and blocking of signal transduction. Moreover, selective deprivation of CD14 from the cellular membrane, and subsequent impairment of TLR4/MD-2 complex formation could be a new mechanism for TLR4 antagonism. A similar mechanism of action has been recently described for monosaccharide **3**, a synthetic TLR4 antagonist [42].

Monosaccharide derivatives

The diphosphorylated diacylated monosaccharide FP7 (compound **3**; Figure 1), is a synthetic molecule with potent TLR4 antagonist action both in cells and in animals [42,43]. Monosaccharide **3** inhibits the LPS-stimulated, TLR4-dependent secretion of proinflammatory cytokines (IL-6, IL-8 and MIP-1β) by monocytes and DCs and prevents DCs maturation upon TLR4 activation by LPS [43]. The mechanism of action of **3** is based on the direct competition with LPS for MD-2 binding probably reinforced by direct binding to CD14 co-receptor. ^{1}H NMR experiments demonstrated that after addition of MD-2, the signals of the two FA chains (C_{14}) of **3** is attenuated [42]

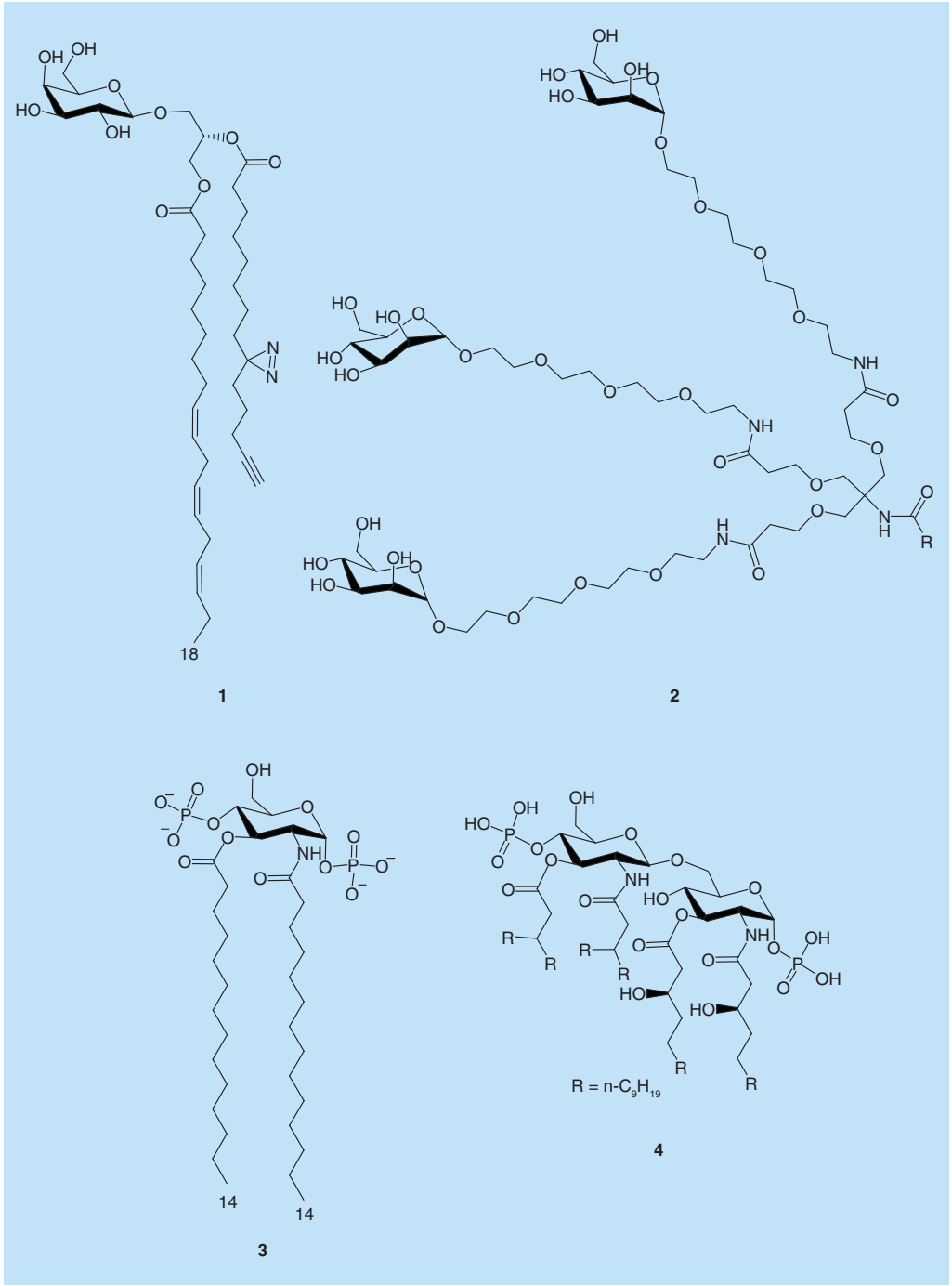

Figure 1. Recently discovered synthetic, glycolipid-based TLR4 modulators: (1) bifunctional MGDG probe, **(2)** trimannoside glycolipid conjugates, R= saturated or unsaturated C_{24} lipophilic chain, **(3)** monosaccharide FP7 and **(4)** vizantin–lipid A conjugate.
MGDG: Monogalactosyldiacylglycerol.

thus suggesting that lipophilic chains are the main interacting units of compound **3** with MD-2 hydrophobic pocket.

The capacity of **3** to induce CD14 and TLR4/MD-2 complex internalization in murine cells was analyzed [42]. Cell exposure to compound **3** caused endocytosis of CD14 but not of the TLR4/MD-2 complex. These results suggest that **3** interact directly with CD14, causing its internalization and deprivation of CD14 on plasma membrane could explain the antagonist action of **3**.

In vitro binding data with purified, functional MD-2 (Facchini FA et al., Unpublished Data) show that **3** is able to displace LPS from human MD-2 (hMD-2), and binds to hMD-2 with an affinity (K_D) in the low micromolar range.

The TLR4 antagonist Eritoran has been recently used to contrast influence lethality in animal models [44]. The infection of some influenza strains induces a TLR4-dependent cytokine storm similar to septic shock. Abnormal TLR4 stimulation is due to the release of endogenous TLR4 agonists (DAMPs) deriving form damage of lung tissue, such as oxidized phospholipids from infected tissue or circulating HMGB1 protein. The DAMP/TLR4 signaling related to influenza inflection is inhibited by Eritoran [44].

Similar to Eritoran, **3** selectively blocked DAMP/TLR4 signaling in animal models, protected mice from PR8 influenza virus-induced lethality and reduced proinflammatory cytokine gene expression in the lungs and acute lung injury (ALI) [43]. In a proof-of-concept experiment, compound **3** inhibited in a dose-dependent manner the DCs activation by endogenous HMGB1 [43]. This suggests that the mechanism of action of **3** in blocking influenza lethality could be based on inhibition of HMGB1/TLR4 signaling. The good bioavailability of **3**, together with its high water solubility, lack of toxicity and selective TLR4 antagonist action, make it a new drug hit targeting TLR4-related microbial and sterile inflammatory diseases.

Lipid A mimetic with Vizantin-like branched chains

In a recent study, it was shown that the trehalose derivative named Vizantin (6,6′-bis-*O*-(3-nonyldodecanoyl)-α,α′-trehalose) displays adjuvant activity based on TLR4 agonism and binding to the TLR4/MD-2 complex. Based on the known biological activity of lipid A and Vizantin, the authors projected a novel bifunctional glycolipid, that combines the structural features of Vizantin (namely, the two branched FA chains 3-nonyldodecanoic acid, 3NDDA) with the glucosamine core of lipid A (compound **4**; Figure 1) [45]. Disaccharide **4** potently antagonizes the LPS/TLR4 signaling pathway in a concentration-dependent manner, in human THP-1 cells, with an IC_{50} of 3.8 nM. Molecular docking simulations with MD-2 and MD-2/TLR4 suggest that the two branched NDDA chains of compound **4** insert into MD-2 binding cavity thus stabilizing the complex by hydrophobic interaction with the receptor.

Nonglycolipid TLR4 modulators

Neoseptins

The screening of 90,000 compounds tested for their ability to activate TNF-α in mouse peritoneal macrophages, led to the identification of a new TLR4 agonist, Neoseptin-1. Structure–activity relationship studies allowed to improve the design of this type of LPS-binding peptide mimetics, leading to Neoseptin-3 hit compound (**5**; Figure 2) [46].

5 is a peptidomimetic with no structural similarity to LPS that activates mouse TLR4 (mTLR4). *In vitro* dose response experiments demonstrated that molecule **5** activates TLR4 in different mouse cells. Induction of TNF-α by **5** was completely abrogated in TLR4- or MD-2-deficient mouse macrophages, while CD14-deficient macrophages that do not respond to LPS, still produced TNF-α in response to **5**.

5 activates mouse TLR4/MD-2 independently of CD14 and triggers canonical MyD88 and Toll IL-1 receptor domain-containing adaptor inducing IFN-β (TRIF)-dependent signaling. On the other hand, **5** is unable to stimulate human TLR4, as turned out from experiments on human THP-1 monocytes. This supported the idea that the TLR4 agonist activity of **5** is species-specific, with a preference toward mouse MD-2 (mMD-2). The direct interaction of **5** with mTLR4/MD-2 heterodimer with formation of a complex was observed by NMR binding experiments and, more directly, by x-ray analysis of the complex. The crystal structures of TLR4/MD-2 complex in the 'apo' form (i.e., without any ligand), in complex with lipid A, and with **5** were compared. In all the three different cases studied, the structure of the mTLR4/MD-2 complexes presented similar conformations. While having completely different chemical structures, lipid A and **5** are capable of inducing similar conformational changes of the MD-2 Phe126 loop region, the typical conformational switch induced by agonists. Interestingly, two molecules of **5** were found asymmetrically bound to MD-2 cavity in the complex with mTLR4/MD-2. The two

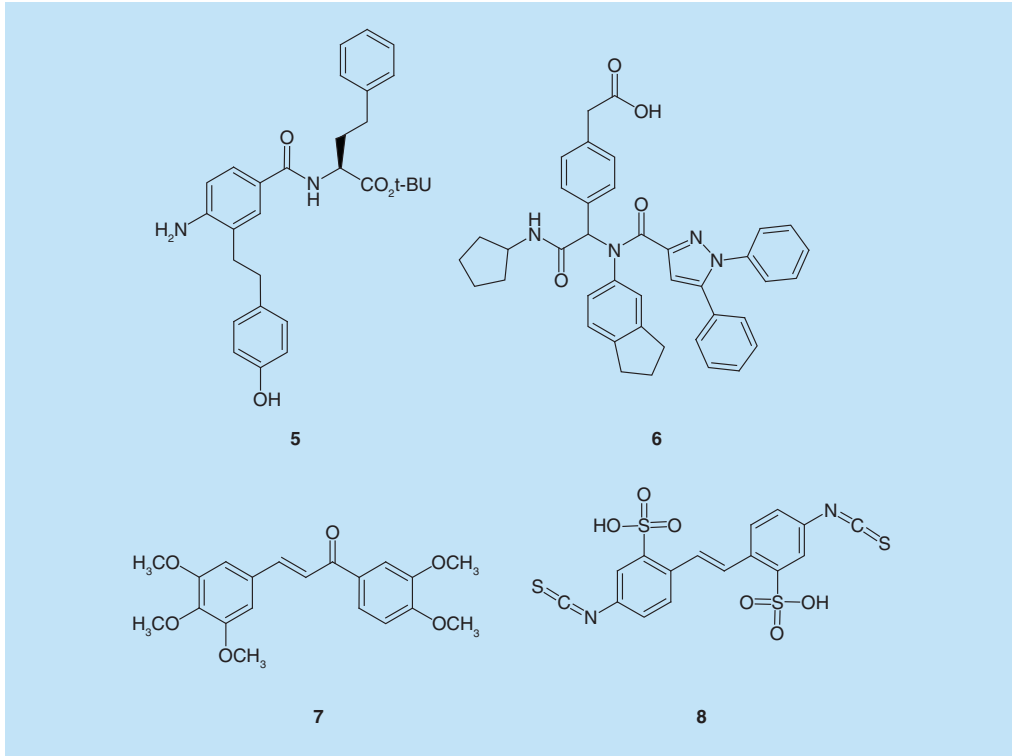

Figure 2. Nonglycolipid synthetic TLR4 modulators. (5) Neoseptin-3, **(6)** compound AZ617, **(7)** chalcone compound 20, and **(8)** 4,4′-Diisothiocyanostilbene-2,2′-disulfonic acid.

molecules occupy different sites at the rim of MD-2 binding cavity and interact with the second TLR4 molecule (TLR4*) thus promoting TLR4 dimerization and activation. The final activated complex (TLR4/MD-2/$\mathbf{5}_2)_2$ contains four molecules of **5**. This study provides new and interesting information on how a molecule different from lipid A can promote the formation of the activated TLR4/MD-2 heterodimer by binding MD-2 and TLR4*. The dissociation between CD14 function and MyD88/TRIF signaling pathways is reminiscent of the mechanism of action of other small-molecular TLR4 agonists, including Ugi compounds presented in the next paragraph. However, the lack of activity on human TLR4 receptor system limits the clinical development of Neoseptins as TLR4-directed therapeutics.

Ugi compounds

A panel of small molecules with TLR4 agonist activity was synthesized through a 4-component Ugi condensation reaction (the more potent molecule being AZ617, compound **6** in Figure 2) [47]. The majority of the synthetic Ugi compounds presented TLR4 agonist in HEK-293 cells transfected with hTLR4/hMD-2/hCD14 while were almost inactive in stimulating HEK cells transfected with mTLR4/mMD-2/mCD14. Species-specific TLR4 activation is due to higher affinity binding of Ugi compounds to hMD-2 than to mMD-2. By comparing the activity of Ugi compounds in HEK 'hybrid' transfectants with a combination of human and mouse receptors, namely hTLR4/mMD-2 and mTLR4/hMD-2, authors observed that Ugi compounds turned out to be more active in the transfectants containing hMD-2. The capacity of Ugi compounds to stimulate human TLR4 receptor system was also confirmed on human peripheral blood mononuclear cells (PBMCs). The preference of human TLR4 receptor system over murine is however peculiar, because LPS and MPLA, show an opposite preference for murine receptors giving a stronger activation in cells expressing mMD-2. Another important difference with LPS and lipid A-derived agonists is that the TLR4 activation mediated by compound **6** is CD14-independent. *In silico* studies

showed two possible sets of binding poses (with almost identical energy) of Ugi compounds into the hydrophobic binding pocket of MD-2.

As Ugi compounds have a TLR4 agonist preference toward human species, and a better water solubility compared with other lipid A analogs, making them a good starting point for the development of adjuvants that can activate TLR4 in cells with physiological low levels of CD14, such as DCs.

Phospholipids

Lung alveolar epithelium secretes a mixture of several proteins and lipids called pulmonary surfactants, which have important immunoregulatory properties, able of regulating the innate immune system by competitively antagonizing ligand-dependent activation of TLR4 [48]. Phospholipids account for 90% of pulmonary surfactants, and it has been reported that minor components of pulmonary surfactants, palmitoyl-oleoyl-phosphatidylglycerol (POPG) and phosphatidylinositol, are capable of inhibiting LPS-induced inflammatory responses in U937 cells, primary rat alveolar macrophages, and primary human alveolar macrophages by blocking LPS-induced phosphorylation of MAPKs and IκBα, and by preventing LPS-induced degradation of IκB and MKP-1 expression [48]. *In vitro* binding studies showed that POPG and phosphatidylinositol bind to LBP, CD14, and MD-2 in a concentration-dependent manner. A recent study screened a library of POPG variants, with the aim to understand the phospholipids' structural features that dictate the antagonistic activity against TLR2 and TLR4 [49]. In summary, POPG analogs with polar head group modifications can antagonize TLR2 and TLR4 activation. POPG analogs strongly bind to CD14 and MD-2 proteins, thus causing TLR4 inhibition. The structural plasticity necessary for TLRs modulation open up possibilities for the design of new POPG-like molecules that can possess individual TLRs specificity.

Chalcone derivatives

Several chalcone derivatives that contain the moiety of (E)-4-phenylbut-3-en-2-one, considered the core structure of currently known MD-2 inhibitors of natural origin such as curcumin, caffeic acid phenethyl ester and 1-dehydro-10-gingerdione, have been designed and synthesized in a recent study [50]. Among all the synthesized chalcone compounds, compound **7** (Figure 2) turned out to be the more potent in antagonizing the TLR4 pathway both *in vitro* and *in vivo*. Fluorescence spectroscopy experiments showed that **7** competitively inhibits the interactions between MD-2 and LPS, and also between TLR4 and MD-2. The direct interaction between **7** and MD-2 was confirmed by surface plasmon resonance experiments. Computational studies shown that in the lower energy binding pose, **7** would interact with MD-2 residues Arg90 and Tyr102, by forming two hydrogen bonds. This finding was experimentally confirmed by using MD-2 mutants [51]. **7** is also able to attenuate LPS-induced lung injuries, in particular by diminishing pulmonary inflammation and by preventing the interaction between MD-2 and TLR4 in lung tissue. Similar to other TLR4 antagonists as Eritoran and monosaccharide **3**, chalcone derivative **7** can be considered a hit compound for the development of drugs for the treatment of ALI and other TLR4-dependent syndromes induced by pathogens infections.

Calcineurin inhibitors

Calcineurin inhibitors (CNIs) cyclosporine A and tacrolimus are active in increasing the production of proinflammatory cytokines and endothelial activation markers through TLR4 activation in cultured murine endothelial and vascular smooth muscle cells as well as in *ex vivo* cultures of murine aortas [52]. Data showed that CNIs were unable to induce inflammation in aortas from *Tlr4*$^{-/-}$ mice and after pharmacological inhibition of TLR4 in endothelial cells. However, further research is required to clarify the exact mechanisms of action by which CNIs are able to activate the TLR4 pathway.

4,4′-Diisothiocyanostilbene-2,2′-disulfonic acid

The anti-inflammatory effects of 4,4′-Diisothiocyanostilbene-2,2′-disulfonic acid (compound **8**, Figure 2), a chloride channel blocker, were investigated in a recent study [53]. **8** significantly inhibits LPS-induced release of proinflammatory cytokines *in vitro* and *in vivo* studies, downregulating the inflammatory cytokines via inhibition of the TLR4/NF-κB pathway, with a clear indication that ClC-3 (a volume-activated chloride channel protein) is involved in the inhibitory effect of **8**. This study showed that abrogating ClC-3 inhibits the LPS-induced inflammatory response by inhibiting the TLR4/NF-κB pathway *in vivo* and *in vitro*, and this mechanism could represent a novel way for TLR4/NF-κB inhibition based on chloride channels.

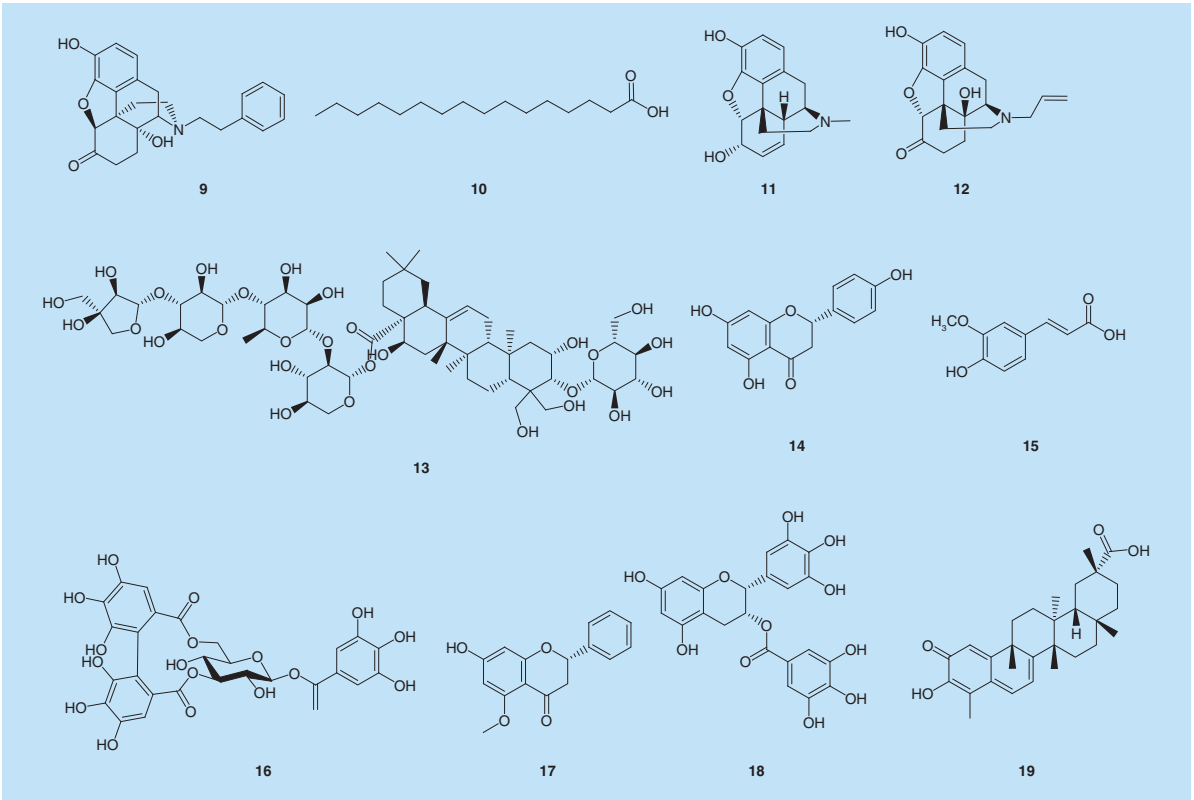

Figure 3. TLR4 modulators of natural origin. (9) *N*-phenethyl-noroxymorphone, **(10)** palmitic acid, **(11)** morphine, **(12)** naloxone, **(13)** platycodin, **(14)** naringenin, **(15)** ferulic acid, **(16)** corilagin, **(17)** alpinetin, **(18)** epigallocatechin-3-gallate and **(19)** celastrol.

Morphine derivatives

Compounds based on simplified morphine analogues (+)-naltrexone and (+)-noroxymorphone have been designed, synthesized and their TLR4 antagonist activities have been evaluated by their effects on inhibiting LPS induced TLR4 downstream nitric oxide production in microglia BV-2 cells [54]. Among all the compounds synthetized, the *N*-phenethyl-noroxymorphone (compound **9**; Figure 3) was the most potent TLR4 antagonist with an IC_{50} of 1.4 μM, and no cell cytotoxicity. This analog also showed *in vivo* efficacy in potentiating morphine analgesia, but further research is required to investigate its exact mechanism of TLR4 inhibition.

TLR4 modulators of natural origin

Plant secondary metabolism provides a vast source of chemically different bioactive and pharmacologically active compounds. Traditional Chinese and Indian medicine use a variety of herbs that are rich in molecules that very likely act as TLR4 modulators [55]. TLR4 activation or inhibition mediated by herbal extracts promoted a vast area of research which focuses on the molecular mechanism of action of these TLR4 modulators [56].

Saturated FAs (palmitic acid)

The molecular mechanism explaining the inflammatory action of palmitic acid (compound **10**, Figure 3; the most abundant circulating saturated fatty acids [SFAs]), has recently been proposed [57]. It has been observed that **10** induces myocardial inflammatory injury and dysfunction through MD-2 in mouse and cell culture experimental models. The paper presented studies of purified protein–ligand interactions indicating that **10** directly binds to MD-2, supporting a mechanism of canonical, MD-2-dependent, TLR4 activation and signaling. However, the MD-2 binding affinity of **10** measured by surface plasmon resonance turned out to be very low

(mM range). **10** is responsible for the production of proinflammatory cytokines in myocardial tissue, causing cardiac tissue remodeling and cardiac dysfunction in mice with hyperlipidemia and/or obesity. In addition, murine cardiomyocytes and macrophages acquired an MD-2-dependent proinflammatory phenotype when challenged with **10**. The computational docking simulation results also supported the hypothesis of direct MD-2/**10** binding and predicted that three molecules of **10** can accommodate into the MD-2 binding cavity. The resulting MD-2/**10** complex appeared to be relatively stable, with appropriate positioning of the FAs.

Interestingly, the findings from this study supported the idea that the ability of **10** (or other SFAs) to activate TLR4 signaling was likely attributed to its saturated nature. The change to unsaturated FAs on the lipid A moiety of LPS results in a complete loss of TLR4 agonist activity, and the unsaturated FA chain plays an important role in MD-2 binding of the antagonist Eritoran [58]. The authors found that, despite the binding to MD-2, unsaturated FAs did not induce TLR4/MD-2 complex formation nor activate downstream TLR4 signaling. Unsaturated FA was unable to induce cardiac inflammatory phenotype both *in vitro* and *in vivo* and did not significantly contribute to myocardial remodeling and injury in obesity. The observation that unsaturated FAs bound MD-2 suggests an intriguing possibility that unsaturated FAs may competitively inhibit SFAs to modulate TLR4 signaling response and chronic inflammation. These results underscore MD-2 as a necessary protein in SFA-mediated myocardial inflammatory injury.

Morphine & opioids

The molecular mechanism of TLR4 stimulation by morphine and opioids has been investigated, and presents several common points with LPS activation [59]. In a recent paper the structural dynamics of the opioid-bound activation mechanism of TLR4/MD-2 complex has been studied using various computational tools [60]. The *in silico* results supported previous findings: the binding of morphine (**11**) and naloxone (**12**) (Figure 3) into the hydrophobic pocket of MD-2 is TLR4-dependent. Binding of **11** induce the typical conformational change of MD-2 into its active form (agonist switch). In particular this is mediated by interaction of **11** with the Phe126 loop of MD-2 that confers stability to the subsequently formed TLR4/MD-2/**11** complex. The interaction with TLR4 also stabilizes the MD-2/**12** complex. However, **12** switches the Phe126 loop of MD-2 to its inactive (antagonist) conformation form. These data confirmed that subtle changes on the morphine structure can induce agonism to antagonism switch and that morphine scaffold could be used to generate potent and specific TLR4 modulators.

Platycodin D

Platycodin D (**13**; Figure 3), the major triterpene saponin in the root of *Platycodon grandiflorum*, exhibits a broad spectrum of anti-inflammatory effects by inhibiting LPS-induced TNF-α and IL-1β production [61] and NF-κB activation [62]. The mechanism of action of **13** in protecting LPS-induced ALI has been recently studied and clarified [63]. In *in vitro* and *in vivo* models, **13** acts as a TLR4 antagonist by mediating the depletion of cholesterol from plasma membrane and therefore by reducing the translocation of TLR4 to lipid rafts. This mechanism was confirmed by the fact that cholesterol replenishment prevented **13**-mediated TLR4 antagonism. Studies on raft-disrupting drugs supported these data, confirming that depletion of cholesterol can antagonize LPS-mediated TLR4 activation by the inhibition of TLR4 translocation into lipid rafts [64]. It has been reported that ethanol also acts by altering the LPS-induced redistribution of TLR4 complex within the lipid raft, thus interfering with receptor clustering and subsequent signaling [65].

P4-ATPases

Phospholipids translocation from exoplasmic to cytoplasmic leaflet is mediated by integral membrane proteins, named P4-ATPases, which have a crucial function in the biogenesis of transport vesicles and in endocytic pathways [66,67]. The hypothesis that P4-ATPases (in particular CDC50A) can play a role in the TLR4 activation pathway has been recently investigated [68]. In this study, the LPS-mediated TLR4 activation has been analyzed by using CDC50A-depleted THP-1 and human monocyte-derived macrophages. LPS challenge of CDC50A-depleted THP-1 is responsible for a hyper-activation of the MyD88-dependent pathway, caused by the impaired endocytic TLR4 retrieval. There are two P4-ATPases (i.e., ATP8B1 and ATP11A) that are expressed in humans, and their deficiency is associated with severe chronic liver disease [69] and pulmonary disorders [70]. The exact contribution of P4-ATPases in TLR4-dependent inflammatory disease remains to be established.

Naringenin

Naringenin (**14**; Figure 3) is a flavonoid naturally present in grapefruit and other citrus species that possess anti-inflammatory and antioxidant activities, particularly important for inflammatory-associated atherosclerosis, arthritis and metabolic syndrome [71]. In a recent study, the underlying mechanism of the anti-inflammatory properties and life-protective efficacy of **14** in LPS-stimulated macrophages and in a murine endotoxaemia model was evaluated [72]. **14** was able to prevent TNF-α and IL-6 upregulation, to inhibit NF-κB activation, and **14** was also responsible for the upregulated expression of ATF3 in LPS-stimulated murine macrophages. In lung tissues, the ATF3 expression is upregulated by the induction of AMPK that is provoked by **14**. In murine models of endotoxaemia, **14** improved the proinflammatory reactions and the survival of mice. This AMPK-ATF3-dependent downregulation of the LPS/TLR4 signaling pathway mediated by **14** represents a novel mechanism of TLR4 modulation.

Nickel & cobalt ions (Ni^{++} & Co^{++})

Allergic contact dermatitis is a very common skin disease, and among over 3,000 allergens, nickel is one of the most common ones [73]. Recent findings revealed that hTLR4, but not TLR4 of other species including mouse, can be directly activated by nickel and cobalt ions [74]. This species-specific activation is due to the coordination of nickel or cobalt ions by a cluster of histidine residues on the ectodomain of hTLR4 that is absent in the majority of other species TLR4. This study identified TLR4 and MD-2 mutants not responsive to LPS that can be activated by nickel and cobalt ions. Starting from these observations, authors proposed a model for the activation of the TLR4/MD-2 complex mediated by transition metal bivalent cations. To enable TLR4 activation several interactions are required and interactions mediated by the histidine residues of the TLR4 ectodomains can be a driving force for TLR4 dimerization. This is confirmed by a study where a single TLR4 mutation (residue N433, important for the interactions of the two TLR4 ectodomains), prevented the dimerization of TLR4 in the presence of cobalt or nickel ions [75].

Interestingly, nickel and cobalt ions turned out to be able to induce the dimerization of TLR4 ectodomain in the absence of MD-2 *in vitro* in cell-free experiments. However, this effect was not observed in cells.

Lead (Pb^{++})

Lead (Pb) exposure is a worldwide problem, and it has been shown that Pb exposure can impact the immune system integrity [76]. Pb neurotoxicity has been researched extensively, however, the proinflammatory role that this metal plays in the brain has not been fully understood. The inflammatory role of Pb has been recently presented [77], and experiments showed that exposure to Pb induce micro and astrogliosis by activating TLR4/MyD88/NF-κB signaling pathway. Increased levels of proinflammatory cytokines were also observed.

Ferulic acid

Ferulic acid (**15**; Figure 3) is a phenolic compound abundant in vegetables and fruits, and it presents several antioxidative and anti-inflammatory activities [78]. **15** pharmacological effects and the underlying mechanisms in mice with acetaminophen-induced hepatotoxicity have been investigated in a recent study [79]. **15** attenuated acetaminophen-induced serum TNF-α and IL-1β production, suppressed TLR4 expression, and dampened MAPK and NF-κB activation. These data suggested that **15** is able to partially suppress TLR4-mediated inflammatory response. However, the molecular mechanism of action of **15** in relation with TLR4 still needs elucidation.

Corilagin

Corilagin (**16**; Figure 3) is a polyphenol isolated from the extract of *Arctostaphylos uvaursi*, it is identified in several plants and it presents anti-inflammatory and antibacterial activity [80]. A recent study found that **16** is able to inhibit both TLR4-dependent MyD88 and TRIF signaling pathways [81]. Cellular and animal models treated with LPS and **16** presented mRNA levels and expression of TLR4, MyD88, TRIF and TRAF6, as well as IL-5 and IL-1β cytokines levels significantly decreased compared with the group treated with LPS alone. The molecular mechanism of action of **16** still needs elucidation.

Alpinetin

Alpinetin (**17**; Figure 3) is a natural flavonoid with known antibacterial, antitumor and other therapeutic activities [82]. A recent study investigates the anti-inflammatory effect of **17** in dextran sulfate sodium-induced colitis in mice [83]. **17** pretreatment inhibited significantly the phosphorylation of IKKa/b, IkBα and p65 NF-κB activation,

and TLR4 expression was downregulated in LPS-induced phorbol myristate acetate (PMA)-differentiated THP-1 cells. According to this study, **17** has a protective effect on dextran sulfate sodium-induced colitis and might be a promising therapeutic treatment. However, further research is required to understand the exact molecular mechanism of action of **17**.

Epigallocatechin-3-gallate

Green tea contains caffeine and polyphenolic compounds known as catechins. The most abundant catechol found in green tea is (−)-epigallocatechin-3-gallate (**18**; Figure 3) [84] which has been suggested to be responsible for many of the potential health effects of tea [82]. A recent study showed that **18** negatively regulates TLR4 pathway through the inhibition of downstream signaling [85]. **18** induced ubiquitination of TLR4, decreased TLR4 expression through E3 ubiquitin-protein ligase RNF216, and increased cGMP levels in macrophages. **18**-induced TLR4 downregulation is completely canceled by the soluble guanylate cyclase (cGMP synthesis enzyme) inhibitor, and cGMP induction is sufficient to suppress TLR4 expression. This is a novel mechanism for the downregulation of TLR4 expression. To study the role of cGMP in downregulation of expression, TLR4 could be particularly valuable.

Celastrol

Celastrol (**19**; Figure 3) is a pharmacologically active cyclic-penta-triterpene, extracted from the roots of the plant *Tripterygium wilfordii*. It has been reported that **19** is a potent immunosuppressive and anti-inflammatory agent [86]. A recent study investigated the protective effects of celastrol on TLR4-dependent liver injury in diabetic rats [87]. Diabetic rats presented steatohepatitis and proinflammatory cytokine significantly upregulated. **19**-treated diabetic rats presented reduced hepatic inflammation and macrophages infiltration. TLR4, MyD88 and NF-κB expression, as well as downstream inflammatory factors IL-1β and TNF-α in the hepatic tissue of **19**-treated rats were downregulated in a dose-dependent manner. Treatment with **19** delayed the progression of diabetic liver disease via the inhibition of TLR4/MyD88/NF-κB signaling pathways and its downstream inflammatory effectors. Further studies are required to clarify the molecular mechanisms of action of **19**, and for the development of new treatments for diabetic liver injury.

Conclusion

After the failure of TLR4 antagonists Eritoran and TAK-242 to pass clinical trials as drugs against acute sepsis and septic shock, the most recent change of direction in TLR4-directed therapeutics is to use TLR4 antagonist, included Eritoran, to block or reduce acute and chronic inflammatory diseases due to TLR4 activation by endogenous factors [88].

Another important paradigm change in the rational design of small-molecular TLR4 modulators is to move away from the structure of lipid A, the natural agonist, and explore new hit compounds derived from combinatorial libraries and natural sources (mainly plant secondary metabolites). Besides the necessity for companies and academic groups to have proprietary structures, the main reason to leave the ligand-based design so far adopted, is the low solubility in aqueous media of lipid A and lipid A-like molecules and their poor pharmacokinetic (adsorption and distribution) properties. Concerning synthetic molecules, new promising directions have been suggested in the use of nonlipid A-like synthetic glycolipids, as in the case of MGDG **1** and tri-MGCs **2** (Figure1) reported in this review [40,41]. This last type of antagonists show a new mechanism of action based on the targeting of membrane lipid rafts that would be essential to TLR4 organization in activated oligomeric species, and in the selective deprivation of CD14 co-receptor from plasma membrane [41]. Interestingly, a very similar mechanism of action based on membrane rafts targeting seems to be at the base of natural molecules such as the steroid **13** [63]. Membrane rafts disruption and impairment of CD14 function are new strategies for TLR4 antagonism that could be used by other molecules and deserve to be investigated more in detail in the perspective to develop new generations of TLR4 modulators. Phosphorylated lipo-monosaccharides as compound **3** [42,43], deriving from molecular simplification of lipid A, present several advantages in the perspective of industrial development, due to the much simpler synthesis compared with Eritoran, and retention of selectivity and antagonist potency. Innovative peptidomimetics (neoseptins) have been proposed in 2016 as interesting hit compounds to develop nonlipid A-like TLR4 agonists [46], while the low potency and the lack of activity on human TLR4 limit the applicability of these compounds. Other nonlipid A-like TLR4 modulators have been reviewed here among synthetic and natural molecules. In general, the main limitation of the studies on new TLR4 modulators reported in this review and

Table 1. Selection of clinical trials testing drugs targeting TLR4.

Compound	Action	Clinical phase	Indications	Ref./clinical trial identifier
MPL plus pollen (Pollinex Quattro)	Agonist	Licensed	Allergy	[89]
AS04 (Stimuvax)	Agonist	Licensed	Protection from HPV	[90]
AS04 (Stimuvax)	Agonist	Phase II	Rectal, prostate and colorectal cancer	NCT01507103, NCT01496131 and NCT01462513
AV-411 (Ibudilast)	Antagonist	Phase II	Asthma and poststroke disorders	[91]
NI-0101[†]	Antagonist	Phase II	Rheumatoid arthritis	[92]
GLA-SE (glucopyranosyl lipid A-stable emulsion)	Agonist	Phase I	Metastatic sarcoma	NCT02180698
GSK1795091	Agonist	Phase I	Cancer	NCT02798978
OM-174 (lipid A analog)	Agonist	Phase I	Solid tumor and melanoma	NCT01800812 and NCT01530698
E5564 (Eritoran)	Antagonist	Withdrawn	Severe sepsis	[13]
TAK-242 (resatorvid)	Antagonist	Withdrawn	Severe sepsis	[30]

[†]First-in-human study of an anti-TLR4 monoclonal antibody.
HPV: Human papillomavirus.

depicted in Figures 1–3 is the lack or very limited investigation of selectivity and toxicity. The TLR4 activity has been rarely compared with the activity on other TLRs or other biological targets, and toxicity studies are lacking as well.

Future perspective

Despite the majority of the natural and synthetic molecules reviewed here are in the early stage of preclinical development, ongoing clinical studies and a few licensed compounds demonstrate the potential of TLR4 modulators (Table 1). TLR4 agonists with a structure related to lipid A (MPL and AS04) have been licenced as vaccine adjuvants. Other lipid A mimetics (AS04, GLA-SE, GSK1795091 and OM-174) are in clinical Phase I or II as anticancer therapeutics. Small molecular TLR4 antagonist AV-411 (Ibudilast) is in Phase II clinical trials for the treatment of asthma and poststroke disorders. NI-0101 is the first anti-TLR4 monoclonal antibody to pass Phase I clinical trials for rheumatoid arthritis, showing safety and tolerability (Table 1).

Because of the very reduced number of chemicals in clinical phase of development as TLR4-based therapeutics, major efforts should be focused in the future to progress in the preclinical characterization of newly discovered hit compounds. To do this, complete data on toxicity and specificity should be collected for every new hit compound presented here. In parallel, it is still important to extend the chemical variety of TLR4 modulators by discovering new active molecules from natural sources (included fruits and vegetables) and from *de novo* designed synthetic molecules.

Executive summary

- TLR4 plays important roles in inflammation but also in repair processes after inflammation. TLR4 signal is activated by bacterial molecules and endogenous factors.
- TLR4 activators (agonists) and inhibitors (antagonists) are, respectively, potential vaccine adjuvants and antitumoral agents (agonists) and anti-inflammatory agents (antagonists).
- In the last 4 years several new synthetic TLR4 modulators have been discovered: some of them have a chemical structure related to lipid A, the natural TLR4 ligand produced by bacteria. Other synthetic molecules, such as neoseptins, Ugi compounds, chalcone and morphine derivatives, have a chemical structure not related to lipid A.
- Several natural compounds showed TLR4 activity: saturated fatty acids and oxidized phospholipids have agonist action.
- Other natural molecules recently discovered are active as TLR4 blockers (antagonists). These molecules are plant secondary metabolites: polyphenols, triterpenes and flavonoids.
- The TLR4-active compounds described in this review are in the early stage of preclinical development. Very few drug candidates targeting TLR4 are in clinical phase.
- It is necessary in the next future to increase the number of molecules that enter into clinical trials by characterizing the toxicity and specificity of action of the TLR4 modulators yet available.

Acknowledgements

The Italian Ministry for Foreign Affairs and International Cooperation (MAECI) is acknowledged.

Financial & competing interests disclosure

This study was financially supported by the H2020-MSC-ETN-642157 project 'TOLLerant'. The authors have no other relevant affiliations or financial involvement with any organization or entity with a financial interest in or financial conflict with the subject matter or materials discussed in the manuscript apart from those disclosed.

No writing assistance was utilized in the production of this manuscript.

References

Papers of special note have been highlighted as: • of interest

1. Akira S, Takeda K. Toll-like receptor signalling. *Nat. Rev. Immunol.* 4(7), 499–511 (2004).
2. Knirel YA, Valvano MA. *Bacterial lipopolysaccharides.* Springer-Verlag Wien, Vienna, Austria (2011).
3. Molinaro A, Holst O, Di Lorenzo F *et al.* Chemistry of lipid A: at the heart of innate immunity. *Chemistry* 21(2), 500–519 (2015).
4. Yu L, Wang L, Chen S. Endogenous toll-like receptor ligands and their biological significance. *J. Cell. Mol. Med.* 14(11), 2592–2603 (2010).
5. Molteni M, Gemma S, Rossetti C. The role of toll-like receptor 4 in infectious and noninfectious inflammation. *Mediators Inflamm.* 2016, (2016).
6. Heneka MT, Carson MJ, El Khoury J *et al.* Neuroinflammation in Alzheimer's disease. *Lancet Neurol.* 14(4), 388–405 (2015).
7. Singer M, Deutschman CS, Seymour CW *et al.* The third international consensus definitions for sepsis and septic shock (Sepsis-3). *JAMA* 315(8), 801–810 (2016).
8. Fleischmann C, Scherag A, Adhikari NK *et al.* Assessment of global incidence and mortality of hospital-treated sepsis. Current estimates and limitations. *Am. J. Respir. Crit. Care Med.* 193(3), 259–272 (2016).
9. Keynan Y, Fowke KR, Ball TB, Meyers AFA. Toll-like receptors dysregulation after influenza virus infection: insights into pathogenesis of subsequent bacterial pneumonia. *ISRN Pulmonology* 2011, 6 (2011).
10. Shah NS, Greenberg JA, McNulty MC *et al.* Bacterial and viral co-infections complicating severe influenza: incidence and impact among 507 US patients, 2013–14. *J. Clin. Virol.* 80, 12–19 (2016).
11. Crum-Cianflone NF. Invasive aspergillosis associated with severe influenza infections. *Open Forum Infect. Dis.* 3(3), ofw171 (2016).
12. Shirey KA, Lai W, Scott AJ *et al.* The TLR4 antagonist, Eritoran, protects mice from lethal influenza infection. *Nature* 497(7450), 498–502 (2013).
13. Opal SM, Laterre PF, Francois B *et al.* Effect of Eritoran, an antagonist of MD2-TLR4, on mortality in patients with severe sepsis: the ACCESS randomized trial. *JAMA* 309(11), 1154–1162 (2013).
14. van Noort JM, Bsibsi M. Toll-like receptors in the CNS: implications for neurodegeneration and repair. *Prog. Brain Res.* 175, 139–148 (2009).
15. Hanamsagar R, Hanke ML, Kielian T. Toll-like receptor (TLR) and inflammasome actions in the central nervous system: new and emerging concepts. *Trends Immunol.* 33(7), 333–342 (2012).
16. Racila DM, Kline JN. Perspectives in asthma: molecular use of microbial products in asthma prevention and treatment. *J. Allergy Clin. Immunol.* 116(6), 1202–1205 (2005).
17. Herrick CA, Bottomly K. To respond or not to respond: T cells in allergic asthma. *Nat. Rev. Immunol.* 3(5), 405–412 (2003).
18. Peri F, Calabrese V. Toll-like receptor 4 (TLR4) modulation by synthetic and natural compounds: an update. *J. Med. Chem.* 57(9), 3612–3622 (2014).
19. Bachtell R, Hutchinson MR, Wang X, Rice KC, Maier SF, Watkins LR. Targeting the toll of drug abuse: the translational potential of toll-like receptor 4. *CNS Neurol. Disord. Drug Targets* 14(6), 692–699 (2015).
20. Wu MK, Huang TL, Huang KW, Huang YL, Hung YY. Association between toll-like receptor 4 expression and symptoms of major depressive disorder. *Neuropsychiatr. Dis. Treat.* 11, 1853–1857 (2015).
21. De Paola M, Sestito SE, Mariani A *et al.* Synthetic and natural small molecule TLR4 antagonists inhibit motoneuron death in cultures from ALS mouse model. *Pharmacol. Res.* 103, 180–187 (2016).
22. Thakur KK, Saini J, Mahajan K *et al.* Therapeutic implications of toll-like receptors in peripheral neuropathic pain. *Pharmacol. Res.* 115, 224–232 (2017).
23. Bettoni I, Comelli F, Rossini C *et al.* Glial TLR4 receptor as new target to treat neuropathic pain: efficacy of a new receptor antagonist in a model of peripheral nerve injury in mice. *Glia* 56(12), 1312–1319 (2008).
24. Gioannini TL, Zhang D, Teghanemt A, Weiss JP. An essential role for albumin in the interaction of endotoxin with lipopolysaccharide-binding protein and sCD14 and resultant cell activation. *J. Biol. Chem.* 277(49), 47818–47825 (2002).

25. Wright SD, Ramos RA, Tobias PS, Ulevitch RJ, Mathison JC. CD14 a receptor for complexes of lipopolysaccharide (LPS) and LPS binding protein. *Science* 249(4975), 1431–1433 (1990).
26. Shimazu R, Akashi S, Ogata H *et al.* MD-2, a molecule that confers lipopolysaccharide responsiveness on toll-like receptor 4. *J. Exp. Med.* 189(11), 1777–1782 (1999).
27. Park BS, Song DH, Kim HM, Choi BS, Lee H, Lee JO. The structural basis of lipopolysaccharide recognition by the TLR4-MD-2 complex. *Nature* 458(7242), 1191–1195 (2009).
28. Gioannini TL, Teghanemt A, Zhang D, Levis EN, Weiss JP. Monomeric endotoxin:protein complexes are essential for TLR4-dependent cell activation. *J. Endotoxin Res.* 11(2), 117–123 (2005).
29. Huber M, Kalis C, Keck S *et al.* R-form LPS, the master key to the activation ofTLR4/MD-2-positive cells. *Eur. J. Immunol.* 36(3), 701–711 (2006).
30. Rice TW, Wheeler AP, Bernard GR *et al.* A randomized, double-blind, placebo-controlled trial of TAK-242 for the treatment of severe sepsis. *Crit. Care Med.* 38(8), 1685–1694 (2010).
31. Miyake K. Innate immune sensing of pathogens and danger signals by cell surface Toll-like receptors. *Semin. Immunol.* 19(1), 3–10 (2007).
32. Mancek-Keber M, Jerala R. Postulates for validating TLR4 agonists. *Eur. J. Immunol.* 45(2), 356–370 (2015).

- **Critically discusses the conditions for the assessment of TLR4 activity of nonlipopolysaccharide agonists.**

33. Li J, Csakai A, Jin J, Zhang F, Yin H. Therapeutic developments targeting toll-like receptor-4-mediated neuroinflammation. *ChemMedChem.* 11(2), 154–165 (2016).
34. Billod JM, Lacetera A, Guzman-Caldentey J, Martin-Santamaria S. Computational approaches to toll-like receptor 4 modulation. *Molecules* 21(8), (2016).
35. Rossignol DP, Lynn M. Antagonism of *in vivo* and *ex vivo* response to endotoxin by E5564, a synthetic lipid A analog. *J. Endotoxin. Res.* 8(6), 483–488 (2002).
36. Mata-Haro V, Cekic C, Martin M, Chilton PM, Casella CR, Mitchell TC. The vaccine adjuvant monophosphoryl lipid A as a TRIF-biased agonist of TLR4. *Science* 316(5831), 1628–1632 (2007).
37. Bowen WS, Minns LA, Johnson DA, Mitchell TC, Hutton MM, Evans JT. Selective TRIF-dependent signaling by a synthetic toll-like receptor 4 agonist. *Sci. Signal.* 5(211), ra13 (2012).
38. Peri F, Piazza M. Therapeutic targeting of innate immunity with toll-like receptor 4 (TLR4) antagonists. *Biotechnol. Adv.* 30(1), 251–260 (2012).
39. Liu X, Dong T, Zhou Y, Huang N, Lei X. Exploring the binding proteins of glycolipids with bifunctional chemical probes. *Angew Chem. Int. Ed. Engl.* 55(46), 14330–14334 (2016).

- **An important chemical work on the synthesis and characterization of a glycolipid-based chemical probe.**

40. Ulivi V, Lenti M, Gentili C, Marcolongo G, Cancedda R, Descalzi Cancedda F. Anti-inflammatory activity of monogalactosyldiacylglycerol in human articular cartilage *in vitro*: activation of an anti-inflammatory cyclooxygenase-2 (COX-2) pathway. *Arthritis Res. Ther.* 13(3), R92 (2011).
41. Flacher V, Neuberg P, Point F *et al.* Mannoside glycolipid conjugates display anti-inflammatory activity by inhibition of toll-like receptor-4 mediated cell activation. *ACS Chem. Biol.* 10(12), 2697–2705 (2015).

- **This paper presents a new type of sugar-based TLR4 antagonists and investigates in detail their mechanism of action.**

42. Cighetti R, Ciaramelli C, Sestito SE *et al.* Modulation of CD14 and TLR4.MD-2 activities by a synthetic lipid A mimetic. *Chembiochem.* 15(2), 250–258 (2014).
43. Perrin-Cocon L, Aublin-Gex A, Sestito SE *et al.* TLR4 antagonist FP7 inhibits LPS-induced cytokine production and glycolytic reprogramming in dendritic cells, and protects mice from lethal influenza infection. *Sci. Rep.* 7, 40791 (2017).
44. Shirey KA, Lai W, Scott AJ *et al.* The TLR4 antagonist Eritoran protects mice from lethal influenza infection. *Nature* 497(7450), 498–502 (2013).

- **First showed that synthetic TLR4 antagonist can be used to block TLR4-dependent influenza lethality.**

45. Yamamoto H, Oda M, Kanno M *et al.* Chemical hybridization of vizantin and lipid A to generate a novel LPS antagonist. *Chem. Pharm. Bull. (Tokyo)* 64(3), 246–257 (2016).
46. Morin MD, Wang Y, Jones BT *et al.* Discovery and structure–activity relationships of the neoseptins: a new class of toll-like receptor-4 (TLR4) agonists. *J. Med. Chem.* 59(10), 4812–4830 (2016).
47. Marshall JD, Heeke DS, Rao E *et al.* A novel class of small molecule agonists with preference for human over mouse TLR4 activation. *PLoS ONE* 11(10), (2016).
48. Kuronuma K, Mitsuzawa H, Takeda K *et al.* Anionic pulmonary surfactant phospholipids inhibit inflammatory responses from alveolar macrophages and U937 cells by binding the lipopolysaccharide-interacting proteins CD14 and MD-2. *J. Biol. Chem.* 284(38), 25488–25500 (2009).

49. Kandasamy P, Numata M, Berry KZ *et al.* Structural analogs of pulmonary surfactant phosphatidylglycerol inhibit toll-like receptor 2 and 4 signaling. *J. Lipid Res.* 57(6), 993–1005 (2016).
50. Zhang Y, Wu J, Ying S *et al.* Discovery of new MD2 inhibitor from chalcone derivatives with anti-inflammatory effects in LPS-induced acute lung injury. *Sci. Rep.* 6, 25130 (2016).
51. Peluso MR, Miranda CL, Hobbs DJ, Proteau RR, Stevens JF. Xanthohumol and related prenylated flavonoids inhibit inflammatory cytokine production in LPS-activated THP-1 monocytes: structure–activity relationships and *in silico* binding to myeloid differentiation protein-2 (MD-2). *Planta Med.* 76(14), 1536–1543 (2010).
52. Rodrigues-Diez R, González-Guerrero C, Ocaña-Salceda C *et al.* Calcineurin inhibitors cyclosporine A and tacrolimus induce vascular inflammation and endothelial activation through TLR4 signaling. *Sci. Rep.* doi: 10.1038/srep27915. (2016).
53. Xiang N, Liu J, Liao Y *et al.* Abrogating ClC-3 inhibits LPS-induced inflammation via blocking the TLR4/NF-κB pathway. *Sci. Rep.* doi:10.1038/srep27583 (2016) (Epub ahead of print).
54. Selfridge BR, Wang X, Zhang Y *et al.* Structure–activity relationships of (+)-naltrexone-inspired toll-like receptor 4 (TLR4) antagonists. *J. Med. Chem.* 58(12), 5038–5052 (2015).
55. Chen CY. TCM Database@Taiwan: the world's largest traditional Chinese medicine database for drug screening *in silico*. *PLoS ONE* 6(1), e15939 (2011).
56. Jeong E, Lee JY. Intrinsic and extrinsic regulation of innate immune receptors. *Yonsei Med. J.* 52(3), 379–392 (2011).
57. Wang Y, Qian Y, Fang Q *et al.* Saturated palmitic acid induces myocardial inflammatory injuries through direct binding to TLR4 accessory protein MD2. *Nat. Commun.* doi:10.1038/ncomms13997 (2017).
58. Huang S, Rutkowsky JM, Snodgrass RG *et al.* Saturated fatty acids activate TLR-mediated proinflammatory signaling pathways. *J. Lipid Res.* 53(9), 2002–2013 (2012).
59. Wang X, Loram LC, Ramos K *et al.* Morphine activates neuroinflammation in a manner parallel to endotoxin. *Proc. Natl Acad. Sci. USA* 109(16), 6325–6330 (2012).
60. Shah M, Anwar MA, Yesudhas D, Krishnan J, Choi S. A structural insight into the negative effects of opioids in analgesia by modulating the TLR4 signaling: an *in silico* approach. *Sci. Rep.* doi:10.1038/srep39271 (2016).
61. Wang C, Schuller Levis GB, Lee EB *et al.* Platycodin D and D3 isolated from the root of *Platycodon grandiflorum* modulate the production of nitric oxide and secretion of TNF-alpha in activated RAW 264.7 cells. *Int. Immunopharmacol.* 4(8), 1039–1049 (2004).
62. Chung JW, Noh EJ, Zhao HL *et al.* Anti-inflammatory activity of prosapogenin methyl ester of platycodin D via nuclear factor-kappaB pathway inhibition. *Biol. Pharm. Bull.* 31(11), 2114–2120 (2008).
63. Hu X, Fu Y, Lu X *et al.* Protective effects of platycodin D on lipopolysaccharide-induced acute lung injury by activating LXRα–ABCA1 signaling pathway. *Front. Immunol.* 7, 644 (2016).
64. Olsson S, Sundler R. The role of lipid rafts in LPS-induced signaling in a macrophage cell line. *Mol. Immunol.* 43(6), 607–612 (2006).
65. Szabo G, Dolganiuc A, Dai Q, Pruett SB. TLR4, ethanol, and lipid rafts: a new mechanism of ethanol action with implications for other receptor-mediated effects. *J. Immunol.* 178(3), 1243–1249 (2007).
66. Lopez-Marques RL, Theorin L, Palmgren MG, Pomorski TG. P4-ATPases: lipid flippases in cell membranes. *Pflugers Arch.* 466(7), 1227–1240 (2014).
67. van der Mark VA, Elferink RP, Paulusma CC. P4 ATPases: flippases in health and disease. *Int. J. Mol. Sci.* 14(4), 7897–7922 (2013).
68. van der Mark VA, Ghiboub M, Marsman C *et al.* Phospholipid flippases attenuate LPS-induced TLR4 signaling by mediating endocytic retrieval of Toll-like receptor 4. *Cell Mol. Life Sci.* 74(4), 715–730 (2017).
69. Pawlikowska L, Strautnieks S, Jankowska I *et al.* Differences in presentation and progression between severe FIC1 and BSEP deficiencies. *J. Hepatol.* 53(1), 170–178 (2010).
70. Fingerlin TE, Murphy E, Zhang W *et al.* Genome-wide association study identifies multiple susceptibility loci for pulmonary fibrosis. *Nat. Genet.* 45(6), 613–620 (2013).
71. Mulvihill EE, Burke AC, Huff MW. Citrus flavonoids as regulators of lipoprotein metabolism and atherosclerosis. *Annu. Rev. Nutr.* 36, 275–299 (2016).
72. Liu X, Wang N, Fan S *et al.* The citrus flavonoid naringenin confers protection in a murine endotoxaemia model through AMPK-ATF3-dependent negative regulation of the TLR4 signalling pathway. *Sci. Rep.* 6, 39735 (2016).
73. Vocanson M, Hennino A, Rozieres A, Poyet G, Nicolas JF. Effector and regulatory mechanisms in allergic contact dermatitis. *Allergy* 64(12), 1699–1714 (2009).
74. Oblak A, Pohar J, Jerala R. MD-2 determinants of nickel and cobalt-mediated activation of human TLR4. *PLoS ONE* 10(3), e0120583 (2015).
75. Raghavan B, Martin SF, Esser PR, Goebeler M, Schmidt M. Metal allergens nickel and cobalt facilitate TLR4 homodimerization independently of MD2. *EMBO Rep.* 13(12), 1109–1115 (2012).

76. Bunn TL, Parsons PJ, Kao E, Dietert RR. Exposure to lead during critical windows of embryonic development: differential immunotoxic outcome based on stage of exposure and gender. *Toxicol. Sci.* 64(1), 57–66 (2001).

77. Chibowska K, Baranowska-Bosiacka I, Falkowska A, Gutowska I, Goschorska M, Chlubek D. Effect of lead (Pb) on inflammatory processes in the brain *Int. J. Mol. Sci.* 17(12), 2140 (2016).

78. Das U, Manna K, Sinha M *et al.* Role of ferulic acid in the amelioration of ionizing radiation induced inflammation: a murine model. *PLoS ONE* 9(5), e97599 (2014).

79. Yuan J, Ge K, Mu J *et al.* Ferulic acid attenuated acetaminophen-induced hepatotoxicity though down-regulating the cytochrome P 2E1 and inhibiting toll-like receptor 4 signaling-mediated inflammation in mice. *Am. J. Transl. Res.* 8(10), 4205–4214 (2016).

80. Dang YP, Chen YF, Li YQ, Zhao L. Developments of anticoagulants and new agents with anti-coagulant effects in deep vein thrombosis. *Mini Rev. Med. Chem.* 17(4), 338–350 (2017).

81. Li HR, Liu J, Zhang SL *et al.* Corilagin ameliorates the extreme inflammatory status in sepsis through TLR4 signaling pathways. *BMC Complement Altern. Med.* 17, 18 (2017).

82. Wolfram S, Wang Y, Thielecke F. Anti-obesity effects of green tea: from bedside to bench. *Mol. Nutr. Food Res.* 50(2), 176–187 (2006).

83. He X, Wei Z, Wang J *et al.* Alpinetin attenuates inflammatory responses by suppressing TLR4 and NLRP3 signaling pathways in DSS-induced acute colitis. *Sci. Rep.* 6, 28370 (2016).

84. Kovacs EM, Lejeune MP, Nijs I, Westerterp-Plantenga MS. Effects of green tea on weight maintenance after body-weight loss. *Br. J. Nutr.* 91(3), 431–437 (2004).

85. Kumazoe M, Nakamura Y, Yamashita M *et al.* Green tea polyphenol epigallocatechin-3-gallate suppresses toll-like receptor 4 expression via upregulation of E3 ubiquitin-protein ligase RNF216. *J. Biol. Chem.* 292(10), 4077–4088 (2017).

86. Shrivastava S, Jeengar MK, Reddy VS, Reddy GB, Naidu VG. Anticancer effect of celastrol on human triple negative breast cancer: possible involvement of oxidative stress, mitochondrial dysfunction, apoptosis and PI3K/Akt pathways. *Exp. Mol. Pathol.* 98(3), 313–327 (2015).

87. Han L, Li C, Sun B *et al.* Protective effects of celastrol on diabetic liver injury via TLR4/MyD88/NF-κB signaling pathway in type 2 diabetic rats. *J. Diabetes Res.* 2016, (2016).

88. Dickinson SE, Wondrak GT. TLR4-directed molecular strategies targeting skin photodamage and carcinogenesis. *Curr. Med. Chem.* doi:10.2174/0929867324666170828125328 (2017) (Epub ahead of print).

89. DuBuske LM, Castells M, Holdich T. Significant reduction in combined symptom and medication score compared with placebo following MPL-adjuvanted uSCIT in patients with seasonal grass pollen allergy. *J. Allergy Clin. Immunol.* 123(Suppl. 2), S216 (2009).

90. Romanowski B, Schwarz TF, Ferguson L *et al.* Sustained immunogenicity of the HPV-16/18 AS04-adjuvanted vaccine administered as a two-dose schedule in adolescent girls: five-year clinical data and modeling predictions from a randomized study. *Hum. Vaccin. Immunother.* 12(1), 20–29 (2016).

91. Jia ZJ, Wu FX, Huang QH, Liu JM. [Toll-like receptor 4: the potential therapeutic target for neuropathic pain]. *Zhongguo Yi Xue Ke Xue Yuan Xue Bao* 34(2), 168–173 (2012).

92. Monnet E, Lapeyre G, Poelgeest EV *et al.* Evidence of NI-0101 pharmacological activity, an anti-TLR4 antibody, in a randomized Phase I dose escalation study in healthy volunteers receiving LPS. *Clin. Pharmacol. Ther.* 101(2), 200–208 (2017).

Journal of Medicinal Chemistry

Article

Cite This: J. Med. Chem. XXXX, XXX, XXX−XXX

pubs.acs.org/jmc

Structure−Activity Relationship in Monosaccharide-Based Toll-Like Receptor 4 (TLR4) Antagonists

Fabio A. Facchini,[†] Lenny Zaffaroni,[†] Alberto Minotti,[†] Silvia Rapisarda,[†] Valentina Calabrese,[†] Matilde Forcella,[†] Paola Fusi,[†] Cristina Airoldi,[†] Carlotta Ciaramelli,[†] Jean-Marc Billod,[‡] Andra Schromm,[§] Harald Braun,[∥] Charys Palmer,[⊥] Rudi Beyaert,[∥] Fabio Lapenta,[#] Roman Jerala,[#] Grisha Pirianov,[⊥] Sonsoles Martin-Santamaria,[‡] and Francesco Peri*[,†]

[†]Department of Biotechnology and Biosciences, University of Milano-Bicocca, Piazza della Scienza, 2, 20126 Milano, Italy

[‡]Department of Structural & Chemical Biology, Centro de Investigaciones Biologicas, CIB-CSIC, C/Ramiro de Maeztu, 9, 28040 Madrid, Spain

[§]Division of Immunobiophysics, Research Center Borstel, Parkallee 1-40, 23845 Borstel, Germany

[∥]VIB-UGent Center for Inflammation Research, UGent Department for Biomedical Molecular Biology, Unit of Molecular Signal Transduction in Inflammation, Technologiepark 927, 9052 Ghent, Belgium

[⊥]Anglia Ruskin Cambridge University, Cambridge CB1 1PT, U.K.

[#]Department of Synthetic Biology and Immunology, Kemijski Institute, National Institute of Chemistry, Hajdrihova 19, SI-1000 Ljubljana, Slovenia

Supporting Information

ABSTRACT: The structure−activity relationship was investigated in a series of synthetic TLR4 antagonists formed by a glucosamine core linked to two phosphate esters and two linear carbon chains. Molecular modeling showed that the compounds with 10, 12, and 14 carbons chains are associated with higher stabilization of the MD-2/TLR4 antagonist conformation than in the case of the C16 variant. Binding experiments with human MD-2 showed that the C12 and C14 variants have higher affinity than C10, while the C16 variant did not interact with the protein. The molecules, with the exception of the C16 variant, inhibited the LPS-stimulated TLR4 signal in human and murine cells, and the antagonist potency mirrored the MD-2 affinity calculated from *in vitro* binding experiments. Fourier-transform infrared, nuclear magnetic resonance, and small angle X-ray scattering measurements suggested that the aggregation state in aqueous solution depends on fatty acid chain lengths and that this property can influence TLR4 activity in this series of compounds.

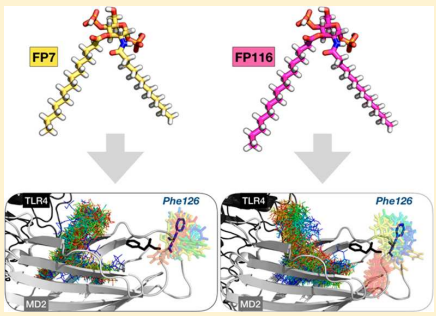

INTRODUCTION

Toll-like receptors (TLRs) are pattern recognition receptors (PRRs) that recognize pathogen-associated molecular patterns (PAMPs). TLR4 is mainly expressed on hematopoietic cells including monocytes, dendritic cells, and macrophages.[1] Lipopolysaccharide (LPS), lipooligosaccharide (LOS), and lipid A from Gram-negative bacteria are generally called endotoxin and are powerful TLR4 agonists.[2] TLR4 responds rapidly to minute amounts of circulating LPS through a multistep molecular recognition process, initiated by transfer of LPS monomers from aggregates in solution to LPS-binding protein (LBP), and subsequently to cluster to differentiation 14 (CD14) and to myeloid differentiation factor 2 (MD-2). MD-2 is associated with TLR4 in MD-2/TLR4 complexes on cell membrane. In the absence of agonist, the complex TLR4/MD-2 is in equilibrium between monomeric and dimeric species. Recent quantitative single-molecule localization microscopy (SMLM) studies[3] have shown that LPS binding to MD-2[4] displaces the equilibrium toward homodimeric complexes $(TLR4/MD\text{-}2/LPS)_2$.[3,5] The homodimer transmits the signal downstream through two distinct pathways. One pathway starts by recruitment of myeloid differentiation primary response gene 88 (MyD88) and adapter myelin and lymphocyte protein (MAL) (MyD88-dependent pathways and production of a number of pro-inflammatory proteins), the other by the activation of TIR-domain-containing adapter-inducing interferon-γ (TRIF) (MyD88-independent pathways and production of interferons).[6]

In addition to bacterial PAMPs, TLR4 can be also activated by damage-associated molecular patterns (DAMPs), endogenous agonists responsible for sterile inflammation, such as

Received: December 11, 2017
Published: March 1, 2018

DOI: 10.1021/acs.jmedchem.7b01803
J. Med. Chem. XXXX, XXX, XXX−XXX

fibronectins,[7] saturated palmitic acid,[8] oxidized phospholipids,[9] or high-mobility group box 1 (HMGB1) protein[10] which have also been shown to activate TLR4. While different LPS chemotypes share a conserved lipid A moiety with chemical determinants that ensure optimal interaction with CD14 and MD-2 (five or six lipophilic fatty acid chains attached to a disaccharide backbone, and one or two phosphate groups), DAMPs are chemically diverse molecules, and the molecular mechanism of TLR4 activation including the role of CD14 and MD-2 in the sensing of these molecules are not entirely understood. DAMPs have been implicated in many pathologies caused by TLR4 activation including atherosclerosis,[11] rheumatoid arthritis,[12] neuroinflammation,[13] trauma,[14] and hemorrhage.[15]

These findings strongly support the idea that regulation of TLR4 activity appears as a potential target for therapeutic control of a variety of inflammatory-based diseases. Manipulation of TLR4-mediated immune responses as a potential approach for pharmacological intervention has been reported in the literature.[16] For the past few years, several TLR4 antagonists have been evaluated in preclinical studies, but only two drugs, E5564[17] (Eritoran, Eisai, Inc.) and TAK-242[18] (Takeda Biological), progressed to clinical trials for treatment of sepsis, which have been discontinued in different phases.[19,20]

Efficient and selective TLR4 antagonists with a chemical structure simpler than lipid A are the basis for development of novel TLR4 modulators. Lipid A consists of a 1,4-diphosphorylated diglucosamine backbone to which variable lengths and numbers of fatty acid (FA) acyl chains are covalently linked.[2] Lipid X (Figure 1),[21] a biosynthetic precursor of lipid A with TLR4 antagonist activity, has been considered a simplified monosaccharide scaffold for the development of novel TLR4 modulators.

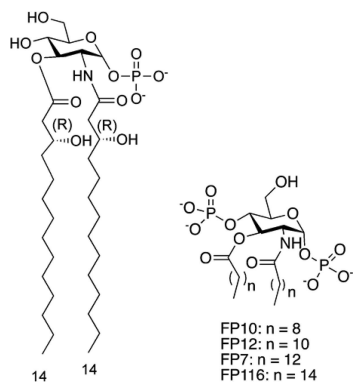

Figure 1. Chemical structures of lipid X and FP7 variants.

Our group developed the lipid X mimetic FP7,[6] a glucosamine derivative with two phosphate groups and two myristic (C14) fatty acid (FA) chains, whose design was inspired by other glucosamine-based TLR4 modulators.[22−24] FP7 is active in inhibiting in a dose-dependent way human[6] and murine[25] TLR4 activation by LPS. Some preliminary observations from nuclear magnetic resonance (NMR) experiments suggest that FP7 interact with MD-2, probably inserting FA chains into hydrophobic binding cavity.[6] This direct competition with LPS for MD-2 binding is probably reinforced by the capacity of FP7 to induce endocytosis of CD14, thus causing the absence of this receptor on the plasma membrane.[6] FP7 is active in blocking PR8 virus lethality that is mainly due to TLR4 overstimulation by endogenous DAMPs (mainly oxidized phospholipids and HMGB-1 protein) derived from viral damage to lung tissue.[25] In a proof-of-concept experiment in support of this *in vivo* mechanism, FP7 inhibited HMGB-1 activation of dendritic cells.[25] Other monosaccharide-based TLR4 modulators were developed, and structure−activity relationship (SAR) studies showed that the length of FA chain is a critical factor determining the potency of TLR4 antagonism or agonism.[22,26] The biological activity and the agonist/antagonist behavior on TLR4 of lipid A variants and other amphiphilic glycolipids including FP7 is not only determined by the interaction with MD-2 but also by the aggregation state in solution. Like LPS and lipid A, FP7 is an anionic amphiphile with a low value of CMC (9 μM).[6] Even though the CMC value of FP7 is higher than its IC_{50} (about 2 μM in HEK cells assays), equilibrium between aggregates and single molecules in solution is present in the concentration range in which FP7 is active.

It has been proposed for lipid A derivatives that the size and the 3D shape of aggregates influence the TLR4 activity, lamellar aggregates being associated with antagonism, and aggregates with nonlamellar cubic symmetry to agonism.[27,28] While the last step of ligand presentation to TLR4 and formation of the activated heterodimer $(TLR4/MD\text{-}2/ligand)_2$ is dominated by single molecule interactions between the ligand and CD14 and MD-2 receptors,[29] the early phases of endotoxin (ligand) recognition by LBP are very likely influenced by the aggregation state of the ligand.

We present here a SAR study on synthetic FP7 variants differing only for FA chains lengths (10, 12, 14, and 16 carbon atoms, Figure 1). In this study we will take into account both the interaction with MD-2 and the aggregation properties of the molecules. Additionally, we show the relationship between the chemical structure of FP7 variants with different fatty acid chains lengths and their effect on functional activity of TLR4 in different *in vitro* cell models.

RESULTS

Computational Design of FP7 Variants as Ligands of Human MD-2 and CD14. Given our previous studies on the lipid X mimetic FP7 as ligand of TLR4/MD-2 and CD14 proteins, with TLR4/MD-2 antagonist activity,[6] we were prompted to investigate the influence of the acyl chain length on the antagonist activity. To address this point, we designed three new FP7 derivatives with different fatty acid (FA) lengths: FP10 (C10), FP12 (C12), FP7 (C14), and FP116 (C16). The ability of these ligands to bind to TLR4/MD-2 complex and to CD14, compared with FP7, was initially assessed through various computational techniques.

We first docked the ligands in the binding site of CD14 using AutoDock Vina. For all the four ligands, docked poses inside the hydrophobic pocket were found. The obtained binding poses were very similar for all the ligands (Figure S1A) with also very close favorable predicted binding energies for the top poses (range from −6.5 to −5.9 kcal mol^{-1}). Therefore, the docking calculation showed that all four ligands are theoretically able to interact with CD14 inside its hydrophobic pocket and to engage in favorable interactions. In the most populated and most favorable docked poses, one phosphate group is interacting with the NH groups of Arg72 and Val73 and with the OH group of Tyr82 (Figure S1B), while the other

DOI: 10.1021/acs.jmedchem.7b01803
J. Med. Chem. XXXX, XXX, XXX−XXX

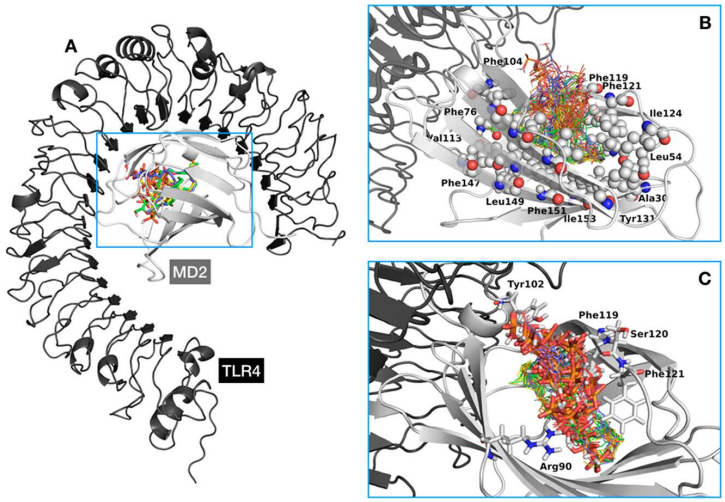

Figure 2. (A) General view of FP10 (in orange), FP12 (in yellow), FP7 (in green), and FP116 (in violet) ligands are shown docked inside TLR4/MD-2 (TLR4 is shown in black and MD-2 in gray). (B) Detail of the MD-2 hydrophobic pocket occupied by all the best docked poses for each ligand (represented as lines). Hydrophobic residues mentioned in the text as interacting with the FA chains of the ligands are represented in spheres. (C) Detail of the polar interactions of the ligands inside the TLR4/MD-2 system. Phosphate groups of the best docked poses of each ligand and the MD-2 residues with which they interact are represented in sticks.

phosphate group is exposed to the solvent. The FA chains are accommodated inside the hydrophobic pocket of CD14 interacting with aliphatic residues, mainly Ala, Val, Leu, and Ile residues and aromatic Phe49 (details are depicted in Figure S1C). The results were in agreement with previous docking studies of FP7 reported by us.[30]

We performed the docking calculations of ligands FP7, FP10, FP12, and FP116 inside the TLR4/MD-2 complex in the antagonist conformation (Figure 2). For all the compounds, favorable docked poses were found, with predicted binding energies, for the best ones, ranging from −7.8 to −6.5 kcal mol^{-1}. The polar head groups are placed at the rim of MD-2 and the FA chains go deep inside the hydrophobic pocket interacting with many hydrophobic residues, namely, Val24, Ala30, Ile32, Ile44, Ile46, Val48, Ile52, Leu54, Leu61, Ile63, Tyr65, Phe76, Leu78, Ile80, Phe104, Val113, Ile117, Phe119, Phe121, Ile124, Tyr131, Val135, Phe147, Leu149, Phe151, and Ile153 (Figure 2B).

Additionally, it was possible to observe more diversity in the predicted binding poses in TLR4/MD-2 than in the case of CD14. Results for FP7 were in agreement with those previously reported in MD-2 protein.[6] In many poses, one of the phosphate groups was close to the hydroxyl group of MD-2 Tyr102 where it establishes hydrogen bonds, and the other one was often close to MD-2 Arg90 establishing hydrogen bonds and electrostatic interactions (Figure 2C). In some docked poses, the phosphate groups were observed to interact with the backbone of residues Phe119, Ser120, and Phe121. Both phosphate groups were often placed at the rim of MD-2 where they are exposed to the solvent, in agreement with the reported X-ray crystallographic complexes of TLR4/MD-2 with glycolipids (for example, complex with Eritoran, PDB-ID 2Z65, or with lipid IVa, PDB-ID 2E59). Two different orientations were also found: type A (antagonist-like binding mode), similar to that found for lipid IVa in PDB-ID 2E59; and type B (agonist-like binding mode), similar to that found for *E. coli* lipid A in PDB-ID 3FXI (Figure S2). It is well-known that these two ligands, lipid IVa and *E. coli* lipid A, bind to TLR4/MD-2 in a different manner, one being rotated 180° compared to the other one, leading to opposed biological activities.

Selected binding poses were used as starting structures for redocking with AutoDock4 resulting in predicted binding energies ranging from −4.6 to +4.3 kcal mol^{-1}. Among the docked solutions, the best poses (from −4.6 to −2.5 kcal mol^{-1}) corresponded to binding poses very similar to those obtained with AutoDock Vina (data not shown). The narrow binding energy range did not permit to rank the ligands by predicted affinity, showing that the four ligands are putative binders of the TLR4/MD-2 system. Given that the main interactions (the polar ones) are common to the four ligands and that the MD-2 pocket is big enough to host two longer FA chains, from the docking calculations, it was not possible to clearly correlate the subtle differences in FA chain length with preferred ligand binding.

Stability of the predicted TLR4/MD-2/ligand complexes was further studied by molecular dynamics (MD) simulations. We selected two of the best binding poses for each ligand (Figure S3): one type A (antagonist-like binding pose) and one type B (agonist-like binding pose), plus two additional poses for compounds FP10 and FP7. Therefore, a total of eight 50 ns MD simulations were run. We monitored the motion of MD-2 over time and examined the root-mean-square deviation (rmsd) and rms fluctuation per residues, as well as the motion of Phe126 side chain over time (Figure S4). All the complexes showed stable ligand−receptor interactions along the MD simulation time as predicted by the docking calculations. In particular, in the MD simulation of the TLR4/MD-2/FP7 complex in the type A (antagonist-like) binding pose, the Phe126 side chain moves around its initial position staying largely exposed to the solvent in a conformation in agreement with the X-ray crystallographic antagonist conformation of MD-2 (Figure 3A).

DOI: 10.1021/acs.jmedchem.7b01803
J. Med. Chem. XXXX, XXX, XXX−XXX

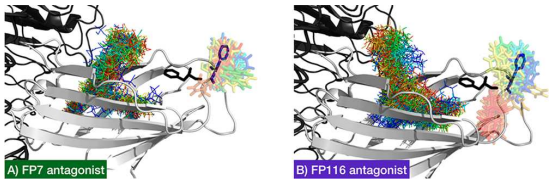

Figure 3. Superimposition of different snapshots (one for each simulated nanosecond), from the MD simulations of the TLR4/MD-2/ligand complexes, colored from blue (t = 0 ns) to red (t = 50 ns). Only ligands (as lines) and Phe126 (in sticks) are made visible. Side chains of Phe126 from the X-ray crystallographic structures have been superimposed to the snapshots to illustrate the antagonist (dark blue, PDB-ID 2E59) and agonist (black, PDB-ID 3FXI) conformations of MD-2. (A) TLR4/MD-2/FP7 complex starting from the type A binding pose (antagonist-like). (B) TLR4/MD-2/FP116 complex starting from the type A binding pose (antagonist-like).

To evaluate the relative orientation between the ligands and MD-2, we arbitrarily defined two vectors, one from the amide carbon atom to the ester and carbon atom of the ligand, and another one from the carbon of residues Pro78 to Thr105 of MD-2 (Figure S5A). The angle between these two vectors was plotted both over time and as a percentage of frames per 0.1 degree angle range (Figure S6). It was observed that none of the ligands undergoes orientation flip during the 50 ns simulations; all remain in the orientation from the docking process. Interestingly, only in the case of the TLR4/MD-2/FP116 complex with FP116 in the type A (antagonist-like) binding pose does the orientation of Phe126 side chain flip over (Figure 3B). We monitored this flipping behavior along the MD simulations, for all the ligands, by arbitrarily choosing two vectors, within MD-2, both starting from the carbon of residue Phe126 to, respectively, the phenyl C-4 atom of the same residue and the carbon of residue Ser21 (data shown in Figures S5B and S7). This observation could suggest that FP116 is not able to efficiently retain an antagonist conformation of MD-2, thus pointing to a poor antagonist capacity.

Additionally, logP values of compounds FP10, FP12, FP7, and FP116 were computationally calculated, ranging from approximately 4 to 10 with a linear distribution (Figure S8). The highest logP value was obtained for FP116 indicating a high lipophilicity that might result in low water solubility. This was in agreement with the lower acyl chain mobility as analyzed by Fourier-transform infrared (FT-IR) spectroscopy (see below). In any case, this did not interfere with the performance of the cell assays. Summarizing, the computational studies assessed the ability of ligands FP7, FP10, FP12, and FP116 to bind both CD14 and TLR4/MD-2, pointing to the long FP116 acyl chain (C16) as the maximum length bordering good

Scheme 1[a]

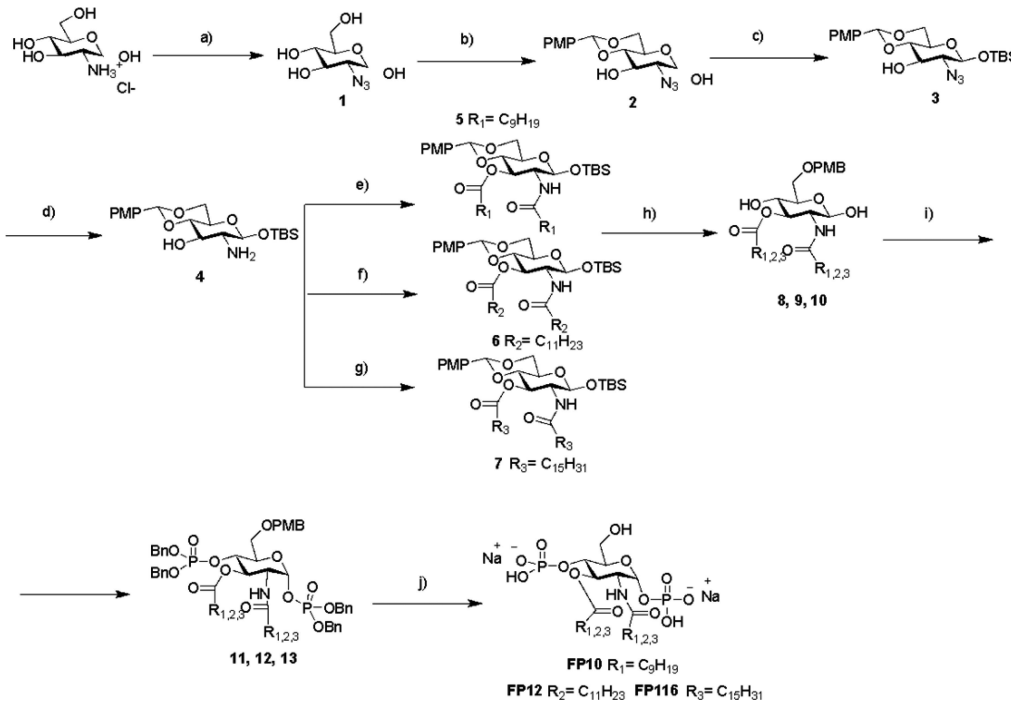

[a]Reagents and conditions: (a) $CuSO_4$, TEA, Py:H_2O, 0 °C, 30 min then TfN_3, Py, 0 °C−rt, O.N., quant.; (b) p-MeOPhCH$(OMe)_2$, CSA, DMF dry, 40 °C, 8 h, 68%; (c) TBSCl, imidazole, CH_2Cl_2 dry, rt, 1.5 h, 62%; (d) PPh_3, THF/H_2O, 60 °C, 2 h, quant.; (e) decanoic acid, EDC, DMAP, CH_2Cl_2 dry, rt, 6 h, 79%; (f) lauroyl chloride, DMAP, Py dry, 0 °C−rt, O.N., 79%; (g) palmitoyl chloride, DMAP, Py dry, rt, O.N., 75%; (h) $NaCNBH_3$, 4 Å MS, THF dry, rt, O.N., then HCl 1 M in dioxane until pH 2, 12−70%; (i) $(BnO)_2PNiPr_2$, imidazolium triflate, CH_2Cl_2 dry, rt, 30 min, then m-CPBA, 0 °C−rt, O.N., 51−56%; (j) (i) H_2, Pd/C, MeOH dry/CH_2Cl_2 dry, rt, O.N., (ii) Et_3N, (iii) IRA 120 H^+ resin, (iv) IR 120 Na^+, 84%-quant.

DOI: 10.1021/acs.jmedchem.7b01803
J. Med. Chem. XXXX, XXX, XXX−XXX

(predicted) binding properties. The compounds were therefore synthesized and tested.

Synthesis of FP Variants. Compounds FP7, FP10, FP12, and FP116 were synthesized according to a divergent synthetic strategy starting from the common precursor **4** (Scheme 1).

Commercially available D-glucosamine hydrochloride was converted into the intermediate **4** by subsequent protection of C-4 and C-6 positions as *p*-methoybenzylidene and the anomeric (C-1) position as *tert*-butyldimethylsislyl (TBDMS) ether.[6] Intermediate **4** was then acylated in positions C2 and C3 according to three different procedures, obtaining monosaccharides **8**, **9**, and **10** with, respectively, C10, C12, and C16 carbon FA chains. Compound FP7, with C14 chains, was obtained similarly following a published procedure.[6] Regioselective *p*-methoxybenzylidene ring opening as *p*-methoxybenzyl (PMB) ether in C-6, followed by phosphorylation of free hydroxyls in positions C1 and C4, and final deprotection of PMB ethers gave final compounds as triethylammonium ions. Exchange of triethylammonium with sodium (IR120 Na^+ ion-exchange resin) followed by reverse-phase purification gave final compounds FP10, FP12, and FP116 with a purity ≥95%.

Aggregation Properties of FP Compounds. *FT-IR Studies.* The mobility of the acyl chains is an important biophysical parameter of aggregated lipids. Biological lipids typically show a temperature-dependent phase transition from a highly ordered gel (Lβ) phase of the hydrocarbon chains at low temperatures (indicated by an absorption peak around 2850 cm^{-1}) to a liquid-cystalline (Lα) phase at higher temperatures (indicated by a absorption peak around 2852 cm^{-1}). The phase transition temperature (T_c) is characteristic of the chemical structure of the lipids. The FP compounds were analyzed by FT-IR spectroscopy to determine the lipid phase in dependence of temperature. FP compounds with shorter acyl chains (FP10, C10 and FP12, C12) were found to be in a fluid Lα phase with high mobility of their acyl chains at all temperatures. FP compounds with longer acyl chains (FP7, C14 and FP116, C16) showed a biphasic behavior with a clear Lβ to Lα phase transition with T_c around 28.5 °C for FP7 and around 40.2 °C for FP116 (Figure 4). Notably, the main phase transition of FP116 at 40.2 °C occurs along a broad temperature range, and a second phase transition is observed around 65 °C. Thus, at a biological relevant temperature of 37 °C, FP10, FP12, and FP7 exhibit a fluid membrane phase, whereas FP116 is still in a rigid membrane phase and requires much higher temperatures for acyl chain melting to occur.

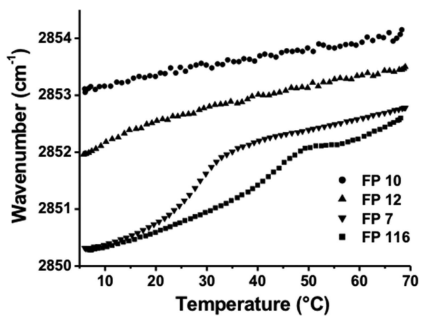

Figure 4. Acyl chain mobility of the aggregated FP compounds in dependence on temperature. The infrared absorption around wavenumbers 2850−2852 cm^{-1} corresponds to the symmetric stretching vibrations ν_s of the CH_2 groups of the acyl chains. The wavenumbers indicated were derived from the peak absorption of $\nu_s(CH_2)$ determined upon constant heating of the samples. Data are representative of two independent measurements.

NMR Studies. The comparison of the ^1H NMR spectra recorded after compound dissolution in phosphate buffer, pH 7.4, 25 °C (Figure S9) suggested a different aggregation state of the bioactive compounds in solution in the micromolar concentration range. The ^1H NMR spectrum acquired on a 100 μM FP7 sample (Figure S9A) clearly showed the presence of two sets of signals, as can be deduced by observing the spectral region between 5.5 and 5.2 ppm. In addition to a doublet of doublet and a triplet, corresponding to H1 and H3 protons (*), also two broad resonances (§) are present that can be assigned to aggregated species. This hypothesis was supported by the comparison of spectrum S9A with FP7 spectra recorded at higher concentrations, in particular 125 μM (Figure S9B) and 250 μM (Figure S9C), where the gradual decrease in sharp signal (*) intensity is associated with the increase of the broad resonance (§) ones, as expected as a consequence of FP7 aggregation. A further confirmation was achieved through the acquisition of relaxation-edited (Figure S9D) and diffusion-edited (Figure S9E) spectra, employed to partially filter out resonances from high molecular weight and low molecular weight species, respectively.[31,32] Indeed, the spectrum acquired with the CPMG sequence (Figure S9D), edited on the basis of relaxation times and thus highlighting the signals from low molecular weight species, showed a decrease of broad signal (§) intensities compared to spectrum S9C; on the contrary, in the diffusion-edited spectrum (Figure S9E), whose parameters were set up to erase resonances from low molecular weight compounds, sharp resonances (*) disappeared. We can conclude that, under our experimental condition, FP7 was present in solution as a mixture of monomer/small aggregates and higher aggregated species (micelles), whose equilibrium changes coherently to the variation of the nominal concentration of the molecule.

Instead, only one set of sharp signals was observed in the ^1H NMR spectra recorded on FP10 and FP12 solutions containing the compounds in the concentration range 100 μM to 1 mM. Representative spectra acquired on 500 μM samples are depicted in Figure S9F−H for FP10 and Figure S9I−M for FP12. Furthermore, FP10 and FP12 resonances appear considerably narrower compared to FP7 signals (Figure S9A). Collectively, these findings suggest an appreciably higher solubility of FP10 and FP12 in aqueous buffer solution and thus a lower propensity to form micelles.

A different behavior can be described for FP116. All the ^1H NMR spectra acquired on this compound present broad resonances and no sharp signals, expected for the free monomer. Thus, in the range of tested concentrations (125−500 μM), FP116 is always present in an aggregated form. Representative spectra acquired on a 250 μM FP116 sample are reported in Figure S9N−P.

SAXS Studies. Small angle X-ray scattering (SAXS) profiles were measured in dependence of temperature to obtain information on the supramolecular organization of the molecules. The data are given in the range of the scattering vectors relevant for structure assignment. All FP compounds showed isotropic scattering, indicating no preference for a predominant orientation of the aggregates. FP10 and FP12 showed diffuse symmetric scattering curves dominated by the

DOI: 10.1021/acs.jmedchem.7b01803
J. Med. Chem. XXXX, XXX, XXX−XXX

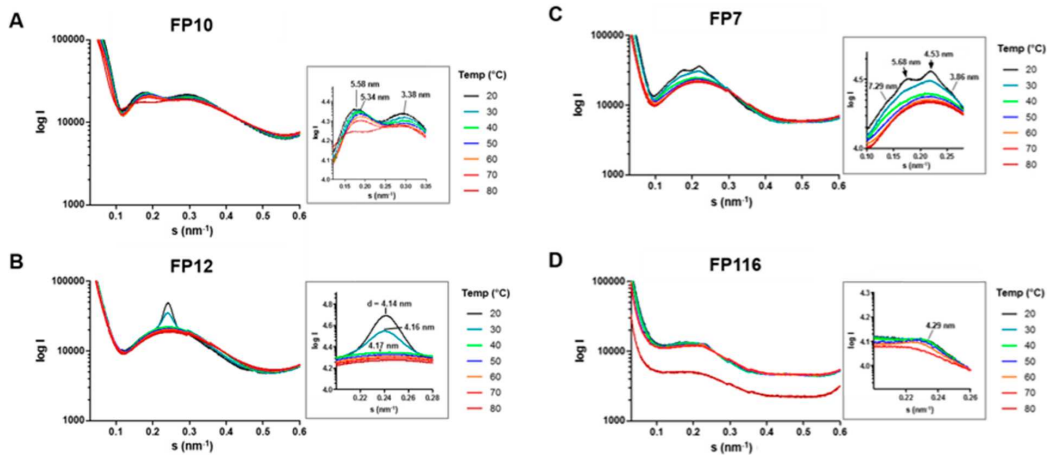

Figure 5. Small angle X-ray diffraction of aggregates in solution for FP10 (A), FP12 (B), FP7 (C), and FP116 (D). Scattering vectors are indicated for temperatures between 20 and 80 °C. Gray squares show enlargements of the relevant scattering vectors. The spacing of the diffraction maxima is indicted as $d = 1/s$ (nm).

form factor, which is characteristic for unilamellar aggregates with large interbilayer distance and probably owing to the negative surface charge of the two adjacent phosphate groups that leads to a net electrostatic repulsion of the bilayers (Figure 5). The scattering of FP10 shows two maxima at 5.58 nm and at 3.38 nm, the latter could indicate the formation of interdigitated bilayers (3.38 nm). For FP12, a single peak is observed at 20 °C (up to 35 °C, data not shown) indicating the formation of correlated multilayers with a *d*-spacing of 4.14 nm, which is also consistent with the formation of an interdigitated bilayer structure. In contrast, FP7 does show a different and more complex scattering pattern, which indicates the occurrence of a nonlamellar structure. The spacing relationship exhibits clear similarity with cubic structures with a space group relationship of aQ 12.7 nm (not visible), $aQ/\sqrt{3}$ (7.29 nm), $aQ/\sqrt{5}$ (5.68 nm), $aQ/\sqrt{8}$ (4.53 nm), and $aQ/\sqrt{11}$ (3.86 nm), agreeing most likely with space group Q_{212}. The tendency to a nonlamellar structure of FP7, however, could explain the slightly lower antagonistic activity of FP7 compared to FP12. In contrast to the above FP compounds, FP116 showed very weak scattering intensities, hardly displaying a form factor, which can be explained by a much lower solubility observed for the FP116 preparation and supports the results obtained by NMR.

Binding to MD-2. *Expression, Purification, and Activity of hMD-2.* Recombinant human MD-2 (hMD-2) was used in *in vitro* binding experiments. The functionality of this protein is a crucial prerequisite to obtain reliable results representative of specific, high-affinity molecular recognition of ligands.[33] Recombinant hMD-2 was expressed in *E. coli*, *Pichia pastoris*, and mammalian HEK293 cells. hMD-2 from different hosts was tested for its activity by incubating HEK/hTLR4 cells with a mixture of recombinant hMD-2 and LPS (100 ng/mL). The TLR4-dependent IL-8 secretion by HEK/hTLR4 cells is indicative of functional MD-2. Figure 6 shows the lowest concentration of MD-2 required for maximum activation of TLR4 (quantified by IL-8 production), for each of the different expressed and purified hMD-2 proteins. hMD-2 produced and purified from HEK293T displayed the highest activity in stimulating the LPS/TLR4 inducible reporter at a concentration of 12 nM, followed by the hMD-2 expressed and purified from *P. pastoris* with its highest biological activity obtained at a concentration of 15 nM. Finally, hMD-2 purified from *E. coli* gave the lowest IL-8 production at the concentration of 245 nM (Figure 6).

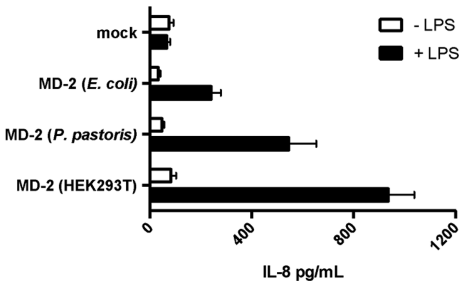

Figure 6. Activity of hMD-2 expressed in different hosts. The figure shows the maximum activation of TLR4 (quantified by IL-8 production) at the lowest concentration of hMD-2 under the different expressed conditions (bacteria 245 nM, yeast 15 nM, and mammalian 12 nM). Results are mean ± SEM from three parallels representative of at least three independent experiments.

The difference in activity of hMD-2 expressed in different hosts most likely reflects minor differences in protein folding and/or glycosylation.[34,35] The higher expression yield and the good activity prompted us to use hMD-2 from *P. pastoris* in *in vitro* binding experiments with synthetic compounds.

Binding studies were carried out by means of fours different techniques: two ELISA-type plate-based assays with immobilized protein, a fluorescence displacement assay, and surface plasmon resonance (SPR).

ELISA Competition Experiments with Anti-hMD-2 Antibody. Direct binding of LPS, FP7, FP10, and FP12 to MD-2 was determined using a monoclonal antibody that binds to free hMD-2 but not to hMD-2 bound to LPS.[36] Monoclonal mouse anti-hMD-2 (9B4) antibody specifically binds to an epitope close to the rim of the LPS-binding pocket of hMD-2, available for recognition by the antibody only when the hMD-2 pocket is empty.

DOI: 10.1021/acs.jmedchem.7b01803
J. Med. Chem. XXXX, XXX, XXX−XXX

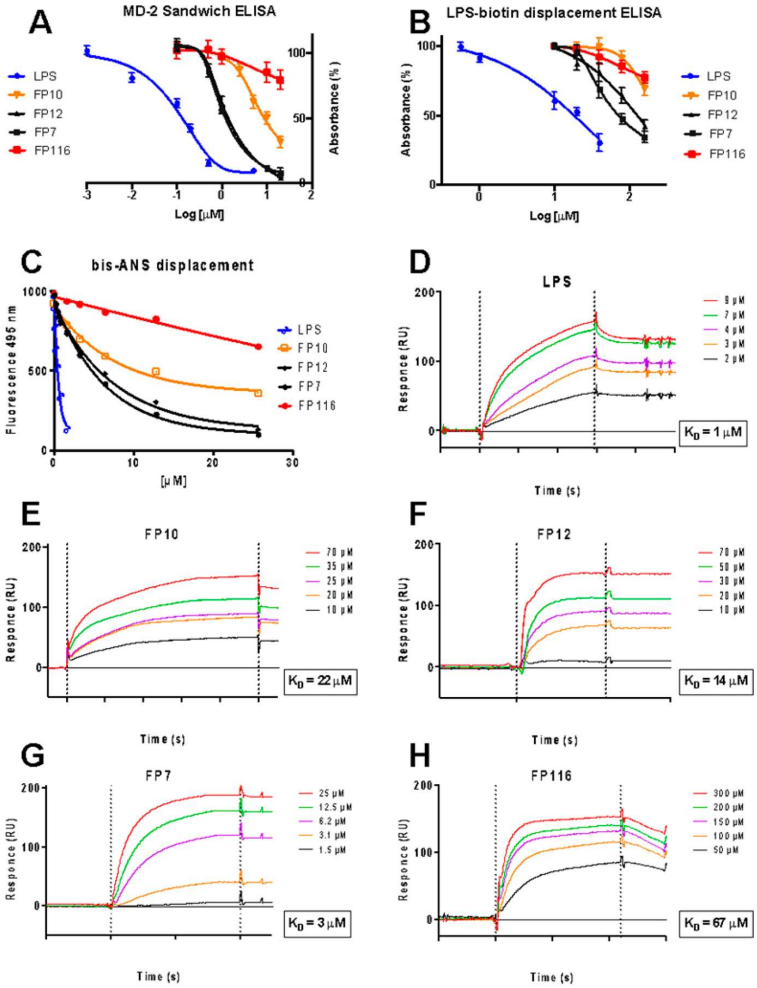

Figure 7. Cell-free binding studies on purified\ hMD-2 receptor. (A) LPS, FP7, FP10, and FP12 prevent anti-human MD-2 monoclonal antibody binding in a dose-dependent manner. (B) LPS, FP7, FP10, FP12, and FP116 activity in competing with biotin-LPS for hMD-2 binding. (C) Fluorescence measurements show that LPS, FP7, FP10, and FP12 dose-dependently inhibit the binding of bis-ANS to MD-2. (D−H) SPR analysis shows direct interaction between LPS, FP10, FP12, FP7, and FP116 and MD-2; K_D values are reported. Results are mean ± SEM from three parallels representative of at least three independent experiments.

This assay detected a decrease in binding to MD-2 in the presence of LPS (Figure 7A), similar to that previously reported.[37] A dose-dependent inhibition of antibody/MD-2 interaction was observed when adding FP7 and FP12, with a 90−95% decrease in binding obtained at concentrations of FP7 and FP12 of 20 μM (Figure 7A). A 70% decrease in binding to hMD-2 was obtained with 20 μM of FP10 (Figure 7A), and a 20% decrease was obtained with 20 μM of FP116 (Figure 7A). These data showed that, while FP7 and FP12 bind hMD-2 with high affinity, FP10 and FP116 are less potent ligands.

ELISA Displacement Experiment with Immobilized hMD-2 and Biotinylated LPS. The ability of FP compounds to displace LPS from the pocket of hMD-2 was assessed by an ELISA plate-based assay. The synthetic molecules were added at increasing concentration to hMD-2, which was already incubated with biotinylated LPS. FP7 and FP12 were able to displace biotin-LPS from hMD-2 in a dose-dependent manner, with the highest displacement of 60−65% obtained at a concentration of 160 μM (Figure 7B). FP10 and FP116, at a concentration of 160 μM, gave a displacement of biotin-LPS of 20−30% (Figure 7B). As a control, LPS at a concentration of 40 μM gave the highest displacement of biotin-LPS of 70% (Figure 7B).

Fluorescence Displacement Assay. It has been previously shown that the fluorescent probe 1,1′-Bis(anilino)-4,4′-bis (naphthalene)-8,8′ disulfonate (*bis*-ANS) binds to MD-2 and is displaced by LPS.[38] bis-ANS presumably binds the same MD-2 binding site as lipid A and of other lipid A-like ligands. TLR4 ligands interacting with MD-2 in a lipid A-like manner are supposed to compete with bis-ANS and displace it from MD-2. LPS, FP7, FP10, and FP12 caused a concentration-dependent decrease of bis-ANS fluorescence, indicating competitive binding of FP7, FP10, and FP12 to hMD-2 (Figure 7C). FP116 induces only a modest decrease of bis-ANS fluorescence

DOI: 10.1021/acs.jmedchem.7b01803
J. Med. Chem. XXXX, XXX, XXX−XXX

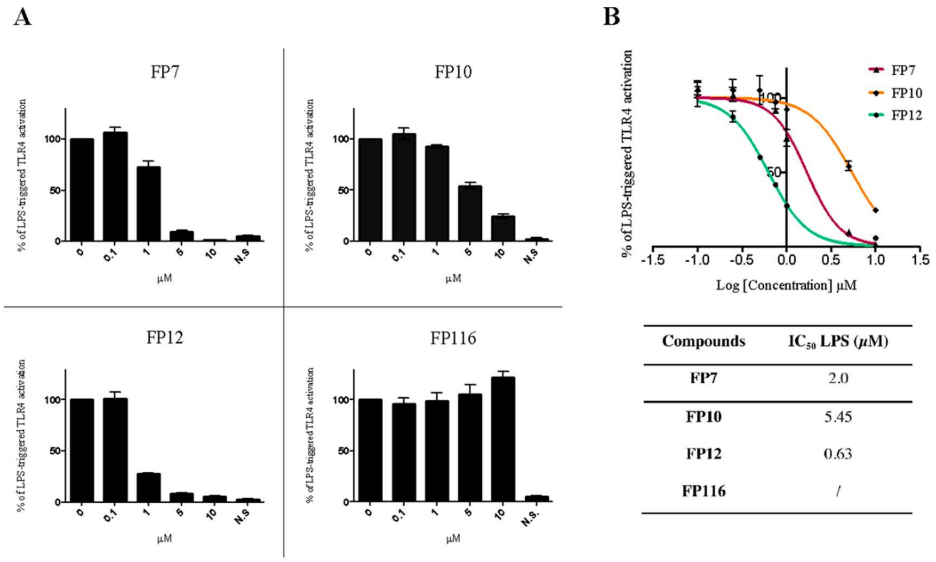

Compounds	IC_{50} LPS (μM)
FP7	2.0
FP10	5.45
FP12	0.63
FP116	/

Figure 8. Dose-dependent inhibition of LPS-triggered TLR4-dependent NF-kB activation in HEK-Blue hTLR4 cells by compounds FP7, FP10, FP12, and FP116. (A) HEK-Blue hTLR4 cells were preincubated with the indicated concentrations of compounds FP7, FP10, FP12, and FP116 and stimulated with LPS (100 ng/mL) after 30 min. Data were normalized to stimulation with LPS alone and expressed as the mean percentage ± SEM of at least three independent experiments. (B) Dose−response curves for compounds FP7, FP10, and FP12 in inducing the TLR4-dependent NF-κB reporter activity. Concentration−effect data were fitted to a sigmoidal four-parameter logistic equation to determine IC_{50} values. Data points represent the mean of percentage ± SEM of at least three independent experiments.

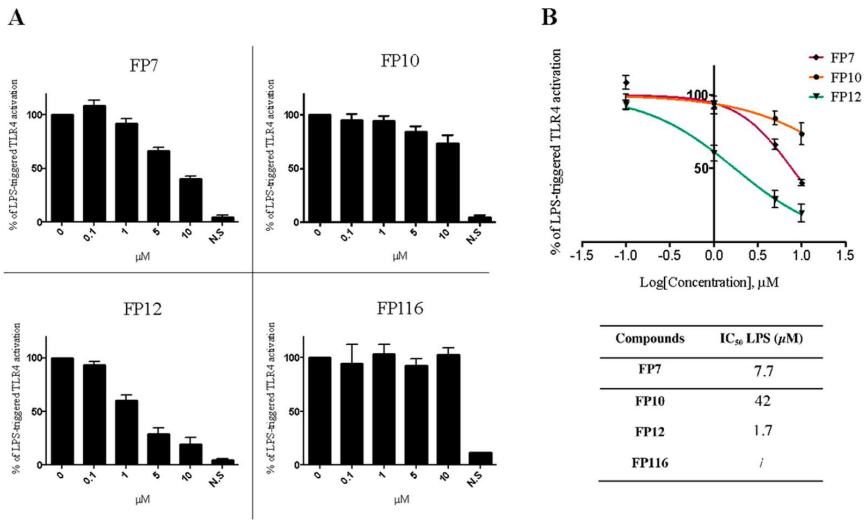

Compounds	IC_{50} LPS (μM)
FP7	7.7
FP10	42
FP12	1.7
FP116	/

Figure 9. Activity of compounds FP10, FP12, and FP116 on RAW-Blue cells. (A) RAW-Blue cells were preincubated with increasing concentrations of synthetic compounds and then stimulated with LPS (10 ng/mL, after 30 min). Data were normalized to the response to LPS and expressed as the mean percentage ± SEM of at least three independent experiments. (B) Dose-dependent inhibition curves of compounds FP7, FP10, and FP12. IC_{50} values in the table on the bottom. Concentration−effect data were fitted to a sigmoidal four-parameter logistic equation to determine IC_{50} values. Data points represent the mean of percentage ± SEM of at least three independent experiments.

at the tested concentrations (Figure 7C), thus confirming that the lack of activity on cells could be related to low affinity binding of this molecule to hMD-2.

Surface Plasmon Resonance (SPR) Analysis. SPR data with immobilized hMD-2 showed direct interaction of the receptor with LPS (control) and with the tested synthetic compounds. K_D values derived from sensorgram analysis were 3, 13.7 , 22, and 66.8 μM for FP12, FP7, FP10, and FP116, respectively (Figure 7E−H). SPR experimental curve optimal fitting was obtained by assuming 1:1 ligand/MD-2 binding stoichiometry.

Together, the results obtained from these *in vitro* cell-free studies clearly indicate that FP7, FP10, FP12, and FP116

DOI: 10.1021/acs.jmedchem.7b01803
J. Med. Chem. XXXX, XXX, XXX−XXX

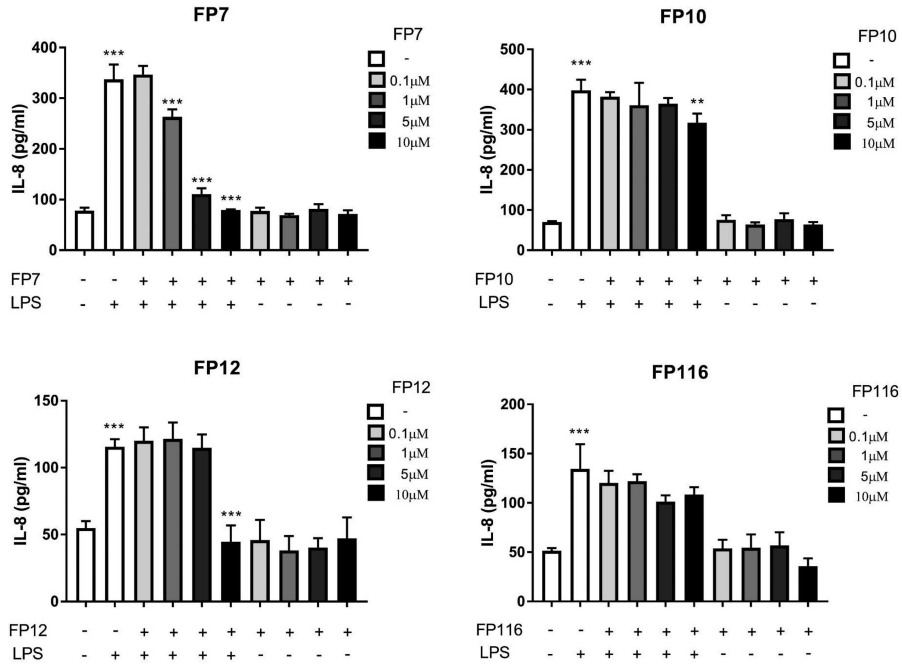

Figure 10. Effect of FP variants on LPS/TLR4 induced production of IL-8 in THP-1 cells. THP-1 cells were pretreated with FP variants (0−10 μM) for 1 h prior to LPS exposure. Cells were then left to incubate 16 h further in the presence or absence of LPS (100 ng/mL). IL-8 production was measured by ELISA. Results are displayed as mean concentration ± SD of three independent experiments. Significant results are indicated as *P > 0.05, **P > 0.01, ***P > 0.001 for LPS vs control and LPS vs FPs treated samples (ANOVA).

directly interacted with MD-2, with the same order of potency found in human and murine cell experiments FP12(C12) > FP7(C14) > FP10(C10) ≫ FP116(C16).

Cell Experiments. *Modulation of LPS-Stimulated TLR4 Signaling in HEK-Blue Cells.* In order to evaluate the influence of the fatty acid length on the TLR4 antagonist activity, molecules FP10, FP12, FP7, and FP116, constituting the homologous series with fatty acid chain lengths C10, C12, C14, and C16, were first tested on HEK-Blue hTLR4 cells. These cells are engineered to stably express the human receptors of the LPS recognition complex (hTLR4, hMD-2, and hCD14) and a reporter gene (SEAP) placed under the control of two TLR4-dependent transcription factors (NF-κB and AP-1). Results from MTT assay revealed that all compounds did not have a negative effect on cell viability at the concentration of 10 μM used in experiments (Figure S10). FP7, FP10, and FP12, but not FP116, inhibited in a concentration-dependent manner the TLR4 signaling in HEK-Blue cells (Figure 8). FP7 displayed the expected antagonistic activity.[6] FP10 and FP12 showed IC_{50} respectively higher (5.45 μM) and lower (0.63 μM) than FP7 (2.0 μM) (Figure 8B). These results demonstrated the efficacy of fatty acid chains lengths (C8, C10, and C12) of FP7 variants to negatively modulate TLR4 signaling in HEK-Blue cells, the order of activity being FP12(C12) > FP7(C14) > FP10(C10) ≫ FP116(C16).

Modulation of LPS-Stimulated TLR4 Signaling in Murine Macrophages. Several TLR4 modulators mimicking lipid A have different effects on human and murine TLR4. In certain cases when passing from murine to human TLR4/MD-2/CD14 system the observed agonistic effect switched to antagonistic effect of the compound of interest.[39] The species specificity is due to differences between hMD-2 and mMD-2 binding regions that induce different positioning of the same ligand, thus causing different activity and, in some cases, switch from agonism to antagonism. In this experiment, we aimed to investigate the effect of glucosamine derivatives in murine RAW-Blue macrophages. These cells are derived from RAW 264.7 and possess the same reporter gene present in HEK-Blue hTLR4 cells (SEAP). We first verified the capacity of FP compounds to stimulate the TLR4 response in RAW-Blue cells, and we found all molecules inactive (Figure S11). When administrated before LPS, FP7, FP10, and FP12 were active in inhibiting TLR4-dependent NF-κB activation in RAW-Blue macrophages (Figure 9A,B). Similarly to what happened in the case of human HEK cells, FP116 turned out to be inactive as antagonist. Notably, FP12 was the most active antagonist compound (IC_{50} = 1.7 μM). The activity order of the tested compounds was found to be the same than in human HEK cells: FP12(C12) > FP7(C14) > FP10(C10) ≫ FP116(C16).

Effect of FP Variants on LPS-Induced TLR4 Signaling in THP-1 Cells. Haematopoietic TLR4 has been shown to play a critical role in any stage of the inflammatory process. Furthermore, immune competent cells use TLR4 signaling to sense danger molecules and produce proinflammatory proteins that initiate and amplify the inflammatory process. To test the potential of FP variants to modulate TLR4 signaling pathways, we utilized THP-1 cells as an *in vitro* model. Initially, we evaluated the effect of FP variants on THP-1 cell viability. THP-1 cells were exposed to different concentrations of FP variants (0−10 μM) in the presence or absence of LPS (100 ng/mL) for up to 24 h. Results from MTT assay demonstrated that FP variants/LPS did not affect cell viability (Figure S12).

DOI: 10.1021/acs.jmedchem.7b01803
J. Med. Chem. XXXX, XXX, XXX−XXX

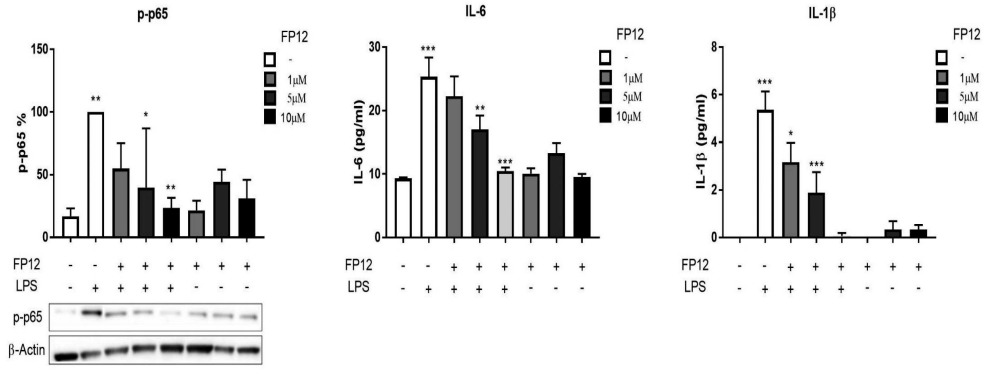

Figure 11. FP12 negatively regulates p65 NF-κB phosphorylation and production of IL-6 and IL-1β in THP-1 cells. THP-1 cells were pretreated with compound FP12 (0−10 μM) for 1 h prior to LPS exposure. Cells were then left to incubate 1 and 16 h further in presence or absence of LPS (100 ng/mL). p65 NF-κB phosphorylation was determined in cell lysates using Western blot analysis, and cytokine production was measured by ELISA after 16 h of LPS exposure, respectively. Results are displayed as mean concentration ± SD of three independent experiments. Significant results are indicated as $*P > 0.05$, $**P > 0.01$, $***P > 0.001$ for LPS vs control and LPS vs FP12 treated samples (ANOVA).

To determine the effect of FP variants on TLR4 signaling, next we analyzed IL-8 expression, a well-known TLR4-dependent proinflammatory cytokine produced in THP-1 cells in response to LPS. ELISA results clearly demonstrated the potential of FP7 and FP12 at 10 μM to inhibit LPS driven IL-8 production (Figure 10). In contrast, FP10 and FP116 had a modest or nonsignificant impact on IL-8 expression, respectively (Figure 10). We have demonstrated that FP7 exerted a negative effect on TLR4 signaling in different cell types (unpublished data). Following on from comparative analysis based on TLR4-dependent IL-8 expression and tendency on the binding affinity with MD-2 of FP7 variants, we found that the structural modification of FP12, but not FP10 and FP116, is related to antagonistic activity of the compound. In support to this notion, we further investigated the ability of FP12 to modulate second messengers in TLR4 signaling. Immunoblotting data revealed that FP12 significantly downregulated p65 NF-κB phosphorylation that was associated with a strong inhibition of the expression of additional TLR4-dependent cytokines, such as IL-6 and IL-1β in a dose-dependent manner (Figure 11). These data clearly demonstrate that FP12 is a potent negative regulator of TLR4 signaling in THP-1 cells.

■ DISCUSSION AND CONCLUSIONS

The homologous series of FP glycolipids with fatty acid chain lengths varying from 10 to 16 carbon atoms was rationally designed as MD-2 ligands and synthesized.

In a first set of *in vitro* experiments, we aimed at studying the SAR of these molecules in binding experiments with functional hMD-2. For this purpose, hMD-2 expressed in yeast (*P. pastoris*) was used because it showed higher activity in responding to LPS stimulus than bacterial (*E. coli*) MD-2 and was produced with higher yields than MD-2 from mammalian (HEK) cells. Four different binding experiments between synthetic compounds and h-MD-2 were carried out. These were competition (displacement) experiments in which the synthetic glycolipids compete with biotin-LPS, with the fluorescent MD-2 ligand bis-ANS, and with anti-MD-2 antibody for MD-2 binding. SPR measurements allowed to analyze directly the binding between synthetic glycolipids and MD-2. All binding experiments consistently provided the same order of affinity among hMD-2 and synthetic molecules: FP12(C12) > FP7(C14) > FP10(C10) > FP116(C16).

The biological activity was then assessed on cells: when provided alone, the synthetic FP compounds did not display any TLR4 agonist activity in human and murine cells. On the contrary, when administrated with LPS, the molecules with 10, 12, and 14 carbon chains (respectively, FP10, FP12, and FP7) were active in blocking LPS/TLR4 signal (antagonism) in human and murine cells, while the molecule with 16 carbons (FP116) showed very weak or no activity. The order of activity of FP variants as TLR4 antagonists was confirmed in human (HEK-TLR4 and THP-1) and murine (RAW macrophages) cells. The molecules with 10, 12, and 14 carbon chains seem to be nonspecies-specific TLR4 antagonists because these compounds are active in both human (HEK and THP-1) and murine cells, with higher potency in human ones. The compound with higher biological activity was FP12, with 12 carbons, followed by FP7 and FP10 with 14 and 10 carbons, while FP116 with 16 carbons showed very weak or no activity in cell models.

The variation of compounds' functional activity was related to the number of carbon atoms of the aliphatic chains, which could be described by a bell-shaped curve with a maximum at C12. This is a common structure−activity trend that is found in a number of series of homologous compounds in medicinal chemistry and can be explained in terms of docking within the binding pocket of the pharmacological target (as it exists an optimal number of carbon atoms that can be accommodated into the pocket) and also in terms of variation of solubility and bioavailability (when the chain length is too long the solubility decreases and also the biological activity). Thus, the difference of TLR4 functional activity of FP monosaccharides related to FA chain length can be explained in terms of their interaction with MD-2(/TLR4) and/or by their aggregation properties in a solution.

The docking and MD simulation studies have shown that FP10, FP7, and FP12 would accomplish optimal binding properties, while FP116 could be bordering the limits of the maximum length compatible with a proper MD-2 binding. Although MD-2 pocket is able to host up to five FA chains, the highly long and flexible C16 acyl chains present in FP116 seem to point to less efficient ability to interact with TLR4/MD-2 in

DOI: 10.1021/acs.jmedchem.7b01803
J. Med. Chem. XXXX, XXX, XXX−XXX

an antagonistic binding mode, given that the required exposed conformation of Phe126 side chain could be jeopardized.

Additionally, calculated logP values for the FP variants point to a very high lipophilicity for FP116, maybe affecting the aggregation properties in solution.

Taken together, these data strongly suggest that the mechanism of TLR4 antagonism of that class of compounds is mainly based on the competition with LPS (or other ligands, as bis-ANS) in the binding to the MD-2/TLR4 complex.

Interestingly, an identical order of activity on TLR4 has been found in a series of monosaccharide TLR4 agonists, the Gifu Lipid As (GLA), and the following order of potency in inducing the production of TNF-α in murine cells was detected: C12 > C14 > C10 ≫ C16.[22] Also in the case of GLA compounds, with three FA chains and one phosphate in C-4 position, the C12 and C14 variants were the most active ones, C10 was less active, and C16 was inactive. Similarly to FP compounds, GLA is more active on murine than on human cells.[22] However, the authors did not provide any evidence or explanation about the link between TLR4 activity of monosaccharide and FA chain length.

Regarding the aggregation properties, some important differences among FP compounds were detected by FT-IR analysis in solution. These measurements showed marked variations in acyl chain fluidity of aggregated FP compounds depending on the chemical structure. The phase transition temperature T_c exhibits a clear inverse correlation with the length of the acyl chains with T_c C16 ≫ T_c C14 > T_c C12 > T_c C10. Of note, this behavior results in marked differences at the biologically relevant temperature of 37 °C, where FP10, FP12, and FP7 are in a fluid membrane phase, whereas FP116 is still in a rigid membrane phase and requires much higher temperatures for acyl chain melting to occur. The occurrence of a very broad phase transition at temperatures above 37 °C and occurrence of a second phase transition at higher temperature as observed for FP116 were also found for inactive glucosamine monosaccharide GLA compounds.[40] Differences in phase behavior have also been shown for the TLR4 ligands lipid A and LPS. The antagonistic tetraacylated synthetic compound 406 is highly fluid at 37 °C, whereas the biologically active hexaacylated compound 506 and LPS Re have phase transition temperatures above 37 °C.[41] The fluidity state of the acyl chains in aggregated glycolipids is thus not an exclusive determinant of inflammatory or antagonistic activity of chemically different compounds. It is rather a modifying parameter of biological activity by affecting aggregate properties such as hydrophobic thickness, packing density, and aggregate stability. NMR and SAXS analysis revealed striking differences in aggregate formation of FP compounds, which are likely to explain differences in their biological activity. Concentration-dependent NMR analysis of the two most antagonistic compounds FP12 and FP7 revealed aggregation of FP7 (C14) at much lower concentrations than FP12 (C12), reflecting further differences in the biophysical state and bioavailability of these compounds. Aggregate structures resolved by SAXS analysis provided evidence for lamellar bilayer structures for FP10 and FP12, which are associated with antagonistic activity; for FP7, a tendency for nonlamellar structures was determined. Considering the crucial role of lipid supramolecular aggregate structure for the presentation to LPS receptor molecules, the different aggregate structures observed by SAXS might explain the slightly lower antagonistic activity of FP7 compared to FP12 in some biological systems.

The present study provides structural and functional biological data demonstrating the ability of novel FP variants to negatively regulate TLR4 signaling in different cell model systems. Having shown the strong potential of FP12 to modulate second messenger activation and various end points of TLR4 signaling pathways including its lack of toxicity, this study supports the idea of further drug development of FP12 as a lead compound in preclinical and clinical studies for pharmacological intervention of inflammatory-based diseases.

EXPERIMENTAL SECTION

Computational Studies. *Structure Construction and Refinement.* The 3D structures of ligands FP10, FP12, FP7, and FP116 were built with PyMOL[42] using 6YA monosaccharide found in the GLYCAM database (http://glycam.org) as a template. The 3D coordinates of human TLR4/MD-2 model in the antagonist conformation is reported elsewhere.[43]

Parameters Derivation. The parameters needed for MD simulations were obtained using the standard Antechamber procedure in Amber14.[44] Briefly, ligand structures, already refined at the AM1 level of theory, were optimized, and their atomic partial charges were calculated with Gaussian09/e1[45] at the Hartree−Fock level (HF/6-31G* Pop = MK iop(6/33 = 2), iop(6/42 = 6)), then the partial charges were derived and formatted for AmberTools15 and Amber14 with Antechamber, assigning the general AMBER force field (GAFF) atom types. Later, the atom types of the atom constituting the saccharide ring were changed to the GLYCAM force field atom types.[46] The GAFF parameters for the phosphate group were modified as shown in the Supporting Information.

Docking Calculations of Ligands FP10, FP12, FP7, and FP116. The Gasteiger charges were computed within the AutoDockTools 1.5.6 program,[47] and the nonpolar hydrogens were merged for all the ligands, the human TLR4/MD-2 antagonist model, and human CD14 (PDB-ID 4GLP). AutoDock VINA 1.1.2 was used for the docking of the ligands, and AutoDock 4.2 was used to redock the best-predicted binding poses. In AutoDock 4.2, the Lamarckian evolutionary algorithm was chosen, and all parameters were kept default except for the number of genetic algorithm runs, which was set to 200 to enhance the sampling. AutoDockTools 1.5.6 was used to assign the Gasteiger−Marsili empirical atomic partial charges to the atoms of both the ligands and the receptors. The structure of the receptors was always kept rigid, whereas the structure of the ligand was set partially flexible by providing freedom to some appropriately selected dihedral angles. Regarding the docking boxes, spacing was set to the default value of 1 Å for VINA, and 0.375 Å for AutoDock. For human CD14 structure, the size of the box was set to 33.00 Å in the *x*-axis, 33.75 Å in the *y*-axis, and 33.75 Å in the *z*-axis, and the center of the box was located equidistant to the center of mass of residues Phe69, Tyr82, and Leu89. For the human TLR4/MD-2 system, the size of the box was set to 33.00 Å in the *x*-axis, 40.50 Å in the *y*-axis, and 35.25 Å in the *z*-axis, and the center of the box was located equidistant to the center of mass of residues Arg90 (MD-2), Lys122 (MD-2), and Arg264 (TLR4).

Molecular Dynamics (MD) Simulations. Selected docked complexes were submitted to MD simulations for 50 ns in Amber14 suite. All the complexes followed the same procedure. First, the system is submitted to 1000 steps of the steepest descent algorithm followed by 7000 steps of the conjugate gradient algorithm. A 100 kcal·mol^{-1}·A^{-2} harmonic potential constraint is applied on both the proteins and the ligand. In the subsequent steps, the harmonic potential is progressively lowered (respectively to 10, 5, and 2.5 kcal·mol^{-1}·A^{-2}) for 600 steps of the conjugate gradient algorithm each time, and then the whole system is minimized uniformly. Next, the system is heated from 0 to 100 K using the Langevin thermostat in the canonical ensemble (NVT) while applying a 20 kcal·mol^{-1}·A^{-2} harmonic potential restraint on the proteins and the ligand. Finally, the system is heated up from 100 to 300 K in the isothermal−isobaric ensemble (NPT) under the same restraint condition as the previous step, followed by a simulation for 100 ps with no harmonic restraint applied. At this point, the system is ready for the production run, which is performed using the Langevin

DOI: 10.1021/acs.jmedchem.7b01803
J. Med. Chem. XXXX, XXX, XXX−XXX

thermostat under NPT ensemble, at a 2 fs time step. All production runs were performed for 50 ns.

LogP Calculations. LogP values of FP10, FP12, FP7, and FP116 were calculated within the Maestro package.[48]

Chemistry. *General.* The reactions were carried out under a nitrogen atmosphere. TLC was performed using prepared plates of silica gel (Merck 60 F254 on aluminum) and revealed using UV light or staining reagents (H_2SO_4 (5% in EtOH), ninhydrin (5% in EtOH), basic solution of $KMnO_4$ (0.75% in H_2O), molibdate solution (molybdatophosphorus acid and Ce(IV) sulfate in 4% sulfuric acid). ^1H NMR (400 MHz) and ^{13}C NMR spectra (100 MHz) were recorded on a Varian spectrometer using partially deuterated solvents as internal standards. Purity of final compounds was ≥95% as assessed by quantitative NMR analysis. Reaction conditions and compound characterization are described in the Supporting Information.

HEK-Blue hTLR4 Cells Assay. HEK-Blue hTLR4 cells (InvivoGen) were cultured according to manufacturer's instructions. Briefly, cells were cultured in DMEM high glucose medium supplemented with 10% fetal bovine serum (FBS), 2 mM glutamine, antibiotics, and 1× HEK-Blue Selection (InvivoGen). Cells were detached using a cell scraper, counted, and seeded in a 96-well multiwell plate at a density of 4×10^4 cells per well. After overnight incubation (37 °C, 5% CO_2, 95% humidity), supernatants were replaced with new medium supplemented by the compound to be tested dissolved in water or DMSO−H_2O (1:1). After 30 min of preincubation, cells were stimulated with 100 ng/mL LPS from *E. coli* O55:B5 (Sigma-Aldrich) and incubated overnight. The SEAP-containing supernatants were collected and incubated with *para*-nitrophenylphosphate (pNPP) for 2−4 h in the dark at room temperature. The well's optical density was determined using a microplate reader set to 405 nm. The results were normalized with positive control (LPS alone) and expressed as the mean of percentage ± SEM of at least three independent experiments.

RAW-Blue Cells. Raw-Blue cells (InvivoGen) were cultured according to the manufacturer's instructions. Briefly, cells were cultured in DMEM high glucose medium supplemented with 10% fetal bovine serum (FBS), 2 mM glutamine, 100 μg/mL Normocin (InvivoGen), and 200 μg/mL Zeocin (InvivoGen). Cells were detached using a cell scraper, and the cell concentration was estimated by using Trypan Blue (Sigma-Aldrich). The cells were diluted in DMEM high glucose medium supplemented as described before and seeded in 96-well multiwell plate at a density of 6×10^4 cells per well in 200 μL. After overnight incubation (37 °C, 5% CO_2, 95% humidity), supernatant was removed, and cell monolayers were washed with warm PBS, treated with increasing concentrations of compounds dissolved in DMSO−H_2O (1:1), and diluted in DMEM. After 30 min, cells were stimulated with 10 ng/mL of LPS from *E. coli* O55:B5 (Sigma-Aldrich) for 16 h. The supernatants were collected and incubated with pNPP for 2−4 h in the dark at room temperature. The optical density of wells was determined using a microplate reader set to 405 nm. The results were normalized with positive control (LPS alone) and expressed as the mean of percentage ± SEM of at least three independent experiments.

THP-1 Cells. THP-1 cells were cultured in RPMI (+10% heat inactivated fetal bovine serum (HiFPS), +1% glutamine, +1% penicillin/streptamycin). Cells were split three times weekly and maintained at a density of 0.3×10^6 cells/mL. For experimental procedures, THP-1 was used at a density 0.5×10^6 cells/mL, 100 L/well (96 wells), and 3 mL/well (six wells) plates, respectively. All cells were pretreated with FP7 variants (0−10 M) for 1 h, then exposed to LPS (100 ng/mL) for 1 or 16 h.

MTT Cell Viability Assay. HEK-Blue hTLR4 cells were grown in DMEM supplemented with 10% FBS, 2 mM glutamine, and antibiotics. Cells were seeded in 100 μL of DMEM without Phenol Red at a density of 4×10^4 cells per well and incubated overnight (37 °C, 5% CO_2, 95% humidity). Cells were treated with the higher dose of compound used in the previous experiments and incubated overnight. MTT solution (5 mg/mL in PBS) was added to each well, and after 3 h incubation, 0.1 N HCl in 2-propanol solution was used to dissolve formazan crystals. Formazan concentration was determined by measuring the absorbance at 570 nm. The results were normalized with untreated control (PBS) and expressed as the mean of percentage ± SEM of three independent experiments.

Preparation of Recombinant hMD-2 in Escherichia coli and Purification. hMD-2 was produced in *E. coli* as described previously,[49] analyzed by SDS−PAGE, and its biological activity tested on 293/hTLR4a cells.

Preparation of Recombinant hMD-2 in Pichia pastoris and Purification. hMD-2 was produced in *Pichia pastoris*, analyzed by SDS−PAGE, and its biological activity tested on 293/hTLR4a cells.

The coding sequence of mature hMD-2 was amplified by PCR (primers F-hMD2-Q19 CAGAAGCAGTATTGGGTCTGC and R-Spe-hMD2 TTTACTAGTATTTGAATTAGGTTGGTGTAGG) from a plasmid template and ligated into the SnaBI/SpeI opened pPpT4AlphaS-His expression vector (under the control of AOX1 promoter), in frame with the N-terminal *S. cerevisiae* α-MF prepro leader sequence and the C-terminal 6xHis tag. The resulting recombinant plasmid pPpT4AlphaS-His was transformed into *E. coli* DH5α competent cells, and the positive recombinant plasmid, which was confirmed by DNA sequencing, was linearized and transformed into *Pichia pastoris* GS115 by electroporation. MD-2 expressing transformant was selected and cultured in a 250 mL shake flask containing 10 mL of YPD liquid media at 28 °C for 24 h. Two liter flasks containing 250 mL of BMGY (1% glycerol) medium at 28 °C were inoculated with 1 mL of overnight inoculum. After being cultured for 24 h, cells were aseptically collected by centrifugation at room temperature for 10 min at 5000 rpm. BMGY medium was replaced with 250 mL of methanol-complex medium BMMY (1% methanol) to induce protein expression at 28 °C (250 rpm), adding 1% of methanol every 12 h. After 2 days of fermentation in BMMY, cells were removed by centrifugation 10 min at 5000 rpm. Supernatant was supplemented with 2 mM $MgCl_2$ (Sigma) and d100 mg/L of reduced glutathione (Sigma), and pH was adjusted to 7.5 with NaOH (Sigma). Precipitate was removed by centrifugation for 20 min at 1900*g*, followed by filtration using Stericup-GP 0.22 μm (Sigma). A 0.5 M solution of Tris HCl pH 7.5 and 1.5 M NaCl (Sigma) was added to the medium to a final concentration of 50 mM Tris HCl and 150 mM NaCl. High density nickel resin (ABT) was added to the medium (30 mL every liter of medium) and incubated in batch at room temperature for 4 h. High density nickel resin was washed several times with 50 mM Tris HCl pH 7.5 and 150 mM NaCl solution. hMD-2 was eluted with 0.5 M imidazole (Sigma) in 2 mL fractions, which were analyzed for protein concentration and by SDS-PAGE. Pooled fractions containing hMD-2 were extensively dialyzed against 50 mM Tris, 150 mM NaCl, and 0.5% Tween 20, pH 7.5 at 4 °C, and purified hMD-2 biological activity was tested on 293/hTLR4a cells.

Preparation of Recombinant hMD-2 in Mammalian Cells and Purification. hMD-2 was produced in HEK293T cells, analyzed by SDS−PAGE, and its biological activity tested on 293/hTLR4a cells.

HEK293T cells were grown in high-glucose DMEM medium supplemented with 10% fetal calf serum, 106 units per L of penicillin G and 1 g L−L of streptomycin in a 5% CO_2 atmosphere at 37 °C. Mammalian expression constructs for secreted proteins carrying a N-terminal FLAG-tag were generated in the pEF vector (Thermo Fisher Scientific). pEF-Flag-DEVD-hMD2-myc/His plasmid was transiently transfected to HEK293T cells, and the cells were harvested 48 h after transfection and resuspended in lysis buffer containing 50 mM Tris, 150 mM NaCl, 1 mM EDTA, and 1% TRITON X-100. The cell suspension was homogenized by Dounce homogenizer and clarified by centrifugation at 10,000*g* for 20 min. ANTI-FLAG M2 affinity gel beads (SIGMA) was added to the lysate, and then it was left shaking at 4 °C overnight. Solution was spin down at 1000 rpm for 2 min and eluted with TBS Flag peptide (100 μL/mL). Recombinant protein hMD-2 was confirmed by Western blot analysis using an HRP-coupled antibody directed against the FLAG-tag at 1:5000 dilution ratio (Invitrogen).

SDS-PAGE and Western Blot. Purified recombinant hMD-2 was analyzed on 15% SDS-PAGE under reducing conditions followed by Coomassie Brilliant Blue staining. For Western blot analysis, proteins were separated by SDS-PAGE under reducing conditions and then electrophoretically transferred onto polyvinylidene difluoride mem-

DOI: 10.1021/acs.jmedchem.7b01803
J. Med. Chem. XXXX, XXX, XXX−XXX

branes (Amersham Biosciences). After protein transfer, the membranes were treated with blocking buffer followed by incubation with anti-His-HRP antibodies (Sigma). Then, the bands were visualized by 3,3′-diaminobenzidine (Sigma) as a peroxidase substrate.

Protein Concentration Determination. The total protein concentration was determined using ultraviolet absorption at 280 nm. The theoretical extinction coefficient (19.285) was obtained using the protein sequence of hMD-2.

hMD-2 Activity Test Using 293/hTLR4a Cells. For measuring the activity of recombinant expressed hMD-2, HEK 293 cells stably transfected with the human TLR4a gene (293/hTLR4a (Invivogen)) were used. Various dilutions of hMD-2 (stock concentration was 10 μM) were incubated with 100 ng/mL of LPS (Sigma) prior to stimulation of 293/hTLR4a cells. Supernatants were analyzed for IL-8 secretion by ELISA assay.

Determination of IL-8 Secretion by Sandwich Enzyme-Linked Immunosorbent Assay. IL-8 concentrations were assayed using the IL-8 Cytosets (Invitrogen) antibody pair kit containing matched, pretitrated, and fully optimized capture and detection antibodies, recombinant IL-8 standard, and streptavidin-horseradish peroxidase (Sigma). The assay was conducted according to the manufacturer's specifications.

Antibody-Sandwich ELISA for the Detection of Binding of Compounds to hMD-2. The method of antibody-sandwich ELISA for the detection of the binding of compounds to MD-2 was modified from a previous study.[36] A microtiter plate was coated overnight at 4 °C with 100 μL/well of 5 μg/mL of chicken polyclonal anti-hMD-2 antibodies, diluted in 50 mM Na_2CO_3 buffer, pH 9.6, and blocked with 1% BSA in PBS. After washing, 1 μM hMD-2 with tested compounds was added and incubated for 2 h. Mouse anti-hMD-2 mAb (0.1 μg/mL, 9B4) and goat antimouse IgG conjugated with HRP (0.1 μg/mL) in PBS were added, followed by detection at 420 nm after the addition of 100 μL of ABTS (Sigma). Chicken anti-hMD-2 polyclonal antibodies were prepared against recombinant hMD-2 by GenTel (Madison, WI, USA), monoclonal mouse anti-hMD-2 9B4 antibodies were from eBioscience (San Diego, CA, USA), and secondary goat antimouse IgG conjugated with horseradish peroxidase was from Santa Cruz Biotechnology (Santa Cruz, CA, USA).

Fluorescence Spectroscopy Assay. Fluorescence was measured on PerkinElmer fluorimeter LS 55 (PerkinElmer, UK) as previously described.[38] All measurements were done at 20 °C in a 5 × 5 mm quartz glass cuvette (Hellma Suprasil, Müllheim, Germany). hMD-2 protein (200 nM) and 1,1′-Bis(anilino)-4,4′-bis (naphthalene)-8,8′ disulfonate (bis-ANS, 200 nM) were mixed and incubated until reaching stable relative fluorescence units (RFUs) emitted at 420−550 nm under excitation at 385 nm. Compounds, at different concentrations, were then added, followed by relative fluorescence unit (RFU) measurement at 420−550 nm.

LPS Displacement Assay. The ability of the compounds to displace LPS from hMD-2 hydrophobic pocket was determined by ELISA. A microtiter plate was coated overnight at 4 °C with 100 μL/well of 5 μg/mL chicken polyclonal anti-hMD-2 antibodies, diluted in 50 mM Na_2CO_3 buffer, pH 9.6, and blocked with 1% BSA in PBS. After washing, 1 μM hMD-2 with biotin-labeled LPS was added and incubated for 2 h. After washing, the compounds were added at different concentrations and incubated for 1.5 h. After washing, 0.5 μg/mL HRP-conjugated streptavidin (Sigma) in PBS was added, followed by detection at 420 nm after the addition of 100 μL of ABTS (Sigma). Chicken anti-hMD-2 polyclonal antibodies were prepared against recombinant hMD-2 by GenTel (Madison, WI, USA).

Surface Plasmon Resonance (SPR) Analysis. The binding affinity of the compounds to recombinant hMD-2 was determined using a Biacore X100 with an NTA sensor chip (Biacore, GE Healthcare, Uppsala, Sweden). Briefly, 0.5 μM hMD-2 (in 50 mM Tris, 150 mM NaCl, 0.5% Tween 20, pH 7.5) was immobilized onto the sensor chip previously activated with 1 min pulse of 10 mM $NiSO_4$. The first flow cell was used as a reference surface to control nonspecific binding. Both flow cells were injected with the analyte (in PBS, 5% DMSO, 5% EtOH, pH 7.5) at a flow rate of 10 μL/min at 25 °C in increasing concentrations. The data were analyzed with Biacore Evaluation software. K_D values were calculated by global fitting of the equilibrium binding responses from various concentrations of analytes using a 1:1 Langmuir binding model.

■ ASSOCIATED CONTENT

Supporting Information

. The Supporting Information is available free of charge on the ACS Publications website at DOI: 10.1021/acs.jmedchem.7b01803.

Molecular formula strings (CSV)

Molecular modeling; docking results; FT-IR spectroscopy; NMR spectroscopy; small-angle X-ray scattering; synthesis and compounds characterization (PDF)

■ AUTHOR INFORMATION

Corresponding Author

*E-mail: francesco.peri@unimib.it. Phone: +39.0264483453.

ORCID

Fabio A. Facchini: 0000-0002-4339-5845

Cristina Airoldi: 0000-0002-3670-6262

Roman Jerala: 0000-0002-6337-5251

Francesco Peri: 0000-0002-3417-8224

Notes

The authors declare no competing financial interest.

■ ACKNOWLEDGMENTS

This study was financially supported by the H2020-MSC-ETN-642157 project TOLLerant. The Italian Ministry for Foreign Affairs and International Cooperation (MAECI), the Slovenian National Agency (grant P4-0176) and the Spanish Ministry for Economy and Competitiveness (MINECO, grants CTQ2014-57141-R and CTQ2017-88353-R) are also acknowledged. SAXS measurements were performed at the EMBL beamline P12 c/o DESY, Hamburg, Germany (beam time grant to A.B.S).

■ ABBREVIATIONS USED

TLR, Toll-like receptor; PRRs, pattern recognition receptors; PAMPs, pathogen-associated molecular patterns; MD-2, myeloid differentiation 2; LOS, lipooligosaccharide; DAMPs, damage-associated molecular patterns; LBP, lipid binding protein; CD14, cluster of differentiation 14

■ REFERENCES

(1) Akira, S.; Takeda, K. Toll-like receptor signalling. *Nat. Rev. Immunol.* **2004**, *4*, 499−511.

(2) Molinaro, A.; Holst, O.; Di Lorenzo, F.; Callaghan, M.; Nurisso, A.; D'Errico, G.; Zamyatina, A.; Peri, F.; Berisio, R.; Jerala, R.; Jiménez-Barbero, J.; Silipo, A.; Martín-Santamaría, S. Chemistry of lipid A: at the heart of innate immunity. *Chem. - Eur. J.* **2015**, *21*, 500−519.

(3) Krüger, C. L.; Zeuner, M. T.; Cottrell, G. S.; Widera, D.; Heilemann, M. Quantitative single-molecule imaging of TLR4 reveals ligand-specific receptor dimerization. *Sci. Signaling* **2017**, *10*, eaan1308.

(4) Gioannini, T.; Teghanemt, A.; Zhang, D.; Levis, E.; Weiss, J. Monomeric endotoxin: protein complexes are essential for TLR4-dependent cell activation. *J. Endotoxin Res.* **2005**, *11*, 117−123.

(5) Park, B.; Song, D.; Kim, H.; Choi, B.; Lee, H.; Lee, J. The structural basis of lipopolysaccharide recognition by the TLR4-MD-2 complex. *Nature* **2009**, *458*, 1191−1195.

(6) Cighetti, R.; Ciaramelli, C.; Sestito, S. E.; Zanoni, I.; Kubik, Ł.; Ardá-Freire, A.; Calabrese, V.; Granucci, F.; Jerala, R.; Martín-Santamaría, S.; Jiménez-Barbero, J.; Peri, F. Modulation of CD14

DOI: 10.1021/acs.jmedchem.7b01803
J. Med. Chem. XXXX, XXX, XXX−XXX

and TLR4·MD-2 activities by a synthetic lipid A mimetic. *ChemBioChem* **2014**, *15*, 250−258.
(7) Okamura, Y.; Watari, M.; Jerud, E.; Young, D.; Ishizaka, S.; Rose, J.; Chow, J.; Strauss, J. r. The extra domain A of fibronectin activates toll-like receptor 4. *J. Biol. Chem.* **2001**, *276*, 10229−10233.
(8) Wang, Y.; Qian, Y.; Fang, Q.; Zhong, P.; Li, W.; Wang, L.; Fu, W.; Zhang, Y.; Xu, Z.; Li, X.; Liang, G. Saturated palmitic acid induces myocardial inflammatory injuries through direct binding to TLR4 accessory protein MD-2. *Nat. Commun.* **2017**, *8*, 13997.
(9) Mancek-Keber, M.; Frank-Bertoncelj, M.; Hafner-Bratkovič, I.; Smole, A.; Zorko, M.; Pirher, N.; Hayer, S.; Kralj-Iglic, V.; Rozman, B.; Ilc, N.; Horvat, S.; Jerala, R. Toll-like receptor 4 senses oxidative stress mediated by the oxidation of phospholipids in extracellular vesicles. *Sci. Signaling* **2015**, *8*, ra60.
(10) Goligorsky, M. S. TLR4 and HMGB1: partners in crime? *Kidney Int.* **2011**, *80*, 450−452.
(11) Erridge, C. The roles of toll-like receptors in atherosclerosis. *J. Innate Immun.* **2009**, *1*, 340−349.
(12) Abdollahi-Roodsaz, S.; Joosten, L. A.; Roelofs, M. F.; Radstake, T. R.; Matera, G.; Popa, C.; van der Meer, J. W.; Netea, M. G.; van den Berg, W. B. Inhibition of toll-like receptor 4 breaks the inflammatory loop in autoimmune destructive arthritis. *Arthritis Rheum.* **2007**, *56*, 2957−2967.
(13) Cao, L.; Tanga, F.; Deleo, J. The contributing role of CD14 in toll-like receptor 4 dependent neuropathic pain. *Neuroscience* **2009**, *158*, 896−903.
(14) Casula, M.; Iyer, A. M.; Spliet, W. G.; Anink, J. J.; Steentjes, K.; Sta, M.; Troost, D.; Aronica, E. Toll-like receptor signaling in amyotrophic lateral sclerosis spinal cord tissue. *Neuroscience* **2011**, *179*, 233−43.
(15) Fan, J.; Li, Y.; Levy, R. M.; Fan, J. J.; Hackam, D. J.; Vodovotz, Y.; Yang, H.; Tracey, K. J.; Billiar, T. R.; Wilson, M. A. Hemorrhagic shock induces NAD(P)H oxidase activation in neutrophils: role of HMGB1-TLR4 signaling. *J. Immunol.* **2007**, *178*, 6573−6580.
(16) Kuzmich, N. N.; Sivak, K. V.; Chubarev, V. N.; Porozov, Y. B.; Savateeva-Lyubimova, T. N.; Peri, F. TLR4 Signaling pathway modulators as potential therapeutics in inflammation and sepsis. *Vaccines (Basel, Switz.)* **2017**, *5*, 34.
(17) Opal, S. M.; Laterre, P. F.; Francois, B.; LaRosa, S. P.; Angus, D. C.; Mira, J. P.; Wittebole, X.; Dugernier, T.; Perrotin, D.; Tidswell, M.; Jauregui, L.; Krell, K.; Pachl, J.; Takahashi, T.; Peckelsen, C.; Cordasco, E.; Chang, C. S.; Oeyen, S.; Aikawa, N.; Maruyama, T.; Schein, R.; Kalil, A. C.; Van Nuffelen, M.; Lynn, M.; Rossignol, D. P.; Gogate, J.; Roberts, M. B.; Wheeler, J. L.; Vincent, J. L. Effect of eritoran, an antagonist of MD-2/TLR4, on mortality in patients with severe sepsis: the ACCESS randomized trial. *JAMA* **2013**, *309*, 1154−1162.
(18) Rice, T.; Wheeler, A.; Bernard, G.; Vincent, J.; Angus, D.; Aikawa, N.; Demeyer, I.; Sainati, S.; Amlot, N.; Cao, C.; Ii, M.; Matsuda, H.; Mouri, K.; Cohen, J. A randomized, double-blind, placebo-controlled trial of TAK-242 for the treatment of severe sepsis. *Crit. Care Med.* **2010**, *38* (8), 1685−1694.
(19) Salluh, J. I.; Póvoa, P. Biomarkers as end points in clinical trials of severe sepsis: a garden of forking paths. *Crit. Care Med.* **2010**, *38*, 1749−1751.
(20) Kalil, A. C.; LaRosa, S. P.; Gogate, J.; Lynn, M.; Opal, S. M. Influence of severity of illness on the effects of eritoran tetrasodium (E5564) and on other therapies for severe sepsis. *Shock* **2011**, *36*, 327−331.
(21) Danner, R. L.; Van Dervort, A. L.; Doerfler, M. E.; Stuetz, P.; Parrillo, J. E. Antiendotoxin activity of lipid A analogues: requirements of the chemical structure. *Pharm. Res.* **1990**, *7*, 260−263.
(22) Matsuura, M.; Kiso, M.; Hasegawa, A. Activity of monosaccharide lipid A analogues in human monocytic cells as agonists or antagonists of bacterial lipopolysaccharide. *Infect. Immun.* **1999**, *67*, 6286−6292.
(23) Yang, D.; Satoh, M.; Ueda, H.; Tsukagoshi, S.; Yamazaki, M. Activation of tumor-infiltrating macrophages by a synthetic lipid A analog (ONO-4007) and its implication in antitumor effects. *Cancer Immunol. Immunother.* **1994**, *38*, 287−293.
(24) Tamai, R.; Asai, Y.; Hashimoto, M.; Fukase, K.; Kusumoto, S.; Ishida, H.; Kiso, M.; Ogawa, T. Cell activation by monosaccharide lipid A analogues utilizing toll-like receptor 4. *Immunology* **2003**, *110*, 66−72.
(25) Perrin-Cocon, L.; Aublin-Gex, A.; Sestito, S. E.; Shirey, K. A.; Patel, M. C.; Andre, P.; Blanco, J. C.; Vogel, S. N.; Peri, F.; Lotteau, V. TLR4 antagonist FP7 inhibits LPS-induced cytokine production and glycolytic reprogramming in dendritic cells, and protects mice from lethal influenza infection. *Sci. Rep.* **2017**, *7*, 40791.
(26) Funatogawa, K.; Matsuura, M.; Nakano, M.; Kiso, M.; Hasegawa, A. Relationship of structure and biological activity of monosaccharide lipid A analogues to induction of nitric oxide production by murine macrophage RAW264.7 cells. *Infect. Immun.* **1998**, *66*, 5792−5798.
(27) Mueller, M.; Lindner, B.; Kusumoto, S.; Fukase, K.; Schromm, A. B.; Seydel, U. Aggregates are the biologically active units of endotoxin. *J. Biol. Chem.* **2004**, *279*, 26307−26313.
(28) Gutsmann, T.; Schromm, A.; Brandenburg, K. The physicochemistry of endotoxins in relation to bioactivity. *Int. J. Med. Microbiol.* **2007**, *297*, 341−352.
(29) Gioannini, T.; Teghanemt, A.; Zhang, D.; Coussens, N.; Dockstader, W.; Ramaswamy, S.; Weiss, J. Isolation of an endotoxin-MD-2 complex that produces toll-like receptor 4-dependent cell activation at picomolar concentrations. *Proc. Natl. Acad. Sci. U. S. A.* **2004**, *101*, 4186−4191.
(30) Ciaramelli, C.; Calabrese, V.; Sestito, S. E.; Pérez-Regidor, L.; Klett, J.; Oblak, A.; Jerala, R.; Piazza, M.; Martín-Santamaría, S.; Peri, F. Glycolipid-based TLR4 modulators and fluorescent probes: rational design, synthesis, and biological properties. *Chem. Biol. Drug Des.* **2016**, *88*, 217−229.
(31) Liu, M.; Nicholson, J. K.; Lindon, J. C. High-resolution diffusion and relaxation edited one- and two-dimensional ^{1}H NMR spectroscopy of biological fluids. *Anal. Chem.* **1996**, *68*, 3370−3376.
(32) Beckonert, O.; Keun, H. C.; Ebbels, T. M. D.; Bundy, J.; Holmes, E.; Lindon, J. C.; Nicholson, J. K. Metabolic profiling, metabolomic and metabonomic procedures for NMR spectroscopy of urine, plasma, serum and tissue extracts. *Nat. Protoc.* **2007**, *2*, 2692.
(33) Manček-Keber, M.; Jerala, R. Postulates for validating TLR4 agonists. *Eur. J. Immunol.* **2015**, *45*, 356−370.
(34) Ohnishi, T.; Muroi, M.; Tanamoto, K.-i. N-Linked Glycosylations at Asn26 and Asn114 of Human MD-2 Are Required for toll-like receptor 4-mediated activation of NF-kB by lipopolysaccharide. *J. Immunol.* **2001**, *167*, 3354−3359.
(35) da Silva Correia, J.; Ulevitch, R. J. MD-2 and TLR4 N-linked glycosylations are important for a functional lipopolysaccharide receptor. *J. Biol. Chem.* **2002**, *277*, 1845−1854.
(36) Viriyakosol, S.; McCray, P. B.; Ashbaugh, M. E.; Chu, J.; Jia, H. P.; Weiss, J.; Kirkland, T. N. Characterization of monoclonal antibodies to human soluble MD-2 protein. *Hybridoma* **2006**, *25*, 349−357.
(37) Resman, N.; Gradisar, H.; Vasl, J.; Keber, M.; Pristovsek, P.; Jerala, R. Taxanes inhibit human TLR4 signaling by binding to MD-2. *FEBS Lett.* **2008**, *582*, 3929−3934.
(38) Mancek-Keber, M.; Jerala, R. Structural similarity between the hydrophobic fluorescent probe and lipid A as a ligand of MD-2. *FASEB J.* **2006**, *20*, 1836−1842.
(39) Ohto, U.; Fukase, K.; Miyake, K.; Shimizu, T. Structural basis of species-specific endotoxin sensing by innate immune receptor TLR4/MD-2. *Proc. Natl. Acad. Sci. U. S. A.* **2012**, *109*, 7421−7426.
(40) Brandenburg, K.; Matsuura, M.; Heine, H.; Müller, M.; Kiso, M.; Ishida, H.; Koch, M. H. J.; Seydel, U. Biophysical characterization of triacyl monosaccharide lipid a partial structures in relation to bioactivity. *Biophys. J.* **2002**, *83*, 322−333.
(41) Seydel, U.; Schromm, A. B.; Brade, L.; Gronow, S.; Andrä, J.; Müller, M.; Koch, M. H. J.; Fukase, K.; Kataoka, M.; Hashimoto, M.; Kusumoto, S.; Brandenburg, K. Physicochemical characterization of

DOI: 10.1021/acs.jmedchem.7b01803
J. Med. Chem. XXXX, XXX, XXX−XXX

carboxymethyl lipid A derivatives in relation to biological activity. *FEBS J.* **2005**, *272*, 327−340.
(42) *The PyMOL Molecular Graphics System*, version 1.8; Schrodinger, LLC, 2015.
(43) Sestito, S. E.; Facchini, F. A.; Morbioli, I.; Billod, J.-M.; Martin-Santamaria, S.; Casnati, A.; Sansone, F.; Peri, F. Amphiphilic guanidinocalixarenes inhibit lipopolysaccharide (LPS)- and lectin-stimulated toll-like receptor 4 (TLR4) Signaling. *J. Med. Chem.* **2017**, *60*, 4882−4892.
(44) Case, D. A.; Babin, V.; Berryman, J.; Betz, R.; Cai, Q.; Cerutti, D.; Cheatham, T.; Darden, T.; Duke, R.; Gohlke, H.; Götz, A.; Gusarov, S.; Homeyer, N.; Janowski, P.; Kaus, J.; Kolossváry, I.; Kovalenko, A.; Lee, T.-S.; Legrand, S.; A. Kollman, P. *Amber 2014*; University of California, San Francisco, 2014.
(45) Frisch, M. J.; Schlegel, H. B.; Scuseria, G. E.; Robb, M. A.; Cheeseman, J. R.; Scalmani, G.; Barone, V.; Mennucci, B.; Petersson, G. A.; Nakatsuji, H.; Caricato, M.; Li, X.; Hratchian, H. P.; Izmaylov, A. F.; Bloino, J.; Zheng, G.; Sonnenberg, J. L.; Hada, M.; Ehara, M.; Toyota, K.; Fukuda, R.; Hasegawa, J.; Ishida, M.; Nakajima, T.; Honda, Y.; Kitao, O.; Nakai, H.; Vreven, T.; Montgomery, J. A., Jr.; Peralta, J. E.; Ogliaro, F.; Bearpark, M. J.; Heyd, J.; Brothers, E. N.; Kudin, K. N.; Staroverov, V. N.; Kobayashi, R.; Normand, J.; Raghavachari, K.; Rendell, A. P.; Burant, J. C.; Iyengar, S. S.; Tomasi, J.; Cossi, M.; Rega, N.; Millam, N. J.; Klene, M.; Knox, J. E.; Cross, J. B.; Bakken, V.; Adamo, C.; Jaramillo, J.; Gomperts, R.; Stratmann, R. E.; Yazyev, O.; Austin, A. J.; Cammi, R.; Pomelli, C.; Ochterski, J. W.; Martin, R. L.; Morokuma, K.; Zakrzewski, V. G.; Voth, G. A.; Salvador, P.; Dannenberg, J. J.; Dapprich, S.; Daniels, A. D.; Farkas, Ö.; Foresman, J. B.; Ortiz, J. V.; Cioslowski, J.; Fox, D. J. *Gaussian 09*; Gaussian, Inc.: Wallingford, CT, 2009.
(46) Kirschner, K. N.; Yongye, A. B.; Tschampel, S. M.; GonzÁLez-OuteiriÑO, J.; Daniels, C. R.; Foley, B. L.; Woods, R. J. GLYCAM06: a generalizable biomolecular force field. Carbohydrates. *J. Comput. Chem.* **2008**, *29*, 622−655.
(47) Morris, G. M.; Huey, R.; Lindstrom, W.; Sanner, M. F.; Belew, R. K.; Goodsell, D. S.; Olson, A. J. Autodock4 and Autodocktools4: automated docking with selective receptor flexibility. *J. Comput. Chem.* **2009**, *30*, 2785−2791.
(48) *Maestro*, release 2017−4; Schrödinger, LLC: New York, 2017.
(49) Gruber, A.; Mancek, M.; Wagner, H.; Kirschning, C. J.; Jerala, R. Structural model of MD-2 and functional role of its basic amino acid clusters involved in cellular lipopolysaccharide recognition. *J. Biol. Chem.* **2004**, *279*, 28475−28482.

DOI: 10.1021/acs.jmedchem.7b01803
J. Med. Chem. XXXX, XXX, XXX−XXX